NEW REACTIONS, MECHANISMS, AND STEREOCHEMICAL THEORY IN ORGANIC CHEMISTRY

By

ROBERT VINCENT KOLAKOWSKI

A dissertation submitted to the

Graduate School-New Brunswick

Rutgers, The State University of New Jersey

In partial fulfillment of the requirements

For the degree of

Doctor of Philosophy

Graduate Program in Chemistry

Written under the direction of

Dr. Lawrence J. Williams, Ph.D.

And approved by

_____

_____

_____

_____

New Brunswick, New Jersey

October, 2010

ABSTRACT OF THE DISSERTATION

New Reactions, Mechanisms, and Stereochemical Theory in Organic Chemistry

By ROBERT V. KOLAKOWSKI

Dissertation Director:

Dr. Lawrence J. Williams, Ph.D.

Here we describe a new method for the formation of allenes utilizing a Grob-like fragmentation along with a mechanistic study. The mechanism of the azide and thio acid amidation is presented. This mechanism was found to go through a thiatriazoline, and the reaction was successfully extended to the isoelectronic coupling of dithio acids with azides to form thioamide. Finally, distortional asymmetry is presented as new model for understanding stereoselectivity in sterically unbiased systems. This model deomonstrates that small ground state perturbations can lead to significant energy differences between diastereomeric tranistion states.

Acknowledgements

I would like to thank Professor Lawrence Williams for providing me with an outstanding scientific education that was facilitated by a laboratory environment that spurred creativity and thoughtful problem solving of unique chemical challenges.

I would also like to thank Professor Spencer Knapp, Professor Daniel Seidel and Dr. Scott Shaw for being on my thesis defense committee.

A special thanks to three key people: First and foremost, Professor Karsten Krogh-Jesperson for his expertise in the area of computational chemistry, his patient and thoughtful discussions helped me decipher the black box that is transition state finding in computational chemistry; Second, Professor Ralph Warmuth for sharing his knowledge of therory and experiment, which was critical in conducting the thio acid/azide kinetic studies; and third Professor Ron Sauers for useful discussions on NBO analysis.

I also want to thank, Yue Zhang, Gaojie Hu, and Kai Liu, who provided the friendship and moral support that to overcome the sometimes daunting tasks of scientific discovery, as well as Williams group memebers both former and current.

Table of Contents

Schemes

Figures

Chapter 1: Allene Synthesis via a Grob Like Fragmentation.

Section 1.1: Allene Fragmentation.

The rich structural and reactive properties of allenes complement the chemistry of alkenes and alkynes and render them versatile synthetic intermediates.[1] Allenes are also present in many natural products[2] and intermediates of certain biosynthetic pathways.[3] The importance of allenes in synthesis is tempered by the lack of methods for their preparation and therefore strategies for their application. The most useful stereoselective methods for allene synthesis are: a) the S_N2' displacement of activated propargyl alcohols by organocuprates and b) the rearrangement of propargyl diazenes.[4] In the course of our synthetic deliberations, we identified instances where available approaches are not expedient and consequently led us to the develop a method of allene synthesis by C-C fragmentation.

Olefin-formation via C-C bond fragmentation was intially recognized in natural product degradation studies[5] and later developed by Grob who showed the fragmentation is stereospecific.[6]

Figure 1.1: C-C Fragmentation Pathway

---

[1] (*a*) Hashmi, A. S. K., in Krause, N.; Hashmi, A. S. K. *Modern Allene Chemistry*, Vol. 1; Wiley-VCH Verlag: Weinhelm, 2004, pp 3-36. (*b*) Ma, S.; in Krause, N.; Hashmi, A. S. K. *Modern Allene Chemistry*, Vol. 2; Wiley-VCH Verlag: Weinhelm, 2004, pp 595-684. (*c*) Wei, L.–L.; Xiong, H.; Hsung, R. P. *Acc. Chem. Res.* **2003**, *36*, 773. (*d*) Brummond, K. M.; DeForrest, J. E. *Synthesis* **2007**, *6*, 795. (*e*) Kim, H.; Williams, L. J. *Curr. Opin. Drug Discovery Dev.* **2008**, *11*, 870.

[2] (*a*) Krause, N.; Hoffmann-Roder, A.; in Krause, N.; Hashmi, A. S. K. *Modern Allene Chemistry*, Vol. 2; Wiley-VCH Verlag: Weinhelm, 2004, pp 997-1017 (*b*) Hu, G.; Liu, K.; Williams, L. J. *Org. Lett.* **2008**, *10*, 5493.

[3] (*a*) Corey, E. J.; D'Alarco, M.; Matsuda, S. P.; Lansbury, Jr.,P. T.; Yamada, Y. *J. Am. Chem. Soc.* **1987**, *109*, 289. (*b*) Song, W. –C.; Brash, A. R. *Science*, **1991**, *253*, 781.

[4] (a) Myers, A. G.; Zheng, B. *J. Am. Chem. Soc.* **1996**, *118*, 4492. (*b*) Shangguan, N.; Kiren, S.; Williams, L. J. *Org. Lett.* **2007**, *9*, 1093. (*c*) Kolakowski, R. V.; Williams, L. J. *Tetrahedron Lett.* **2007**, *48*, 4761. (*d*) Wang, Z.; Shangguan, N.; Cusick, J. R.; Williams, L. J. *Synlett*, **2008**, *2*, 213.

[5] (*a*) Prelog, V.; Zalan, E. *Helv. Chim. Acta.* **1944**, *27*, 535. (*b*) Prelog, V.; Haflinger, O. *Helv. Chim. Acta.* **1950**, *33*, 2021. for the first synthesis of allenes see . Burton, B. S.; von Pechmann, H. *Ber. Dtsch. Chem. Ges.* **1887**, *20*, 145.

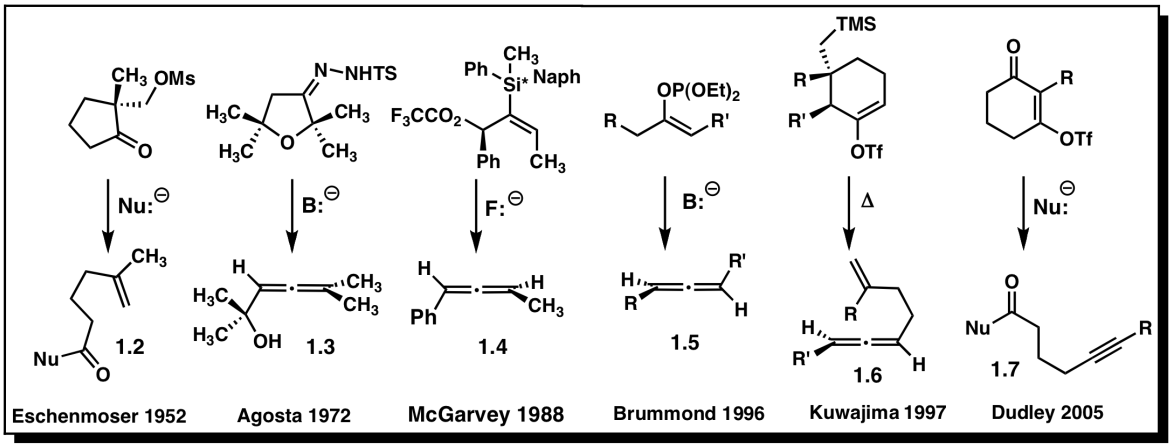

Figure 1.2: Related Reactions

Eschenmoser disclosed a mechanistically relevant fragmentation induced by nucleophilic attack to give **1.2**, Figure 1.2.[7] The first recorded allene-producing fragmentation was introduced by Agosta[8] and is based on a Shipiro-type intermediate to fragment a furan to the corresponding allenol **1.3**. McGarvey[9] showed that the fragmentation of a vinal triflate β to a chiral silyl group could produce an allene with maintenance of chirality **1.4**. Brummond in 1996 showed a vinyl phosphate ester, **1.5,** could undergo base mediate fragmentation to produce an allene.[10] Kuwajima[11] showed that vinyl triflates, **1.6,** could undergo thermally induced fragmentation to produce allenes. The use of a polar aprotic solvent such as DMF was found necessary for the reaction, which pointed to a cationic-like intermediate. Recently, Dudley reported that β-triflyl-α,β-unsaturated ketones also

---

[6] Grob, C. A. *Angew. Chem. Int. Ed.* **1969**, *8,* 535.

[7] Eschenmoser, A.; Frey, A. *Helv. Chim. Acta.* **1952**, *35*, 1660.

[8] Foster, A. M.; Agosta, W. C. *J. Org. Chem.* **1972**, *37*, 61.

[9] Torres, E.; Larson, G. L.; McGarvey, G. J. *Tetrahedron Lett.* **1988**, 1355.

[10] (*a*) Brummond, K. M.; Dingess, E. A.; Kent, J. L. *J.Org. Chem.* **1996**, *61*, 6096. (*b*) Brummond, K. M.; Wan, H.; Kent, J. L. *J.Org. Chem.* **1998**, *63*, 6535.

[11] Sugai, M.; Tanino, K.; Kuwajima, I. *Synthesis* **1997**, 461.

undergo efficient C-C bond fragmentation to give alkynes **1.7**.[12] As this fragmentation strategy has not yet been applied to allene synthesis we wondered whether vinyl triflates would fragment to give the corresponding allenes via a framework that complements the Grob and Dudley reactions and whether this transformation could be used to prepare allenes stereospecifically.

Addition of carbon nucleophiles to **1.8** generated a transient alkoxide that induced fragmentation/allene formation Table 1.1. Use of approximately stoichiometric quantities of nucleophile gave allenic ketones **1.9a-e**. Use of excess reagent gave allenic alcohols **1.10a-c**. Alkyl, aryl, and alkynyl nucleophiles, delivered as their corresponding organolithium or Grignard reagents, added smoothly and induced fragmentation. Ketone, ester enolates and dithiane anions also add efficiently and induce fragmetnation. Use of cerium chloride was necessary to suppress competitive enolate formation of this substrate in instances where hard carbon nucleophiles were used.[13] Addition of alkoxides or lithiated amines as nucleophiles for carbonyl addition, which in principle would give ester or amide products, gave recovered **1.8** or complex mixtures. As suggested by the selective preparation of compounds **1.10a-1.10c** fragmentation appears rate limiting for at least some substrates. For example, when a reaction mixture of **1.9a** with $CeCl_3$ (2.5 equiv.) and *n*-BuLi (2.5 equiv.) at -78 ºC was quenched after 10 min, the non-fragmented tertiary alcohol **1.11** was isolated in 20% yield (*c.f.* **1.9a**). These data demonstrate that allenes form rapidly from carbon nucleophile addition/vinyl triflate fragmentation for suitable substrates.

---

[12] (*a*) Kamijo, S.; Dudley, G. B. *J. Am. Chem. Soc.* **2005**, *127*, 5028. (*b*) Kamijo, S.; Dudley, G. B. *J. Am. Chem. Soc.* **2006**, *128*, 6499.

[13] Imamoto, T.; Takiyama, N.; Nakamura, K.; Hatajima, T.; Kamiya, Y. *J. Am. Chem. Soc.* **1989**, *111*, 4392.

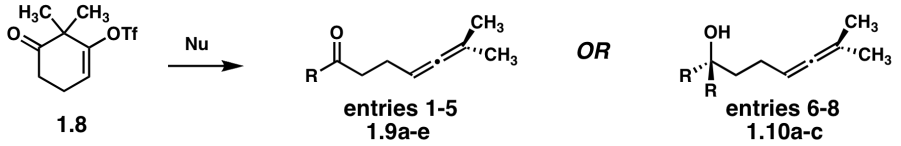

1.8 entries 1-5 1.9a-e entries 6-8 1.10a-c

entry	product	R-	yield (%)	entry	product	R-	yield (%)
1	1.9a	Ph	76[a]	6	1.10a	Ph	86[f]
2	1.9b	O, Ph	78[b]	7	1.10b	nBu	81[g]
3	1.9c	O, EtO	89[c]	8	1.10c	S, S	74[h]
4	1.9d	S, S	87[d]				
5	1.9e	TMS	75[e]				

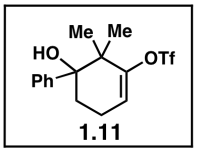

1.11

[a]1.0 equiv PhLi, 45 min, THF -78 ºC - rt, 1 h. [b]1.3 equiv NaHMDS, 1.3 equiv $PhCOCH_3$, THF, -78 ºC, 15 min. [c]1.4 equiv LiHMDS, 1.3 equiv EtOAc, THF, -78 ºC, 15 min. [d]1.1 equiv *n*BuLi, 1.2 equiv dithiane, THF, -78 ºC - rt, 1 h. [e]1.1 equiv *n*BuLi, 1.2 equiv TMSCCH, THF, -78 ºC - rt, 1 h. [f]3.0 equiv $CeCl_3$, 3.0 equiv PhMgBr, THF, -78 ºC - rt, 1h. [g]3.0 equiv $CeCl_3$, 3.0 eq *n*-BuLi, THF, -78 ºC – rt. [h]3.0 eq *n*-BuLi, 3.0 equiv dithiane, THF, -78 ºC – rt.

Table 1.1: Nucleophilic Induced Allene Fragmentation.

Scheme 1.2 summarizes our findings that allenes form from other vinyl triflates and, where relevant, that stereogenic allenes form stereospecifically. Exposure of carvone-derived silyl ether **1.12** to fluoride ion led to rapid and clean formation of allenic aldehyde. For convenience, the reaction mixture was then treated with reducing agent, which gave the corresponding acyclic alcohol **1.13**. Excess phenyl magnesium bromide smoothly added to cyclopentenone **1.14** to give allenic alcohol **1.15**. Following this procedure, Yue Zhang synthesized ten-membered cyclic allene **1.17**. Reaction efficiency for these more complex substrates is primarily a reflection of triflate hydrolysis as a competing side reaction. Brief treatment of **1.16** to the reaction conditions gave allene

1.17 (52%) and partially cleaved ether **1.22**. The yield of **1.17** based on recovered **1.22** was 85%. The fragmentations are stereospecific. My coworker Dr. Madhuri Manpadi showed that highly enantioenriched acyclic vinyl triflates **1.18** and **1.20** fragment upon treatment with fluoride to give the corresponding enantioenriched allenes. Mosher ester analysis showed that in this fragmentation allene **1.18** did not form **1.21** from **1.18→1.19** and allene **1.19** was not formed from **1.21**.

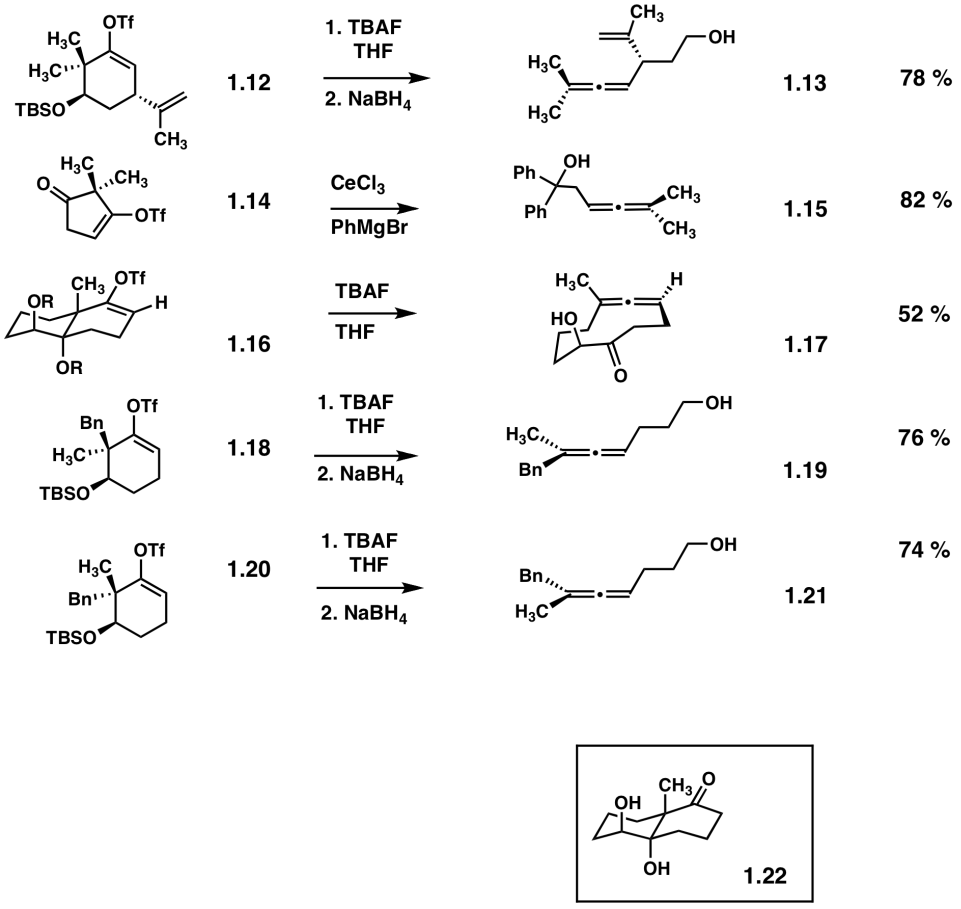

Scheme 1.2: Vinyl triflate to allene fragmentation

Section 1.2: Mechanistic Framework

In principle, anionic *O*-triflyl piperidone **1.23** could give an allene of type **1.24** or an alkyne of type **1.25** (*cf*. Dudley fragmentation). The corresponding trifluoroacetate salt was treated with excess PhMgBr in diethyl ether at -20 ºC.[14] Only **1.24** was observed after 5 min (>20:1, **1.24**:**1.25**, 5% yield, 5% conversion). As the reaction proceeded, **1.25** became evident and the ratio of **1.24**:**1.25** gradually decreased. After 1 h the ratio of **1.24:1.25** was 3:1 (82% yield, 82% conversion). The increase in alkyne is readily understood in terms of the known propensity of terminal allenes to isomerize to terminal alkynylides under strongly basic conditions.

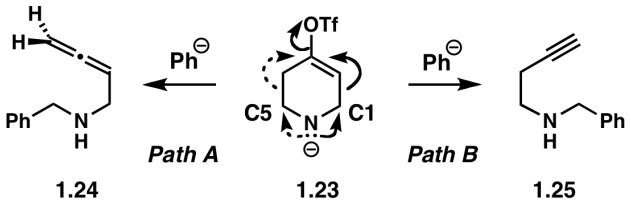

time (min)	1.24:1.25	yield (%)
5	>20:1	5
15	10:1	45
30	5:1	73
60	3:1	82

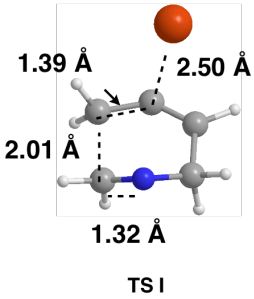

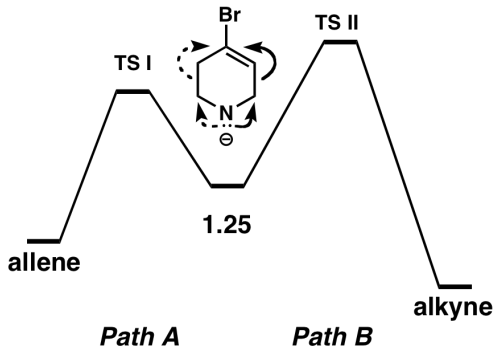

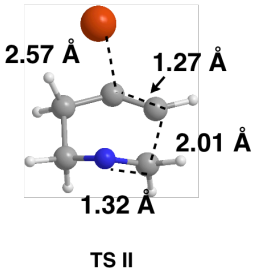

[14] The immediate fragmentation products (not observed) are imines. Use of THF accelerated the isomerization process (1 h: **26**:**27** = 1:1, 85% yield, 85% conversion).

Scheme 1.3: Mechanistic framework study

These data demonstrate that fragmentation of this system favors allene over alkyne formation.

Why does the allene form faster than the alkyne? Computed transition states were found for allene and alkyne formation using B3LYP/6-31G+(2d,2p). The $\Delta H^{\ddagger}_{calc}$ for the computed transition structures **TS I** and **TS II** was 2.39 kcal/mol, favoring allene formation.[15] Moreover, NBO population analysis of the optimized ground state energy of **1.23** indicates a greater positive charge on C5 than on C1.[16] Hence the calculated transition structures are consistent with a rationale wherein the triflate polarizes the carbon framework. Despite proper stereoelectronics for both pathways, the sp^3 network, being more polarized than the sp^2 network, interacts more strongly with the anionic nitrogen and allene formation becomes the kinetically more facile transformation.

We have shown that suitably functionalized vinyl triflates can be induced to fragment to give allenes. Mechanistic studies provide a framework for understanding this reaction in relation to other known modes of fragmentation, and as such, these findings complement methods of alkene and alkyne synthesis that rely upon C-C bond fragmentation. Importantly, this work complements allene synthesis methods that use alkyne precursors and provides access to 1,3-disubstituted allenes which are often difficult to synthesize. The stereospecificity of this reaction type also allows access to highly enantioenriched allenes.

---

[15] Caution must be exercised in light of the known difficulties in calculating allene and alkyne isomers. (See: Wodrich, M. D.; Corminboeuf, C.; Schleyer, P. V. R. *Org. Lett.* **2006**, *8*, 3631.) The good correlation between $\Delta H^{\ddagger}_{calc}$ and experiment is likely due to the degree of separation that exists between the transition states and the product ground states.

[16] F. Weinhold, C. Landis, *Valency and Bonding*. Cambridge University Press: Cambridge UK, 2005.

Chapter 2: Thioamides via Thiatriazolines.

Section 2.1: Examples of Thioamides from Dithio Acids and Azides

Our group has previously disclosed an amide coupling between thio acids and azides.[17] This reaction was discovered to be mechanistically distinct from amine based strategies and will be discussed further in Chapter 3.[18] We were curious to see whether thio acid/azide coupling could be extended to dithio acids and azides to produce thioamides.

Thioamides serve as isosteric replacements for amides in peptides and as versatile synthetic precursors to thiazolines and thiazoles.[19] Most approaches to the construction of thioamides involve formation of the parent amide followed by thionation.[20] Figure 2.1 illustrates the mechanistic hypothesis we set forth to explore. The azide and dithioacid would couple directly to form a thiatriazoline, and then fragment to form amide, N_2, and S_8 products (Eq. 1, X = O,S).

---

[17] Shangguan, N.; Katukojvala, S.; Greenberg, R.; Williams, L. J. *J. Am. Chem. Soc.* **2003**, *125*, 7754. For a detailed mechanistic study: Kolakowski, Robert V.; Shangguan, N.; Sauers, R. R.; Williams, L. J. *J. Am. Chem. Soc.* **2006**, *128*, 5695.

[18] Larock, R. C. Comprehensive Organic Transformations (Wiley-VCH, New York, ed. 2, 1999)

[19] Jagodzinski, T. S. *Chem. Rev.* **2003**, *103*, 197.

[20] For recent amide thionations see: Charette, A. B.; Grenon, M. J. *Org.Chem.* **2003**, *68*, 5792.; Coats, S. J.; Link, J. S.; Hlasta, D. J. *Org.Lett.* **2003**, *5*, 721.; Zbruyev, O. I.; Stiasni, N.; Kappe, C. O. *J. Comb. Chem.* **2003**, *5*, 145.; Curphey, T. J. *J.Org.Chem.* 2002, 67, 6461.; Ilankumaran, P.; Ramesha, A. R.; Chandrasekaran, S. *Tetrahedron Lett.* **1995**, *36*, 8311.; For an important report see: Lajoie, G.; Lepine, F.; Mazaik, L.; Belleau, B. *TetrahedronLett.* **1983**, *24*,3815.; For other approaches using dithiocarboxylates or isothiacyanates see: Schaumann, E. In Comprehensive Organic Synthesis; Trost, B. M., Fleming, I., Eds.; Pergamon Press: Oxford, 1991; Vol.6, pp419. ; Schaumann, E.; Moeller, M.; Adiwidjaja, G. *Chem. Ber.***1988**,*121*,689.; Papadopoulos, E. P. *J. Org. Chem.* **1975**, *41*, 962.; For an interesting side reaction that was noted to produce a thioamide see: Paulsen, H.; Bielfeldt, T.; Peters, S.; Bock, K. *Liebigs Ann.Chem.***1994**, 369.

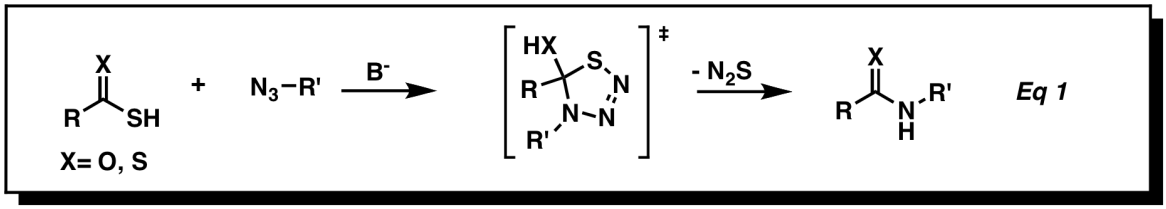

Figure 2.1: Thioamide Hypothesis.

Our initial study of thio acids and azides revealed that electron deficient azides couple with thio acids rapidly and quantitatively.[17] With this knowledge we set out to react dithiobenzoic acid **2.1** and benzene sulfonazide **2.2** as shown in Figure 2.1.

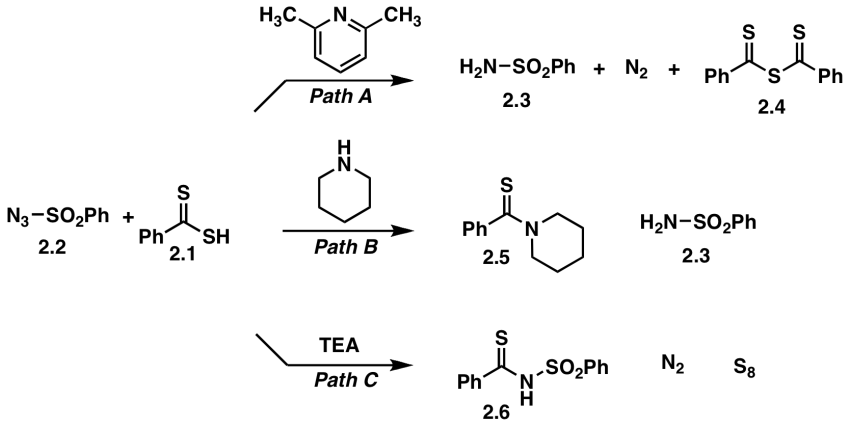

Figure 2.2: Initial base screen for thioamide coupling.

The reaction outcome is remarkably dependent on the nature of the base promoter, unlike the parent reaction to form amides. We focused on the effects of 2,6-lutidine, piperidine, and triethylamine. In the presence of 2,6-lutidine (Path A), **2.1** converted **2.2** rapidly and completely to benzenesulfonamide **2.3**, nitrogen, and sulfur.

Dithiobenzoic anhydride **2.4** also formed.[21] Thus, while being the base of choice for the thioacid/azide amidation, 2,6-lutidine is ineffective for the thioamide coupling. Piperidinium salts of dithioacids are easy to handle and are stable at room temperature. The piperidine salt of **2.1** also proved stable in solution;[22] however, subsequent addition of **2.2** led to rapid formation of piperidine-derived thioamide **2.5**, as well as **2.3**, nitrogen, and sulfur (Path B). **Table 2.1**. summarizes a series of experiments that more completely probe this outcome. Piperidinium dithiobenzoate **2.7** (1.3 equiv) formed small quantities of **2.5** (10%) in methanol at room temperature over the course of 30 min. In the presence of azide **2.2**, piperidinium dithiobenzoate effected the nearly quantitative conversion to the sulfonamide (**2.3)** as well as the formation of significantly more **2.5** than expected under these conditions. As the amount of sulfonazide was increased, the amount of **2.3** and **2.5** isolated from the reaction mixture increased as well, while the relative ratio of **2.3**:**2.5** remained 1:1. These experiments establish that the conversion of piperidinium dithiobenzoate to **2.5** is stoichiometric in sulfonyl azide **2.2** and produces an equivalent amount of **2.3**. In contrast to the weakly basic 2,6-lutidine and the highly nucleophilic piperidine, triethylamine promoted the smooth coupling of **2.1** with **2.2** to give *N*-benzenesulfonyl thioamide **2.7** in excellent yield (Path C, Scheme 2.2).

---

[21] Kato, S; Masumoto, H.; Kimura, M.; Murai, T.; Ishida, M. *Synthesis*, **1987**, 304.

[22] Tani, K.; Hanabusa, S.-i.; Kato, S.; Mutoh, S.-y.; Suzuki, S.-i.; Ishida, M. *J. Chem. Soc., Dalton Trans*. **2001**, 518.; Kato, S.; Ono, Y.; Miyagawa, K.; Murai, T.; Ishida, M. *Tetrahedron Lett*. **1986**, *27*, 4595.; Kato, S.; Shibahashi, H.; Katada, T.; Takagi, T.; Noda, I.; Mizuta, M.; Goto, M. *Liebigs Ann. Chem*. **1982**, *7*, 1229.

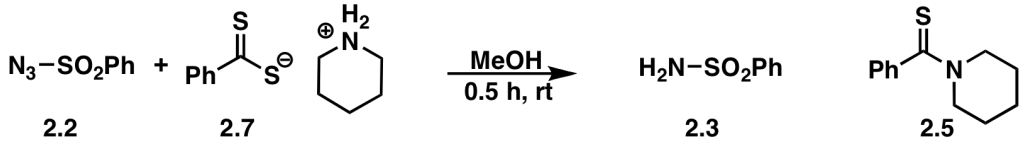

2.2 2.7 2.3 2.5

Eqv.	yield (%)	
0.0	10%	0.0%
0.25	34%	95%
0.5	54%	93%
0.75	63%	83%
1.0	62%	62%

Table 2.1: Linear Intermediate Interception Study

Having determined that triethylamine displays the desired properties for the coupling, we moved to develop a dithioacid/azide thioamidation method. We generated the dithioacid from the corresponding Grignard reagent and carbon disulfide. Exposure of the dithioacid to the azide in the presence of triethylamine gave the desired thioamide. Examples of these thioamidations are shown in Table 2.2. The most convenient method was to generate the dithioacid under standard conditions described above followed by an aqueous acid workup in order to remove magnesium salts, and then sequential treatment of the dithioacid with triethylamine then azide. By using a slight excess of dithioacid (1.3 equiv crude), triethylamine (2 equiv), and azide (1.0 equiv) in a suitable solvent at 0 °C for 1–4 h, the desired thioamide could be obtained in good overall yield.

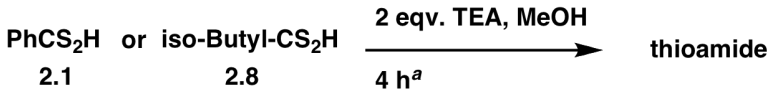

azide	dithio acid	conditions	yield[d] (%)
N_3-SO_2Ph	2.1	a	83
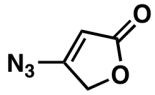	2.1	a	85
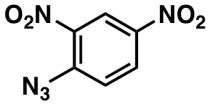	2.1	a	75
N_3-Bn	2.1	b	56
N_3-SO_2Ph	2.8	a	93
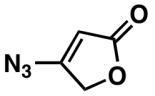	2.8	a	67
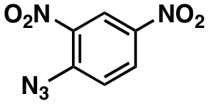	2.8	a	75
N_3-Bn	2.8	b	36
N_3-SO_2Ph	2.1	c	86

[a] Conditions: MeOH, 0° C-rt, 4 h
[b] Conditions: $CHCl_3$, reflux, 36 h
[c] Conditions: H_2O, 0° C-rt, 30 min
[d] Yield determined from silica gel chromatography purification.

Table 2.2: Examples of Dithio Acid Thioamidation

As with our thioacid/azide amidation, electron deficient azides react rapidly and efficiently with dithioacids, while electron rich azides require heating for prolonged periods in order to achieve good conversions. Thionation of amides *N*-substituted with electron withdrawing groups, such as *e.g.* sulfonyl, often require heating at 150 °C with phosphorous pentasulfide or exposure to Lawesson's reagent in refluxing toluene for

24 h.[23]

Section 2.2: Mechanistic Framework

The mechanistic framework in Scheme **2.2** readily rationalizes the reaction outcomes in Scheme **2.1**. In the presence of base, the thiolate adds to the terminal nitrogen of the azide forming a linear anionic intermediate in equilibrium with the neutral species (**I/II**). Intermediate **I** would be expected to exhibit active ester character. The weaker base, lutidine, should favor the protonated form to a much greater degree than piperidine or triethylamine.

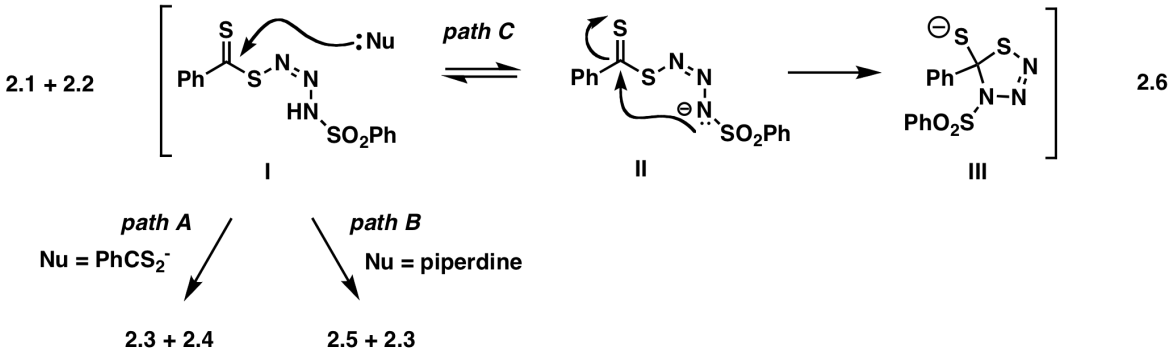

Scheme 2.2: Thioamide Mechanistic Rationale

Nucleophilic attack of a second molecule of dithioacid at the thiocarbonyl of **I** should result in fragmentation to **2.3, 2.4**, nitrogen, and sulfur as shown (path A). In principle, **I** could be intercepted by 2,6-lutidine and form the *N*-thioacyllutidinium species, which

[23] Walter, W.; Roehr, A. *Liebigs Ann. Chem.* **1975**, 41.; Cava, M. P.; Levinson, M. I. *Tetrahedron* 1985, 41, 5061.; Santilli, A. A.; Scotese, A. C.; Morris, R. L.; Schiehser, G. A.; Teller, D. M.; Nielsen, S. T.; Strike, D. P. *J. Med. Chem.* **1988**, *31*, 1480.; Brillon, D. *Synth. Commun.* **1990**, *20*, 3085.; Jesberger, M.; Davis, T. P.; Barner, L. *Synthesis* **2003**, 1929.; Meadow, F. R.; Cavagnol, J. C. *J. Org. Chem.* **1951**, *16*, 1582.

could then be attacked by dithiobenzoate **2.1** to give the observed products. However, intermediates this type are not observed in the parent thio acid/azide amidation probably due to the increased reactivity of the carbonyl versus the thio carbonyl.[24] This pathway would be less relevant in the presence of stronger bases; however, the active ester could undergo nucleophilic acyl substitution by the highly nucleophilic piperidine (path B). Addition of piperidine to **I** followed by collapse of the tetrahedral intermediate would give the observed products.[25] In this way, benzenesulfonyl azide appears to serve as a stoichiometric activator of a dithioacid, and piperidine appears sufficiently nucleophilic to intercept the linear intermediate (**I/II**). As shown in path C, triethylamine enforces formation of the anion (**I→II**) but does not otherwise interfere and thus enables **II** to cyclize to thiatriazoline **III**. The thiatriazoline then undergoes fragmentation, either stepwise or in a concerted retro [3+2] mechanism,[26] to give the thioamide **2.6**.

Additional control experiments support this mechanistic framework. Benzenesulfonamide **2.3** does not react under these conditions with dithiobenzoic acid **2.1** or dithiobenzoic anhydride **2.4**, even in the presence of triethylamine,[27] thus demonstrating that the dithioacid/azide amidation does not proceed through an amine intermediate. Examination of the reaction profile by ESI-MS revealed the presence of a species that corresponds to a 1:1 adduct of dithioacid:azide. ESI-MS/MS of this species indicates loss

---

[24] Wiberg, K. B.; Wang, K. B.; Miller, S. J. Puchlopek, A. L.; Bailey, W. F. Fair, J. D. *J. Org. Chem.* **2009**, *74*, 3659.

[25] The alternative mechanism, wherein dithiobenzoic anhydride is formed as in path A and then reacts with piperidine to give the observed acylation product (5) and benzenesulfonamide (3), can be ruled out, as **2.3** is not generated in significant quantities in the presence of triethylamine (see path C), and **2.3** is not acylated by dithiobenzoic anhydride.

[26] Lieber, E.; Oftedahl, E.; Rao, C. N. R. *J. Am. Chem. Soc.* **1963**, *28*, 194.; Loock, E. V.; Vandensavel, J.-M.; L'abbe, G.; Smets, G. *J. Org. Chem.* **1973**, *38*, 2916.; L'abbe, G.; Verhelst, G.; Yu, C.-C.; Toppet, S. *J. Org. Chem.* **1975**, *40*, 1728.; L'abbe, G. *Angew. Chem., Int. Ed. Engl.* **1980**, *19*, 276.; L'Abbe, G.; Dekerk, J. P.; Martens, C.; Toppet, S. *J. Org. Chem.* **1980**, *45*, 4366.; L'abbe, G.; Brems, P.; Albrecht, E. J. *Heterocycl. Chem.* **1990**, *27*, 1059.; Wentrup, C.; Kambouris, P. *Chem. Rev.* **1991**, *91*, 363.; Adam, W.; Bargon, R. M. *Eur. J. Org. Chem.* **2001**, 1959.

[27] We believe the lack of *N*-acylsulfonamide formed in this reaction rules out the role of triethylamine as a nucleophilic catalyst in the parent reaction.

of fragments corresponding to phenyl (77), benzenesulfonyl (141), sulfhydryl (33), and nitrous sulfide (60), consistent with the structural assignment of thiatriazoline **III**.

The thioacid/azide amidation may prove to be broadly applicable for the synthesis of complex amides. The reactivity principles deduced from the amidation provided the conceptual basis for this new route to thioamides. We have shown that dithioacids couple efficiently with electron deficient azides to give thioamide products under very mild conditions. The dithioacid/azide thioamidation does not proceed through an amine intermediate, but rather through a thiatriazoline. The attributes of the thioacid/azide amidation, namely the high degree of chemoselectivity, solvent compatibility, excellent coupling efficiency of electron deficient azides, and the non-toxic byproducts nitrogen and sulfur, appear to be retained for thioamide synthesis as well.

Chapter 3: The Mechanism of Thio Acid Amidation

Section 3.1: Introduction to Amide Coupling

It is of considerable interest to develop new amidation reactions that can accommodate a broader range of substrates than conventional amidation and that are compatible with a wider range of reaction conditions, including *in vitro* and *in vivo* studies.[28] Systematic mechanistic and methodological investigations have shown that chemoselectivity, solvent compatibility, and rate of intermolecular coupling limit conventional intermolecular amidation. One alternative, and the basis for most new methods, is to apply a nonacylation reaction to bring the amine, or amine equivalent, and the acyl group into proximity.[29] To be broadly effective, the nonacylating reaction must be chemically orthogonal to the functionality of the coupling partners and the solvent. This prior-capture strategy has the potential to facilitate amide bond formation by rendering the amidation reaction intramolecular. If the prior-capture reaction is faster than conventional intermolecular amidation and leads to a favorable geometry for a subsequent intramolecular amidation,[30] then the overall rate of amide formation by prior-capture may be significantly faster than conventional amidation. Native peptide ligation,[31] a powerful amidation reaction, is

---

[28] Wieland, T., Bodanszky, M.; *World of Peptides: A Brief History of Peptide Chemistry*; Springer-Verlag: New York, 1991.

[29] (*a*) Prescher, J. A.; Bertozzi, C. R. *Nat. Chem. Biol.* **2005**, *1*, 13. (*b*) Saxon, E.; Bertozzi, C. R. *Science* **2000**, *287*, 2007. (*c*) Kochendeoerfer, G. G.; Kent, S. B. H. *Curr. Opin.Chem. Biol.* **1999**, *3*, 665. (*d*) Tam, J. P.; Yu, Q.; Miao, Z. *Biopolymers* **1999**, *51*, 311. (*e*) Humphrey, J. M.; Chamberlin. R. *Chem. Rev.* **1997**, *97*, 2243. (*f*) Kohn, M.; Breinbauer, R. *Angew. Chem. Int. Ed.* **2004**, *43*, 3106. (*g*) Brase, S.; Gil, C.; Knepper, K.; Zimmermann, V. *Angew. Chem., Int. Ed.* **2005**, *44*, 5188. (*h*) Bode, J. W.; Fox, R. M.; Baucom, K. D. *Angew. Chem. Int. Ed.* **2006**, *25*, 1248. (*i*) W.-J. Yoo, C.-J. Li, *J. Am. Chem. Soc.*, **2006**, *128*, 13064. (*g*) Li X, Danishefsky S. J. *J. Am. Chem. Soc.* **2008**, *130*, 5446.

[30] (*a*) Wieland, T.; Bokelmann, E.; Bauer, L.; Lang, H.; Lau, H.; Schafer, W. *Liebigs Ann.* **1953**, *583*, 129. (*b*) Brenner, M.; Zimmerman, J. P.; Wehrmüller, J.; Quitt, P., Hardtmann, A.; Sneider, W.; Beglinger, U. *Helv. Chim. Acta* **1957**, *40*, 1497. (*c*) Kemp, D. S. *Biopolymers* **1981**, *20*, 1793.

[31] Avoidance of steric congestion in the transition state has been shown to be critically important for prior-capture strategies, see (*a*) Kemp, D. S.; Carey, R. I. *J. Org. Chem.* **1993**, *58*, 2216. reviewed in: (*b*) Coltart, D. M. *Tetrahedron* **2000**, *56*, 3449.

chemoselective, can be performed on unprotected peptide segments, and is effective in water. This and related methods rely on amino acid side-chain functionality to facilitate the prior-capture step.[32] Recent reports suggest that methods for the chemical synthesis of fully elaborated post-translationally modified protein targets may soon be within reach.[33] Among the most impressive displays of the advances in this area, the Staudinger ligation has been combined with metabolic engineering to effect post-translational-like modification of a cell-surface protein in an animal model.[34] These advances constitute milestone achievements and are suggestive of the benefits that would accrue if additional methodologies were available. Ideal methods would impose minimal structural requirements upon the coupling partners, and the full range of amide target systems, peptide, non-peptide, and hybrids, would be accessible using reactions that are rapid, selective and produce innocuous byproducts.[35]

Our research toward the development of new reactions that enable the synthesis of complex amides led us to reevaluate the acetylation of alkylazides with thioacetic acid.

---

[32] *C*-terminal thio ester peptide segments couple with *N*-terminal cysteine peptide segments to form an amide. Thus, trans-thioesterification is a suitably fast prior-capture reaction. Intramolecular *S*- to *N*-acyl transfer via a five-membered transition state constitutes a geometry that is not overly congested. Consequently, the chemical synthesis of proteins and protein-like compounds of approximately one hundred residues is feasible, see: (*a*) Dawson, P. E.; Muir, T. W.; Clark-Lewis, I.; Kent, S. B. *Science* **1994**, *266*, 776. (*b*) Muir, T.; Dawson, P. E.; Kent, S. B. H. *Methods Enzymol.* **1997**, *289*, 266. See also, ref 2c. Compare with: (*c*) Gutte, B.; Merrifield, R. B. *J. Am. Chem. Soc.* **1969**, *91*, 501. (*d*) Denkewalter, R. G.; Veber, D. F.; Holly, F. W.; Hirschmann, R. *J. Am. Chem. Soc.* **1969**, *91*, 502. (*e*) Yajima, H.; Fujii, N. *J. Chem. Soc., Chem. Commun.* **1980**, *3*, 115.

[33] Alternatives to cysteine include: (*a*) Offer, J.; Dawson, P. E. *Org. Lett.* **2000**, *2*, 23. (*b*) Hacking, T. M.; Griffin, J. H.; Dawson, P. E. *Proc. Natl. Acad. Sci. USA* **1999**, *96*, 10068. (*c*) Canne, L. E.; Bark, S. J.; Kent, S. B. H. *J. Am. Chem. Soc.* **1996**, *118*, 5891. Alternatives to native amide linkages have been explored and reviewed, see ref 2d and (*d*) Liu, C.-F.; Tam, J. P. *Proc. Natl. Acad. Sci. U.S.A.* **1994**, *91*, 6584. See also: (*e*) Tolbert, T. J.; Wong, C. H. *J. Am. Chem. Soc.* **2000**, *122*, 5421. (*f*) Hohsaka, T.; Ashizuka, Y.; Sasaki, H.; Murakami, H.; Sisido, M. *J. Am. Chem. Soc.* **1999**, *121*, 12194. (g) Cornish, V. W.; Mendel, D.; Schultz, P. G. *Angew. Chem., Int. Ed. Eng.* **1995**, *34*, 621. See also: (*h*) Leleu, S.; Penhoat, M.; Bouet, A.; Dupas, G.; Papamicaël, C.; Marsais, F.; and Levacher, V. *J. Am. Chem. Soc.* **2005**, *127*, 15668

[34] Prescher, J. A.; Dube, D. H.; Bertozzi, C. R. *Nature* **2004**, *430*, 873.

[35] For example, Click Reactions: (a) Lewis, W. G.; Green, L. G.; Grynszpan, F.; Radic, Z.; Carlier, P. R.; Taylor, P.; Finn, M. G.; Sharpless, K. B. *Angew. Chem., Int. Ed.* **2002**, *41*, 1053. (b) Demko, Z. P.; Sharpless, K. B. *Angew. Chem., Int. Ed.* **2002**, *41*, 2110. (c) Kolb, H. C.; Finn, M. G.; Sharpless, K. B. *Angew. Chem., Int. Ed.* **2001**, *40*, 2004.

This reaction was first noted in the literature in 1980.[36] Subsequently, thioacetic acid was shown to be generally useful for the conversion of organic azides to the corresponding acetamide products when applied as solvent or cosolvent.[37] It was proposed that adventitious hydrogen sulfide reduces the azide to the corresponding amine, which undergoes rapid acetylation with thioacetic acid to regenerate hydrogen sulfide and to allow the cycle to be repeated. Hence, thioacetic acid-induced formation of amides from azides was postulated to be a very rapid, but otherwise conventional, nucleophilic acyl substitution reaction. A few observations inconsistent with this mechanism have been noted,[38] but perhaps since the reaction appeared to be a conventional amidation, no mechanistic studies had been disclosed.

We, however, demonstrated that the reaction of thio acids and azides must proceed through a mechanism different than that originally suggested. Azide substrates participate in the reaction, whereas the corresponding amines fail to couple: hence amines are not intermediates. Interestingly, the reaction is accelerated by the presence of base. Unlike other amidation, the thio acid/azide coupling can be used to readily fashion amides from electron-deficient azides and hence from nonnucleophilic amine equivalents.[39] Indeed, a variety of thio acids, including *N*-protected α-amino thio acids, chemoselectively couple with organic azides bearing electron-withdrawing or electron-

---

[36] Hakimelahi, G. H.; Just, G. *Tetrahedron Lett.* **1980**, *21*, 2119.

[37] (*a*) Rosen, T.; Lico, I. M.; Chu, T. W. *J. Org. Chem.* **1988**, *53*, 1580. (*b*) Rakotomanomana, N.; Pavia, J.-M. *Carbohydr. Res.* **1990**, *197*, 318.

[38] (*a*) Paulsen, H.; Bielfeldt, T.; Peters, S.; Bock, K. *Liebigs Ann. Chem.* **1994**, 369. (*b*) Elofsson, M.; Salvador, L. A.; Kihlberg, J. *Tetrahedron* **1997**, *53*, 369. (*c*) Marcaurelle, L. A.: Bertozzi, C. R. *J. Am. Chem. Soc.* **2001**, *123*, 1587. (*d*) Chou, S.-S. P.; Chow, T. J.; Hsu, C.-H.; Yang, C.; Long, S.-H.; Lin, C.-D. *J. Chem. Soc., Perkin Trans. 1* **1997**, 1691. (*e*) McKervey, M. A.; Sullivan, B. O.; Myers, P. L.; Green, R. H. *J. Chem. Soc., Chem. Commun.* **1993**, 94. (*f*) Yamashiro, D.; Blake, J. *Int. J. Pept. Prot. Res.* **1981**, *18*, 383.

[39] Amidation of electron-deficient azides via the Staudinger reaction appears to be very slow compared to electron-rich azides, opposite the trend observed for the thio acid/azide amidation, see: Lin, F. L.; Hoyt, H. M.; van Halbeek, H.; Bergman, R. G.; Bertozzi, C. R. *J. Am. Chem. Soc.* **2005**, *127*, 2686.

donating functionality. For example, *N*-acyl sulfonamides, *N*-aryl amides, enamides, unprotected hydroxy amides, and β-N-amidoglycosides are readily prepared in solvents ranging from chloroform to water and give rise to amides ranging from sensitive alkyl amides to safety-catch linkers and fluorescently labeled amino acid derivatives.[40] The reaction also represents a traceless ligation method, since as with conventional amidation, the substrate requirements are minimal, the reaction can be fast, and only the native amide function remains after coupling.[41] Hence the thio acid/azide amidation appears to be a potentially useful synthetic method.

Section 3.2: Mechanistic Studies

The transformation, however, was not well understood on a mechanistic level. We set out to gain mechanistic insight into the coupling of thio acids with electron-poor and electron-rich azides in order to better understand the reaction, further improve the methodology, and facilitate the discovery of mechanistically related transformations. Two frameworks consistent with the available data are outlined below in Scheme 3.1, and were advanced as models of the reaction mechanism. The proposals, Path 1 and Path 2, have in common the involvement of a thiatriazoline **3.4** as opposed to an amine intermediate. They differ in the exact timing of the bond formation process.[42] While Path 2 forms a thiatriazoline in a

---

[40] (a) Wu, X.; Hu, L. *Tetrahedron Lett*. **2005**, *46*, 8401. (b) Knapp, S.; Darout, E. *Org. Lett*. **2005**, *7*, 203. (c) Fazio, F.; Wong, C.-H. *Tetrahedron Lett*. **2003**, *44*, 9083. (d) Zhu, X.; Pachamuthu, K.; Schmidt, R. R. *Org. Lett*. **2004**, *6*, 1083.

[41] (a) Merkx, R.; Brouwer, A. J.; Rijkers, D. T. S.; Liskamp, R. M. J. *Org. Lett*. **2005**, *7*, 1125. (b) Barlett, K. N.; Kolakowski, R.; Katukojvala, S.; Williams, L. J. *Org. Lett*. **2006**, *8*, 823.

[42] A third path not shown in Scheme 1 can be advanced: Formation of the carbon nitrogen bond in *Path 2* could be faster than formation of the sulfur nitrogen bond. The Schmidt amidation is mechanistically analogous to this proposal; however, since azides bearing electron-withdrawing groups react with thio acids more rapidly than azides bearing electron-donating functionality, it seems unlikely that this path represents a generally relevant mechanism. If, however, the mechanism were substrate dependent, this possibility should not be ignored and might be promoted by a suitable additive, including metals or acid.

single [3+2] cycloaddition step, the first step of Path 1 is intermolecular coupling between the sulfur of the thio acid and the terminal nitrogen of the azide and is reminiscent of a prior-capture reaction. The second step of Path 1 is analogous to the S- to *N*-acyl transfer **3.3** of the most powerful protein ligation strategies advanced to date and proceeds via a five-membered transition state. Thiatriazoline **3.4** is proposed as the key intermediate for both paths, which could decompose either stepwise or in a single retro-[3+2][60] reaction to give the amide and the observed nitrogen and sulfur products.[43] Protonation in this base-promoted reaction may occur either before or after thiatriazoline conversion to amide and is represented as occurring prior to amide formation. Herein, we disclose experimental

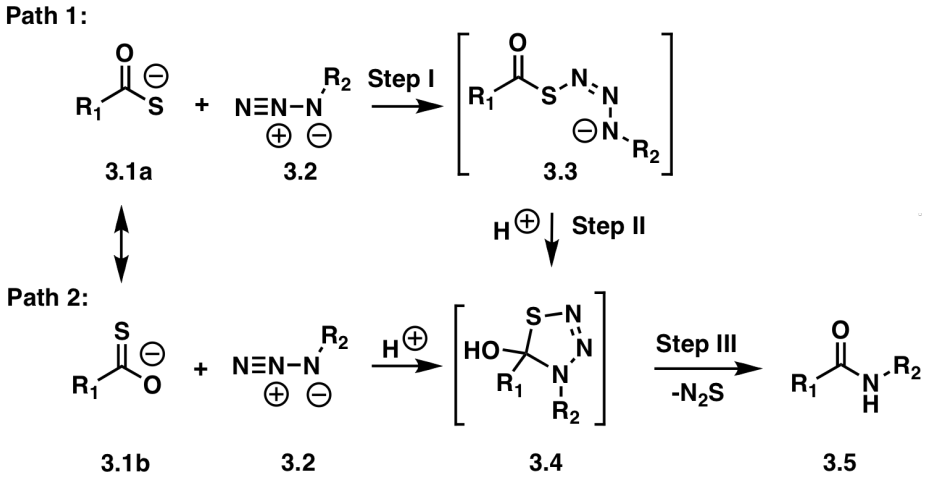

and computational data consistent with Path 1 for electron-deficient azides and Path 2 for electron-rich azides.

Scheme 3.1: Proposed Mechanistic Framework for Thio Acid/Azide Amidation

[43] During the reaction there is a significant amount of bubbling/off-gassing which is attributed to nitrogen. At the end of the reaction elemental sulfur is deposited at the bottom of the reaction flask and has been filtered, weighed and shown to stoichiometrically correlate with the reaction stoichiometry.

Kinetic studies on both classes of azide are summarized in Table 3.1. We consider benzene sulfonyl azide representative of electron-deficient azides and benzyl azide representative of electron-rich azides.[44] While electron-deficient azides react much more rapidly with thio acids than electron-rich azides, both classes of reaction are accelerated by addition of base. In the reaction of thiobenzoic acid and sulfonyl azides, 1 equiv. of lutidine increased the reaction rate by a factor of 80; similar rate acceleration was observed for benzyl azide. The reactions are first order in thio acid and first order in azide. Variable temperature kinetic analysis revealed similar activation parameters for the two classes of azide, with benzyl azide having higher enthalpies and entropies of activation.

Azide	E_a *(kcal mol^{-1})*	$\Delta H^{\ddagger}$*(kcal mol^{-1})*	$\Delta S^{\ddagger}$(eu)
$PhSO_2N_3$	11.3 ±0.1[b]	10.69 ±0.1	-32 ±0.2
BnN_3	11.7 ±0.2	11.04 ±0.2	-45 ±0.2

R = SO_2Ph $\quad k_{obs} = 5.7 \times 10^{-3}\ M^{-1}\ S^{-1} \pm 0.1$ @ 21 ºC

R = CH_2Ph $\quad k_{obs} = 4.5 \times 10^{-6}\ M^{-1}\ S^{-1} \pm 0.1$ @ 21 ºC

[a] Activation parameters were determined by variable temperature pseudo first-order kinetics and fit to the model: *rate* = $k_{obs}[PhCOSH][N_3R]$. Arrhenius plot correlation coefficients ≥ 0.999. [b]σ for the activation parameters was estimated via a least-squares regression method of the corresponding Arrhenius plots.[45] For experimental details and plots, see experimental for chapter 3, pg 135.

44 Benzyl azide represents alkyl azides in general, the amide products of which are typical of most amidation reactions. The amidation products of sulfonyl azides, N-acyl sulfonamides, are also useful intermediates in medicinal chemistry as well as in solution and solid support-based safety-catch chemistry. See: (*a*) Kenner, G. W. *Chem. Commun*. **1971**, 636. (*b*) Backes, B. J.; Ellman, J. A. *J. Org. Chem*. **1999**, *64*, 2322. (*c*) Shin, Y.; Winans, K. A.; Backes, B. J.; Kent, S. B. H.; Ellman, J. A.; Bertozzi, C. R. *J. Am. Chem. Soc*. **1999**, *121*, 11684. (*d*) Ingenito, R.; Dreznjak, D.; Guffler, S.; Wenschuh, H.; *Org. Lett*. **2002**, *4*, 1187. (*e*) Mclean, D.; Hale, R.; Chen, M. *Org. Lett*. **2001**, *3*, 2977. (*f*) Abbate, F.; Supuran, C. T.; Scozzafava, A.; Orioli, P.; Stubbs M. T.; Klebe, G. A.; Jones, B. R. *J. Med. Chem*. **2002**, *45*, 3583.

45 *Data Reduction and Error Analysis for the Physical Sciences*; Beving, P. R.; McGraw-Hill, Inc.: New York, 1969.

Table 3.1. Amidation Activation Parameters with Thiobenzoic Acid and Azides

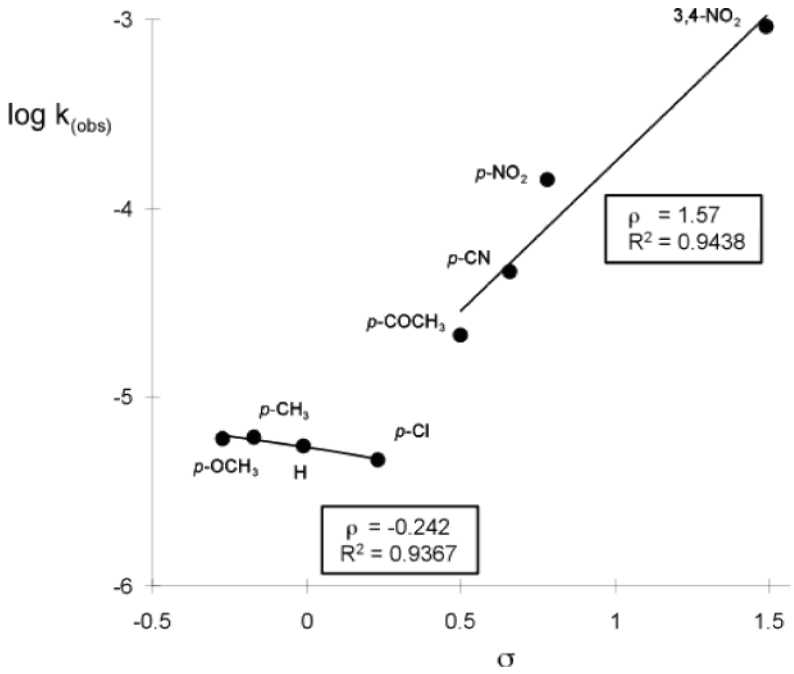

Figure 3.1: Hammett Correlation Study Hammett correlation of phenyl azides. Rate determined by monitoring UV disappearance of thiobenzoic acid. Rate is weakly dependent on $\sigma < 0.3$. Rate increases markedly with increasing $\sigma > 0.4$.

We also conducted a Hammett correlation study with substituted phenyl azides. As shown in Figure 3.1, there is a distinct break in the σ plot. Two lines model the data well, with $\sigma < 0.3$ substituents fitted to $\varrho = -0.242$ ($R^2 = 0.9367$) and $\sigma > 0.4$ fitted to $\varrho = 1.57$ ($R^2 = 0.9438$). Within the limit $\sigma < 0.3$, the $\varrho = -0.242$ plot is indicative of a reaction pathway that is relatively insensitive to azide electronics, whereas the pathway represented by $\varrho = 1.57$ is highly sensitive, within the limit $\sigma > 0.4$, to the electronic properties of theazide. Taken together, the nonlinear Hammett correlation provides strong

evidence that the mechanism for electron-poor azides is different from the mechanism for relatively electron-rich azides.

To gain further insight, we sought to intercept the proposed intermediate of type **3.3**. If Path 1 represents the relevant mechanism, electron-deficient azides should undergo bimolecular coupling, step **I**, faster than electron-rich azides; however, intramolecular cyclization, step **II**, should be comparatively slow. The linear intermediate might be relatively long-lived for electron-deficient azides, and thus it might be possible to intercept **3.3** with a good nucleophile. For example, thio acid coupling with a sulfonazide in the presence of an amine nucleophile might give amine-derived acylation products in addition to, or instead of, the expected *N*-acyl sulfonamide. Indeed, the linear intermediate could be intercepted, as described below and shown in Scheme 3.2.

When benzene sulfonazide **3.7** was added to a solution of piperidinium thiobenzoate **3.6** in methylene chloride that did not have excess piperidine, *N*-benzoyl sulfonamide **3.10** was produced in near quantitative yield in 30 min, as expected Scheme 3.2. Trace amounts of amide **3.8** and benzene sulfonamide **3.9** were measurable, but insignificant. In contrast, when benzene sulfonazide **3.7** was added to piperidinium thiobenzoate **3.6** in the presence of excess piperidine, amide **3.6** was produced in 54% yield.[46] In addition to molecular sulfur and nitrogen, the reaction also gave benzene sulfonamide in 45% yield and produced *N*-benzoyl sulfonamide in only 50% yield.[47] It is important to note that amine salts of thiobenzoic acid are relatively stable in solution and

[46] (*a*) For further experimental data, procedures, and characterization see Supporting Information. (*b*) Related observations were noted for the reaction of dithio acids with azides. See: (*c*) Kolakowski, R. V.; Shangguan, N.; Williams, L. J. *Tetrahedron Lett*. **2006**, *47*, 1163

[47] Similar results were noted for related couplings of electron deficient azides (e.g. 4-nitrophenyl azide), but not for electron-rich azides (data not shown).

that piperidinium thiobenzoate **3.6** in methylene chloride gave only trace amounts of amide product **3.8** over the course of 30 min. Similar results were noted for **3.6** in 5.0 M piperidine. Therefore, the formation of amide **3.8** is induced by addition of benzene sulfonazide. The simplest interpretation of these results invokes **3.11** as an active ester-like species formed in solution in the course of the thio acid/azide amidation with electron-deficient azides Scheme 3.2.

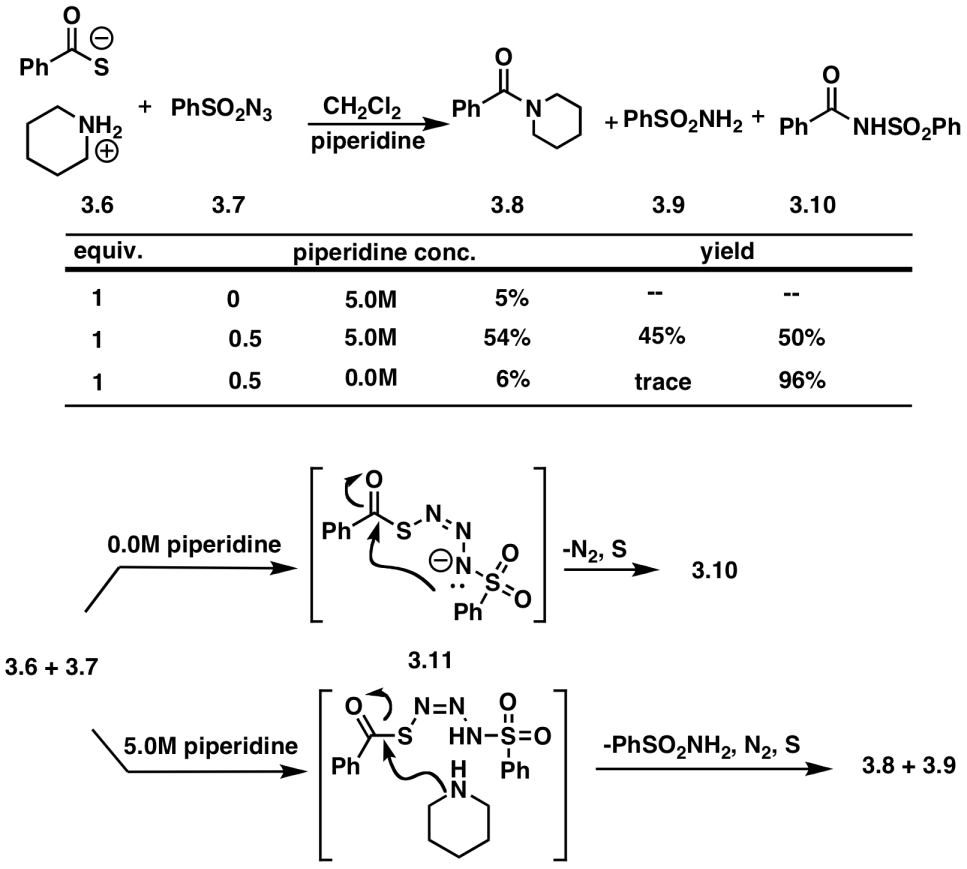

equiv.	piperidine conc.		yield		
1	0	5.0M	5%	--	--
1	0.5	5.0M	54%	45%	50%
1	0.5	0.0M	6%	trace	96%

Scheme 3.2: Linear intermediate interception study.

In light of the known propensity of thionoesters to couple with organic azides at elevated temperatures (vide infra), we examined the viability of Path 2 under our more

mild conditions. If Path 2 represents the primary mechanistic route to amide product, conditions that favor the thiono form of a thio acid could accelerate the reaction. Addition of trimethylsilyl triflate to thiobenzoic acid and triethylamine or lutidine effected complete conversion to trimethylsilyl thionobenzoate **3.13**, Scheme 3.3.[48] Subsequent treatment of **3.13** with benzyl azide or benzene sulfonazide under our original amidation conditions gave only trace amounts of the corresponding amide products.[49] Importantly, if trimethylsilyl triflate is omitted from these reactions, the amide products are obtained in

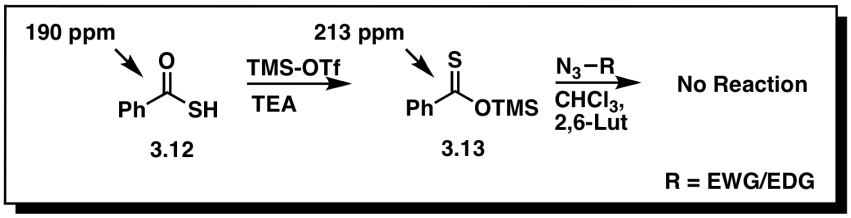

excellent yield. These data indicate that under these conditions either minimal steric interactions or the retention of the anionic character of **3.1**, or both, are required for amidation.

Scheme 3.3. Silyl Thionoester Reaction with Organic Azides.

Careful monitoring of thio acid/azide reactions by standard spectroscopic techniques yielded no measurable intermediates; however, several intriguing observations were documented with electrospray mass spectrometry (Scheme 4). Reaction mixtures of thio acids **3.14a–c** and electron-rich or electron-poor azides **3.15a–d** gave ionic adducts

[48] For synthesis and characterization of trimethylsilyl thionobenzoate, see: (a) Kato, S.; Wataru, A.; Mizuta, M.; Ishii, Y. *Bull. Chem. Soc. Jpn.* **1973**, *46*, 244. See also: (b) Perlmutter, P.; Rose, M.; Vounatos, F. *Eur. J. Org. Chem.* **2003**. (c) Shalaby, M. A. and Rapoport, H. *J. Org. Chem.* **1999**, *64*, 1065.

[49] If the thio acid is not distilled or sparged with nitrogen prior to reaction, false coupling results may be observed, which we have found are an indication of the presence of impurities and/or incomplete formation of the thionoester.

corresponding to a 1:1 ratio of thio acid:azide. ESI–MS/MS revealed that these species fragment uniformly. Specifically, the loss of fragments corresponding to R_1, R_2, OH, and N_2S were readily apparent for each set of coupling partners, regardless of the nature of the azide or complexity of the thio acid.

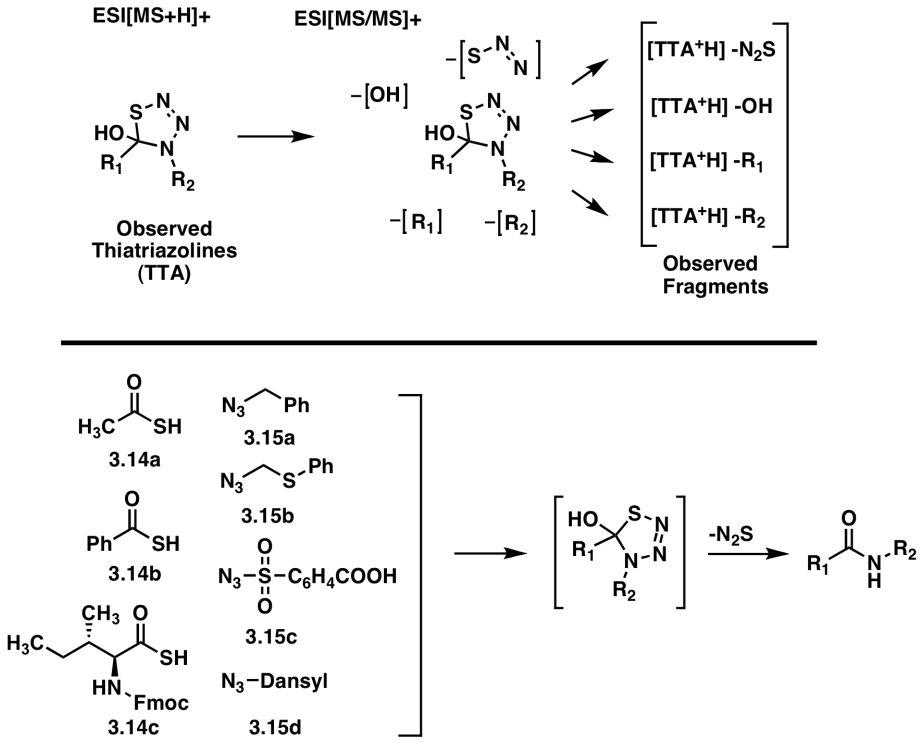

Scheme 3.4. ESI Analysis of Thiatriazolines.

These data are inconsistent with linear structures of type **3.3** and isomeric thiatriazoline **3.16 (**Figure 3.2) but are consistent with a cyclic intermediate corresponding to a thiatriazoline of type **3.4**.

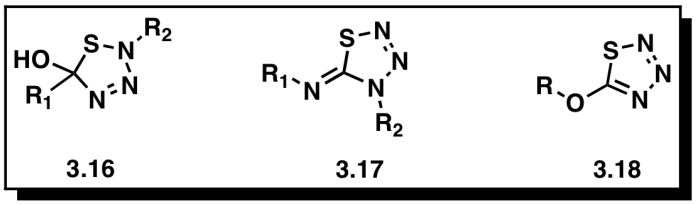

Figure 3.2 Related heterocycles.

We also examined the potential energy surfaces of the reactions of thioacetate ion and thioacetic acid with methane sulfonazide and methyl azide using Density Functional (DFT) calculations in collaboration with Dr. Ronald Sauers. The mechanism was found to be dependent on the electronic character of the azide and protonation state of the thio acid. As outlined in Scheme 1, Path 1 is found to be favored for the reaction with methane sulfonazide and thioacetate. Path 2 is favored for the reaction of methyl azide and thioacetate. In contrast, Path 2 is preferred for both azides when the coupling partner is thioacetic acid. Figures 3.3 and 3.4 show computed stationary points for these reactions.

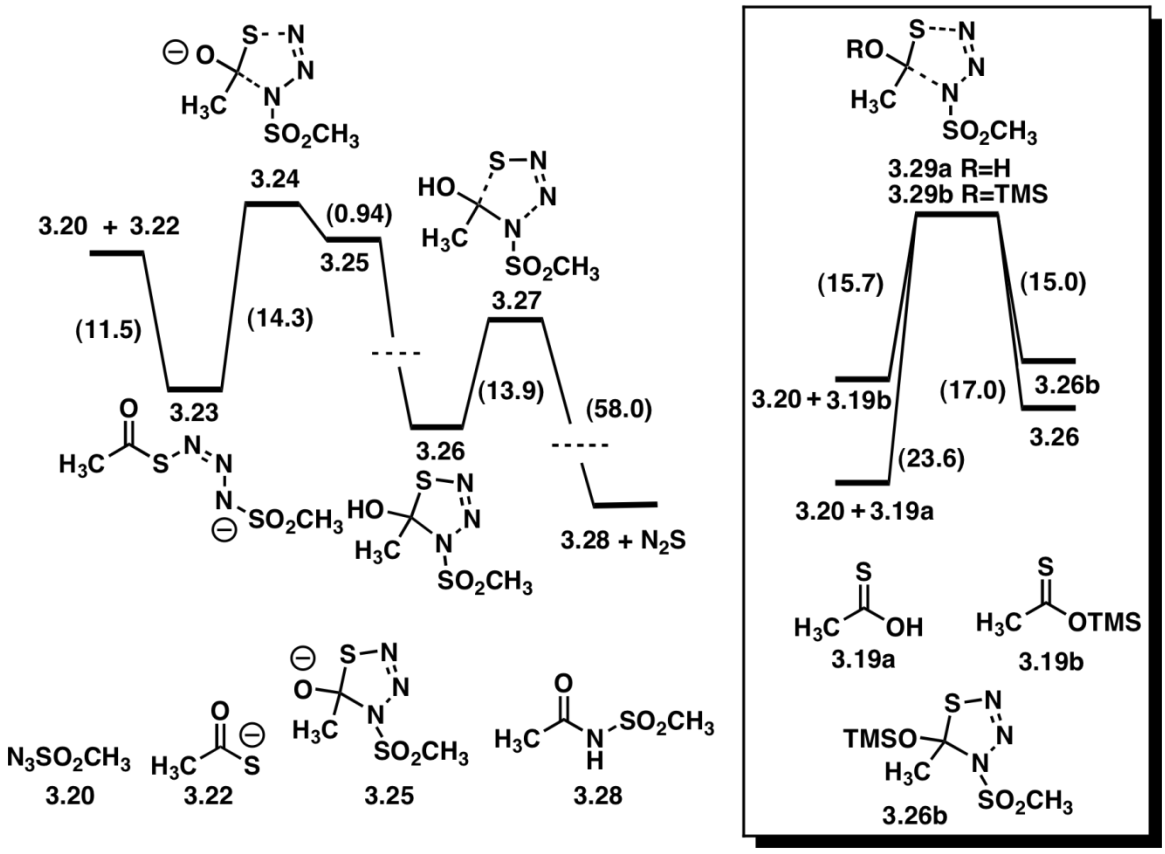

Figure 3.3: DFT Potential Energy Surface for Electron Withdrawing Azides

Relative enthalpies (kcal/mol) for methane sulfonazide reactions at 298.15 K in simulated acetone**.**

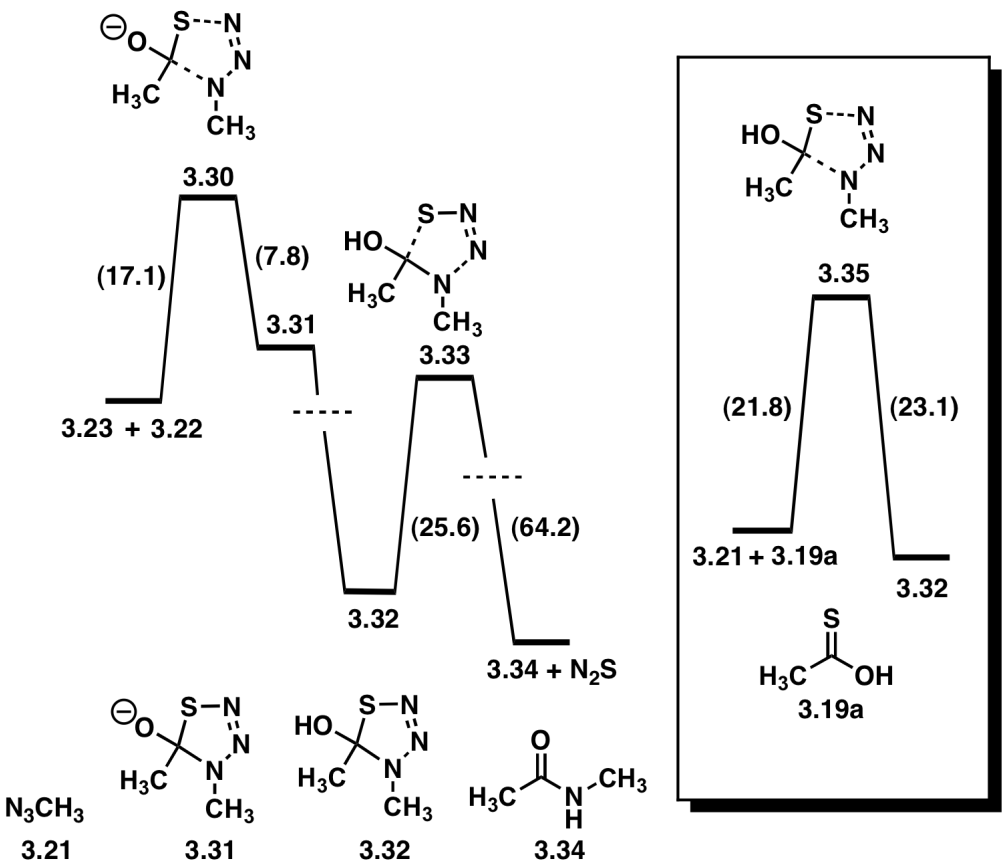

Figure 3.4: DFT Potential Energy Surface for Electron Donating Azides

Relative enthalpies (kcal/mol) for methyl azide reactions at 298.15 K in simulated acetone.

In Figure 3.3 we compare the reactions of electron-deficient methane sulfonazide **3.20** with thioacetate **3.22** and thioacetic acid (depicted as thiono tautomer **3.19a**, inset). Both systems produce thiatriazoline **3.26** and subsequently undergo retro-[3+2] cycloaddition to produce nitrous sulfide and amide **3.38**. The detailed pathways are found to be quite different, however. Thioacetate **3.22** adds to methane sulfonazide **3.20** to form a stable linear adduct **3.23**, which is 11.5 kcal/mol lower in energy. Transition structure **3.24** connects this intermediate with anionic thiatriazoline **3.25** as shown by intrinsic

reaction coordinate (IRC) calculations. At this stage, protonation of the unstable anion **3.25** leads to intermediate **3.26**, which ultimately produces **3.28** and nitrous sulfide via retro-[3+2] cycloaddition transition structure **3.27**. In contrast, thio acetic acid **3.19a** undergoes direct [3+2] cycloaddition with methane sulfonazide **3.20** via transition structure **3.29a** to form thiatriazoline **3.26** (see inset), a path that poses a significantly higher barrier compared to **3.24**. This pathway is supported by IRC calculations, which link **3.29a** to **3.19a** and **3.20** to thiatriazoline **3.26**.

The reaction of **3.20** with the related *O*-trimethylsilyl acetate **3.19b** was also studied computationally (Figure 3.3, inset). The activation barrier computed for the concerted cycloaddition step to produce silyl thiatriazoline **3.26b** was found to be 15.7 kcal/mol, significantly lower than that found for thioacetic acid (23.6 kcal/mol). As before, thiatriazolines **3.26** and **3.26b** were shown to undergo retro-[3+2] cycloadditions with barriers of 13.9 kcal/mol and 15.8 kcal/mol, respectively.

Figure 3.4 describes the related chemistry of reactions between methyl azide with thioacetic acid and thioacetate. Examination of the coupling of thioacetate **3.22** with comparatively electron-rich methyl azide **3.21** shows that the reactants undergo [3+2] cycloaddition via transition structure **3.30** to form anionic thiatriazoline **3.31**. Although a stable linear adduct was found (not shown), IRC calculations link transition structure **3.30** with **3.31** along with methyl azide **3.21** and thioacetate **3.22**. As expected, protonation of **3.31** is highly favorable and gives thiatriazoline **3.32**, which undergoes retro-[3+2] cycloaddition via transition structure **3.33** to produce amide **3.34** and nitrous sulfide.[50] The coupling of thioacetic acid **3.19a** with methyl azide produces **3.32** directly by way of

[50] Anionic transition states related to **3.33** and leading to **3.34** were not found. This does not preclude retro-[3+2] nor stepwise decomposition pathways of such anionic intermediates.

transition structure **3.35,** Figure 3.4 inset, albeit with a higher activation energy (21.8 kcal/mol) than observed for the anionic counterpart (17.1 kcal/mol). Importantly, IRC calculations also established connectivity between **3.33** and components **3.32**, **3.34** and nitrous-sulfide.

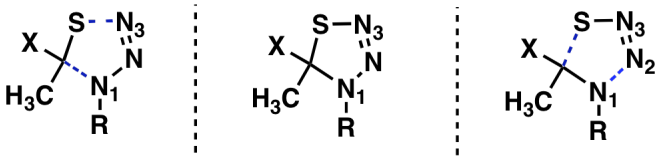

R, X	C-N^1	S-N^3	C-N^1	S-N^3	N^1-N^2	C-S
1. CH_3, O^-	2.29	1.94	1.55	1.77	-	-
2. CH_3, OH	2.09	2.43	1.46	1.78	1.67	2.46
3. CH_3SO_2, O^-	1.73	1.77	1.61	1.76	-	-
4. CH_3SO_2 ,OH	2.20	2.21	1.50	1.88	1.91	2.22

Table 3.2: Key atomic distances. (in Ångstroms) computed for the stationary states discussed above.

Table 3.2 presents key atomic distances computed for the stationary states discussed above. For the alkyl azide (entries 1 and 2), the [3+2] cycloaddition transition states (I) are not symmetric, and the protonation state of the thio acid dictates the relative rate of bond formation. Thus, C–N^1 bond formation is less advanced (2.29 Å) than S–N^3 bond formation for the thiocarboxylate (entry 1). The reverse is observed for the higher energy thio acid transition state (entry 2). Comparison of the C–N^1 and S–N^3 distances of the thiatriazoline-forming transition structure for entry 1 and 3 reveals the distinct

mechanistic differences between electron-deficient azide (entry 3) and the electron-rich azide (entry 1) when coupling with thioacetate. For the sulfonyl azide (entry 3), the S–N^3 bond is already established (1.77 Å) and consequently does not change significantly during C–N^1 bond formation. In contrast, the C–N^1 and S–N^3 distances for entry 2 and entry 4 are similar for the transition structures leading to thiatriazoline and are reflective of analogous [3+2] cycloadditions. As expected, the C–N^1 distances of the anionic thiatriazolines (II) are greater than the C–N^1 distances of the neutral analogues (*cf*. entries 1 and 3 with entries 2 and 4). As with the [3+2] cycloaddition, the [3+2] cycloreversion transition (III) structures are highly asymmetric. This is most pronounced for the methyl azide-derived substrate (entry 2). In this transition structure, the C–S bond is long and weak (2.46 Å), whereas the N^1–N^2 bond is still substantial. Similar though less pronounced trends are observed for the sulfonyl azide-derived substrate.

Section 3.3: Discussion

The above data are in accord with two related but distinctly different mechanisms. The mechanisms differ primarily in the manner and rate at which the common thiatriazoline intermediate forms.

The stoichiometry of the transition states, as shown by kinetic analysis, consists of one molecule of the anion of the thio acid and one molecule of the azide, regardless of the electronic character of the azide. Amidation for the sulfonazide is fast ($k_{obs} = 5.7 \times 10^{-3}$ M^{-1} s^{-1} ± 0.1, 21 °C), whereas the reaction rate for the alkyl azide is comparatively slow. Thus thio acid/azide amidation strongly complements Staudinger amidation, which is slow for

electron-deficient azides and fast ($k_{obs} = 2.5 \times 10^{-3}$ $M^{-1}s^{-1} \pm 0.2$, 20–21 °C) for electron-rich azides.[51]

The enthalpy of activation ($\Delta H^{\ddagger}$) for the more polarized electron-deficient benzene sulfonazide is smaller than that of benzyl azide. Alone this small difference cannot rule out either pathway. The entropy of activation ($\Delta S^{\ddagger}$) is large and negative for both azides, although it is significantly larger in magnitude for the electron-rich benzyl azide. This accounts for the significant differences in rates for the two substrates. It is difficult to further interpret $\Delta S^{\ddagger}$ with certainty. For the coupling of thiobenzoic acid and benzyl azide, the significantly larger $\Delta S^{\ddagger}$ may indicate that electron-rich azides couple via a more entropically demanding bimolecular cycloaddition transition state (Path 2), a rationale that is supported by our computational studies, *vide infra*. Thus, the difference in rate of amidation for the two classes of azides is due primarily to differences in the entropies of activation and is reflective of the fundamentally different mechanisms represented in Scheme 1, Path 1 and Path 2.

The Hammett correlation study of substituted phenyl azides Figure 3.1 is indicative of two mechanisms and is not attributable to a change in rate determining step (e.g. a switch from Step **I** to Step **II** in Path 1, Scheme 1). Crossover from one mechanism to the other occurs near σ 0.35. Thus electron-rich azides and modestly electron-poor azides follow one reaction path, whereas highly electron-deficient azides follow a separate reaction path. The reaction mechanism for comparatively electron-rich azides is otherwise relatively insensitive to azide electronics ($\varrho = -0.242$), findings consistent with a cycloaddition reaction pathway. In contrast, the reaction mechanism for electron-poor

[51] Interpretation of the data is complicated by the sensitivity of $\Delta S^{\ddagger}$ to reaction solvent. *Organic Reactions: Equilibria, Kinetics and Mechanism*; Csizmadia, I. G., Ruff, F., Eds.; Elsevier: New York, 1994.

azides is highly sensitive to azide electronics (ρ = 1.57), findings consistent with a stepwise reaction pathway that proceeds by way of an anionic intermediate that can be stabilized by the electron-withdrawing substituent of the azide.

The chemical trapping experiments Scheme 3.2 strongly support the presence of a linear intermediate for sulfonazides, and by analogy, other fast-reacting electron-deficient azides. At high concentrations of piperidine, benzene sulfonazide induces the rapid conversion of the piperidinium thiobenzoate salt to the piperidine-derived benzamide. These findings are readily rationalized by considering an acyclic precursor with active ester character, such as **3.11** (compare with **3.3**). Thus, at high concentrations the amine nucleophile intercepts the intermediate in an intermolecular reaction with formation of benzene sulfonamide, nitrogen and sulfur, whereas under dilute conditions intramolecular cyclization dominates ultimately leading to the *N*-acyl sulfonamide product.[52] In principle, the failure to intercept the corresponding intermediate of benzyl azide could imply that the linear intermediate formed from benzyl azide cyclizes faster than piperidine interception. The Hammett correlation study provides strong evidence that an alternate mechanism is operative and that the amidation of electron-rich azides may not proceed through a linear intermediate.

Thiatriazolines appear to be intermediates for both classes of azide. ESI has been applied to detect transient species in the Wittig, Mitsunobo, and Staundinger reactions, as well as related tetrahedral intermediates **3.4**.[53] For the full range of thio acids and azides studied, ESI reveals the presence of a 1:1 ratio of adducts derived from the thio acid and

---

[52] These experiments do not directly establish that compounds of type **3** are on the reaction path, since they do not address the important issue of the nature of the equilibrium between intermediates of type **3** and **4**. However, given the computational findings, **3** does indeed appear to be a relevant intermediate.

[53] Although **3.3**, if present, could cyclize under these conditions to give the observed thiatriazoline **3.4** and is not distinguishable via the ESI–MS experiment

the azide coupling partner. The fragmentation pattern of these adducts includes loss of substituents associated with the parent thio acid and azide, as well as loss of hydroxyl and nitrous sulfide see Scheme 3.2. It is difficult to establish unequivocally that ionic species detected in electrospray ionization mass spectrometry experiments are present as neutral, relevant intermediates in the reaction; nevertheless, the fragmentation pattern rules out isomeric structures such as **3.3** and **3.16** and is only consistent with thiatriazolines of type **3.4**.[54]

Since ethyl thiono esters and methyl dithio esters are known to react with alkyl azides at elevated temperatures (110 °C) to form imidates and thioimidates[55] it seemed reasonable that such intermediates might be relevant to the thio acid/azide amidation. Under the mild reaction conditions of our amidation, however, neither class of azide reacted with silyl thionoesters. The steric, electronic, and conformational properties of the silyl thionoesters are significantly different from thiocarboxylates, and consequently, this finding is difficult to interpret. In agreement with the DFT calculations discussed below, the [3+2] cycloaddition of neutral coupling partners would appear to require higher temperatures than the coupling of thiocarboxylates.

The available experimental data on known thiatriazolines and thiatriazoles suggest likely routes by which thiatriazolines of type **3.4** form amides. Thiatriazolines of type **3.17,** Figure 3.2, have been demonstrated to decompose stepwise, first expunging molecular nitrogen and ultimately losing sulfur. The corresponding reactive intermediates

---

[54] Mlostoñ, G.; Romañski, R.; Heimgartner, H. *Polish J. Chem*. **2001**, *75*, 975.

[55] The DFT calculations reported here strongly implicate Path 2 as the likely mechanism by which the putative thiatriazolines of ref. 52 lead to the observed imidates. The amidation reactions in ref 39a and 39b likely follow reaction mechanisms analogous to those outlined here as well. for examples see: Hartman, G. D.; L. M. Weinstock, L. M. *Synthesis*, **1976**, 681.

have been intercepted.[56] In contrast to **3.17**, which houses an exocyclic electron-withdrawing group, thiatriazoles of type **3.18** bear an exocyclic electron-donating group. This type of heterocycle loses nitrous sulfide (N_2S), in what is probably a single step process, which rapidly decomposes to nitrogen and sulfur.[57] Nitrous sulfide generated from thiatriazoles has been characterized and used to deliver sulfur to strained alkenes, generating thiiranes.[58] While ESI does not provide insight to the nature of the bond breaking process, data summarized in Scheme 3.4 show that thiatriazolines formed from thio acids and azides can lose a fragment corresponding to nitrous sulfide.[59]

The DFT calculations also support the experimental conclusions in that two discrete reaction paths have been identified and that the mechanism is dictated by the electronic properties of the azide. The electron-deficient azide reacts via a stepwise mechanism[60] to form a thiatriazoline intermediate. Thus the anion of the thio acid adds to the polarized azide terminus. This establishes the S–N connectivity and generates a stabilized aza-anion (**3.23**, Figure 3.3). This species cyclizes to form the C–N bond leading to **3.25**. There is virtually no barrier to ring opening and reversion to the linear intermediate.[61] Protonation of this anion, however, prevents reversion to the linear

---

[56] (*a*) Loock, E. V.; Vandensavel, J. M.; L'Abbe, G.; Smets, G. *J. Org. Chem.* **1973**, *38*, 2916. (*b*) L'Abbe, G.; Verhelst, G.; Yu, C-C.; Toppet. S. *J. Org. Chem.* **1975**, *40*, 1728. (*c*) L'Abbe, G.; Brems, P.; Albrecht, E. *J. Heterocyclic Chem.* **1990**, *27*, 1059. Metal analogues are also known, see: (*d*) Fruhauf, H. W. *Chem. Rev.* **1997**, *97*, 523.

[57] Wentrup, C.; Kambouris, P. *Chem. Rev.* **1991**, *91*, 363.

[58] Adam, W.; Bargon, R. M. *Eur. J. Org. Chem.* **2001**, 1959.

[59] To date, capture of nitrous sulfide or S_1 according to the procedure of Adam (see ref. 56) has failed to provide unequivocal experimental evidence that nitrous sulfide is being generated under the reaction conditions.

[60] Related to diazotransfer, see: Regitz, M. *Synthesis* **1972**, 351.

[61] This finding is analogous to the very low barrier to hydroxide addition/chloride elimination from acyl chlorides [(*a*) Fox, J. M.; Dmitrenko, O.; Liao, L. A.; Bach, R. D. *J. Org. Chem.* **2004**, *69*, 7317]. It is noteworthy in this regard that the pK_a of protonated **3.23** may well be near that of an *N*-acyl sulfonamide ($pK_a \approx 2.5$, see ref. 41a) and the pK_a of thiatriazoline **3.26** near other tetrahedral intermediates [(*b*) $pK_a \approx 12$, see: Deslongchamps, P. *Tetrahedron*, **1975**, *31*, 2463. (c) Perrin, C. L.; Nunez, O. *J. Am. Chem. Soc.* **1986**, *108*, 5997.; and (*d*) Perrin, *Acc. Chem. Res.* **2002**, *35*, 28.] and hence represents a pK_a difference of approximately 10 orders of magnitude. This difference in anion stability anticipates the small reaction barrier separating **3.25** from **3.23**.

intermediate and leads to the relatively stable, neutral thiatriazoline **3.26**. In contrast to thio acetate, thioacetic acid **3.19a** was found to undergo a one-step cycloaddition with methyl sulfonylazide to form **3.26** directly. While both routes converge on the same intermediate, the reaction barrier for the one-step process is significantly higher in comparison to the anion (Figure 3.3). Intermediate **3.26** undergoes a [3+2] cycloreversion to form the enol form of the product amide plus nitrous sulfide, which decomposes to the observed nitrogen and sulfur.

Electron-rich alkyl azide participates in a concerted process for both the thiocarboxylate and the thio acid to give the thiatriazoline in a single step. However, the reaction proceeds via a lower activation barrier for the thiocarboxylate (17.1 kcal/mol vs 21.8 kcal/mol, see Figure 3.4). Thus for both the electron-rich and the electron-poor azides, the anionic reactions are accelerated relative to the neutral reactions.

The computed activation energy difference between reactions of methyl sulfonazide and methyl azide with thioacetic acid (1.8 kcal/mol) is somewhat larger than the experimentally determined value (0.35 kcal/mol). There are two likely causes for this difference. First, the single point (polarizable continuum model) PCM computations only approximate the kinetic medium; and second, the use of methyl groups in the calculations in place of phenyl and benzyl used in the experiments ignores steric interactions that may be relevant. This minor difference aside, the studies indicate that the thio acid/azide coupling of azides bearing electron-donating substituents constitutes an anion-accelerated [3+2] cycloaddition process that results in the formation of a stable thiatriazoline.[62] This

[62] Analogous anion accelerated [3+2] cycloadditions, though known, appear to be very rare (for an example, see: (*a*) Shindo, M., Kotaro, I.; Tsuchiya, C.; Shishido, K. *Org. Lett.* **2002**, *4*, 3119.) and models for predicting the effect of an exo-anion on a [3+2] cycloaddition do not appear to be developed (see for example: (*b*) Carpenter, B. K. *Tetrahedron* **1978**, *34*, 1877.).

comparatively more sterically demanding transition state is consistent with our experimental findings and the trend wherein primary azides react more rapidly than secondary azides and much more rapidly than tertiary azides. The anionic thiatriazoline **3.31** is significantly more stable than **3.25** and is not as prone to C–N cleavage and conversion to a linear intermediate. Protonation of **3.31** and retro-[3+2] reaction gives the amide product as well as nitrous sulfide in a manner completely analogous to the pathway outlined for the thio acid reaction with electron-deficient azides.

The experimental results from kinetic studies, Hammett correlation, trapping experiments, and ESI–MS/MS data coupled with computational analysis uniquely support our contention that the reaction pathway for relatively electron-rich azides is different from the pathway for highly electron-deficient azides. The mechanisms shown above summarize our current understanding of these reactions.

Section 3.4: Conclusions

For relatively electron-rich azides Scheme 3.5 the nitrogen–sulfur and nitrogen–carbon connectivity of the thiatriazoline intermediate is formed in a single step by anion-accelerated [3+2] cycloaddition.

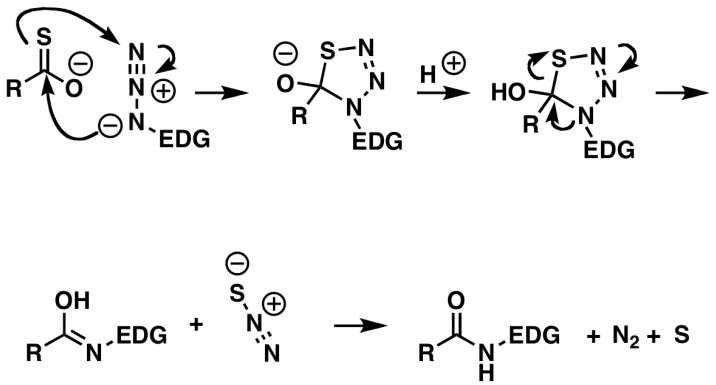

Scheme 3.5: Mechanism of Amidation: Electron-Rich Azide

Subsequent protonation and loss of nitrous sulfide via retro-[3+2] cycloaddition gives the amide product. Highly electron-poor azides first form the nitrogen–sulfur bond to give a linear intermediate Scheme 3.6. In a separate step, formation of the nitrogen–carbon bond and protonation gives the thiatriazoline intermediate. Retro-[3+2] cycloaddition gives the amide product. This mechanism is in complete accord with the prior capture concept.

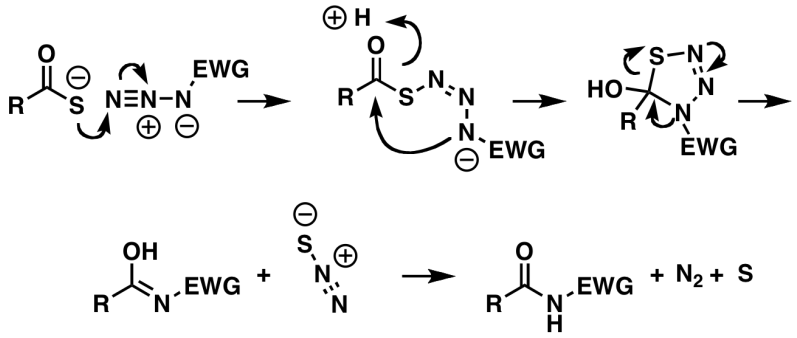

Scheme 3.6. Mechanism of Amidation: Electron-Deficient Azide

The mechanistic data provide a basis for understanding the thio acid/azide amidation and explain why this reaction approaches the ideal click-type reaction profile for highly electron-poor azide substrates. Such azides form the desired amide products in high yield under dilute or concentrated solutions at room temperature. The coupling is effective in solvents ranging from organic to aqueous. Nearly equimolar quantities of the coupling partners provide high yield of the desired product. These observations are directly attributable to the efficient, chemoselective capture of the thiocarboxylate by the polarized azide followed by efficient intramolecular nucleophilic addition. Molecular nitrogen and sulfur, both of which are innocuous, form as the only identifiable byproducts by spontaneous and exothermic decomposition of the thiatriazoline. Virtually all of these characteristics are retained in the amidation of electron-rich azides. However, since the

azide is not highly polarized, the thiatriazoline is formed directly and extended heating of more concentrated reaction mixtures is required to induce satisfactory reaction rates.

Since our original disclosure on the thio acid/azide amidation as a method for complex amide synthesis and as a potential ligation strategy, several advances and applications of the reaction have appeared, including selenium variants[39a,b] and metal promoted couplings.[39c] New applications include the preparation of neoglycopeptides,[39d] thioamides, *N*-acyl sulfonamides and their conjugates,[35,40b] including the promising *N*-acyl β-substituted aminoethane sulfonamides.[40a]

Thio acid/azide amidation provides an alternative chemoselective strategy to amide synthesis that complements the Staudinger amidation method, as it is especially effective for electron-deficient azide partners and effective over a range of solvents, including water. This report lays a mechanistic foundation for amide synthesis via thio acid/azide amidation and should enable hypothesis-driven approaches to other amide forming reactions and methodological improvements.

Chapter 4: One-pot Synthesis of *N*-acylsulfonamides

Section 4.1: Introduction

Sulfonyl azides react very rapidly with thio acids Scheme 1 to give *N*-acyl sulfonamides, a product class useful in medicinal chemistry,[63] solid support linking strategies,[64] and for conjugation and ligation applications among others.[65]

Our group[66] has shown that trimethoxybenzyl (TMOB) thio esters could be an efficient method prepare thio acid precursors; however, this approach is limited to acid stable precursors, as illustrated in Scheme 1. TMOB thioesters are readily prepared [67] from the corresponding carboxylic acid and TMOB thiol.[68] Conversion of protected threonine **4.5** to TMOB thioester **4.6** and removal of the Fmoc protection gave amine **4.7**, and DCC-mediated coupling of **4.7** with dipeptide **4.8**[69] gave peptide thio ester **4.9** in excellent yield.[70] TFA cleavage of both the TMOB and the *tert*-butyl groups gave the crude peptide thio acid (tert-butyl group cleaves rapidly in this process, whereas the TMOB group

---

[63] (*a*) Abbate, F.; Supuran, C. T.; Scozzafava, A.; Orioli, P.; Stubbs M. T.; Klebe, G. A.; Jones, B. R. *J. Med. Chem.* **2002**, *45*, 3583. (*b*) Uehling, D. E.; Donaldson, K. H.; Deaton, D. N.; Hyman, C. E.; Sugg, E. E.; Barrett, D. G.; Hughes, R. G.; Reitter, B.; Adkison, K. K.; Lancaster, M. E.; Lee, F.; Hart, R.; Paulik, M. A.; Sherman, B. W.; True, T.; Cowan, C. *J. Med. Chem.* **2002**, *45*, 567. (*c*) Mader, M.; Shih, C.; Considine, E.; De Dios, A.; Grossman, S.; Hipskind, P.; Lin, H.; Lobb, K.; Lopez, B.; Lopez, J.; et al. Bioorg. Med. *Chem. Lett.* **2005**, *15*, 617. (*d*) Johansson, A.; Poliakov, A.; Åkerblom, E.; Wiklund, K.; Lindeberg, G.; Winiwarter, S.; Danielson, U.; Samuelsson, B.; Hallberg, A. *Bioorg. Med. Chem.* **2003**, *11*, 2551.

[64] (*a*) Kenner, G. W. *Chem. Commun.* **1971**, 636. (*b*) Backes, B. J.; Ellman, J. A. *J. Org. Chem.* **1999**, *64*, 2322. (*c*) Shin, Y.; Winans, K. A.; Backes, B. J.; Kent, S. B. H.; Ellman, J. A.; Bertozzi, C. R. *J. Am. Chem. Soc.* **1999**, *121*, 11684. (*d*) Ingenito, R.; Drezniak, D.; Guffler, S.; Wenschuh, H. *Org. Lett.***2002**, *4*, 1187. (*e*) Mclean, D.; Hale, R.; Chen, M. *Org. Lett.***2001**, *3*, 2977.

[65] Merkx, R.; Brouwer, A. J.; Rijkers, D. T. S.; Liskamp, R. M. J. *Org. Lett.* **2005**, *7*, 1125.

[66] Shangguan, N.; Katukojvala, S.; Greenberg, R.; Williams, L. J. *J. Am. Chem. Soc.* **2003**, *125*, 7754.

[67] Neises, B.; Steglich, W. *Angew. Chem., Int. Ed. Engl.* **1978**, *17*, 522.

[68] Vetter, S. *Synth. Commun.* **1998**, *28*, 3219.

[69] Katukojvala, S.; Barlett, K. N.; Lotesta, S. D.; Williams, L. J. *J. Am. Chem. Soc.***2004**, *126*, 15348.

[70] No epimerization was observed for the coupling.

cleaves slower >2 h), which upon treatment with trimethylsilylethyl sulfonyl azide **4.10**[71] gave the peptide conjugate **4.11** in 92% yield. Similar treatment of **4.6** gave the corresponding amide product **4.12**. These experiments demonstrate the ease with which thio acid/azide amidation can be adapted to ligation/conjugation reactions. However, limitations being that TMOB removal is slow, prolonged exposure to TFA is required for good conversion, and preparation of **4.11** by way of **4.6**, while high yielding, is an uneconomical route to simple amino acid-derived *N*-acyl sulfonamides. Furthermore, this approach is not compatible with acid-sensitive functional and specifically protecting groups commonly used in peptide couplings. e.g. Boc, **4.5**→**4.6**.

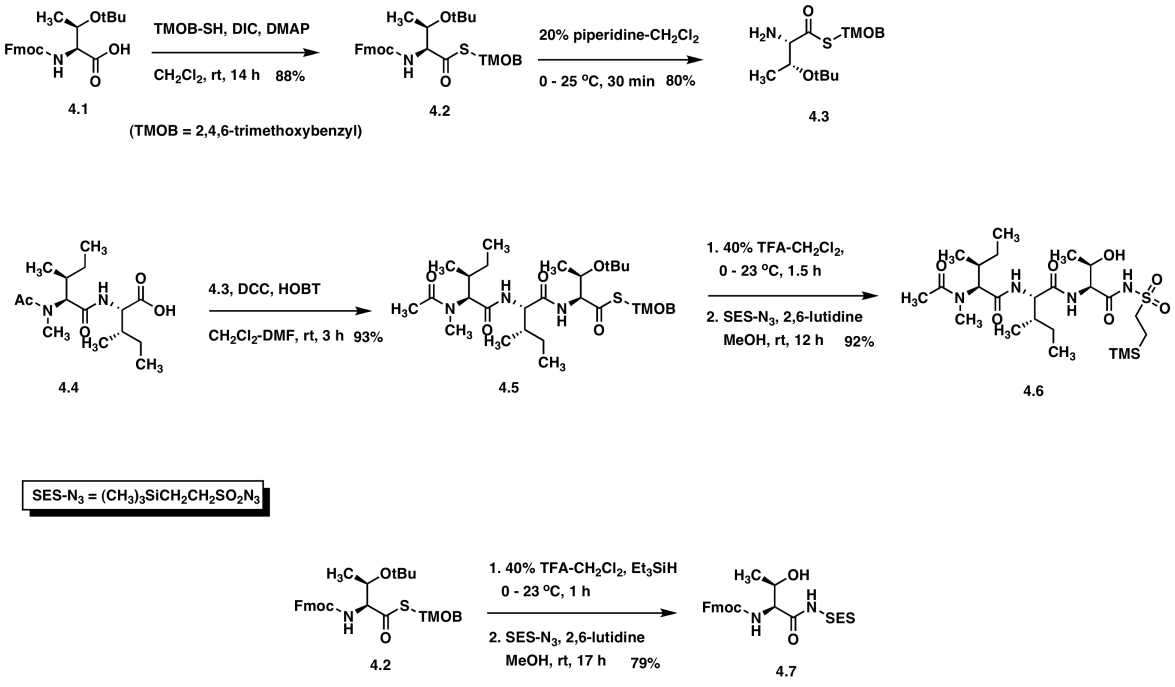

Scheme 4.1: TMOB mediated formation of thio acids and their reaction with azides.

[71] Weinreb, S. M.; Chase, C. E.; Wipf, P.; Venkatraman, S. *Organic Syntheses*; Wiley & Sons: New York; Collect. Vol. 10, p 707.

Section 4.2: One Pot Procedure for Generating Thio Acids and Their Reactions With N-Acylsulfonamides

Our goal, therefore, was to develop an *N*-acyl sulfonamide synthesis procedure compatible with acid- and base-sensitive functionality. Scheme 4.2 summarizes the general approach, and Table 4.1 provides several examples of the method. Protected amino acids **4.8a-e**, were transformed to amino thio acids by exposure to isobutyl chloroformate,[72] and then trimethylsilyl thiolate, followed by dilution with methanol and then removal of volatiles under reduced pressure. The *N*-acyl sulfonamide products **4.10a-e** were formed by dilution of the thio acid in mildly basic methanol, addition of sulfonyl azide, stirring at room temperature, followed by removal of solvent, presumably, a trimethylsilyl thioester generated from addition of the thiolate to the mixed anhydride rearranges to the trimethylsilyl thionoester under the reaction conditions. Upon methanolysis, the thio acid is liberated. Anhydrous trimethylsilyl thiolate was prepared from bis(trimethylsilyl) sulfide upon treatment with methyllithium.

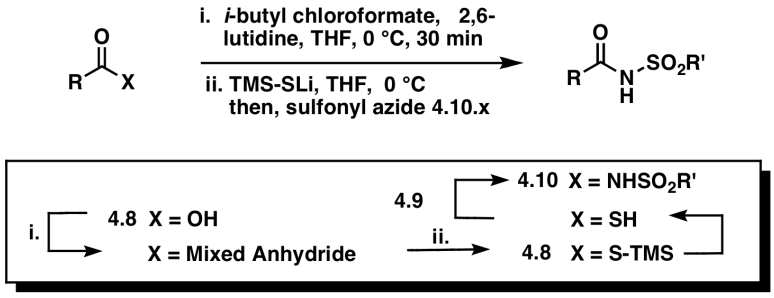

Scheme 4.2: Carboxylic Acid Conversion to a Thio Acid

Subsequent exposure to the azide leads to the amide. This approach to generating thio

[72] Dudash, J.; Jiang, J.; Mayer, S. C.; Joullie, M. M. *Synth. Commun.***1993**, *23*, 349.

acids has many favorable qualities, including reactant stoichiometry (near 1:1 for all reagents), volatility of most reagents and reaction byproducts, reliably high yields, and that the choice of solvent in the coupling reaction can be determined by the solubility properties of the reactants since the thio acid/azide amidation is effective in a range of organic and aqueous solvents. Moreover, *N*-acyl sulfonamides often display significant water solubility. Avoidance of aqueous workup and the lack of significant byproducts and excess reagents, commonly used for other sulfonamide couplings, also adds to the attractiveness of the method. In generating the thio acid, the less convenient use of hydrogen sulfide, sodium sulfide,[73c-f] or the less atom economical use of thiols, such TMOB-thiol and related hydrogen sulfide equivalents,[72g,h] is avoided by hexamethyldisilathiane (HMDT). The generation of trimethylsilyl thiolate from HMDT with methyllithium conveniently leads to excellent overall yields of amide.[72a] Solutions of tetrabutylammonium fluoride in THF dried over activated molecular sieves performed as well as methyllithium and gave yields that were superior to those obtained with wet tetrabutylammonium fluoride;[72b] however, methyllithium reactions are easier to monitor and are not contaminated by nonvolatile tetrabutylammonium salts. In addition to the qualities mentioned above, this method is highly complementary to other *N*-acyl sulfonamide syntheses. Direct amidation of sulfonamides with active esters usually requires strong base and/or highly active esters and excess reagents.[74] The conditions

---

[73] (a) Kraus, G. A.; Andersh, B. Tetrahedron Lett. **1991**, *32*, 2189. (*b*) Schwabacher, A. W.; Maynard, T. L. *Tetrahedron Lett*. **1993**, *34*, 1269. and references therein. (*c*) Yamashiro, D.; Blake, *J. Int. J. Peptide Protein Res*. **1981**, *18*, 383. and references therein. (*d*) Pansare, S. V.; Vederas, *J. C. J. Org. Chem*. **1989**, *54*, 2311. (*e*) Hoeg-Jensen, T.; Holm, A.; Sorensen, H. *Synthesis* **1996**, 383. (*f*) Lee, A. H. F.; Chan, A. S. C.; Li, T. *Tetrahedron* **2003**, *59*, 833. (*g*) Goldstein, A. S. Gleb, M. H. *Tetrahedron Lett*. **2000**, *41*, 2797. (*h*) Gartner, H.; Villain, M.; Botti, P.; Canne, L. *Tetrahedron Lett*. **2004**, *45*, 2239.

[74] DMSO is an exception. We believe this is due to oxidation of thethio acid. Selenocarboxylates appear to behave similarly. See: Wu, X.; Hu, L.; Tetrahedron Lett. 2005, 46, 8401.

presented here are mildly basic and compatible with a range of functionality, including acid- and base-sensitive protecting groups as well as certain unprotected functionality.

For the entries in Table 4.1, the same procedure was followed, modified only by the reaction time allowed for the consumption of mixed anhydride by thiolate, a parameter readily monitored by TLC. Coupling partners include base-sensitive substrates (entries **4.8a–c**), acid-sensitive substrates (entries **4.8d-e**), protected alcohol (entry **4.8d**), free alcohol (entry **4.8e**), and free carboxylic acid **4.9a**, (entries 1–3). Methyllithium and dried tetrabutylammonium fluoride were used for the trimethylsilyl thiolate formation step of entry **4.8e**, and the overall yields were equally effective within experimental error.

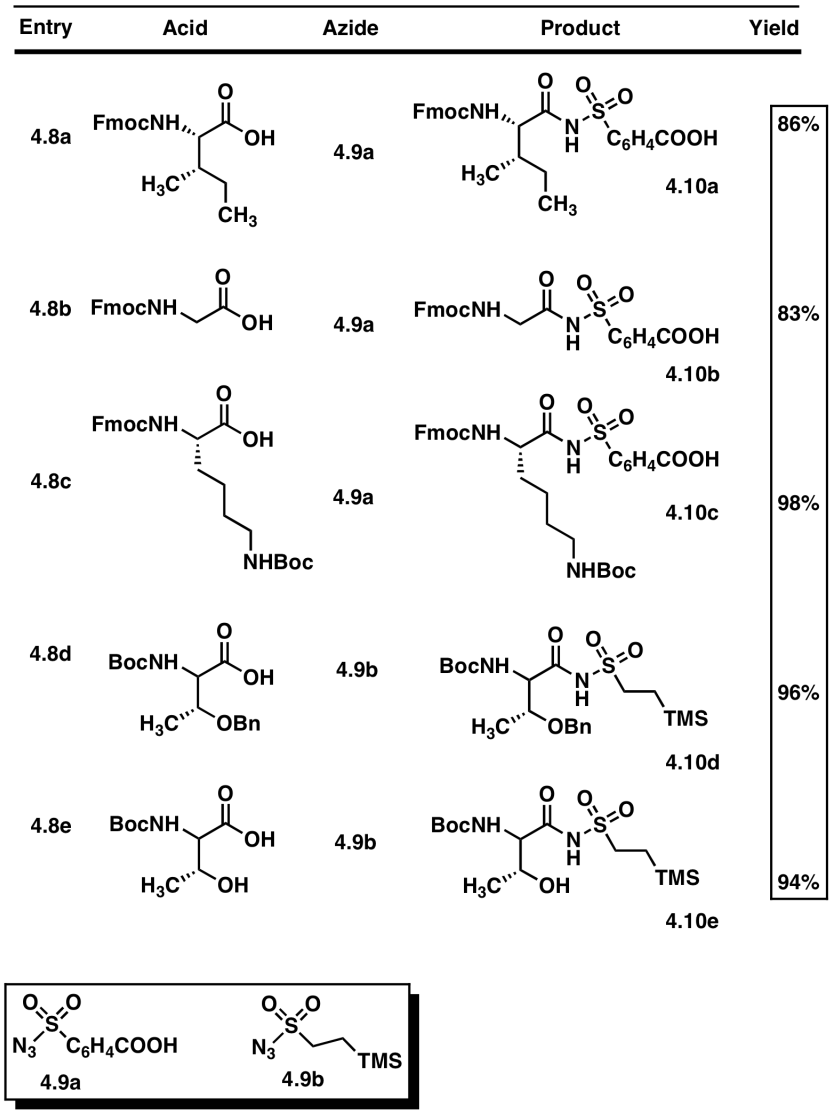

Table 4.1: Acid and base sensitive substrates.

The ability to employ unprotected coupling partners, such as 4-carboxy-benzenesulfonyl azide **4.9a**, enables direct subsequent functionalization without having to implement a protecting group strategy. For example, Fmoc-Ile-OH, was converted to the thio acid and taken directly and immobilized on the amine-functionalized Wang amide resin. The same overall sequence, leading to an identically functionalized resin, was achieved by formation of the *N*-acyl sulfonamide on solid support

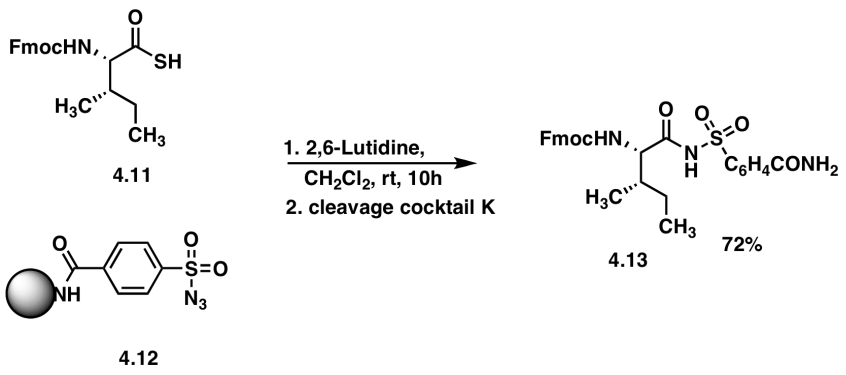

Scheme 4.3: *N*-Acylsulfonamides Generated on Solid Support

Thus, Wang amide resin was coupled with commercial **4.9a** and then exposed to the crude Fmoc-Ile-SH prepared according to our method. The consumption of resin-bound azide was readily monitored, and the only modification to the amidation protocol was the use of excess Fmoc-Ile-SH (2 equiv. based on the parent carboxylic acid) and methylene chloride instead of methanol. Proof that we had indeed succeeded in effecting thio acid/azide amidation on solid support was secured by comparison of the spectral characteristics of the purified cleavage products from the two resins, which were shown to be identical. The overall isolated yield of the **4.13** was 72% based on the loading capacity of the resin.

This report offers a mild, chemoselective alternative to the preparation of *N*-acyl sulfonamides from active esters and sulfonamides that is compatible with acid- and base-sensitive protecting groups and, in certain cases, unprotected functionality. Generation of the thio acid from the parent carboxylic acid followed by addition of sulfonyl azide gives the desired product in excellent yield. The feasibility of *N*-acyl sulfonamide synthesis with peptide segments and solid support has also been demonstrated. Similarly, SES-N_3 has been shown to give *N*-acyl sulfonamides. Following *N*-alkylation, the SES group is

readily cleaved upon brief, room temperature fluoride treatment. The generality of these findings, including applications in target-oriented synthesis, studies in chemical biology, and related amidations, will be reported in due course.

Chapter 5: Distortional Asymmetry and its Role in Stereoselection.

Section 5.1: Introduction

Several theoretically sound qualitative models for predicting the lowest energy transition state for face selective reactions have been developed and applied as rationales for stereoinduction in organic synthesis. The most widely used models[75] are based on steric, torsion, stereoelectronic, and polar effects and pay special attention to stabilizing and destabilizing interactions that may emerge as reactants approach the transition region on the path to product. Combined, these constitute the framework organic chemists use to rationalize the selectivity in chemical reactions. However, there is a large body of data where these models fail, particularly in constrained cyclic systems.[76] This is surprising, since many of these systems were designed to enable partitioning of the various contributions and to thereby facilitate a deeper understanding of the factors that govern face selectivity. We propose a distortional asymmetry new model to explain of these findings. This model identifies circumstances where asymmetric distortional contributions to transition state energies influence, and perhaps even dictate, face selectivity in highly constrained compounds.

---

[75] Extensive data and the most widely used stereochemical models, such as those of Cram, Felkin, and many others, are reviewed in a special issue of Chemical Reviews *Chem. Rev.* **1999**. *5*, 1067-1480. For an overview of each model see ref. 83a.

[76] (*a*) Dannenberg, J. J. *Chem. Rev.***1999***, 5*, 1225. (*b*) Tomoda, S. *Chem. Rev.* **1999***, 5*, 1243. (*c*) Cieplak, A. S. *Chem. Rev.* **1999**, *5*, 1265. (*d*) Ohwada, T. *Chem. Rev.* **1999**, *5*, 1337. (*e*) Gung, B. W. *Chem. Rev.* **1999**, *5*, 1377. (f) Kaselji, M.; Chung, W.-S.; le Noble, W. J. *Chem. Rev.* **1999**, *5*, 1387. (g) Adcock, W. ; Trout, N. A. *Chem. Rev.* **1999***, 5*, 1415. (h) Wipf, P.; Jung, J.-K. *Chem. Rev.* **1999**, *5*, 1469.

Section 5.2: Torsional Model

Our interest in stereoselective synthesis, specifically in contemplating the stereochemical led us to consider the possibility that distortional effects could contribute to the facial outcome of a reaction. In our explorations we took note of norbornene, an archetypal system to probe stereo-inducing effects. Huisgen[77] noted that not only was norbornene exo face selective but it reacted ~1000 times faster than bicyclooctene in cycloadditions. This was attributed to strain release and deemed "factor *x*". The debate

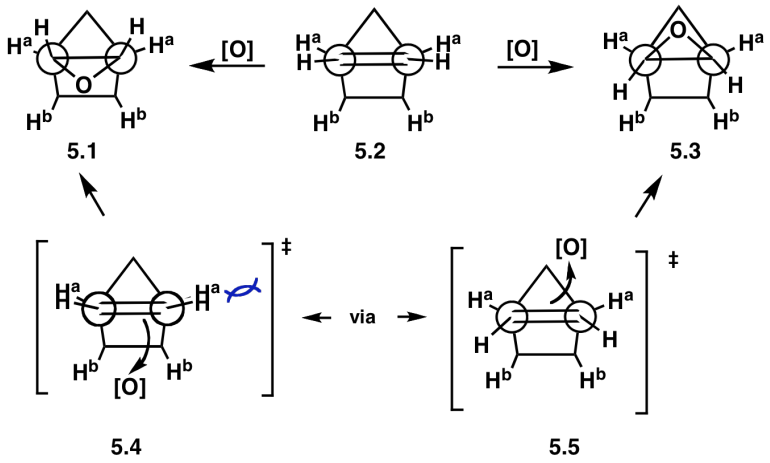

Figure 5.1: Torsional Effects Destabilizing Endo Attack of an Oxidant

was focused on HOMO differentials,[78] steric effects,[79] and torisonal effects.[80] The most prominent argument, made by Houk et. al.,[81] states that the steric torsional interaction of H^a and H clash as norbornene **5.2** procedes through intermediate **5.4** to endo product **5.1**. Conversely, if an electrophile attacks the exo face the olefinic hydrogens never

[77] Huisgen, R.; Ooms, P. H. J.; Mingin, M.; Allinger, N. L. *J. Am. Chem. Soc*. **1980,** *102*, 3951.
[78] Inagaki, S.**;** Fujimoto, H.; Fukui, K. *J. Am. Chem. Soc*. **1976**, *98*, 4054.
[79] Brown, H. C.; Hammar, W. J.; Kawakami, J. H.; Rothberg, I.; Van der Jugt, D. L. *J. Am. Chem. Soc*. **1967**, *89*, 6381.
[80] Schleyer, P. v. R. *J. Am. Chem. Soc*. **1967**, *89*, 701.
[81] Rondan, N. G.; Paddon-Row, M. N.; Caramella, P.; Mareda, J.; Mueller, P. H.; Houk, K. N. *J. Am. Chem. Soc*. **1982**, *104*, 4976.

eclipse protons H^a. Thus exo approach represents the lower energy pathway. These destabilizing eclipsing interactions were used to explain the 7° olefin pyramidization in the exo direction observed in the ground state. Hyperconjugative stabilization, not unlike the type argued to cause the barrier of rotation in ethane,[82] was ruled out due to a 1000 fold increase in rate of cycloaddition when compared with bicyclo[2.2.2]oct-2-ene and bicyclo[2.1.1]hex-2-ene.

Section 5.3:The Distortional Asymmetry Model

In contrast, **5.6-5.9** were studied by the Ohwada group.[83] The stereochemical outcome of these reactions cannot be attributed to torsional effects due to the near symmetric nature of the allylic bonds. It was found that preferred approach of *m*-CPBA to tricycle **5.10** is opposite the cyclopropyl moiety, consistent with through-space interactions analogous to the class findings on the 7-norbornenyl cation.[84] Remarkably, the preferred approach of reagent to **5.6-5.9** is from the same side as the cyclopropyl moiety, and yet the cyclobutyl analog **5.9** reacts with the opposite face selectivity. Also of note is the degree of selectivity – high for **5.6-5.8**, low for **5.9** and high for **5.10**. The observed face selectivity is difficult to rationalize, especially the data for tricycle **5.6**, a compound unbiased by steric, torsional, or polar contributions.

---

[82] Mo. Y.; Gao, J. *Acc. Chem. Res.* **2007**, *40*, 113.

[83] Tsuji, M.; Ohwada, T. Shudo, K. J. *Tetrahedron Lett.* **1997**, *38,* 6693.

[84] Winstein, S; Shatavsky, M.; Norton, C.; Woodward, R. B. *J. Am. Chem. Soc.* **1952**, *77*, 4183.

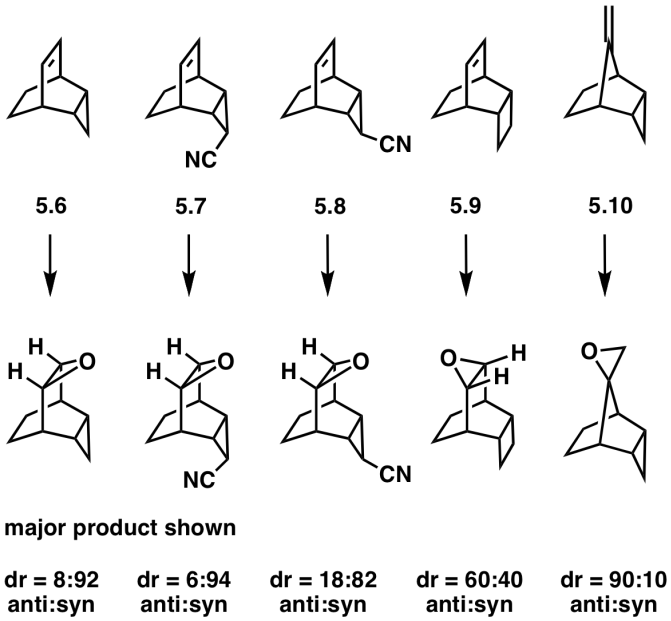

Figure 5.2: Experimental Results for Treatment of the Above Olefins with *m*-CPBA

We approximate the distortional asymmetry contribution by evaluating the symmetric out-of-plane bend of the olefinic hydrogens of **5.6-5.9**, Figure **5.3c**.[85] We used two methods for this evaluation. Presented here is the vibrational model. This model isolates the bending mode of the olefin then plots the single point energy calculation for each isolated structure. Alternatively, one could mechanically move the hydrogen to bend at the desired dihedral angle and then choose to optimize the structures ground state with the bond dihedral angles held in place. Both techniques yield similar results, we will focus on the vibrational olefin bend for this discussion. The calculated distortional potential diagrams are presented in **c.** The energy differential for displacement of the olefin hydrogens ±10˚ is indicated. The

[85] Note that: (a) the reactant vibrations (~ 800 cm^{-1} for **5.6-5.9**) are symmetric out-of-plane olefin hydrogen bends; (b) the vibrations under discussion are comparatively low energy (~ 700-800 cm^{-1}) and are significantly populated ~ 5% at the reaction temperature (room temperature); (c) the reaction barriers are low ~ 3500 cm^{-1}.

diastereomeric transition states for epoxidation of these olefins **a.** with *m*-CPBA as oxidant were calculated, and the energy differential determined ($\Delta H^{\ddagger}_{DCM}$, entries 1-4). Transition states for epoxidation with performic acid (PFA) were also assessed and indicate the observed trends are not unique to *m*-CPBA (entries 5-8). The extent of distortion of the olefinic hydrogens in each transition state is given as $°\theta_{syn}$ and $°\theta_{anti}$. Although not shown, TS states for the oxidation of **5.6-5.9** with OsO_4 displayed a similar energy trend.[86] For further insight, we calculated the relative energies of the epoxidation transition structures with the olefin hydrogens adjusted to $\theta = 0°$ $\Delta H_{\%}$. Importantly, the diastereomeric products are nearly isoenergetic $\Delta H_{product}$ = 0.0 - 0.9 kcal/mol, and the transition states are early, as assessed by the degree of bond forming and bond breaking, the small reaction barriers (10 ± 2 kcal/mol), and the exothermicity of the epoxidations (53 ± 1 kcal/mol).

[86] Note: for detailed energies see the supporting experimental information.

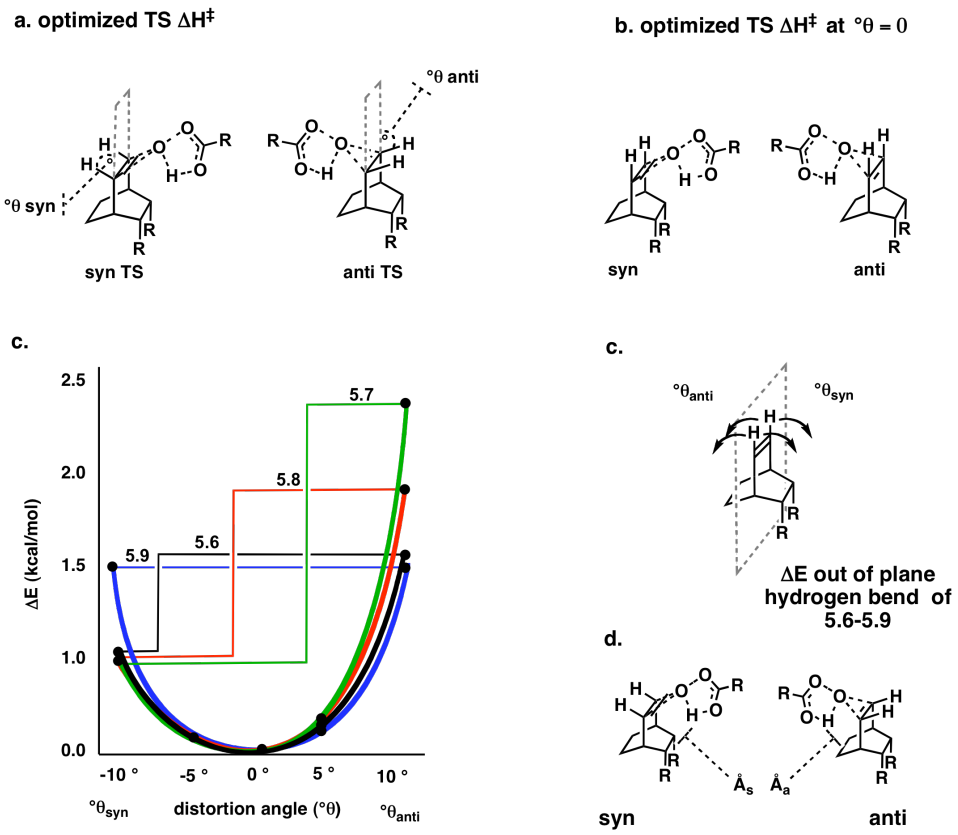

entry	olefin-reagent	a. ΔH‡DCM (kcal/mol)	°θ syn	°θ anti	b. $\Delta H_{\%}$ (kcal/mol)	c .$\delta\Delta E_{dis}$ (kcal/mol)	d. $Å_s$	$Å_a$
1	5.6-*m*CPBA	1.39 (1.51)	11 (13)	10 (12)	1.07/ -23 %	0.60/ 43 %	2.37	2.19
2	5.7-*m*CPBA	1.75 (3.22)	13 (14)	10 (12)	0.57 -67 %	1.54/ 88 %	2.36	2.18
3	5.8-*m*CPBA	1.03 (0.77)	13 (14)	11 (12)	0.49/ -52 %	1.01/ 98 %	2.44	2.19
4	5.9-*m*CPBA	0.03 (-0.04)	11 (13)	11 (13)	0.00/ -	-0.02/ -	2.20	2.21
5	5.6-PFA	1.33 (1.44)	11 (13)	10 (12)	1.01/ -23 %	0.60/ 45 %	2.37	2.20
6	5.7-PFA	1.79 (3.28)	12 (13)	10 (12)	1.23/ -31 %	1.54/ 86 %	2.28	2.13
7	5.8-PFA	1.09 (0.71)	12 (14)	10 (13)	0.73/ -33 %	1.01/ 93%	2.36	2.14
8	5.9-PFA	0.02 (0.00)	11 (12)	11 (13)	0.00/ -	-0.02/ -	2.16	2.15

Figure 5.3: Computational Results

a. Tabulated are calculated transition structure parameters for syn and anti approach of reagent and the corresponding transition state distortional angle. Values are given for $\Delta H^{‡}$DCM (gas phase values in parenthesis), θ_{syn} and θ_{anti} (gas phase values in parenthesis), **b.**$\delta\Delta E_{dis}$. indicates the SPE difference between the syn and anti TS when the hydrogen olefin dihedral angle is set to zero ($\theta_{syn} = \theta_{anti} = 0^{\circ}$);**c**. Calculated symmetric out-of-plane vibrational potentials of **5.6-5.8c** in comparison to **5.9c** are highly asymmetric. The distortional differential at $\theta = 10^{\circ}$ is highlighted for **5.6** (black), **5.7** (green), **5.8** (red), **5.9** (blue). The percentage of $\Delta H^{‡}$DCM is also given as $\Delta H_{\%}$. **d**. The distance between the reagent and substrate sector in the transition states for both anti and syn labled ($Å_{syn}$ and $Å_{anti}$).

Examination of the aforementioned data reveals five important findings. **1**) The distortion potentials for **5.6-5.9c** favor distortions away from the preferred face of attack and $\delta\Delta E_{dis}$, Figure 5.3c. **2**) This includes compound **5.9**, whose relative face selectivity is opposite that of **5.6-5.9.2**. The out-of-plane bend geometries for the olefinic hydrogens in the calculated transition states are near 10˚, and in all cases, the degree of distortion is lower for the side corresponding to the steeper distortional potential (compare $°\theta_{anti}$ with $°\theta_{syn}$ in Figure5.3a).[87] **3**) The distortional differentials (Figure 5.3c) at 10˚ approximate these energies and range from 43–98 % of the corresponding transition state differentials, except for compound **5.9**, for which the differential is very small (compare $\delta\Delta E_{dis}$, $\Delta H^{\ddagger}_{DCM}$ in Figure 5.3). **4**) The anti-periplanar vicinal bonds lengthen in the transition states in the same way and to the same degree as that observed for coupled vibrational motion of the olefin ground state out-of-plane bend at 10˚ (Figure 5.3c).[88] **5**) A significant portion of the energy differences between each set of diastereomeric transition states is lost, 23-67 %, when the distortion angle is restricted to 0˚ and the SPE of the structure is reevaluated (compare and $\Delta H^{\ddagger}_{DCM}$ and ΔH_q in entries 1-8, Figure 5.3).

[87] The TS and potentials were calculated using DFT/B3LYP were carried out with the G03.E suite of programs, with 6-31+G(d,p) and 6-31G(2d,2p) basis sets. General solvent effects were incorporated with the polarizable conductor self-consistent reaction field model, CPCM, dichloromethane dielectric (8.93 D). Frequency calculations confirmed the nature of the stationary points.

[88] For example, for **5.1** the vicinal bond lengths, Figure X,a , are: 1.555 Å (ground state), 1.565 Å (vibrational distortion θ_{syn} = 10˚), and 1.563 Å (TS, θ_{syn} = 11˚). Tables of these data and related bond lengths for ± 20˚ vibrational distortions for **5.1-5.4** are included in the supporting experimental

Section 5.4: Discussion

The observed selectivities are not attributable to differences in steric effects, torsional effects, product energies or transition state stabilizing factors because these factors are not present to any significant degree in the studied system. Although steric interactions are often the largest contributor to face selectivity, the faces of the olefins in **5.6-5.9** are isosteric.[89] In each case, the oxidant occupies a region that is further away from the substrate on the cyclopropyl side (see $Å_{anti}$ and $Å_{syn}$, entries 1-3 and 5-7, Figure 5.3). The opposite trend would be expected if steric interactions were contributing to face selectivity. There are no significant torsional contributions to the differences observed in these diastereomeric transition states. The olefin/bridgehead torsion angles are very small for these compounds in the ground state (**5.6** = -1.7°; **5.7** = -2.3°; **5.8** = -1.8°; **5.9** = 0.1°) and differ only slightly for the diastereomeric transition states (~2°, determined by $\theta_{syn} - \theta_{anti}$, Figure 5.3b). The difference in transition state energies for this series cannot be attributed to product energies. Since distortional energy is repulsive, it is expected to be offset, at least in part, by energy redistribution in transition structures. Still, the enforced return to planarity, as for structures of type $°\theta_{syn} = °\theta_{anti} = °0$, should simulate removal of distortional contributions that persist in the transition structures. Remarkably, when planarity is enforced, the energy difference between the transition structures drops significantly (ΔH_q, entries 1-8, Figure 5.3).

The computational data presented here derive from the use of well established density functionals and basis sets notable for their ability to model well the relative

[89] As assessed by Connelly model of sovalation for accessible surfaces.

energies of many organic reactions, including epoxidation.[90] As shown in Figure 5.3, reactant ground state-based approximations suggest that distortional contributions constitute the bulk of the transition state differential for these reactions (ΔE). These values are consistent with approximations that assess residual distortional contributions in the transition state that have not been redistributed in the transition structure ($\Delta H_{\%}$). Vicinal bond extension observed in ground state vibrational distortions parallel those in the transition states (Figure 5.3a). We conclude that the observed outcome is due to distortional asymmetry, specifically the influence of asymmetric vibrational contributions to the reaction barrier.

This ground state-induced difference in transition states is readily understood in terms of reaction theory.[91] For example, and despite virtually identical product energies, Marcus theory accommodates this outcome. As shown in Figure 5.4a, when reactant **R** follows a steeper potential due to these distortional asymmetry contributions a higher barrier (**TS′**) must be traversed to reach product **P′** than when the reactant follows a more gradual distortional potential to the other diastereomer (**R→TS″→P″**). The product ratio (**P′**:**P″**) will reflect these differences.

[90] Singleton, D. A.; Merrigan, S. R.; Liu, J.; Houk, K. N. *J. Am. Chem. Soc.* **1997**, *119*, 3385.
[91] Marcus, R. *Pure Appl. Chem.* 1997, *69*, 13 (1997).

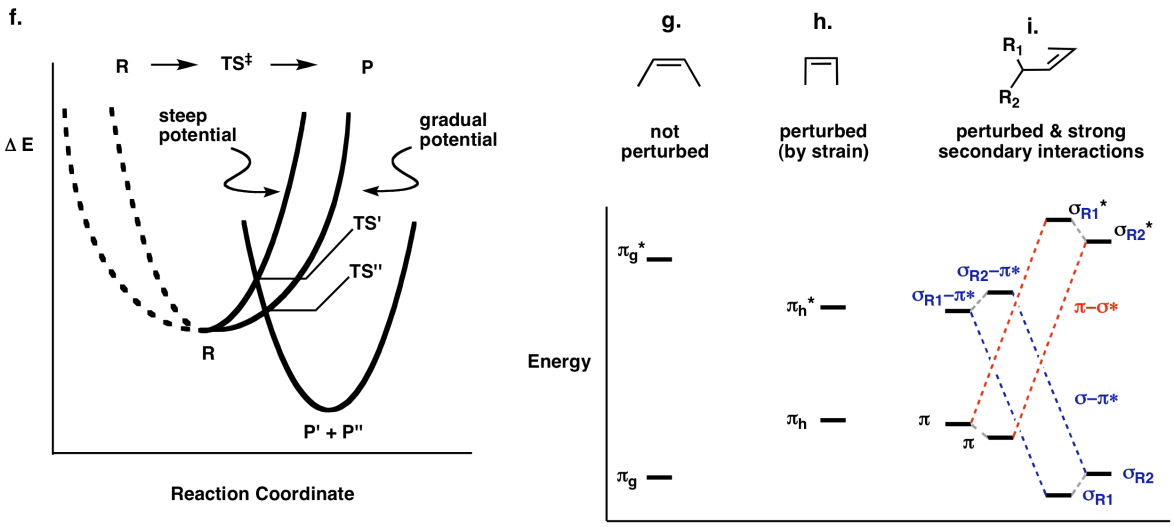

Figure 5.4: As the distortional potential steepens so does the TS energy.

What is the origin of the distortional asymmetry? We suggest that the most important factor is that the perturbed π-bond interacts strongly with its neighbors. In a series such as **5.6-5.9**, π* is lowered and π is raised relative to acyclic systems due to ring strain (compare Figure 5.4g to 5.4h). This leads to enhanced orbital mixing, for example with vicinal substituents of proper symmetry. There will be no distortional differential for symmetrically substituted π-systems, whether or not such systems are perturbed (e.g. $R^1 = R^2$, Figure 5.4i). In instances where the substituents are not identical ($R^1 \neq R^2$), distortional asymmetry may arise: the more efficient the orbital mixing of the vicinal bond the stronger the expected interaction (e.g. σ→π* and π→σ*); and the greater the difference in orbital mixing, dictated by the identity and orientation of R^1 and R^2, the greater the asymmetry.

Further evidence revealing the importance of donor-acceptor interactions was demonstrated by the deletion study of NBO study of difluorocyclobutene, Figure 5.5. In this study the donor bond contributing to the olefin is shut off and the structure is

then reoptimized and the dihedral angle is measured. As expected the hydrogen bond has the greatest effect on pyramidization. Also, noted is that when both orbital interactions are shut off the structure is nearly planar.

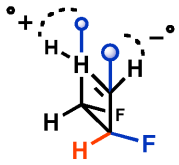

degrees from planarity	NBO deletion element
3.6°	optimized structure
5.6° Δ 2.0°	F donor orbital shut off
-0.1° Δ -3.7°	H donor shut off
-0.2° Δ -3.8°	all donors shut off

Figure 5.5 NBO deletion study of diflurorocyclobutene

Two other important factors are the early transition state of the reaction and the lack of conformational freedom in the olefin substrate. Starting material-like transition states have a small degree of bond breaking and bond formation. The major product of a face selective reaction in this context is, therefore, a consequence of the transition state that, among other factors, requires the minimal amount of bond breaking. Since repulsive and attractive forces are nearly balanced in the transition region, the reactant favors an approach that coincides with the most readily distorted potential of the π-face. Note, however, that in conformationally dynamic systems, although conformers with strong secondary orbital mixing may exist, these conformers

may not be relevant to the lowest energy pathway.[92] In contrast, in constrained systems distortional asymmetry effects, where they are present, necessarily contribute to the transition state energies.

The behavior of **5.6-5.9** is readily understood. Strain induced by the ring system perturbs the π bond and gives rise to strong secondary orbital mixing that includes the C-C bonds of the vicinal methylene. The C-C bonds emanating from the cyclopropyl fusion in **1** should mix much less efficiently, owing to the nature of the bonding in three membered-rings. Introduction of electron-withdrawing nitrile functionality in **5.6** and **5.9** further attenuates the polarizability of the C-C bonds emanating from the cyclopropyl group and simultaneously introduces a dipole effect. Polar contributions are manifest in the strong dependence of the transition state energies on the medium dielectric for **5.7** and **5.8**, but not **5.6** and **5.9** (compare $\Delta H^{\ddagger}_{DCM}$ in entries 1-8, Figure 2).[93] In the case of the endo-nitrile, this dipole effect is cooperative with the distortional potential, whereas for the exo-nitrile the effect is competitive. In contrast to the cyclopropyl derivatives, the cyclobutyl moiety of **5.9** participates in orbital mixing to essentially the same degree as the methylene substituent. Hence, the overall asymmetry is modest. Fully constrained, the resultant distortional asymmetry contributions are necessarily reflected in the transition state energies for these starting material-like reactions. The reagent approaches the π-face from the side of the least efficient orbital mixing. Approach from this side minimizes

[92] Other factors notwithstanding, conformers with these interactions should be less reactive, since π is lowered and π* is raised, relative to conformers that lack these interactions.

[93] Application of a continuum dielectric to model solvent is a crude approximation of medium effects. Nevertheless, medium dependence is evident: in vacuum the polar effect is maximal, whereas in a dielectric field of low strength the effect is greatly attenuated.

bond-breaking necessary to reach the transition state. For **5.6-5.9** distortional asymmetry is significant; for **5.9** the effect is modest.

Section 5.5: Conclusion

From the aforementioned analysis we can surmise, distortional asymmetry applies to kinetically controlled reactions where (*a*) the transition state is starting material-like, (*b*) the conformation is constrained, and (*c*) secondary orbital interactions are strong but asymmetric. Hence, the greater the distortional asymmetry contribution the greater the potential selectivity.[94]

Distortional asymmetry should apply to other prochiral systems in addition to olefins. For example, nucleophilic addition to constrained ketones should be strongly influenced by these effects, since Lewis acid coordination to the carbonyl oxygen serves to lower π* and would thereby lead to strong secondary orbital interactions. This model also provides clarifying insight into the relevance of pyramidalization, the observation that prochiral functionality may deviate slightly from planarity, even in the absence of obvious distorting geometric constraints.[95] Such non-planar structures arise from asymmetric secondary orbital mixing in the ground state and the greater this mixing the greater the deviation from planarity. Pyramidalization alone does not guarantee face selectivity. However, where distortional asymmetry effects come into play (*a-c*, above) pyramidalization is expected and should be indicative of the face favored by this effect. Torsional effects were not pertinent to the series described here.

---

[94] For very early transition states the selectivity should be lower than somewhat later early transition states, for example dichlorocarbene addition to and olefin.

[95] Vázquez, S.; Camps, P. *Tetrahedron* **2005,** *61*, 5147.

Nevertheless, where both torsional and distortional asymmetry effects are relevant they are expected to be cooperative, given directional component torsional strain and the symmetry requirement for orbital mixing in distorional asymmetry. In general, as described above, distortional asymmetry effects may not be relevant to face selectivity in acyclic systems due to conformational freedom.[96] In these systems, other factors, such as steric, polar, torsional, and other stereoelectronic effects combine to govern selectivity, *c.f.* Felkin-Anh-Eisenstein approach.

The distortional asymmetry model complements recent findings on reagent distortion/interaction energy,[97] is consistent with reaction theory, and is a previously unrecognized consequence of ground state strain-induced orbital mixing,[98] on transition state energies. Importantly, distortional asymmetry should be a significant contributor, indeed perhaps the governing contribution, to a large body of poorly understood data in the field of organic chemistry.

---

[96] Seebach, D.; Zimmerman, J.; Gysel, U.; Ziegler, R.; Ha., T. K. *J. Am. Chem. Soc.* **1988**, *110*, 4763.

[97] Ess, D. H.; Houk, K. N. *J. Am. Chem. Soc.* **2007**, *129*, 10646.

[98] Bent, H. A. *Chem. Rev.* **1961**, *61*, 275.

General procedure

Starting materials, reagents and solvents were purchased from commercial suppliers (Sigma-Aldrich and Fischer). All reactions were conducted in oven-dried (145 °C) glassware under an inert atmosphere of dry argon. The progress of reactions was monitored by silica gel thin layer chromatography (TLC)[99] plates (pore size 60Å, 250 μm layer thickness, glass support, with fluorescent indicator, Silicycle) visualized under 254 nm UV and charred using vanillin[100] or *p*-anisaldehyde stain[101] . Products were purified by flash column chromatography (FCC) on 230-400 mesh, pore size 60Å, Silicycle, ultra pure silica gel. Infrared (FTIR) spectra were recorded on an ATI MattsonGenesis Series FT-Infrared spectrophotometer. Characterized reactant products were homogeneous by TLC. Proton nuclear magnetic resonance spectra ^{1}H NMR were recorded on either a Varian-400 *I-Nova* (400 MHz), or a Varian-500 *I-Nova* (500 MHz). Data are reported as follows: chemical shift, integration, multiplicity (s = singlet, d = doublet, t = triplet, qt = quartet, q = quintet, n = nonet, td = triplet of a doublet, dt = doublet of a triplet, b = broad, m = multiplet), and coupling constants in Hz. ^{13}C NMR were recorded on either a Varian-300 instrument (75 MHz) or a Varian-400 instrument (100 MHz). Chemical shifts are reported in ppm relative to tetramethylsilane (TMS) as the internal standard, Mass spectra were recorded on a Finnigan LCQ-DUO.

---

100 LeRosen, A. L.; Moravek, R. T.; Carlton, J. K. *Anal. Chem.*,**1952**, *24*, 1335
101 Stahl, E.; Kaltenbach, U. *J. Chromatogr. A*, **1961**, *5*, 351

Computational Experimental Details

Electronic structure calculations, based on density functional theory (DFT), were carried out with the Gaussian 03 suite[1] of programs. We utilized the B3LYP functional [2] with 6-31++g(d,p), 6-31+g(d,p), 6-31g(2d,2p), and 6-31g(d,p) basis sets.[3] General solvent effects were incorporated with the polarizable conductor self-consistent reaction field model (CPCM).[4] All transition states were verified by observing the nature of the negative imaginary frequency.

(1) Gaussian 03, Revision E.01,
M. J. Frisch, G. W. Trucks, H. B. Schlegel, G. E. Scuseria,
M. A. Robb, J. R. Cheeseman, J. A. Montgomery, Jr., T. Vreven,
K. N. Kudin, J. C. Burant, J. M. Millam, S. S. Iyengar, J. Tomasi,
V. Barone, B. Mennucci, M. Cossi, G. Scalmani, N. Rega,
G. A. Petersson, H. Nakatsuji, M. Hada, M. Ehara, K. Toyota,
R. Fukuda, J. Hasegawa, M. Ishida, T. Nakajima, Y. Honda, O. Kitao,
H. Nakai, M. Klene, X. Li, J. E. Knox, H. P. Hratchian, J. B. Cross,
V. Bakken, C. Adamo, J. Jaramillo, R. Gomperts, R. E. Stratmann,
O. Yazyev, A. J. Austin, R. Cammi, C. Pomelli, J. W. Ochterski,
P. Y. Ayala, K. Morokuma, G. A. Voth, P. Salvador, J. J. Dannenberg,
V. G. Zakrzewski, S. Dapprich, A. D. Daniels, M. C. Strain,
O. Farkas, D. K. Malick, A. D. Rabuck, K. Raghavachari,
J. B. Foresman, J. V. Ortiz, Q. Cui, A. G. Baboul, S. Clifford,
J. Cioslowski, B. B. Stefanov, G. Liu, A. Liashenko, P. Piskorz,

I. Komaromi, R. L. Martin, D. J. Fox, T. Keith, M. A. Al-Laham,

C. Y. Peng, A. Nanayakkara, M. Challacombe, P. M. W. Gill,

B. Johnson, W. Chen, M. W. Wong, C. Gonzalez, and J. A. Pople,

Gaussian, Inc., Wallingford CT, 2004.

(2) Becke, A.D. *J. Chem. Phys.* **1993**, *98*, 5648; Lee, C.; Yang, W.; Parr, R.G. *Phys. Rev. B.* **1988**, *37*, 785.

(3) Ditchfield, R.; Hehre, W.J.; Pople, J.A. *J. Chem. Phys.* **1971**, *54*, 721. Hariharan, P.C.; Pople, J.A. *Mol. Phys.* **1974**, *27*, 209. Krishnan, R.; Binkley, J.S.; Seeger, R.; Pople, J.A. *J. Chem. Phys.* **1980**, *72*, 650. McLean, A.D.; Chandler, G.S. *J. Chem. Phys.* **1980**, *72*, 5639. Clark, T.; Chandrasekhar, J.; Spitznagel, G.W.; Schleyer, P.v.R. *J. Comp. Chem.* **1983**, *4*, 294.

(4) Cossi, M.; Barone, V. *J. Phys. Chem. A* **1998**, *102*, 1995.

Experimental Chapter 1:

Protocol for the formation of triflates:

One of two methods was employed for the formation of the vinyl triflates used in this work. First the use of a stoichiometric amide base such as NaHMDS or LDA for the deprotonation of the corresponding ketone and than treatment with (bis)trifilamide.[102] Second we used 2,6-ditertbutyl-3-methylpyrindine for deprotonation of the carbonyl compound and then treatment of the enolate with triflic anhydride.[103]

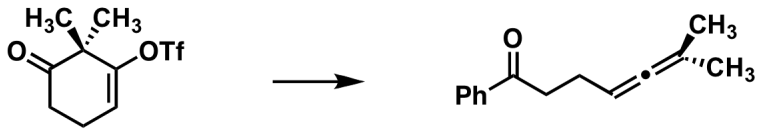

1.8 **1.9a**

6-methyl-1-phenylhepta-4,5-dien-1-one (1.9a): To an oven dried round bottom flask (15 ml) equipped with a magnetic stir bar and septum was added dry ether (1.3 ml) and vinyl triflate **1.8** (70 mg, 0.258 mmol) under an argon atmosphere. The reaction mixture was cooled to -78 ºC, and 1.8 M phenyl lithium (145 μl, 0.290 mmol) was added dropwise via syringe. The reaction mixture was stirred for 1 h at -78 ºC and additional 1 h at rt. The reaction mixture was dried *in vacuo* and subjected to flash column chromatography (hexanes 98 %: ethyl acetate 2%) to provide a colorless oil (39 mg, 76 %); IR ν_{max}(KBr)/cm^{-1} 2907, 1967, 1687, 1597 δ_H (500 MHz, $CDCl_3$) 7.97 (2H, d, J = 8.0 Hz), 7.56 (1H, t, J = 7.34 Hz), 7.47 (2H, t, J = 7.6 Hz), 5.09 (1H, n, J = 2.8 Hz), 3.06 (2H, t, J = 6.9 Hz), 2.43 (2H, qt, J = 7.03), 1.58 (3H, s), 1.57 (3H, s); δ_C (125 $CDCl_3$, MHz) 201.9,

[102] Stang, P. J.; Treptow, W. *Synthesis* **1980**, *4*, 283.

[103] McMurry, J. E.; Scott, W. J. *Tetrahedron Lett*. **1983**, *24*, 979.

199.9, 137.5, 133.0, 128.7, 128.2, 96.9, 88.2, 37.4, 23.9, 20.8; (ESI/MS) *m/z* Calcd for $C_{28}H_{32}NaO_2$: 423.2 [M x 2 + Na]; found: 423.2

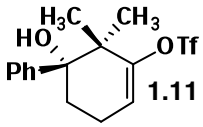

1.11

1.11 was isolated in 20 % yield when the reaction was quenched after stirring for 20 min at -78 ºC. IR ν_{max}(KBr)/cm^{-1} 3447, 2909, 1447; δ_H (500 MHz, $CDCl_3$) 7.53 (2H, d, *J* =7.6 Hz), 7.38 (2H, t, *J* = 8.0 Hz), 7.31 (1H, t, *J* = 7.0 Hz), 5.83 (1H, dd, *J* = 2.5 Hz), 2.61 (1H, m), 2.53 (1H, m), 2.35(1H, dt, *J* = 8.6 Hz), 1.88 (1H, s), 1.78 (1H, m), 1.14 (3H, s), 0.97 (3H, s); δ_C (125 $CDCl_3$, MHz) 154.5, 143.3, 127.9, 127.7, 127.3, 115.7, 77.8, 44.2, 30.5, 25.8, 20.7, 18.1; (ESI/MS) *m/z* Calcd for $C_{15}H_{17}F_3NaO_4S$: 372.9 [M + Na]; found: 372.9.

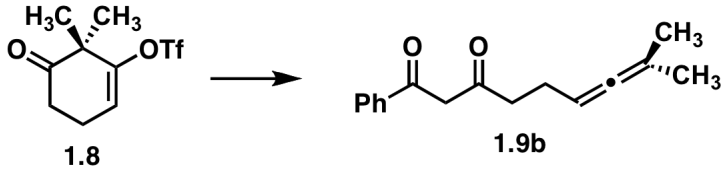

8-methyl-1-phenylnona-6,7-diene-1,3-dione (1.9b): To an oven dried round bottom flask (15 ml) equipped with a magnetic stir bar and septum was added dry THF (1.3 ml) and acetophenone (67 μl, 0.573 mmol). At -78 ºC, 1.0 M NaHMDS (620 μl, 0.617 mmol) was added dropwise and stirred for 45 min. A solution of vinyl triflate **1.8** (120 mg, 0.441 mmol) in 1 ml of dry THF was added dropwise. The reaction mixture was stirred for an additional 1 h at -78 ºC, and 1 h at rt. The reaction mixture was then dried *in vacuo* and subjected to flash column chromatography (hexanes 95 %: ethyl acetate 5%) to provide a colorless oil (83 mg, 78 %). IR ν_{max}(KBr)/cm^{-1} 3438, 2916, 1967, 1603; δ_H (500 MHz, $CDCl_3$) 7.89 (2H, d, *J* = 7.9 Hz), 7.53 (1H, t, *J* = 7.4 Hz), 7.46 (2H, t, *J* = 7.9 Hz), 5.05

(1H, n, J = 2.9 Hz), 2.54 (1H, t, J = 7.4 Hz), 2.36 (2H, d, J = 6.9 Hz), 1.65 (3H, s), 1.64 (3H, s); δ_C (125 $CDCl_3$, MHz) 202.1, 197.2, 182.9, 135.2, 132.4, 128.9, 128.2, 97.1, 96.5, 87.8, 38.6, 25.2, 20.9; (ESI/MS) *m/z* Calcd for $C_{32}H_{36}NaO_4$: 507.2 [M x 2 + Na]; found: 507.2.

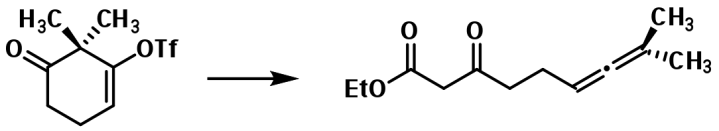

7 **8c**

Ethyl 8-methyl-3-oxonona-6,7-dienoate (1.9c): To an oven dried round bottom flask (15 ml) equipped with a magnetic stir bar and septum was added dry THF (1.8 ml) and ethyl acetate (77 μl, 0.872 mmol). At -78 ºC, 1.0 M NaHMDS (837 μl, 0.837 mmol) was added dropwise and stirred for 45 min. A solution of vinyl triflate **1.8** (95 mg, 0.350 mmol) in 1 ml of dry THF was added dropwise. The reaction mixture was stirred for an additional 1 h at -78 ºC, and 1 h at rt. The reaction mixture was dried *in vacuo* and subjected to flash column chromatography (hexanes 95%: ethyl acetate 5%) to provide a colorless oil (61 mg, 83 %). IR ν_{max}(neat)/cm^{-1} 2981, 1968, 1744, 1717; δ_H (500 MHz, $CDCl_3$) 4.99 (1H, n, J = 2.9 Hz), 4.18 (2H, qt, J = 6.9 Hz), 3.43 (2H, s), 2.61 (2H, t, J = 6.8 Hz), 2.26 (2H, qt, J = 6.9 Hz), 1.65 (3H, s), 1.63 (3H, s), 1.27 (3H, t, J = 7.0); δ_C (125 MHz, $CDCl_3$) 202.4, 201.9, 167.5, 97.1, 87.7, 81.5, 49.6, 41.9, 23.2, 20.8, 14.3; (ESI/MS) *m/z* Calcd for $C_{24}H_{36}NaO_6$: 443.2 [M x 2 + Na]; found: 443.2.

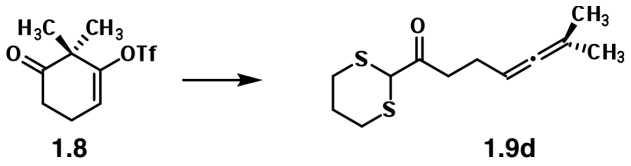

1.8 **1.9d**

1-(1,3-dithian-2-yl)-6-methylhepta-4,5-dien-1-one (1.9d): To an oven dried round bottom flask (15 ml) equipped with a magnetic stir bar and septa was added dry THF (1.9 ml) and dithiane (56 mg, 0.463 mmol). At -40 ºC, 2.5 M *n*-butyllithium (170 μl, 0.424 mmol) was added dropwise gradually warmed to -20 ºC over the course of 1 h. The solution was cooled to -78 ºC and vinyl triflate **1.8** (105 mg, 0.386 mmol) in 1 ml of dry THF was added dropwise. The reaction mixture was stirred for an additional 1 h at -78 ºC, and 1 h at rt. The reaction mixture was dried *in vacuo* and subjected to flash column chromatography (hexanes 95%: ethyl acetate 5%) to provide a colorless oil (81 mg, 87 %). IR ν_{max}(neat)/cm^{-1} 3425.0, 2905, 1995, 1711, 1213; δ_H (500 MHz, $CDCl_3$) 5.02 (1H, n, J = 2.9 Hz), 4.26 (1H, s), 3.23 (2H, t, J = 6.4 Hz), 2.76 (2H, t, J = 7.4 Hz), 2.60 (2H, ddd, J = 2.7 Hz), 2.29 (2H, qt, J = 2.9 Hz), 2.06 (2H, m), 1.68 (3H, s), 1.67 (3H, s); δ_C (125 MHz, $CDCl_3$) 202.6, 201.8, 97.1, 87.8, 47.4, 39.5, 26.6, 25.5, 23.8, 20.9; (ESI/MS) *m/z* Calcd for $C_{24}H_{36}NaO_2S_4$: 507.0 [M x 2 + Na]; found: 507.0.

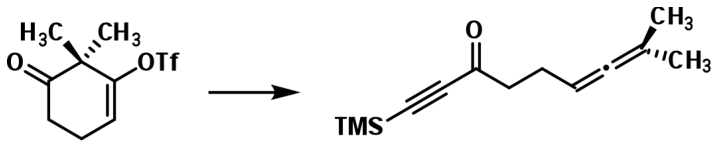

1.8 **1.9e**

8-methyl-1-(trimethylsilyl)nona-6,7-dien-1-yn-3-one (1.9e): To an oven dried round bottom flask (15 ml) equipped with a magnetic stir bar and septa was added dry THF (2.2 ml) and ethynyltrimethylsilane (75 μl, 0.529 mmol). At -78 ºC, 2.5 M *n*-butyllithium (194 μl, 0.485 mmol) was added dropwise and maintained at 0 ºC for 10 min. The solution was cooled to -78 ºC and vinyl triflate **1.8** (105 mg, 0.386 mmol) in 1 ml of dry THF was added dropwise. The reaction mixture was stirred for an additional 1 h at -78 ºC, and 1 h at rt. The reaction mixture was dried *in vacuo* and subjected to flash column chromatography (hexanes 95%: ethyl acetate 5%) to provide a colorless oil (73 mg, 75 %). IR ν_{max}(neat)/cm^{-1} 2979, 2153, 1968, 1734, 1210; δ_H (500 MHz, $CDCl_3$) 5.01 (2H, n, J = 2.9 Hz), 2.64 (2H, t, J = 7.0 Hz), 2.34 (2H, qt, J = 7.0Hz), 1.67 (3H, s), 1.6 (3H, s), 0.25 (9H, s); δ_C (125 MHz, $CDCl_3$) 201.2, 187.5, 102.3, 97.6, 97.5, 87.5, 44.2, 23.8, 50.8, -0.4; (ESI/MS) *m/z* Calcd for $C_{13}H_{20}NaOSi$: 243.1 [M + Na]; found 243.1.

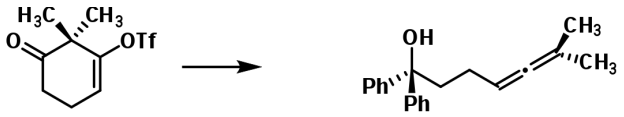

1.8 **1.10a**

6-methyl-1,1-diphenylhepta-4,5-dien-1-ol (1.10a): To a flamed dried round bottom flask (15 ml) equipped with a magnetic stir bar and septum, anhydrous $CeCl_3$[104] (360 mg, 1.466 mmol) was dispensed in an argon glove bag. The reaction flask was then gradually warmed to 130-145 ºC over 30 min and held at that range for 30 min. The flask was

104 For a detailed procedure on the preparation of anhydrous $CeCl_3$ used here see: Ballentine, S.; Hart, D. J. *Org. Syn., Coll. Vol. 10,* **2004**, 200 .

cooled to rt, dry THF (1 ml) was added and the flask was sonicated for 1 h. At -78 ºC, 1M phenylmagnesium bromide in ether (1.466 ml, 1.466 mmol) was added dropwise and stirred for 45 min. Vinyl triflate **1.8** (133 mg, 0.489 mmol) in 1 ml of dry THF was then added dropwise. The reaction mixture was stirred for an additional 1 h at -78 ºC, and 1 h at rt. The reaction was quenched with saturated $NaHCO_3$ (10 ml) and extracted with ethyl acetate (3 X 15 ml), the organic portion was dried over Na_2SO_4. The resultant extract was dried *in vacuo* subjected to flash column chromatography (hexanes 95%: ethyl acetate 5%) to provide a colorless oil (117 mg, 86 %). IR ν_{max}(neat)/cm^{-1} 3473, 2932, 1965, 1446; δ_H (500MHz, $CDCl_3$) 7.43 (4H, d, *J* = 8.0 Hz), 7.33 (4H, d, *J* = 8.2 Hz), 7.24 (2H, d, *J* = 6.6 Hz), 5.01 (1H, n, *J* = 2.8 Hz), 2.40 (2H, t, *J* = 8.0 Hz), 2.29 (1H, s), 1.98 (2H, qt, *J* = 8.6), 1.70 (3H, s), 1.69 (3H,s); δ_C (125 MHz, $CDCl_3$) 201.8, 147.3, 128.4, 127.0, 126.3, 96.0, 89.0, 78.6, 41.3, 24.2, 20.9; (ESI/MS) *m/z* Calcd for $C_{40}H_{44}NaO_2$: 578.9 [M x 2+ Na]; found: 578.9.

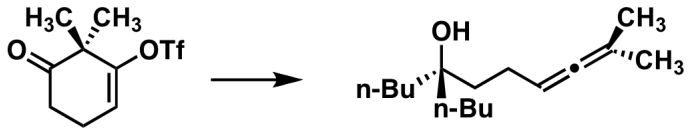

1.8 **1.10b**

5-butyl-10-methylundeca-8,9-dien-5-ol (1.10b): To a flamed dried round bottom flask (15 ml) equipped with a magnetic stir bar and septum, anhydrous $CeCl_3$[6] (299 mg, 1.212 mmol) was dispensed in an argon glove bag. The reaction flask was the gradually warmed to 130-145 ºC over 30 min and held at that range for 30 min. The flask was cooled to rt, dry THF (1 ml) was added and the flask was sonicated for 1 h. At -78 ºC, 2.5 M *n*-

butyllithium (485 μl, 1.212 mmol) was added dropwise and stirred for 45 min. Vinyl triflate **1.8** (110 mg, 0.404 mmol) in 1 ml of dry THF was then added dropwise. The reaction mixture was stirred for an additional 1 h at -78 ºC, and 1 h at rt. The reaction was quenched with satuarated $NaHCO_3$ (10 ml) and extracted with ethyl acetate (3 X 15 ml), the organic portion was dried over Na_2SO_4. The resultant extract was dried *in vacuo* subjected to flash column chromatography (hexanes 95 %: ethyl acetate 5%) to provide a colorless oil (78 mg, 81 %). IR ν_{max}(neat)/cm^{-1} 3403, 2932, 1967; δ_H (500 MHz, $CDCl_3$) 4.98 (2H, n, J = 2.9 Hz), 1.98 (2H, m), 1.68 (3H, s), 1.67 (3H, s), 1.63 (1H, bs), 1.52 (2H, m), 1.43 (4H, m), 1.28 (8H, m), 0.91 (6H, t, J = 7.2 Hz); δ_C (125 MHz, $CDCl_3$) 201.7, 95.7, 89.3, 74.7, 39.2, 38.8, 26.0, 23.8, 23.6, 21.0, 14.3; (ESI/MS) *m/z* Calcd for $C_{32}H_{60}NaO_2$: 500.1 [M x 2+ Na]; found: 500.1.

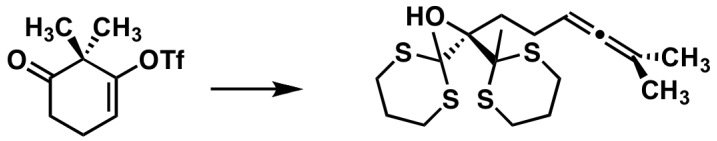

1.8 **1.10c**

6-methyl-1,1-bis(2-methyl-1,3-dithian-2-yl)hepta-4,5-dien-1-ol (1.10c): To an oven dried round bottom flask (15 ml) equipped with a magnetic stir bar and septum was added dry THF (2.1 ml) and methyldithiane (111 mg, 0.826 mmol). At -20 ºC, 2.5 M *n*-butyllithium (0.294 μl, 0.735 mmol) was added dropwise, warmed to 22 ºC and stirred for 30 min. The solution was cooled to -78 ºC and vinyl triflate **1.8** (50 mg, 0.184 mmol) in 1 ml of dry THF was added dropwise. The reaction mixture was stirred at rt for 15 min at which time TLC indicated the consumption of the starting material. The reaction mixture

was dried *in vacuo* and subjected to flash column chromatography (hexanes 95 %: ethyl acetate 5%) to provide a colorless oil (57 mg, 79 %). IR ν_{max}(neat)/cm^{-1} 3744, 2927, 1966, 1444, 1275; δ_H (400 MHz, $CDCl_3$) 5.02 (1H, n, *J* = 2.9 Hz), 3.45 (1H, s), 2.91 (8H, m), 2.34 (4H, m), 2.05 (6H, s), 1.93 (4H, m), 1.69 (6H, d, *J* = 2.9 Hz); δ_C (100 MHz, $CDCl_3$) 201.7, 95.27, 89.0, 85.7, 65.1, 34.4, 28.0, 27.6, 27.5, 27.2, 24.6, 21.1; (ESI/MS) *m/z* Calcd for $C_{18}H_{30}NaOS_4$: 413.1 [M+Na]; found: 413.2 .

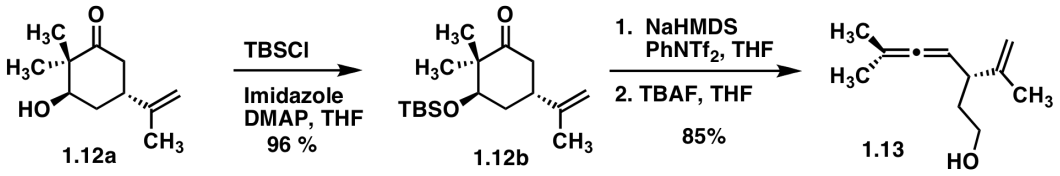

(R)-6-methyl-3-(prop-1-en-2-yl)hepta-4,5-dien-1-ol (1.12): Keto alcohol **1.12** was protected using TBSCl, Imidazole and DMAP in THF. 96 %; IR ν_{max}(neat)/cm^{-1} 2973, 1966, 1413, 1212; δ_H (500 MHz, $CDCl_3$) 4.77 (1H, m), 4.71 (1H, m), 3.83 (m, 1H), 2.84 (1H, m), 2.51 (1H, m), 2.32 (1H, m), 2.05 (1H, m), 1.83 (1H, m), 1.73 (3H, s), 0.90 (6H, s), 0.84 (9H, bs), 0.03 (3H, s), 0.02 (s, 3H); δ_C (125 MHz, $CDCl_3$) 215.3, 147.9, 110.1, 78.5,50.4, 42.4, 39.5, 34.1, 26.0, 24.7, 21.6, 18.2; (ESI/MS) *m/z* Calcd for $C_{17}H_{33}O_2Si$: 297.2 [M+H]; found: 297.2. Unstable triflate **1.12b** was synthesized and flushed through silica gel with hexanes and utilized for the next step without further purification.

To an oven dried round bottom flask (10 ml) equipped with a magnetic stir bar and septum was added dry THF (0.580 ml) and vinyl triflate **1.12** (50 mg, 0.117 mmol). At 0 ºC, was added 1 M TBAF in THF *cf.* 5 % H_2O (0.233 ml, 0.233 mmol) drop wise and warmed to 22 ºC and stirred 1 h. At which time TLC indicated consumption of the starting

material. The flask was then charged with 2 ml of MeOH[105] and excess $NaBH_4$ was added. When the bubbling subsided the reaction mixture was dried *in vacuo* and subjected to flash column chromatography (hexanes 95 %: ethyl acetate 5%) to provide a colorless oil (17 mg, 75 %). IR ν_{max}(neat)/cm^{-1} 3416, 2973, 1966, 1413, 1212; δ_H (500 MHz, $CDCl_3$) 4.89 (1H, m), 4.80 (1H, m), 4.76 (1H, m), 3.67 (2H, t, *J* = 6.4 Hz), 2.82 (1H, qt, *J* = 7.4 Hz), 1.73 (2H, m), 1.71 (3H, s), 1.70 (6H, s), 1.69 (1H, bs); δ_C (125 MHz, $CDCl_3$) 201.7, 148.0, 111.0, 96.7, 91.9, 61.8, 44.4, 35.3, 21.0, 20.8, 19.5; (ESI/MS) *m/z* Calcd for $C_{11}H_{19}O$: 167.2 [M+H]; found 167.2.

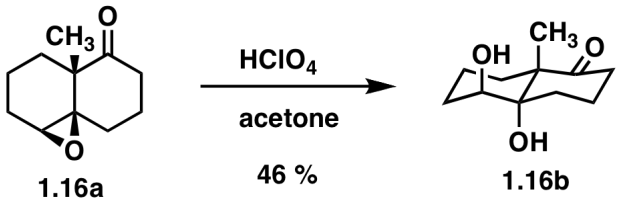

1.16a 1.16b

(4aS,5S,8aS)-4a,5-dihydroxy-8a-methyloctahydronaphthalen-1(2H)-one (1.16b):

To the solution of the epoxide **1.16** (740 mg, 4.1 mmol) in acetone (10 mL) at 0 °C, was added conc $HClO_4$ (1 ml) dropwise and stirred at that temperature for 1 h. The reaction was then neutralized with 10% NaOH. Acetone was evaporated and the reaction mixture was dissolved in water (50 mL) and extracted with EtOAc (3 x 100 mL). The combined organic layer was washed with brine (50 mL), dried *in vacuo* and subjected to flash column chromatography (hexanes 20 %: ethyl acetate 80%) to give the diol **1.16b** (370 mg, 46% yield) as white crystal. IR ν_{max}(neat)/cm^{-1} 3444, 2927, 2871, 1697, 1456, 1089, 961; δ_H (400 MHz, CD_3OD) 3.51 (1H, t, *J* = 2.8 Hz), 2.80-2.63 (1H, m), 2.62-2.50 (1H, m), 2.20-1.71 (6H, m), 1.60-1.50 (1H, m), 1.49-1.41 (1H, m), 1.41-1.33 (1H, m), 1.38

105 Note: The aldehyde was reduced *in situ* due to its inherent instability to silica chromatography.

(3H, d, J = 0.5 Hz), 1.31-1.23 (1H, m); δ_C (100 MHz, CD_3OD) 219.0, 77.8, 76.3, 53.0, 37.2, 30.8, 29.6, 28.4, 21.4, 20.8, 17.1; (ESI/MS) m/z Calcd for $C_{11}H_{18}NaO_3$: 221.1 [M+Na]; found: 221.1.

The stereochemistry of the diol **1.16b** was confirmed by x-ray crystallography. Slow evaporation of a sample of diol **1.16b** in minimum amount of EtOAc gave crystals suitable for X-ray analysis. CCDC 741826 contains the supplementary crystallographic data for diol **1.16b**. These data can be obtained free of charge from The Cambridge Crystallographic Data Centre via www.ccdc.cam.ac.uk/data_request/cif.

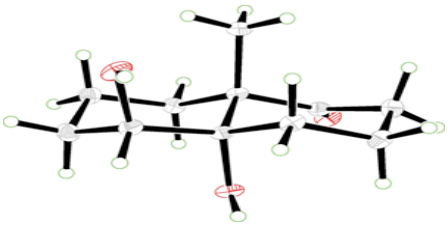

Figure 1.0 Crystal Structure of diol 1.16b

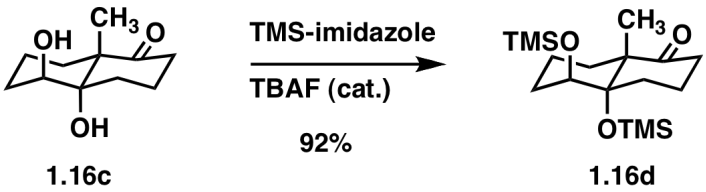

1.16c **1.16d**

(4aS,5S,8aS)-8a-methyl-4a,5-bis(trimethylsilyloxy)octahydronaphthalen-1(2H)-one (1.16d):

Diol **1.16c** (87mg, 0.439 mmol) was dissolved in 0.6 mL 1-(trimethylsilyl)-1H-imidazole at room temperature. Then two drops of TBAF (1.0 M solution in THF) was added. Reaction was stirred at room temperature for 2 h. The reaction was then quenched with water (30 mL), and extracted with DCM (3 x 30 mL). The combined organic phase was washed with water (20 mL), brine (20 mL) and dried over anhydrous Na_2SO_4. Evaporation of solvent and FCC purification using 5% EtOAc in hexanes gave di silyl ether **1.16d** (138 mg, 92% yield) as a colorless oil. IR ν_{max}(neat)/cm^{-1} 2954, 2872, 1716, 1455, 1251, 948, 840, 753; δ_H (500 MHz, $CDCl_3$) 3.64 (1H, t, *J* = 2.5 Hz), 2.62 (1H, ddd, *J* = 15.4, 11.2, 9.1 Hz), 2.45 (1H, ddd, *J* = 14.3, 11.9, 7.2 Hz), 2.21-2.14 (1H, m), 2.00-1.87 (3H, m), 1.84 (1H, ddd, *J* = 14.1, 4.6, 3.0 Hz), 1.81-1.68 (1H, m), 1.49-1.39 (2H, m), 1.40-1.22 (2H, m), 1.31 (3H, s), 0.12 (9H, s), 0.10 (9H, s); δ_C (125 MHz, $CDCl_3$) 216.4, 82.5, 75.1, 53.4, 35.7, 29.4, 29.2, 27.4, 21.0, 20.0, 16.0, 2.8(3), 0.4(3); ESI/MS) *m/z* Calcd for $C_{17}H_{34}NaO_3Si_2$: 365.2 [M+Na]; found 365.2.

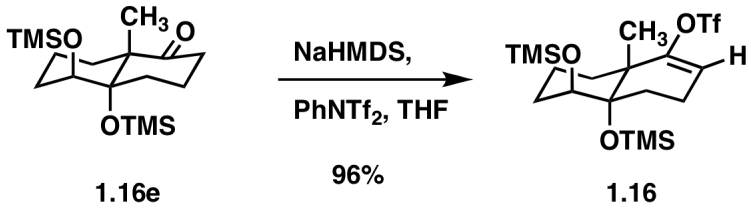

(4aS,5S,8aS)-8a-methyl-4a,5-bis(trimethylsilyloxy)-3,4,4a,5,6,7,8,8a-octahydronaphthalen-1-yl trifluoromethanesulfonate (1.16): 92%; IR ν_{max}(neat)/cm^{-1} 2955, 2873, 1416, 1209, 1088, 942, 840, 754; δ_H (500 MHz, $CDCl_3$) 5.49 (1H, t, *J* = 3.7 Hz), 3.70 (1H, t, *J* = 2.7 Hz), 2.30-2.15 (3H, m), 1.98 (1H, dtd, *J* = 11.2, 5.2, 2.7 Hz), 1.89 (1H, td, *J* = 13.1, 3.4 Hz), 1.82-1.69 (1H, m), 1.50-1.41 (2H, m), 1.4-1.32 (2H, m), 1.35

(3H, s), 0.12 (9H, s), 0.10 (9H, s); δ_C (125 MHz, $CDCl_3$) 156.8, 118.7 (1C, q, *J* = 320 Hz), 112.7 (1C, d, *J* = 0.9 Hz), 78.8, 74.8, 44.0, 29.2, 27.6, 26.6, 23.7, 20.9, 16.1, 2.6(3), 0.3(3); ESI/MS) *m/z* Calcd for $C_{15}H_{26}F_3O_6SSi$: 419.1 [M+H_2O-TMS]; found 419.5.

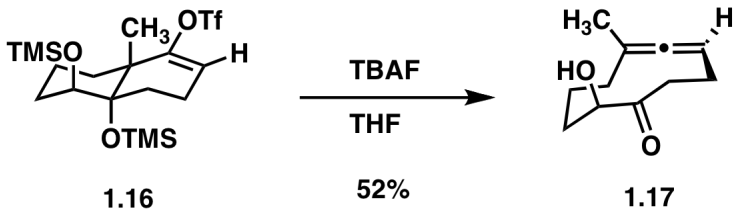

1.16 1.17

(5R,10S)-10-hydroxy-6-methylcyclodeca-4,5-dienone (1.17): To a solution of triflate **15** (60 mg, 0.126 mmol) in THF (1 mL), was added TBAF (1.0 M, 0.50 mL, 0.50 mmol) in one portion and stirred at rt for 15 min. The reaction was then quenched with saturated NH_4Cl (20 mL) and extracted with Et_2O (3 x 20 mL). The combined organic phase was washed with brine (5 mL) and dried over anhydrous Na_2SO_4. Evaporation of solvent and FCC purification using 20% EtOAc in hexanes gave allene **16** (12 mg, 52% yield) as a colorless oil. IR ν_{max}(neat)/cm^{-1} 3417, 2925, 2855, 1964, 1705, 1445, 1043, 926, 774; δ_H (500 MHz, $CDCl_3$) 5.13-5.07 (1H, m), 4.21 (1H, dt, *J* = 7.3, 3.6 Hz), 3.33 (1H, d, *J* = 3.5 Hz), 2.73-2.64 (2H, m), 2.61-2.53 (1H, m), 2.28-2.17 (2H, m), 2.17-2.09 (1H, m), 2.04-1.96 (1H, m), 1.94-1.87 (1H, m), 1.87-1.77 (1H, m), 1.60-1.50 (1H, m), 1.57 (3H, d, *J* = 2.9 Hz); δ_C (125 MHz, $CDCl_3$) 211.7, 203.3, 102.0, 88.4, 34.7, 34.4, 32.3, 23.5, 18.7, 17.9; ESI/MS) *m/z* Calcd for $C_{11}H_{16}NaO_2$: 203.1 [M+Na]; found 203.1.

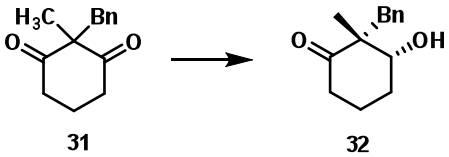

31 32

(2*R*,3*R*)-2-benzyl-3-hydroxy-2-methylcyclohexanone (32): Modified CBS reduction[8] of diketone **31** utilizing oxazoborolidinone-*S* catalyst provided (2*R*,3*R*)-2-benzyl-3-hydroxy-2-methylcyclohexanone **32** in 72 % yield and 74 % ee; $[\alpha]_D^{25}$ -24.1 (*c* 3.0, $CHCl_3$); IR ν_{max}(neat)/cm^{-1} 3444, 3060, 3028, 2941, 2873,1697,1602, 1495, 1452, 1065, 1032, 993, 705; δ_H (500 MHz, $CDCl_3$) 7.29-7.13 (5H, m), 3.75 (1H, m), 3.10 (1H, d, *J* = 13.7 Hz), 2.96 (1H, d, *J* = 13.7 Hz), 2.55 (2H, t, *J* = 6.9 Hz), 2.12 (1H, m), 2.05 (1H, m), 1.86 (1H, m), 1.76 (1H, m), 1.06 (3H, s) ; δ_C (500 MHz, $CDCl_3$) 214.4, 137.8, 130.7, 128.3, 126.6, 75.9, 54.8, 38.0, 37.6, 28.7, 20.9, 20.5, ; (ESI/MS) *m/z* Calcd for $C_{14}H_{18}NaO_2$: 241.1 [M+Na]; found: 241.2.

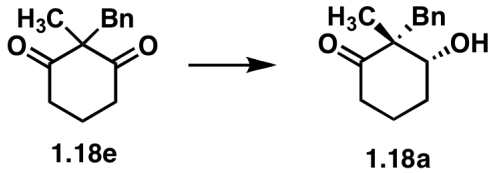

1.18e 1.18a

(2*S*,3*S*)-2-benzyl-3-hydroxy-2-methylcyclohexanone (1.18a): Modified CBS reduction[8] of diketone **1.18e** utilizing oxazoborolidinone-*R* catalyst provided (2*S*,3*S*)-2-benzyl-3-hydroxy-2-methylcyclohexanone **1.18a** in 69 % yield and 67 % ee; $[\alpha]_D^{25}$ + 18.6 (*c* 1.2, $CHCl_3$).

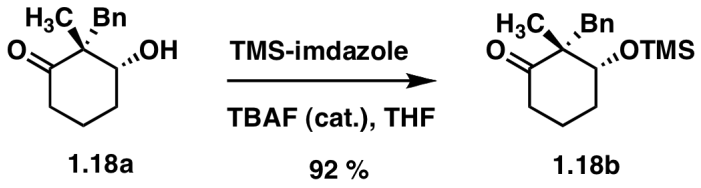

1.18a 1.18b

(2*S*,3*S*)-2-benzyl-2-methyl-3-(trimethylsilyloxy)cyclohexanone (1.18b): 92 %; ; $[\alpha]_D^{25}$ -43.2 (*c* 1.0, $CHCl_3$); IR ν_{max}(neat)/cm^{-1} 2953, 1708, 1495, 1453, 1251, 1079, 881, 840, 747, 702; δ_H (500 MHz, $CDCl_3$) 7.14 – 6.89 (m, 5H), 3.55 (t, 1H, *J* = 6.0 Hz), 2.91 (d, 1H, *J* = 13.9 Hz), 2.81 (d, 1H, *J* = 13.9 Hz), 2.45 (m, 1H), 2.31 (m, 1H), 1.88 (m, 1H), 1.75 (m, 2H), 1.47 (m, 1H), 0.82 (s, 3H), 0.00 (s, 9H); δ_C (500 MHz, $CDCl_3$) 213.8, 138.2, 130.2, 127.8, 127.6, 77.6, 56.0, 37.7, 29.4, 20.8, 20.1, 0.4 ; (ESI/MS) *m/z* Calcd for $C_{17}H_{26}NaO_2Si$: 313.5 [M+Na]; found 313.5.

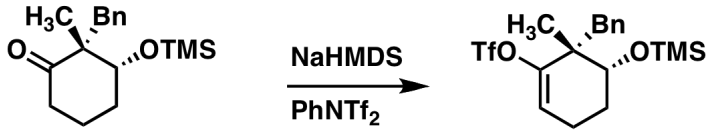

1.18c 1.18

(5*R*,6*R*)-6-benzyl-6-methyl-5-(trimethylsilyloxy)cyclohex-1-enyl trifluoromethanesulfonate (1.18): 93 %, $[\alpha]_D^{25}$ -32.5 (*c* 1.5, $CHCl_3$); IR ν_{max}(neat)/cm^{-1} 2955, 1676, 1495, 1454, 1413, 1251, 1211, 1144, 992, 840 ; δ_H (500 MHz, $CDCl_3$) 7.14 – 6.98 (5H, m), 5.58 (1H, m), 3.51 (1H, dd, *J* = 3.6, 11.0 Hz), 2.67 (2H, s), 1.92 (2H, m), 1.37 (1H, m), 1.25 (1H, m), 1.00 (3H, s), 0.01 (9H, s); δ_C (500 MHz, $CDCl_3$) 151.8, 137.7, 130.6, 129.6, 127.3, 125.7, 116.2, 75.3, 44.7, 39.3, 25.9, 22.7, 20.6, 0.0 ; (ESI/MS) *m/z* Calcd for $C_{18}H_{26}F_3O_4SSi$: 423.5 [M+H]; found 423.5.

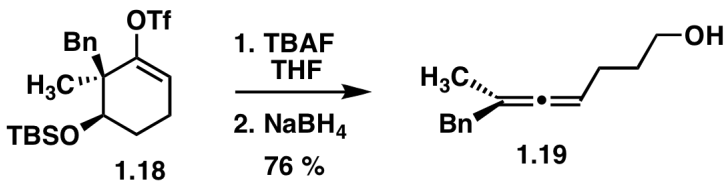

(*R*)-6-methyl-7-phenylhepta-4,5-dien-1-ol (1.19): To an oven dried round bottom flask (15 ml) equipped with a magnetic stir bar and septum was added dry THF (5 ml) and vinyl triflate **18** (270 mg, 0.64 mmol). At 0 ºC, was added 1 M TBAF in THF *cf*. 5 % H_2O (3.2 ml, 3.2 mmol) dropwise and warmed to 22 ºC and stirred for 1 h. At which time TLC indicated consumption of the starting material. The flask was then charged with 2 ml of MeOH [7] and excess $NaBH_4$ was added. When the bubbling subsided the reaction mixture was concentrated *in vacuo* and subjected to flash column chromatography (hexanes 95 %: ethyl acetate 5%) to provide a colorless oil 76 %, $[\alpha]_D^{25}$ +24.9 (*c* 1.2, $CHCl_3$); IR ν_{max}(neat)/cm^{-1} 3582, 3360, 2933, 1981, 1494, 1381, 1212, 1145, 1029, 665; δ_H (500 MHz, $CDCl_3$) 7.35 – 7.14 (5H, m), 5.02 (1H, m), 3.60 (2H, td, *J* = 1.8, 6.6 Hz), 3.26 (2H, s), 2.02 (2H, m), 1.64 (3H, d, *J* = 2.8 Hz), 1.61 (2H, t, *J* = 7.2 Hz); δ_C (500 MHz, $CDCl_3$) 202.8, 135.9, 129.8, 129.2, 128.4, 126.3, 99.8, 89.9, 62.8, 41.7, 32.4, 25.8, 19.2 ; (ESI/MS) *m/z* Calcd for $C_{14}H_{19}O$: 203.3 [M+H]; found: 203.3.

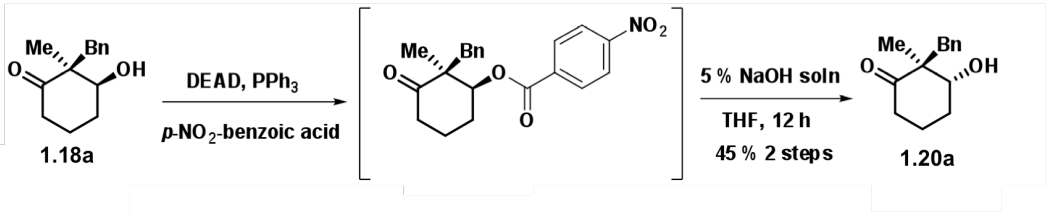

(2*S*,3*R*)-2-benzyl-3-hydroxy-2-methylcyclohexanone (1.20a). To alcohol **1.18a** (439 mg, 2.01 mmol) in 30 mL THF under argon was added triphenylphosphine (2.6 g, 10.05 mmol) and *p*-nitrobenzoic acid (1.68 g, 10.05 mmol). Then the solution was cooled to 0 ºC and DIAD (1.97 mL, 10.05 mmol) was added dropwise. The reaction was warmed to rt, and stirred at rt for 12 h, and then at 60 ºC for 4 h. The reaction mixture was cooled to rt and quenched with 3N HCl (10 mL). 15 mL water was added and extracted with ether (3 x 30 mL). The combined organic layer was washed with brine (20 mL), dried and concentrated *in vacuo* and subjected to flash column chromatography (hexanes 90 %: ethyl acetate 10%) to give the benzoate ester as a yellow oil. The benzoate ester was diluted with 5 mL THF and 10 mL 5 % aq. NaOH solution was added and stirred at 40 ºC for 12 h. The reaction mixture was cooled to rt and diluted with 10 mL $CHCl_3$ and washed with water, 1N HCl and brine. Organic layer was dried, and concentrated *in vacuo* and subjected to flash column chromatography (hexanes 85 %: ethyl acetate 15%) to yield Mitsunobu inverted 2*S*, 3*R* diastereomer[9] (195 mg, 45 %); $[\alpha]_D^{25}$ +24.7 (*c* 1.4, $CHCl_3$); δ_H (500 MHz, $CDCl_3$) 7.21 – 7.07 (5H, m), 3.72 (1H, m), 3.03 (1H, d, *J* = 13.6 Hz), 2.89 (1H, d, *J* = 13.6 Hz), 2.47 (2H, m), 2.04 (1H, m), 1.94 (1H, m), 1.79 (1H, m), 1.69 (1H, m), 0.97 (3H, m); δ_C (500 MHz, $CDCl_3$) 214.4, 137.9, 130.9, 128.3, 128.2, 75.9, 54.7, 37.9, 37.6, 28.7, 21.0, 20.5; (ESI/MS) *m/z* Calcd for $C_{14}H_{18}NaO_2$: 241.1 [M+Na]; found: 241.1.

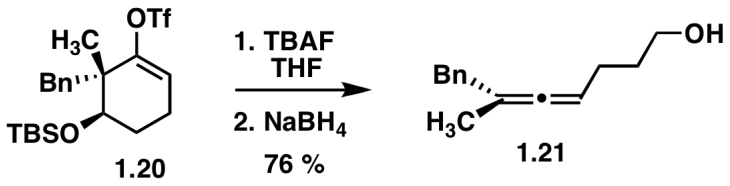

(*S*)-6-methyl-7-phenylhepta-4,5-dien-1-ol (1.21): 74 %, $[\alpha]_D^{25}$ -22.3 (*c* 0.9, $CHCl_3$). Mosher ester analysis of enantiomeric allenes **18** and **20** using ^1H, and ^{19}F NMR showed one enantiomer.

Typical procedure for mechanistic study:

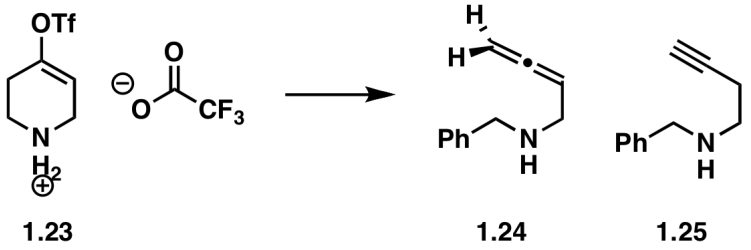

***N*-benzylbuta-2,3-dien-1-amine (1.22), *N*-benzylbut-3-yn-1-amine (1.25):** To an oven dried round bottom flask (15 ml) equipped with a magnetic stir bar and septum was added piperidinevinylOTf **1.23**, (220 mg, 0.637 mmol). Dry ether (6.40 ml) was added via syringe and under an argon atmosphere. The partially dissolved solid was cooled to -20 ºC at which time (1.05 μl, 3.19 mmol) of 3.0 M phenyl magnesium bromide in ether was

slowly added via syringe. The cooling bath was then removed and the turbid reaction mixture began to dissolve. After 1 h the reaction was quenched with saturated $NaHCO_3$ (5 ml). The reaction mixture was then added to a separatory funnel followed by ether (10 ml) and an additional portion of saturated $NaHCO_3$ (10 ml). The ethereal layer was separated and the organic layer was extracted with 3 X 10 ml portions of ether. The ethereal layers were combined and dried over anhydrous Na_2SO_4, filtered and dried *in vacuo*. Flash column chromatography of the resultant oil with (dichloromethane 97 % : $MeO^-NH_4^+$ 2%) as a solvent provided a slightly off white oil (85 mg, 84 %) of a combined mixture of allene **1.24** and alkyne **1.25**. **1.24** IR ν_{max}(KBr)/cm^{-1} 3374, 2922, 1955, 1454 δ_H (500 MHz, $CDCl_3$) 7.37 (4H, m), 5.18 (1H, q, *J* = 2.2 Hz), 4.89 (2H, dt, *J* = 6.6 Hz), 3.39 (2H, dt, *J* =2.2 Hz), δ_C (125 MHz, $CDCl_3$) 208.7, 140.1, 128.7, 128.5 127.2, 89.5, 76.3, 53.3, 47.4 ; (ESI/MS) *m/z* Calcd for $C_{11}H_{14}N$: 160.1 [M+H]; found: 160.1. **1.25** IR ν_{max}(KBr)/cm^{-1} 3307, 3063, 2918, 2098, 1203 δ_H (500 MHz, $CDCl_3$) 7.33 (4H, m), 3.85 (1H, q, *J* = 2.2 Hz), 2.84 (2H, t, *J* = 6.6 Hz), 2.43 (2H, td, 2.4 Hz), 2.2 (1H, bs), 2.08 (1H, td, *J* = 2.0 Hz); δ_C (125 MHz, $CDCl_3$) 140.2, 128.5, 127.5, 89.5, 76.3, 53.3, 47.4, 19.5; (ESI/MS) *m/z* Calcd for $C_{11}H_{14}N$: 160.1[M+H]; found: 160.1.

Computational Experimental Details

Electronic structure calculations, based on density functional theory (DFT), were carried out with the Gaussian 03 suite[10] of programs. We utilized the B3LYP functional[11] with 6-31+g(d)basis sets.[12] All transition states were verified by observing the nature of the negative imaginary frequency.

Calculated ground and TS states and ΔH for the piperidine halogen series.

4-bromo-1,2,3,6-tetrahydropiperidide

Center Number	Atomic Number	Atomic Type	Coordinates (Angstroms) X	Y	Z
1	6	0	0.710520	-1.201619	0.074192
2	6	0	2.260387	-1.200110	0.045420
3	7	0	2.870292	-0.011932	-0.419715
4	6	0	2.273680	1.086742	0.239832
5	6	0	0.732769	1.285120	-0.081701
6	6	0	0.066659	-0.044176	-0.009456
7	1	0	2.312730	1.020734	1.370740
8	1	0	2.776766	2.030370	-0.031938
9	1	0	0.606453	1.723222	-1.083262
10	1	0	0.283945	1.985642	0.642523

11	1	0	2.528825	-1.474509	1.116623
12	1	0	2.577034	-2.066754	-0.561225
13	1	0	0.190270	-2.153755	0.172204
14	35	0	-1.932347	-0.015348	-0.008497

SCF Done: E(RB+HF-LYP) = -2821.19494633

[8] Yeung, Y. -Y.; Chein, R. –J; Corey, E. J. *J. Am. Chem. Soc.* **2007**, *129*, 10346

[9] Carr, J. M.; Snowden, T. S. *Tetrahedron* **2008**, *64*, 2897

4-bromo-1,2,3,6-tetrahydropiperidide TS I

Center Number	Atomic Number	Atomic Type	Coordinates (Angstroms) X	Y	Z
1	6	0	0.811697	-1.092137	0.052705
2	6	0	2.379978	-1.264529	0.097830
3	7	0	3.072144	-0.154390	-0.462708
4	6	0	2.779366	0.966142	0.189199
5	6	0	0.825290	1.404901	-0.039666
6	6	0	0.306348	0.115235	0.015457
7	1	0	2.684305	0.960817	1.294275
8	1	0	3.229630	1.888317	-0.192921

9	1	0	0.739377	1.926407	-0.996569
10	1	0	0.628188	2.062749	0.811263
11	1	0	2.621654	-1.442665	1.171135
12	1	0	2.626780	-2.187616	-0.445563
13	1	0	0.220148	-2.000103	0.056345
14	35	0	-2.196319	-0.025853	-0.010062

Low frequencies --- -295.9546 -4.2714

Zero-point correction	0.106347 (Hartree/Particle)
Thermal correction to Energy	0.113565
Thermal correction to Enthalpy	0.114509
Thermal correction to Gibbs Free Energy	0.073168
Sum of electronic and zero-point Energies	-2821.075333
Sum of electronic and thermal Energies	-2821.068115
Sum of electronic and thermal Enthalpies	-2821.067171
Sum of electronic and thermal Free Energies	-2821.108512

SCF Done: E(RB+HF-LYP) = -2821.18167997

4-bromo-1,2,3,6-tetrahydropiperidide TS II

Center	Atomic	Atomic	Coordinates (Angstroms)		
Number	Number	Type	X	Y	Z

1	6	0	0.000000	0.000000	0.000000
2	6	0	0.000000	0.000000	2.017564
3	7	0	1.259301	0.000000	2.433321
4	6	0	1.956440	1.131256	1.933710
5	6	0	2.295206	0.977000	0.368390
6	6	0	1.110688	0.509359	-0.339151
7	1	0	1.382821	2.080253	2.019948
8	1	0	2.918727	1.266413	2.446604
9	1	0	3.122394	0.269236	0.235754
10	1	0	2.633831	1.952288	0.003286
11	1	0	-0.593832	0.933565	2.019239
12	1	0	-0.594456	-0.891066	2.243135
13	1	0	-0.882482	-0.395455	-0.474851
14	35	0	1.710816	0.786954	-2.819961

Low frequencies --- -315.3985 -8.1281 -0.0149 -0.0148 0.0080 11.4756

Zero-point correction	0.106624 (Hartree/Particle)
Thermal correction to Energy	0.113946
Thermal correction to Enthalpy	0.114890
Thermal correction to Gibbs Free Energy	0.073264
Sum of electronic and zero-point Energies	-2821.071594
Sum of electronic and thermal Energies	-2821.064272
Sum of electronic and thermal Enthalpies	-2821.063327
Sum of electronic and thermal Free Energies	-2821.104954

SCF Done: E(RB+HF-LYP) = -2821.17821776

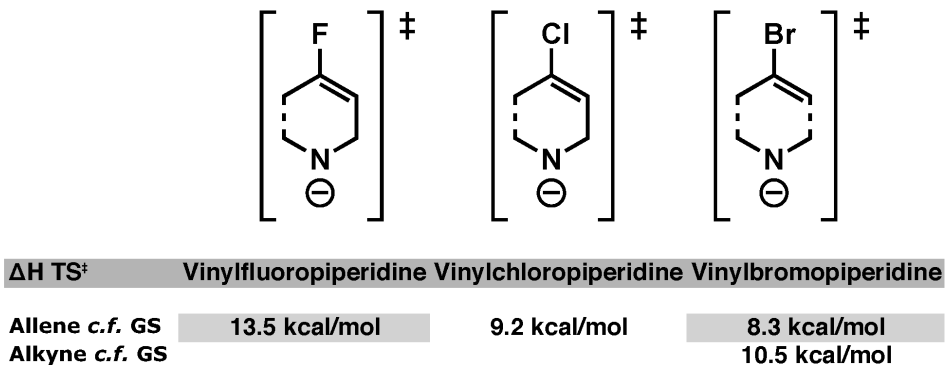

ΔH TS‡	Vinylfluoropiperidine	Vinylchloropiperidine	Vinylbromopiperidine
Allene *c.f.* GS	13.5 kcal/mol	9.2 kcal/mol	8.3 kcal/mol
Alkyne *c.f.* GS			10.5 kcal/mol

Figure 2 Calculated TS states and ΔH for the piperidine halogen series.

4-fluoro-1,2,3,6-tetrahydropiperidide

Center Number	Atomic Number	Atomic Type	Coordinates (Angstroms) X	Y	Z
1	6	0	0.298299	-1.228027	0.063618
2	6	0	-1.240698	-1.182022	0.047852
3	7	0	-1.816303	0.037989	-0.405098
4	6	0	-1.179540	1.121701	0.249647
5	6	0	0.353366	1.269124	-0.094785
6	6	0	0.969034	-0.084710	-0.029520
7	1	0	-1.670577	2.075077	-0.010625
8	1	0	-1.207856	1.053281	1.383299
9	1	0	0.860293	1.941042	0.622785
10	1	0	0.477609	1.703209	-1.099138

11	1	0	-1.600886	-2.024202	-0.568930
12	1	0	-1.530974	-1.455392	1.114333
13	1	0	0.823923	-2.178426	0.172570
14	9	0	2.373315	-0.084101	-0.022164

SCF Done: E(RB+HF-LYP) = -349.305781532

4-fluoro-1,2,3,6-tetrahydropiperidide TS (analogous to TS I)

Center Number	Atomic Number	Atomic Type	Coordinates (Angstroms) X	Y	Z
1	6	0	0.000000	0.000000	0.000000
2	6	0	0.000000	0.000000	1.524619
3	7	0	1.391286	0.000000	1.947007
4	6	0	1.896464	1.221373	1.849477
5	6	0	1.530265	1.963448	-0.147000
6	6	0	0.800738	0.858047	-0.675586
7	1	0	1.318384	2.089773	2.228541
8	1	0	2.978835	1.326248	1.979309
9	1	0	2.404527	2.264389	-0.731403
10	1	0	0.949440	2.813717	0.209306
11	1	0	-0.564353	0.870405	1.948510
12	1	0	-0.506401	-0.909746	1.878337
13	1	0	-0.415781	-0.857264	-0.526029
14	9	0	1.155214	0.469001	-2.003693

Low frequencies --- -321.1759 -22.3101 -15.8295

Zero-point correction	0.107617 (Hartree/Particle)
Thermal correction to Energy	0.113811
Thermal correction to Enthalpy	0.114755
Thermal correction to Gibbs Free Energy	0.077599
Sum of electronic and zero-point Energies	-349.176664
Sum of electronic and thermal Energies	-349.170469
Sum of electronic and thermal Enthalpies	-349.169525
Sum of electronic and thermal Free Energies	-349.206682

SCF Done: E(RB+HF-LYP) = -349.284280603

4-chloro-1,2,3,6-tetrahydropiperidide

Center Number	Atomic Number	Atomic Type	Coordinates (Angstroms) X	Y	Z
1	6	0	0.104118	-1.208530	0.067032
2	6	0	1.647929	-1.198314	0.044693
3	7	0	2.257402	-0.001891	-0.408749
4	6	0	1.646490	1.095164	0.246064
5	6	0	0.113297	1.284146	-0.091694
6	6	0	-0.547745	-0.052465	-0.018175
7	1	0	1.676180	1.028545	1.378322
8	1	0	2.152609	2.039426	-0.018544

9	1	0	-0.004318	1.713030	-1.098472
10	1	0	-0.356269	1.982510	0.622769
11	1	0	1.917396	-1.481005	1.115058
12	1	0	1.976308	-2.057431	-0.566742
13	1	0	-0.420543	-2.158681	0.171063
14	17	0	-2.383983	-0.033716	-0.013514

SCF Done: E(RB+HF-LYP) = -709.663483888

4-chloro-1,2,3,6-tetrahydropiperidide TS (analogous to TS I)

Center Number	Atomic Number	Atomic Type	Coordinates (Angstroms) X	Y	Z
1	6	0	0.142288	-1.106034	0.082269
2	6	0	1.716818	-1.255070	0.098669
3	7	0	2.375585	-0.141164	-0.491051
4	6	0	2.076629	0.982813	0.160215
5	6	0	0.135679	1.393970	-0.005484
6	6	0	-0.368984	0.097548	0.061825
7	1	0	2.033060	0.983908	1.269725
8	1	0	2.506863	1.906439	-0.241844
9	1	0	0.008144	1.912722	-0.959283
10	1	0	-0.048951	2.048931	0.850726
11	1	0	1.981794	-1.414917	1.170085
12	1	0	1.965605	-2.181727	-0.437692

13	1	0	-0.442968	-2.017794	0.081459
14	17	0	-2.755719	-0.054634	-0.040046

Low frequencies --- -301.1029 -3.3624

Zero-point correction	0.106409 (Hartree/Particle)
Thermal correction to Energy	0.113575
Thermal correction to Enthalpy	0.114520
Thermal correction to Gibbs Free Energy	0.074133
Sum of electronic and zero-point Energies	-709.542443
Sum of electronic and thermal Energies	-709.535277
Sum of electronic and thermal Enthalpies	-709.534333
Sum of electronic and thermal Free Energies	-709.574719

SCF Done: E(RB+HF-LYP) = -709.648852263

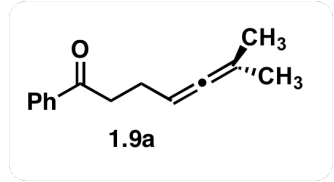
O
Ph
CH3
CH3

1.9a

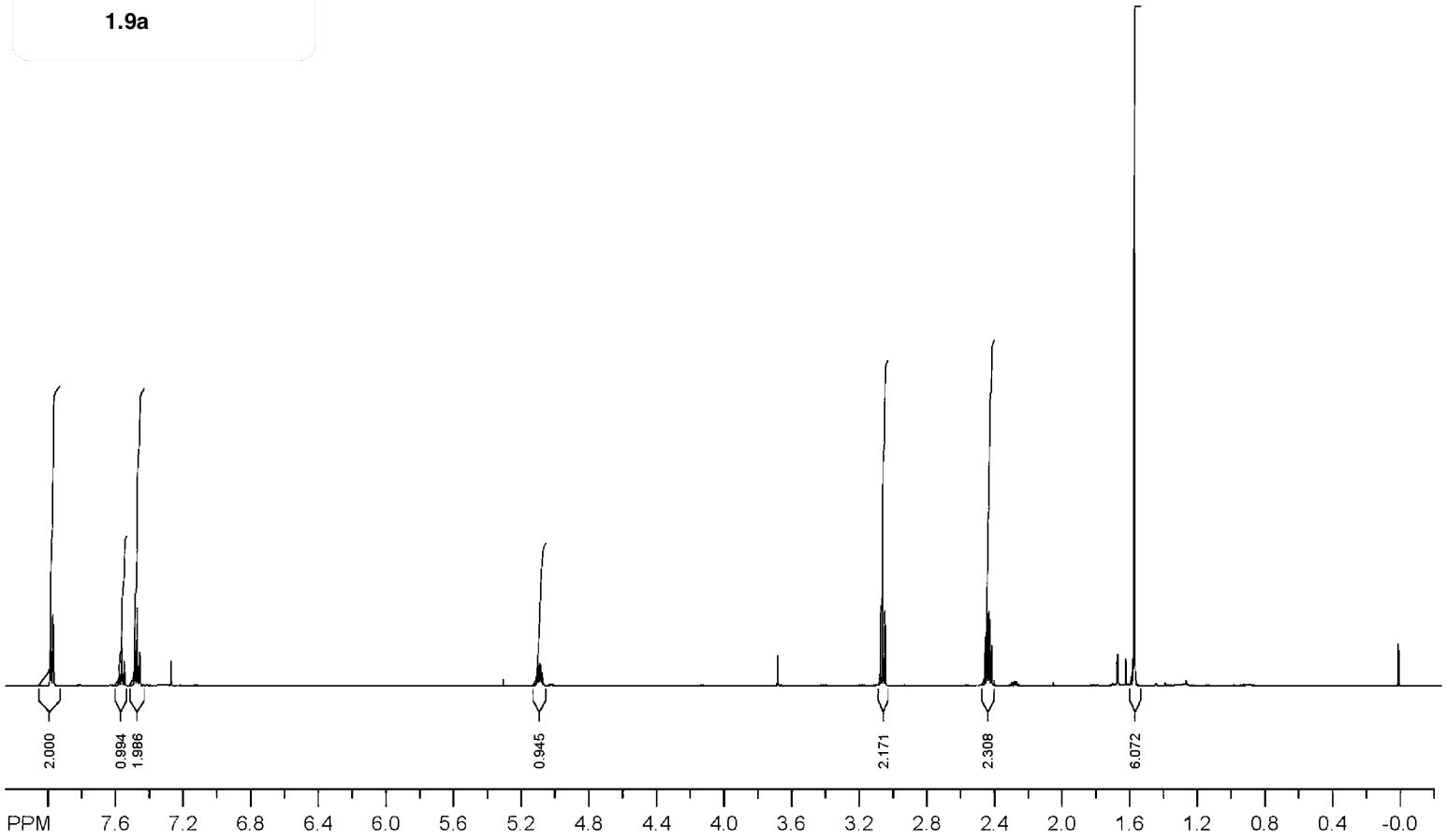
2.000
0.994
1.986
0.945
2.171
2.308
6.072
PPM
7.6
7.2
6.8
6.4
6.0
5.6
5.2
4.8
4.4
4.0
3.6
3.2
2.8
2.4
2.0
1.6
1.2
0.8
0.4
-0.0

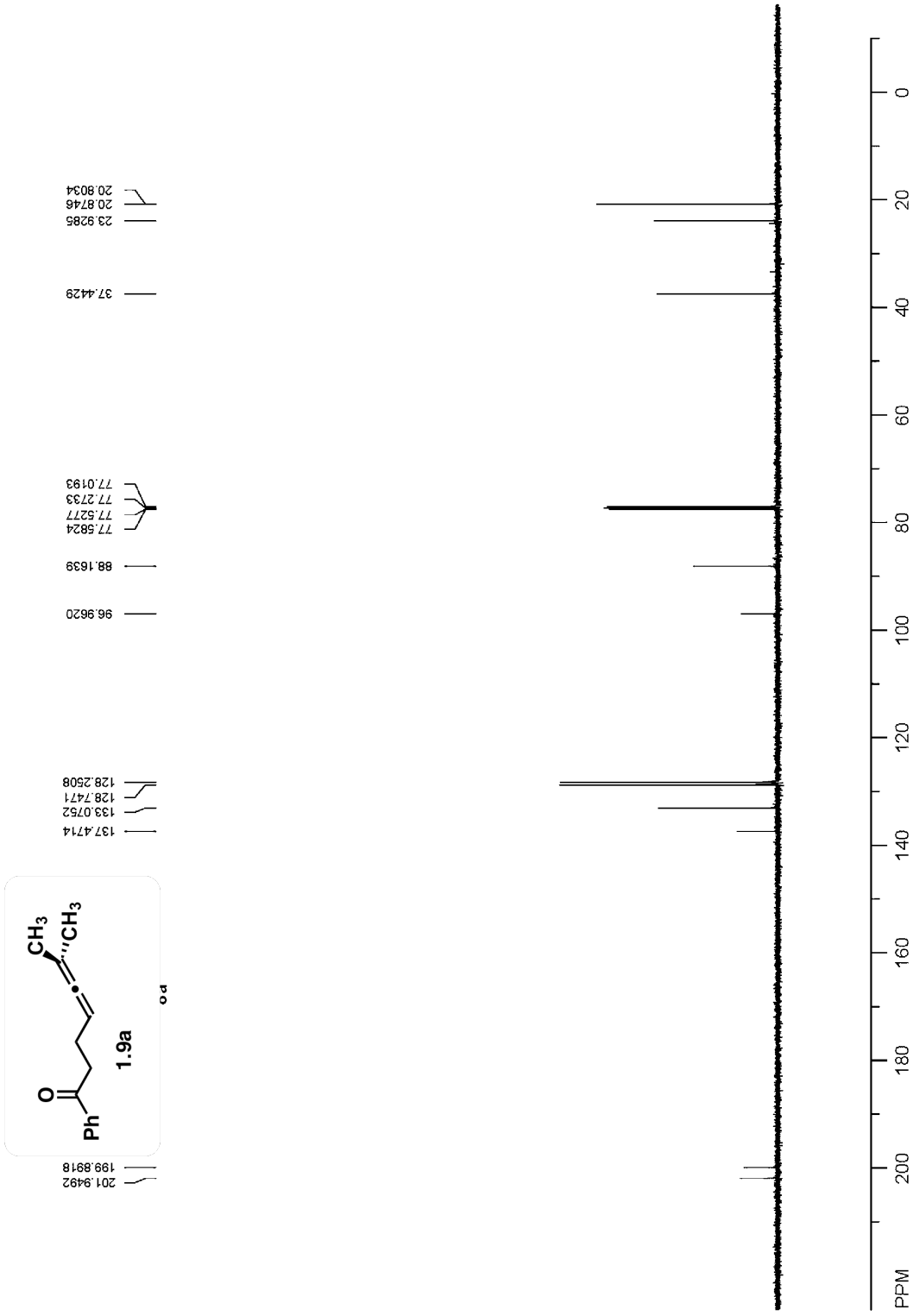
201.9492
199.8918
137.4714
133.0752
128.7471
128.2508
96.9620
88.1639
77.5824
77.5277
77.2733
77.0193
37.4429
23.9285
20.8746
20.8034
CH3
CH3
O
Ph
1.9a
PPM
0
20
40
60
80
100
120
140
160
180
200

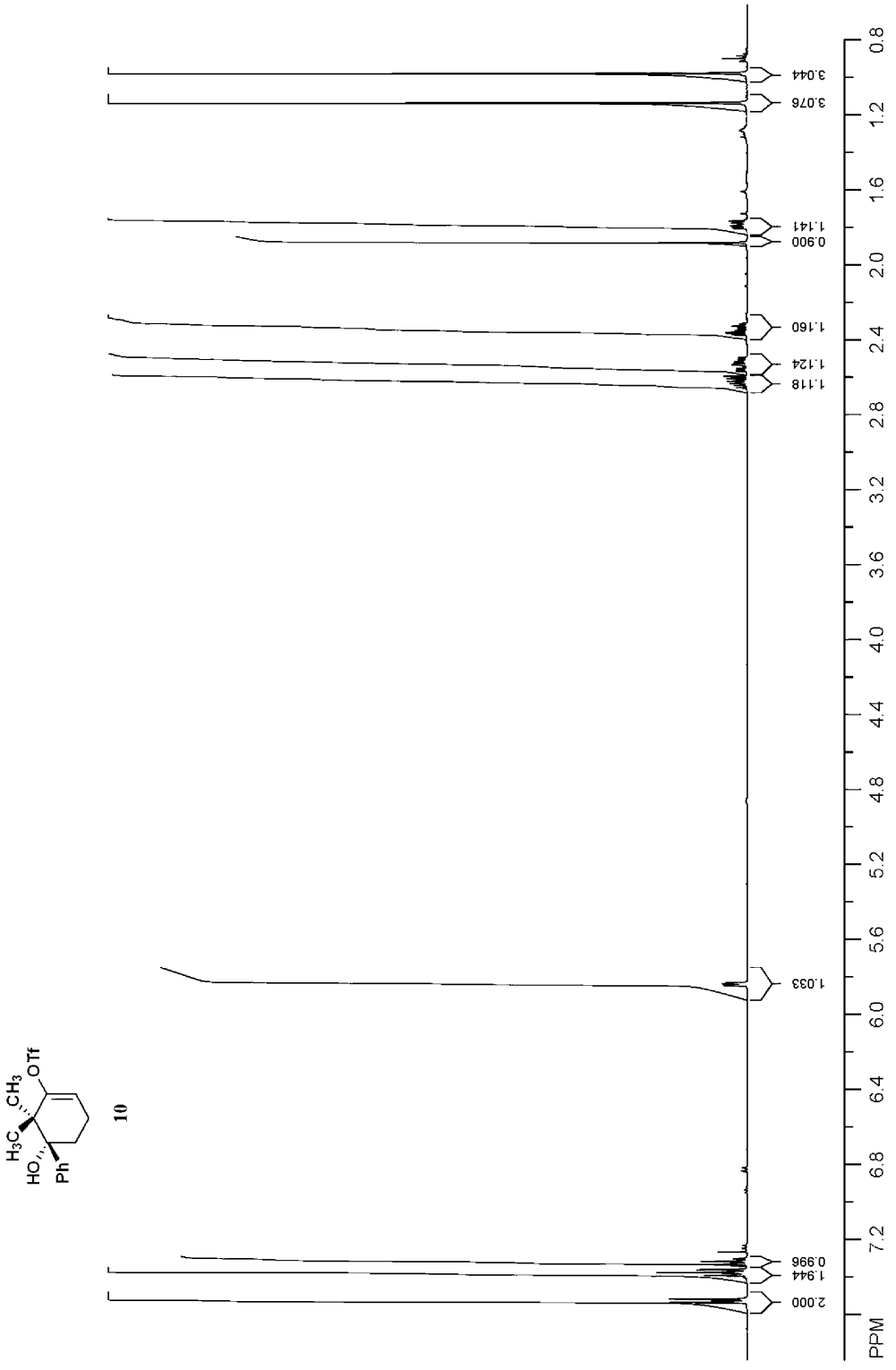
10
PPM
0.8
1.2
1.6
2.0
2.4
2.8
3.2
3.6
4.0
4.4
4.8
5.2
5.6
6.0
6.4
6.8
7.2
3.044
3.076
1.141
0.900
1.160
1.124
1.118
1.033
0.996
1.944
2.000

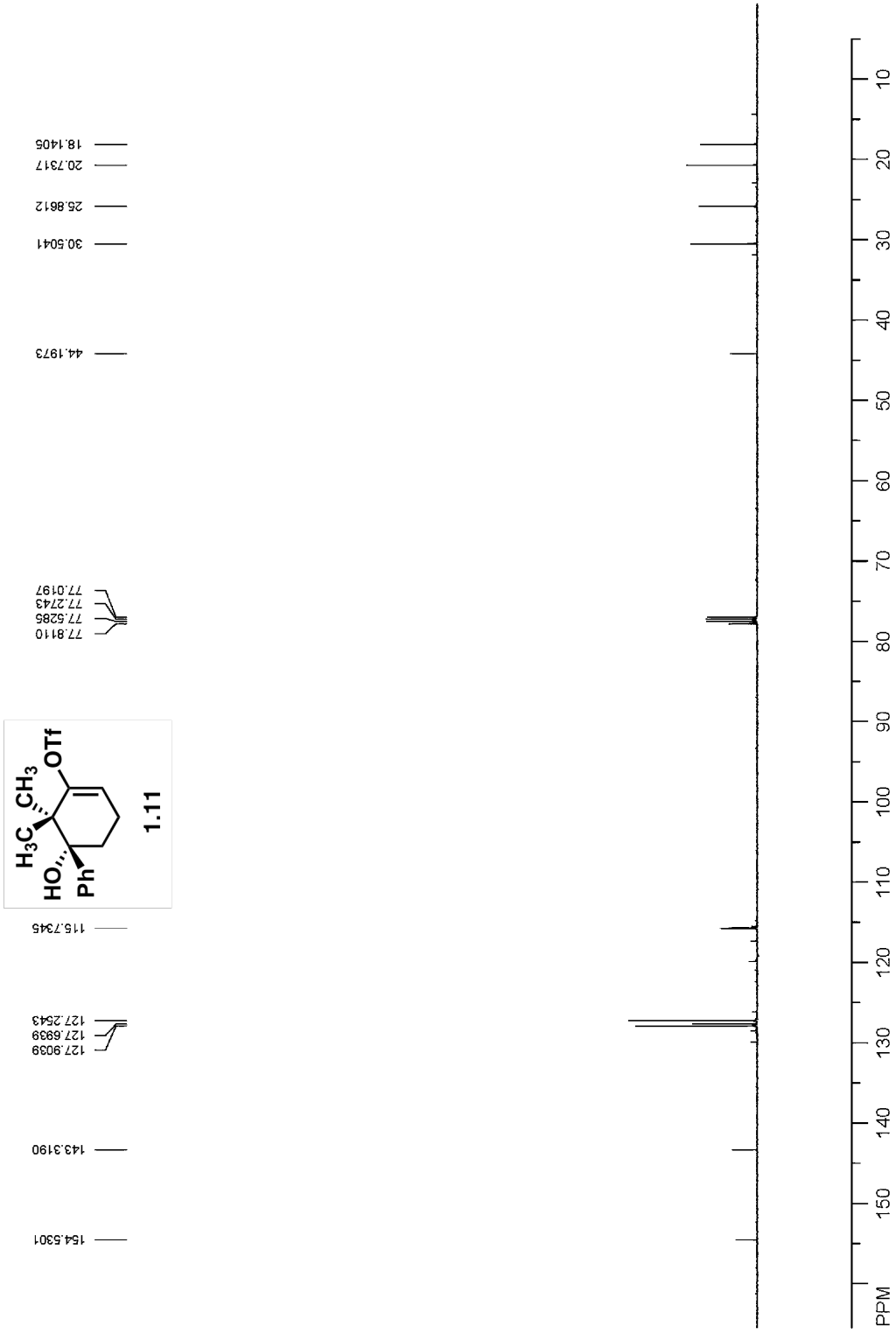
18.1405
20.7317
25.8612
30.5041
44.1973
77.0197
77.2743
77.5285
77.8110
115.7345
127.2543
127.6939
127.9039
143.3190
154.5301
1.11
PPM

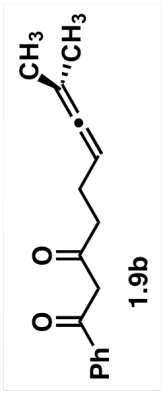
CH3
CH3
O
O
Ph

1.9b

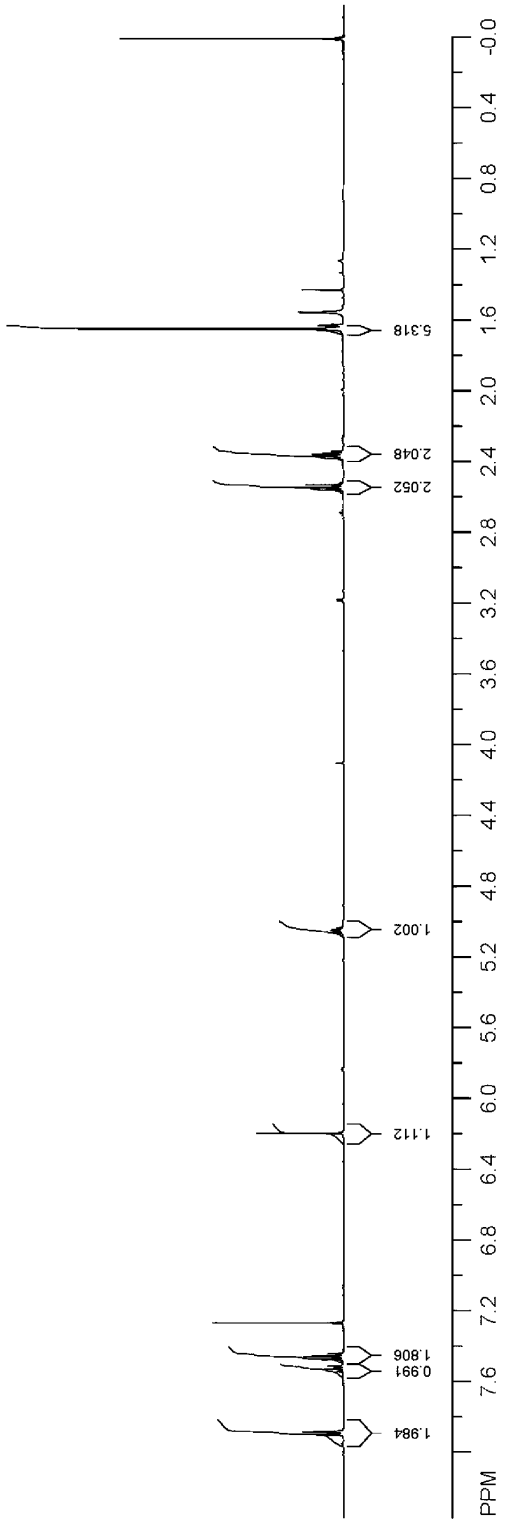
5.318
2.048
2.052
1.002
1.112
1.984
0.991
1.806
PPM
7.6
7.2
6.8
6.4
6.0
5.6
5.2
4.8
4.4
4.0
3.6
3.2
2.8
2.4
2.0
1.6
1.2
0.8
0.4
-0.0

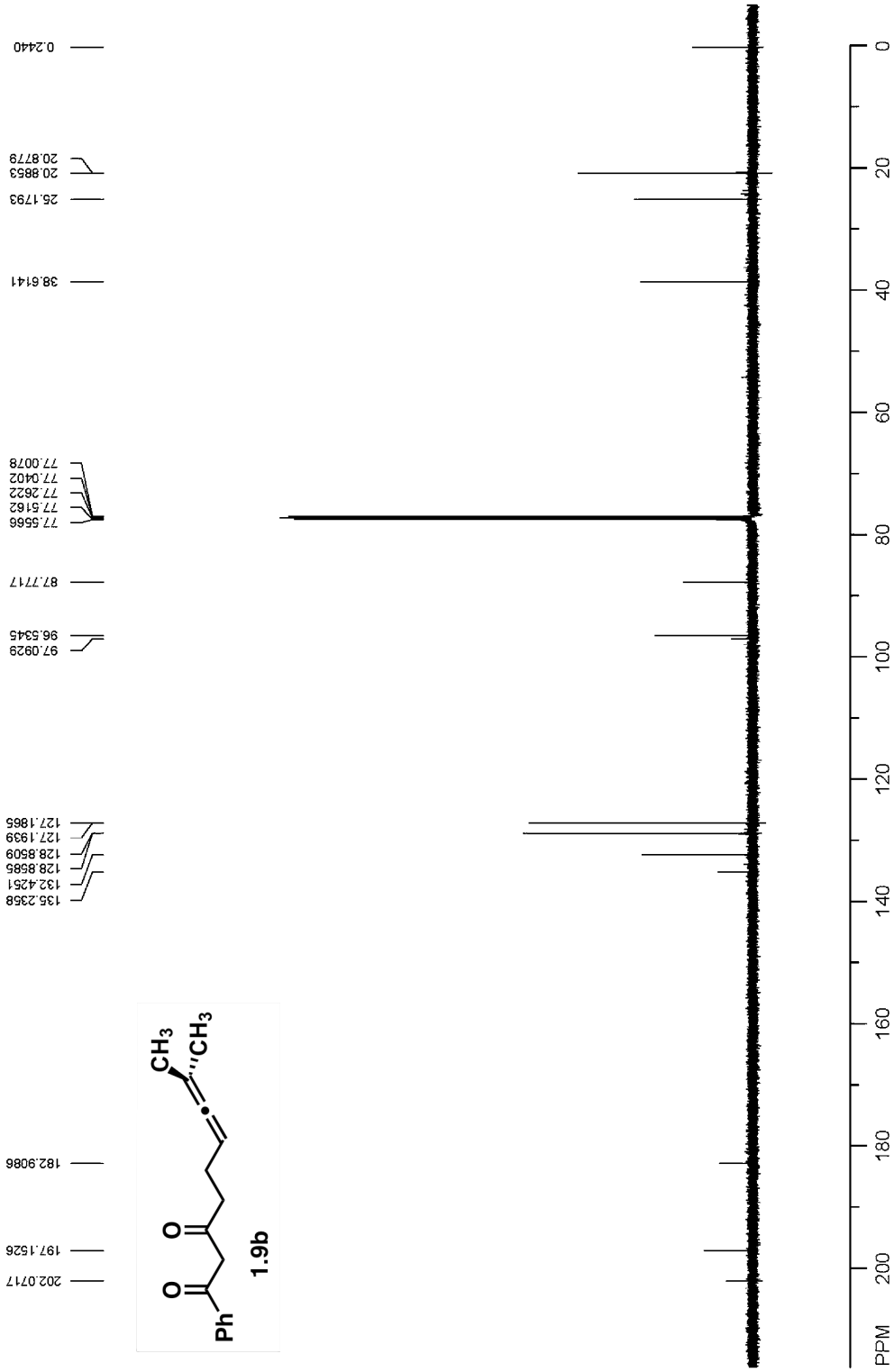
0.2440
20.8779
20.8853
26.1793
38.6141
77.0078
77.0402
77.2622
77.5162
77.5566
87.7717
96.5345
97.0929
127.1865
127.1939
128.8509
128.8586
132.4251
135.2358
182.9086
197.1526
202.0717
O
O
Ph
CH3
CH3
1.9b
PPM
0
20
40
60
80
100
120
140
160
180
200

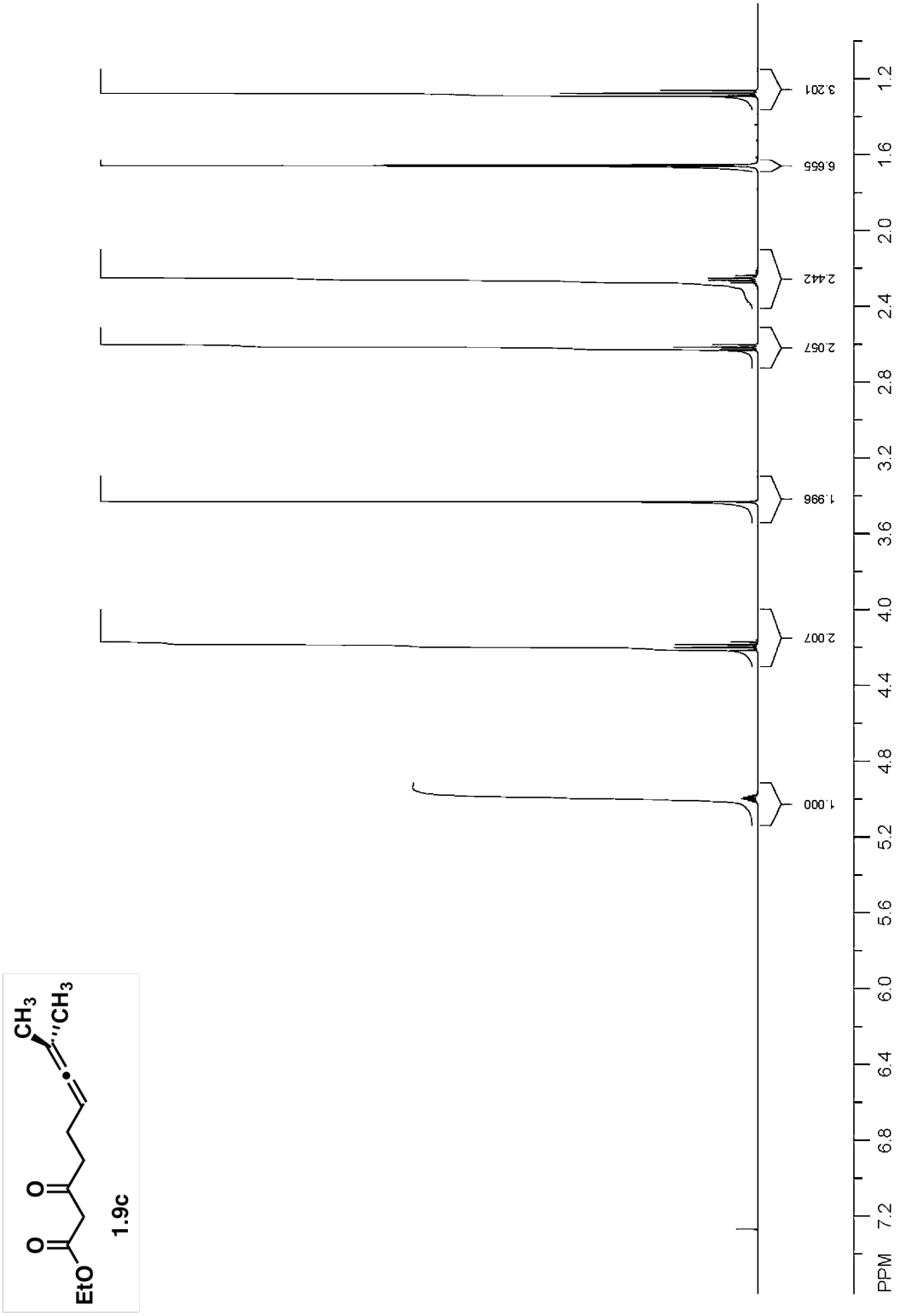
CH3
CH3
O
O
EtO
1.9c
3.201
6.655
2.442
2.057
1.996
2.007
1.000
PPM
7.2
6.8
6.4
6.0
5.6
5.2
4.8
4.4
4.0
3.6
3.2
2.8
2.4
2.0
1.6
1.2

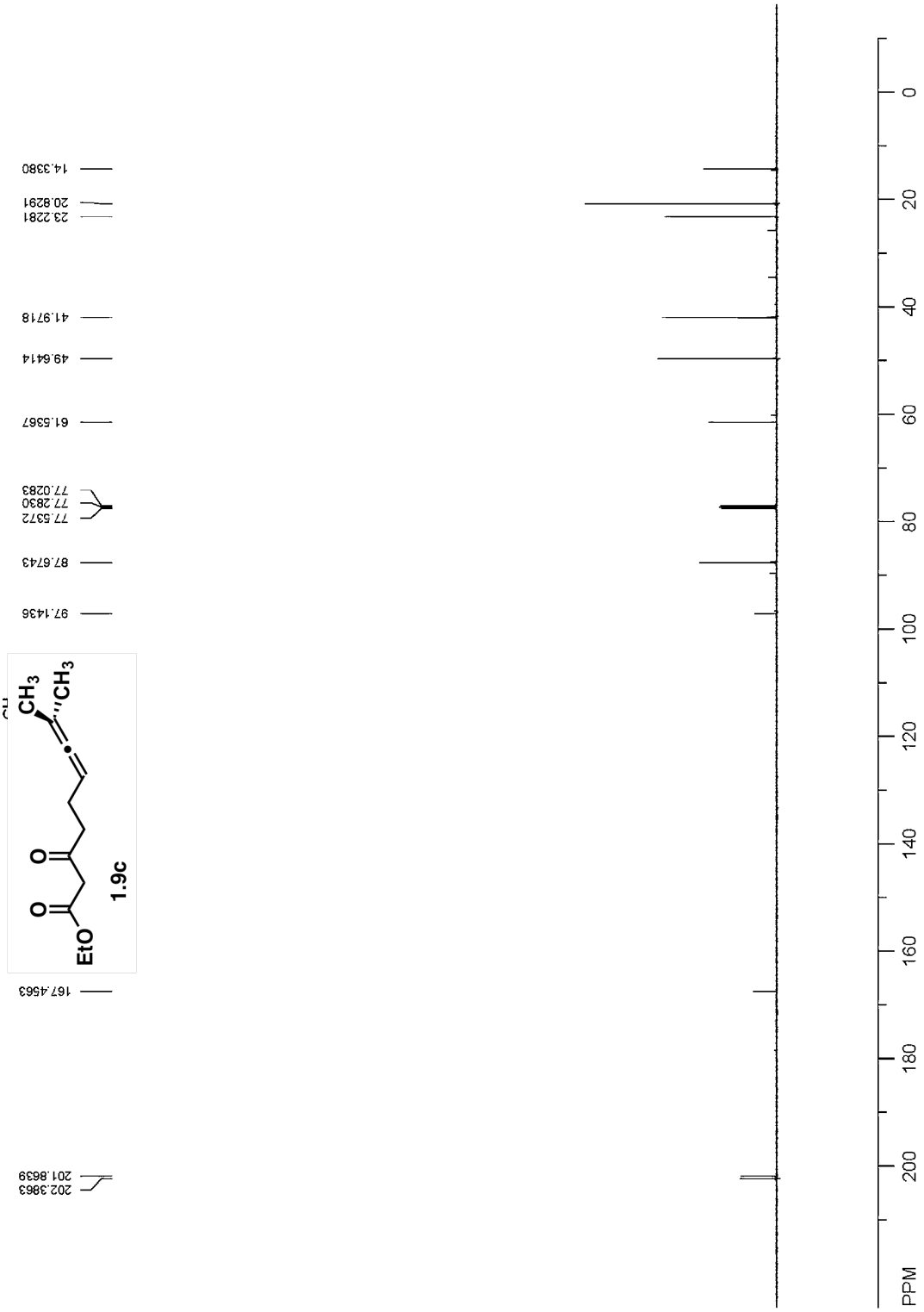
14.3380
20.8291
23.2281
41.9718
49.6414
61.5367
77.0283
77.2830
77.5372
87.6743
97.1436
167.4563
201.8639
202.3863
EtO
O
O
CH3
CH3
1.9c
PPM
0
20
40
60
80
100
120
140
160
180
200

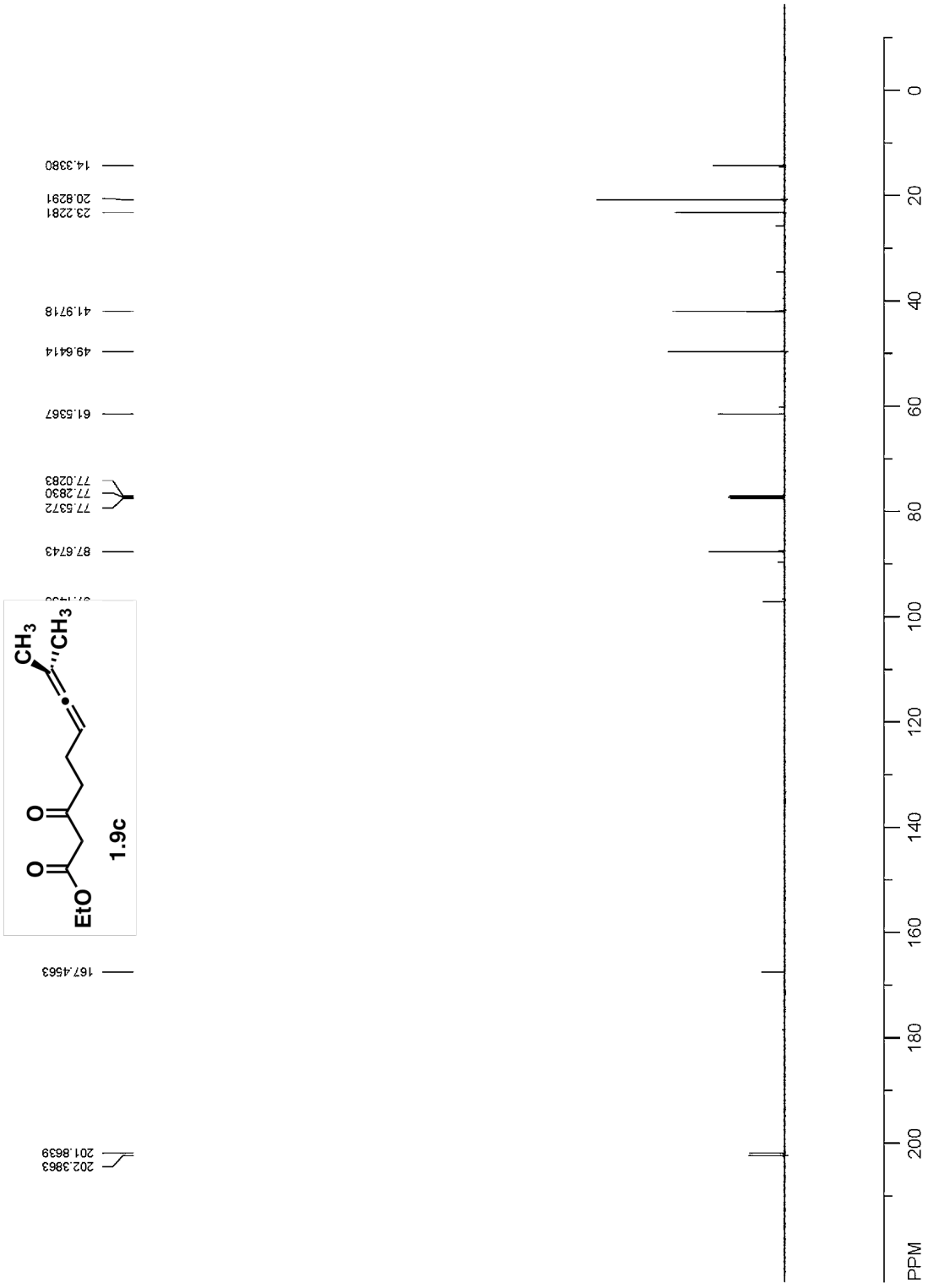
14.3380
20.8291
23.2281
41.9718
49.6414
61.5367
77.0283
77.2830
77.5372
87.6743
167.4563
201.8639
202.3863
CH3
CH3
O
O
EtO
1.9c
PPM
0
20
40
60
80
100
120
140
160
180
200

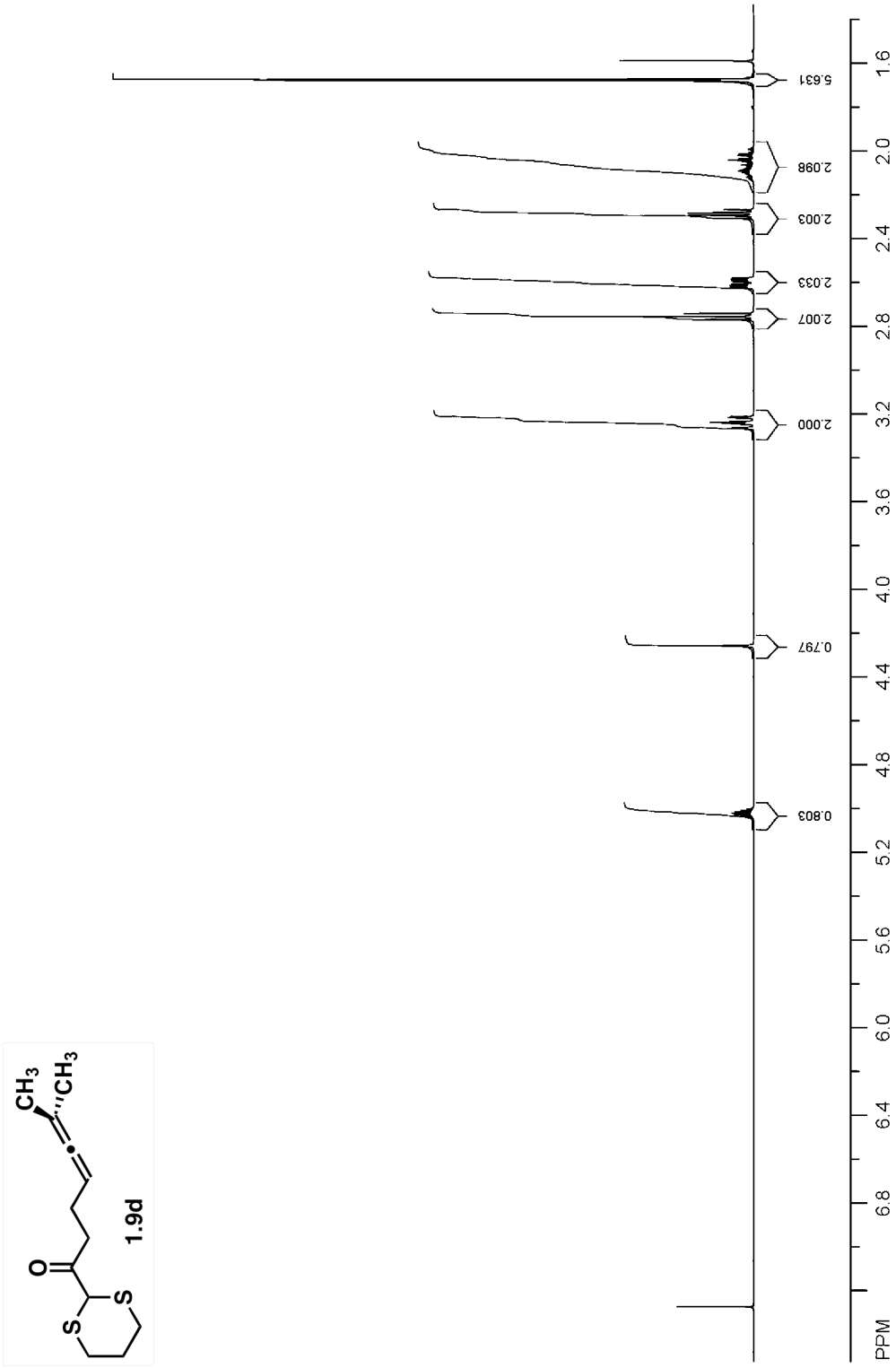
5.631
2.098
2.003
2.033
2.007
2.000
0.797
0.803
PPM
1.6
2.0
2.4
2.8
3.2
3.6
4.0
4.4
4.8
5.2
5.6
6.0
6.4
6.8
CH3
CH3
O
S
S
1.9d

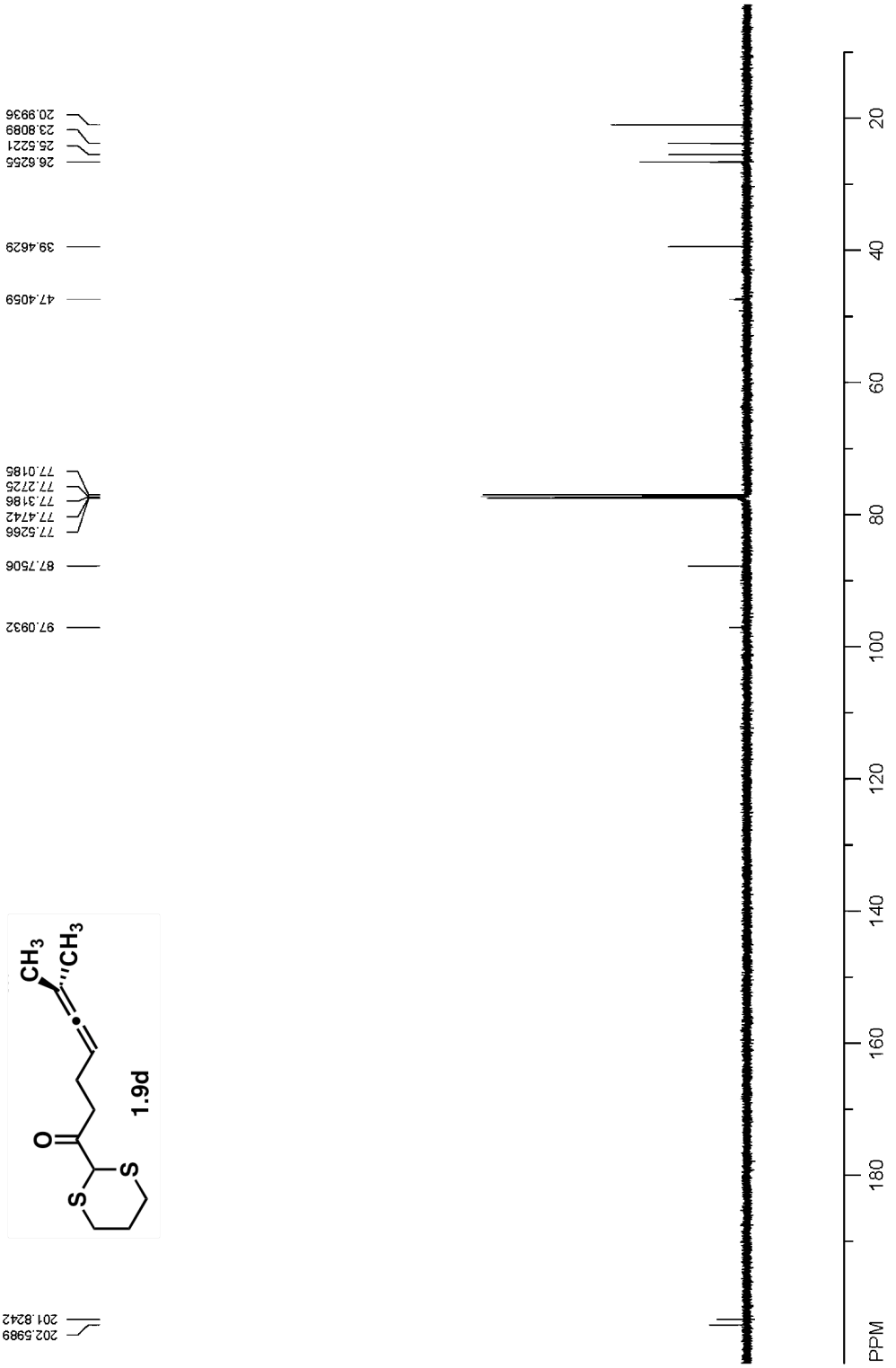
20.9936
23.8089
25.5221
26.6255
39.4629
47.4059
77.0186
77.2725
77.3186
77.4742
77.5266
87.7506
97.0932
201.8242
202.5989
1.9d
O
S
S
CH3
CH3
PPM
20
40
60
80
100
120
140
160
180

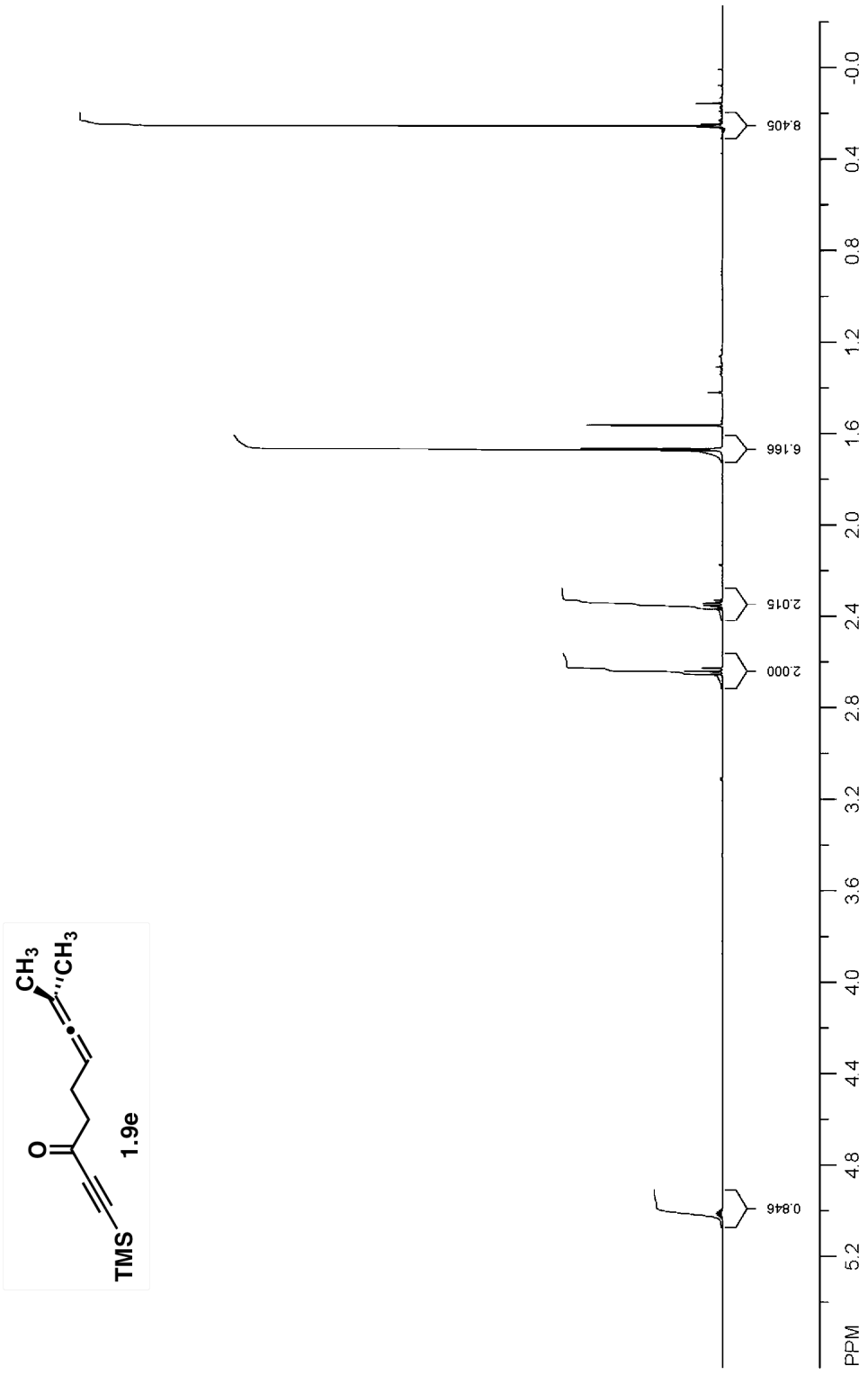
CH3
CH3
O
TMS
1.9e
8.405
6.166
2.015
2.000
0.846
PPM
5.2
4.8
4.4
4.0
3.6
3.2
2.8
2.4
2.0
1.6
1.2
0.8
0.4
-0.0

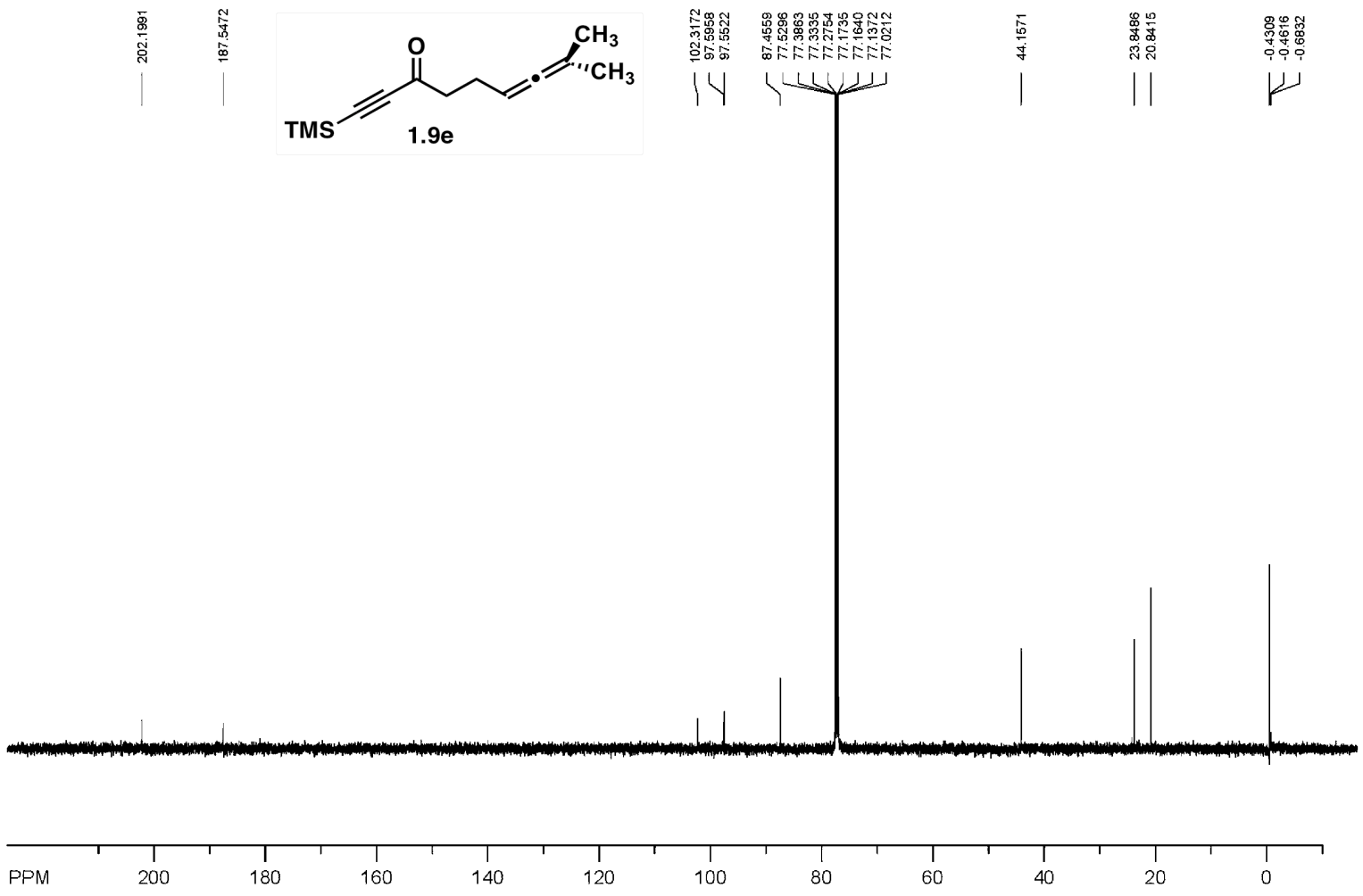
202.1981
187.5472
102.3172
97.5958
97.5522
87.4559
77.5296
77.3863
77.3335
77.2754
77.1735
77.1640
77.1372
77.0212
44.1571
23.8486
20.8415
-0.4309
-0.4616
-0.6832
O
CH3
CH3
TMS
1.9e
PPM
200
180
160
140
120
100
80
60
40
20
0

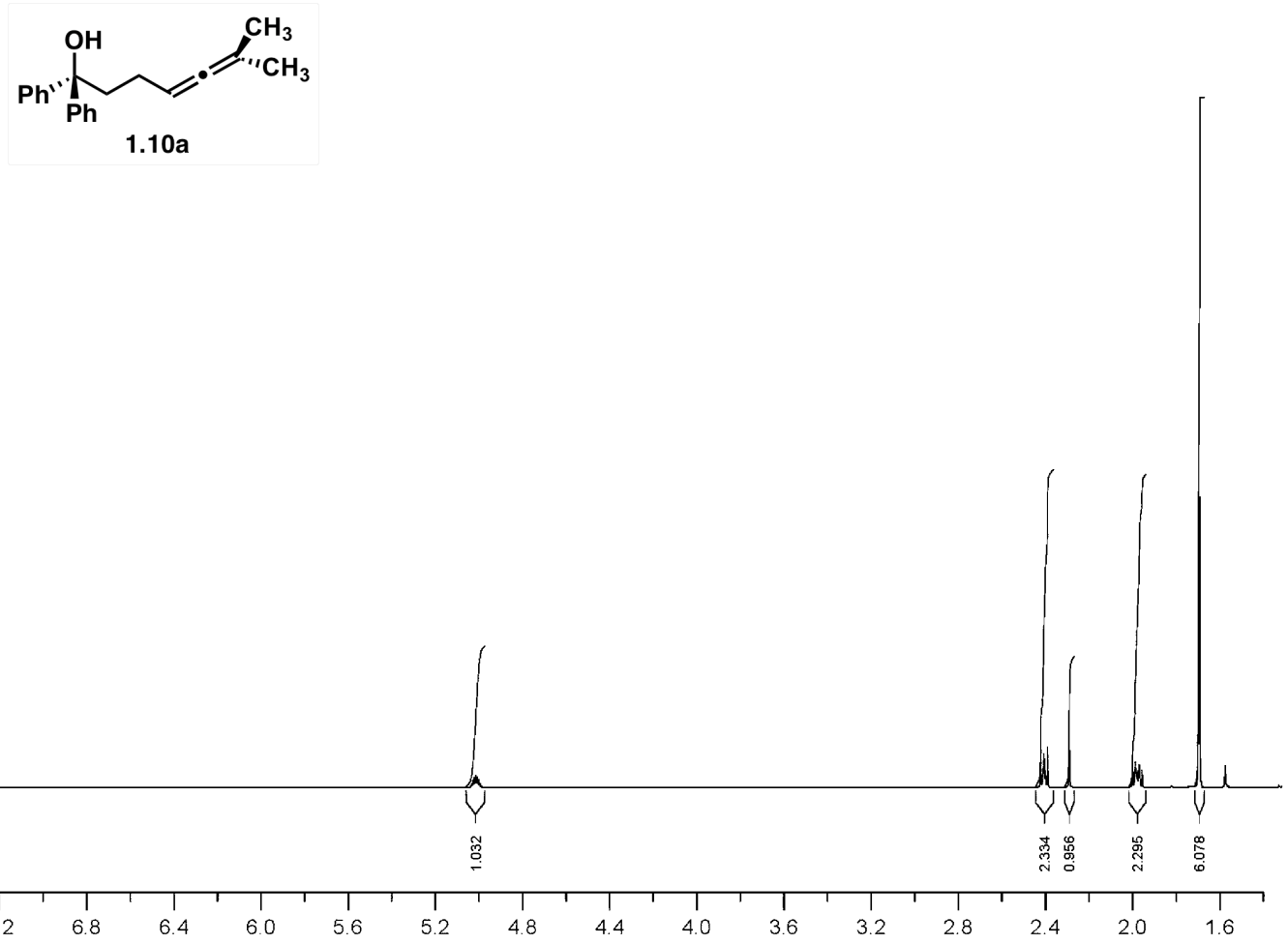
OH
CH3
CH3
Ph
Ph
1.10a
4.000
3.865
1.867
1.032
2.334
0.956
2.295
6.078
PPM
7.6
7.2
6.8
6.4
6.0
5.6
5.2
4.8
4.4
4.0
3.6
3.2
2.8
2.4
2.0
1.6

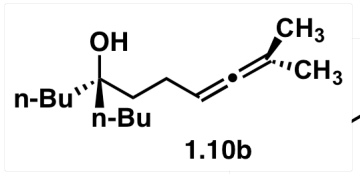
OH
CH3
CH3
n-Bu
n-Bu

1.10b

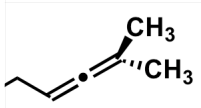
CH3
CH3

1.10a

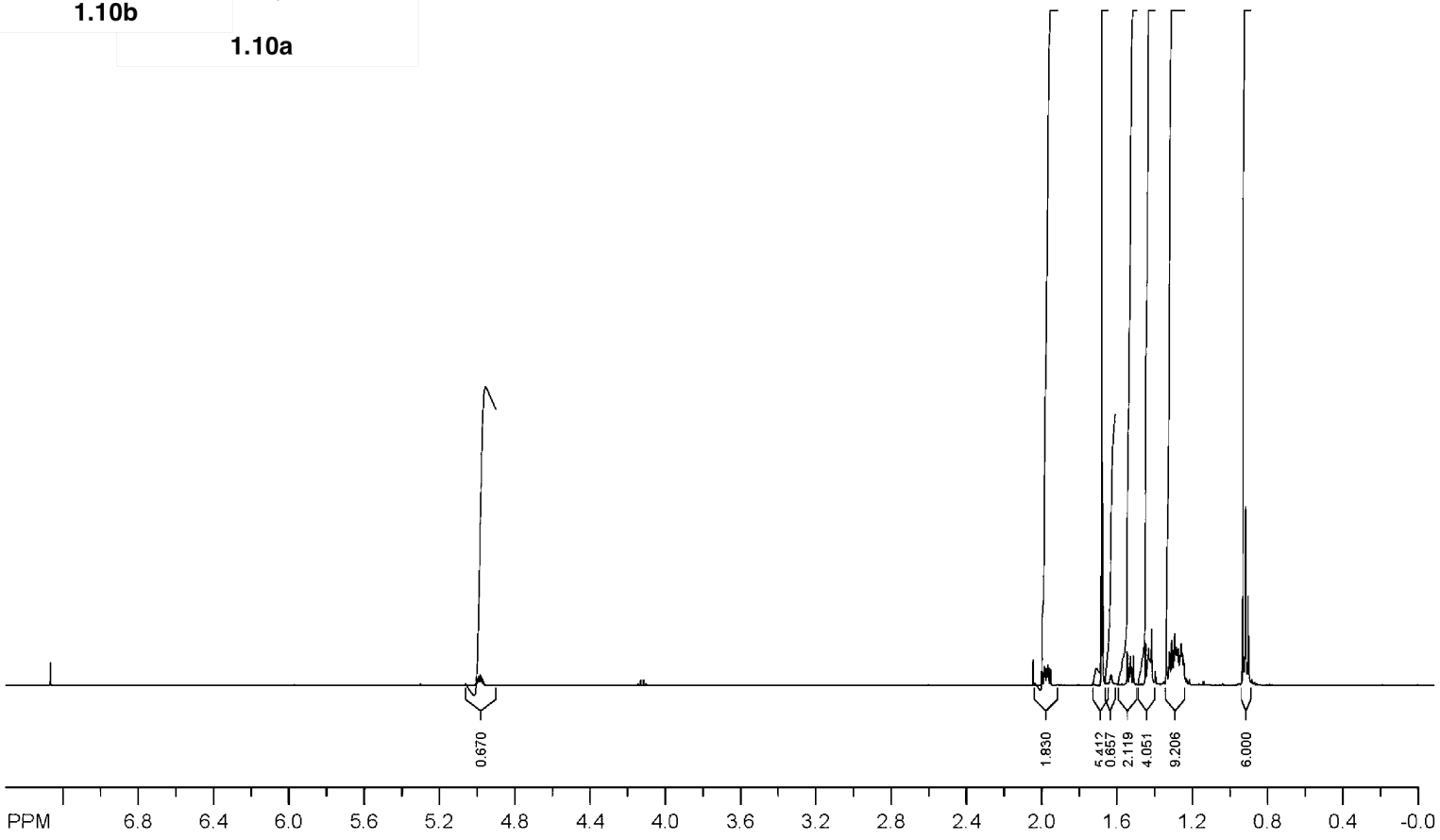
0.670
1.830
5.412
0.657
2.119
4.051
9.206
6.000
PPM
6.8
6.4
6.0
5.6
5.2
4.8
4.4
4.0
3.6
3.2
2.8
2.4
2.0
1.6
1.2
0.8
0.4
-0.0

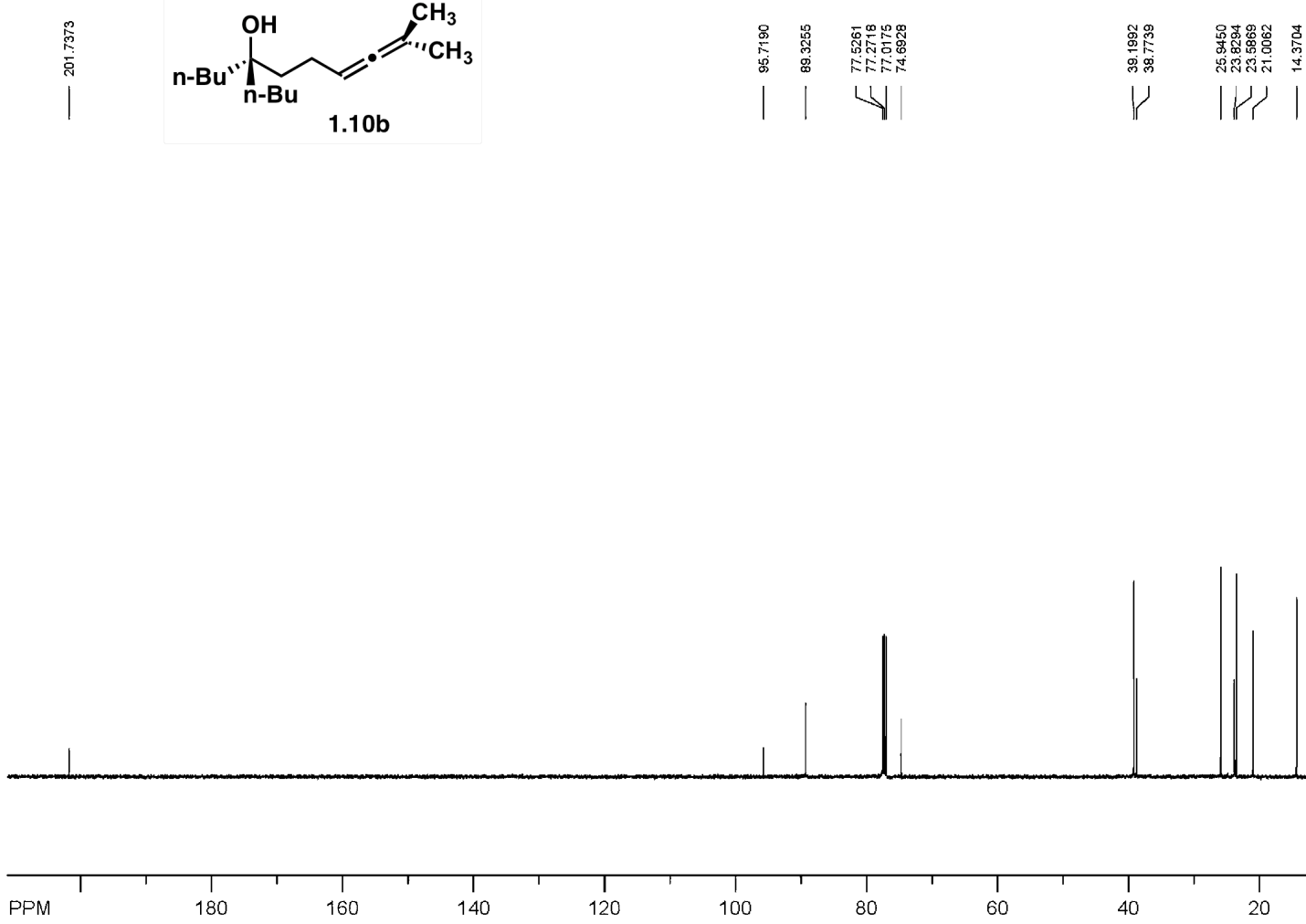
201.7373
OH
CH3
CH3
n-Bu
n-Bu
1.10b
95.7190
89.3255
77.5261
77.2718
77.0175
74.6928
39.1992
38.7739
25.9450
23.8294
23.5869
21.0062
14.3704
PPM
180
160
140
120
100
80
60
40
20

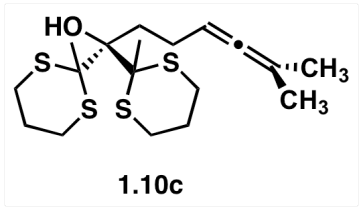
HO
S
S
S
S
CH3
CH3

1.10c

0.835
0.878
8.146
3.968
6.000
4.436
5.519
PPM
7.2
6.8
6.4
6.0
5.6
5.2
4.8
4.4
4.0
3.6
3.2
2.8
2.4
2.0
1.6

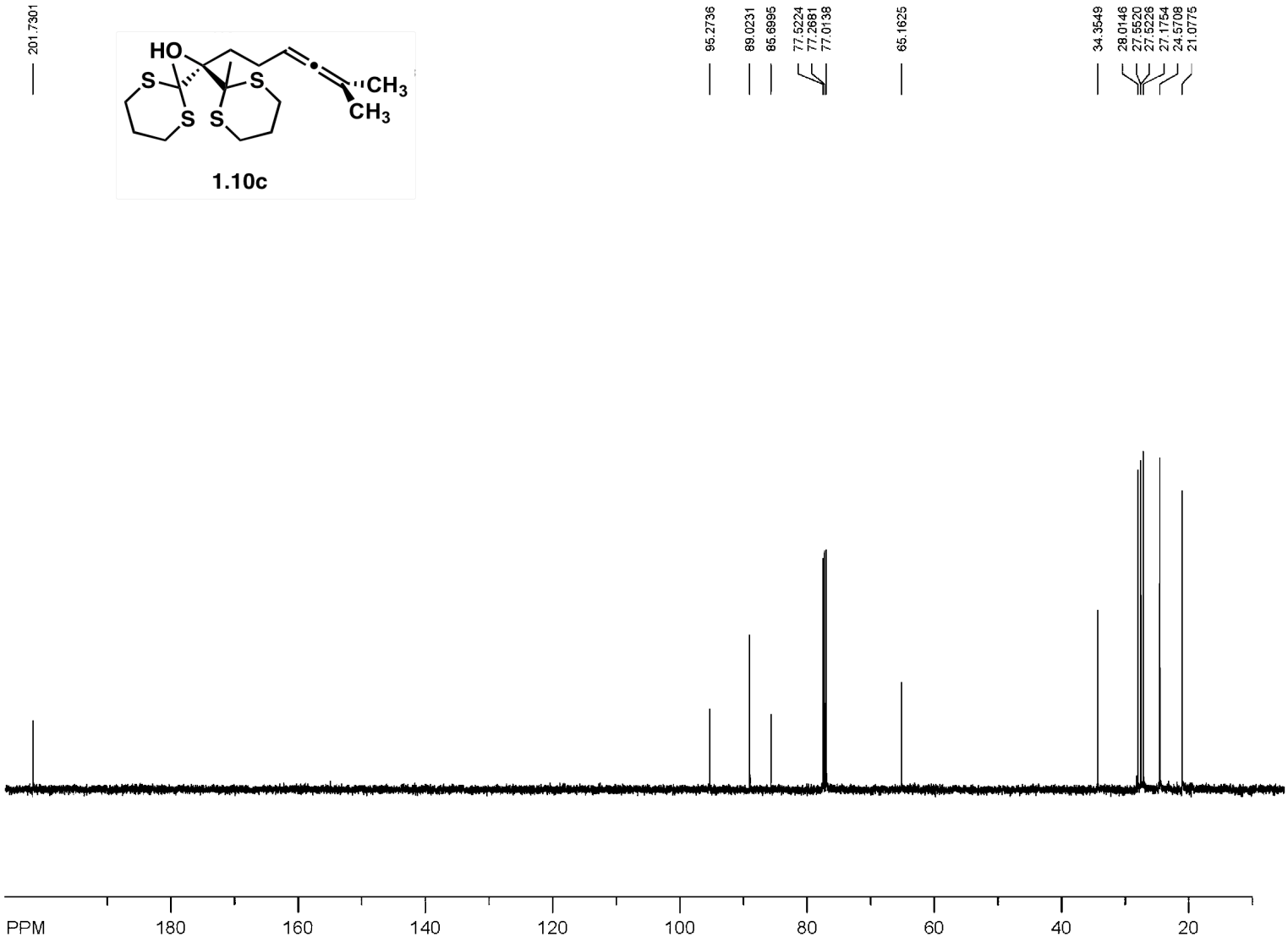
201.7301
95.2736
89.0231
85.6995
77.5224
77.2681
77.0138
65.1625
34.3549
28.0146
27.5520
27.5226
27.1754
24.5708
21.0775
HO
S
S
S
S
CH3
CH3
1.10c
PPM
180
160
140
120
100
80
60
40
20

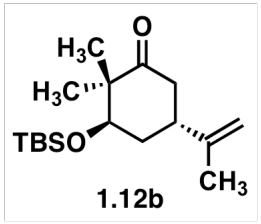
O
H3C
H3C
TBSO
CH3

1.12b

0.954
0.999
1.156
1.216
1.181
1.205
2.887
2.734
2.792
5.475
PPM
9.0
8.0
7.0
6.0
5.0
4.0
3.0
2.0
1.0
0.0

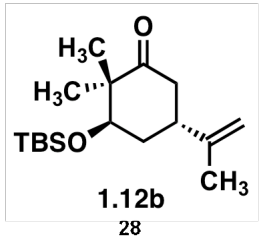
O
H3C
H3C
TBSO
CH3
1.12b
28

110.0564
78.4910
77.4994
77.2456
76.9912
50.4116
42.4536
39.4840
34.1479
25.9904
25.9219
25.8779
24.7595
21.6218
20.9362
18.2684
PPM
200
180
160
140
120
100
80
60
40
20
0

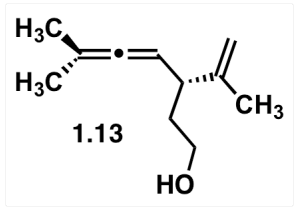
H3C
H3C
CH3
1.13
HO

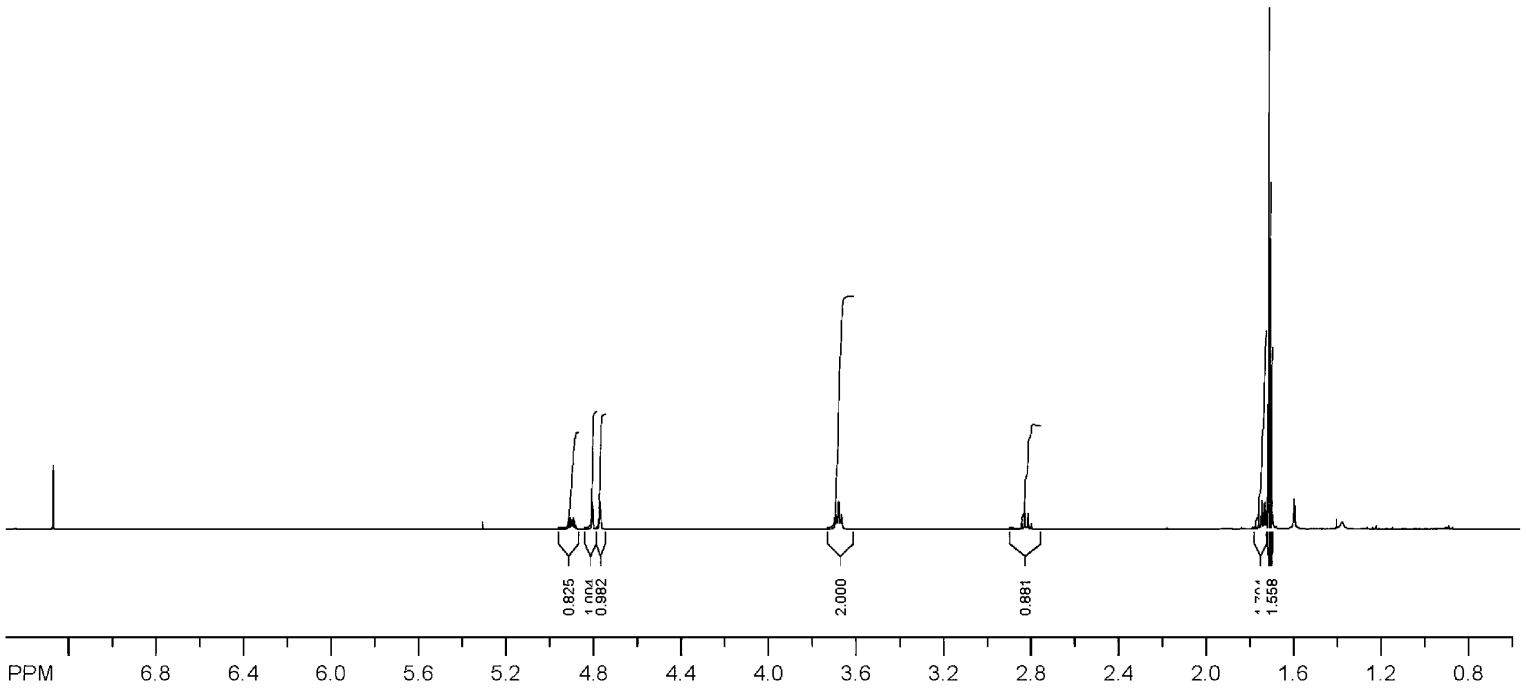
0.825
2.000
0.881
1.558
PPM
6.8
6.4
6.0
5.6
5.2
4.8
4.4
4.0
3.6
3.2
2.8
2.4
2.0
1.6
1.2
0.8

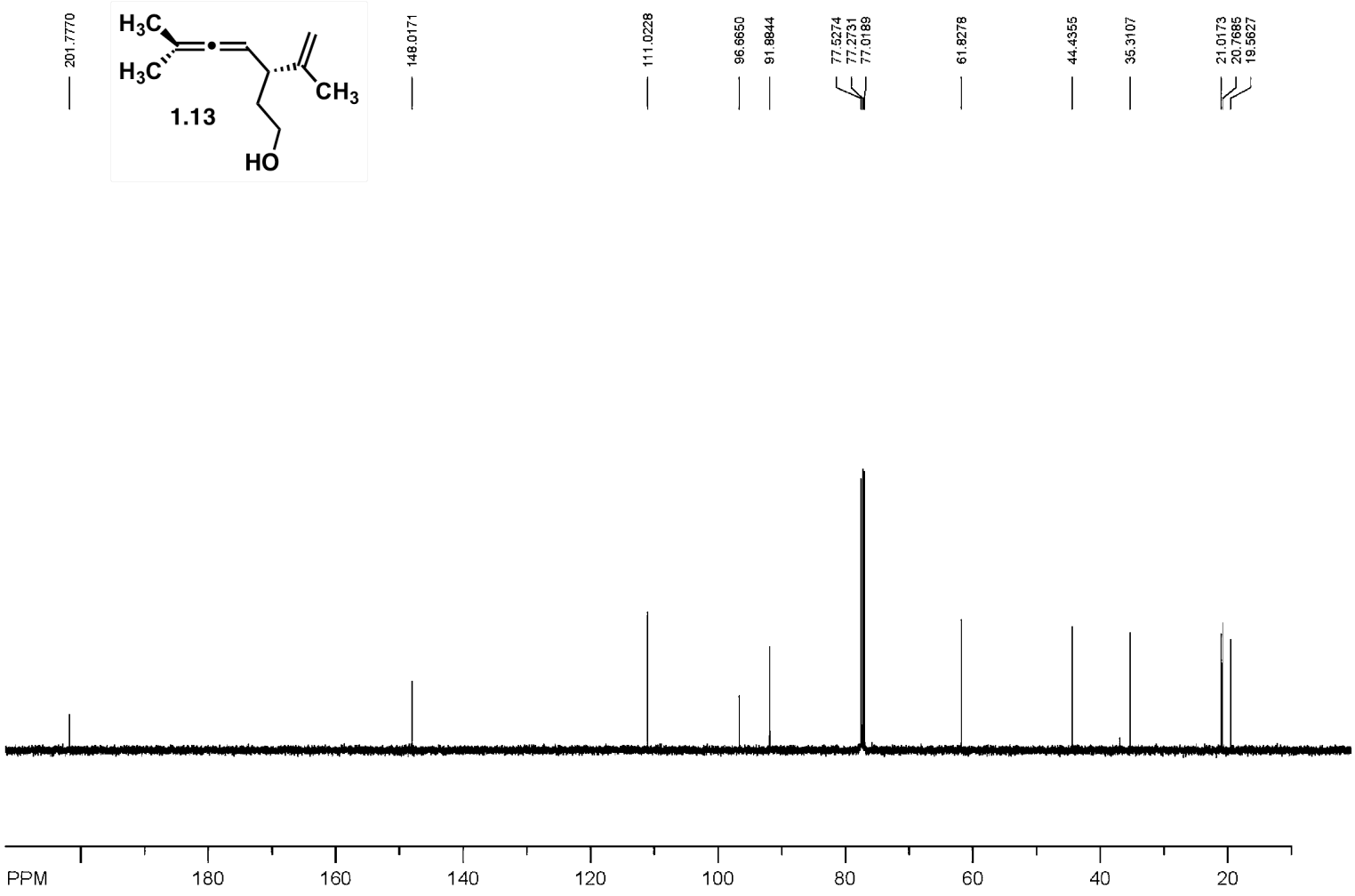
201.7770
148.0171
111.0228
96.6650
91.8844
77.5274
77.2731
77.0189
61.8278
44.4355
35.3107
21.0173
20.7685
19.5627
H3C
H3C
CH3
1.13
HO
PPM
180
160
140
120
100
80
60
40
20

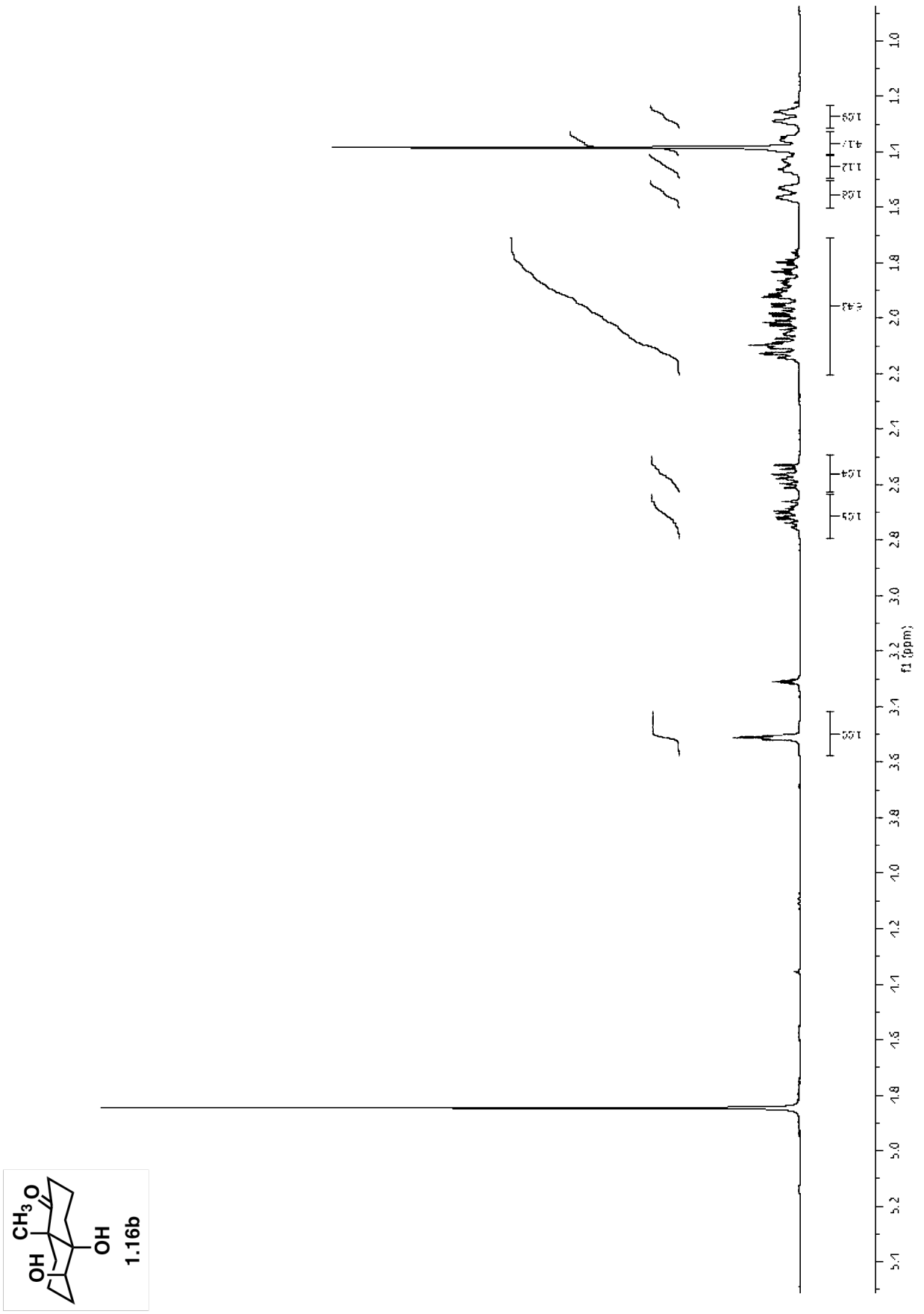
CH3O
OH
OH
1.16b
f1 (ppm)

1.16b

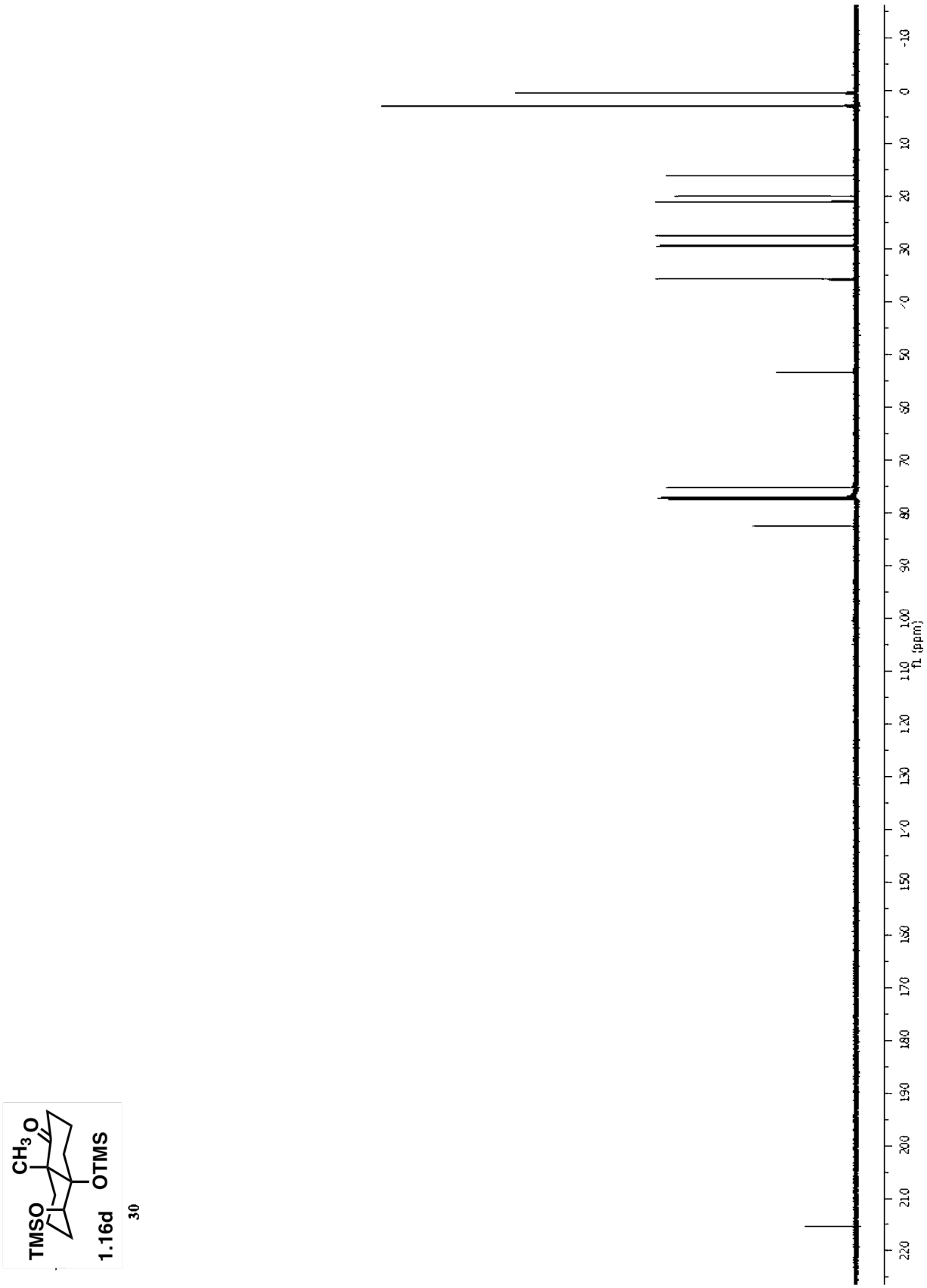
TMSO
CH3O
OTMS
1.16d
30
f1 (ppm)

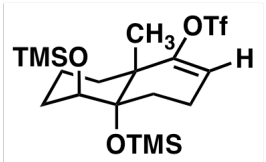

1.16

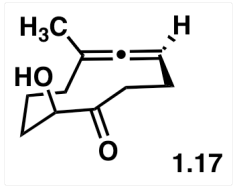

1.17

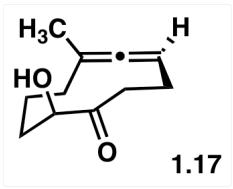
H3C
H
HO
O

1.17

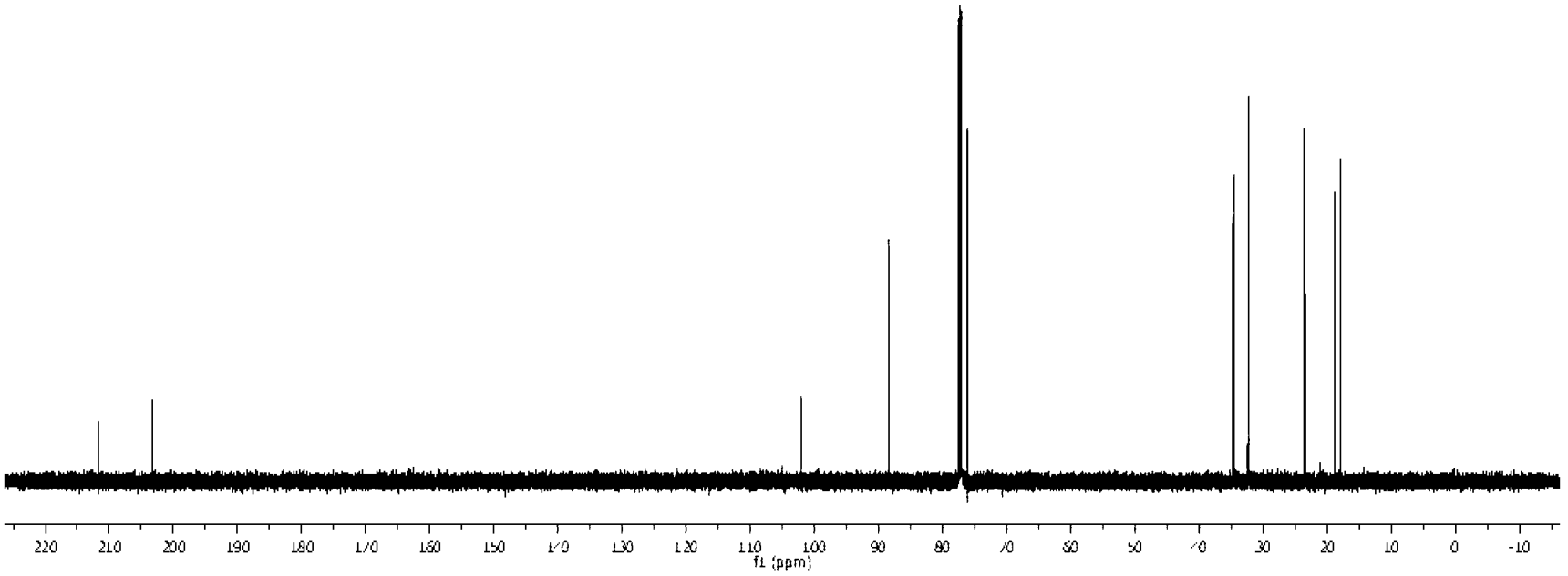
220
210
200
190
180
170
160
150
140
130
120
110
100
90
80
70
60
50
40
30
20
10
0
-10
f1 (ppm)

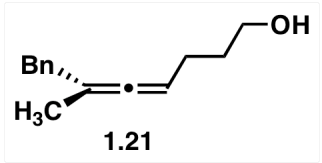
OH
Bn
H3C

1.21

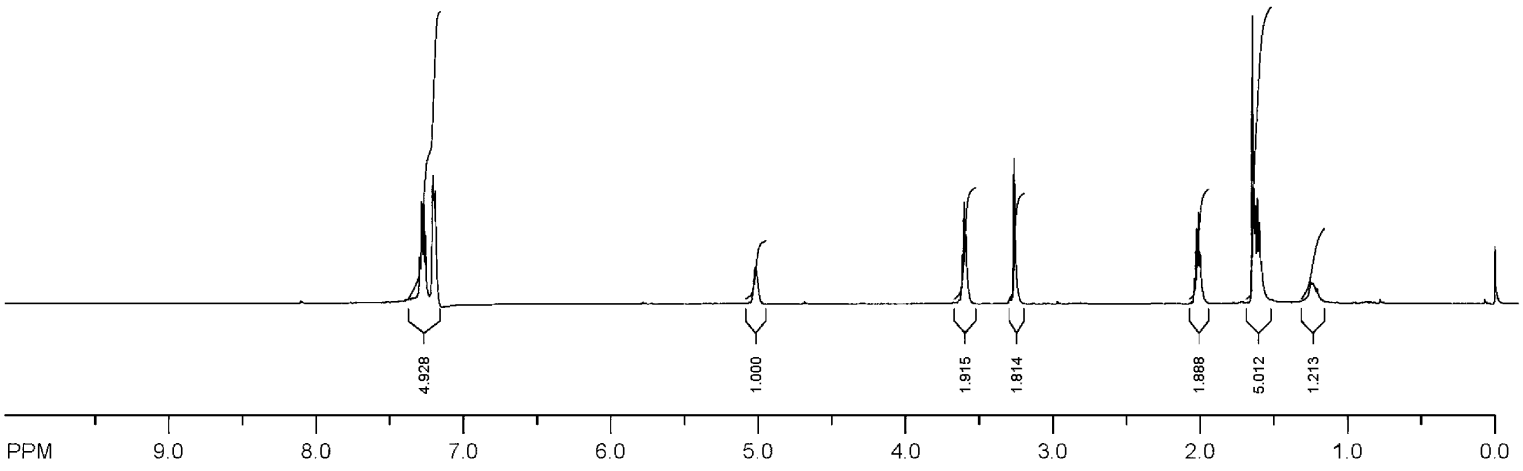
4.928
1.000
1.915
1.814
1.888
5.012
1.213
PPM
9.0
8.0
7.0
6.0
5.0
4.0
3.0
2.0
1.0
0.0

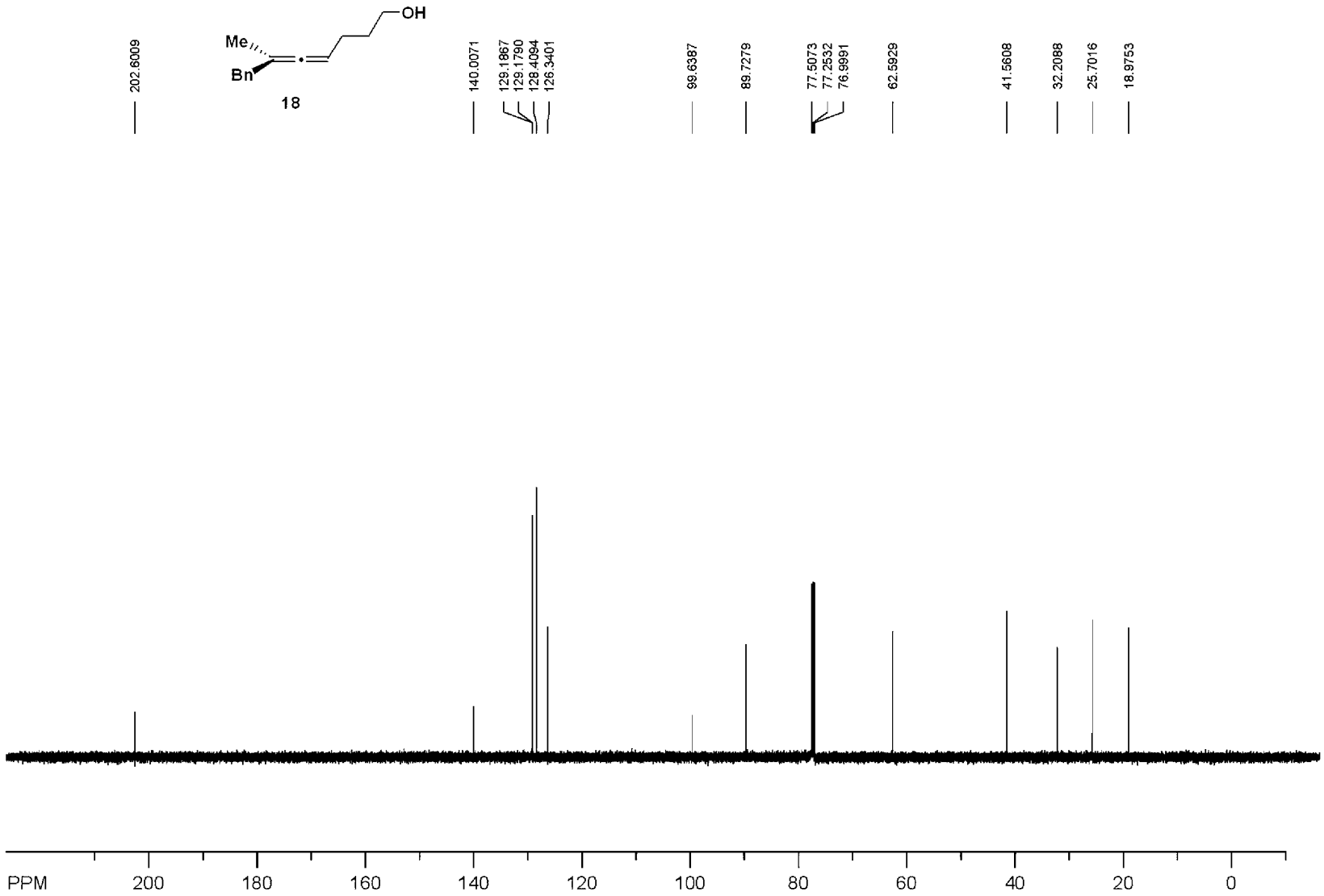
OH
Me
Bn
18
202.6009
140.0071
129.1867
129.1790
128.4094
126.3401
99.6387
89.7279
77.5073
77.2532
76.9991
62.5929
41.5608
32.2088
25.7016
18.9753
PPM
200
180
160
140
120
100
80
60
40
20
0

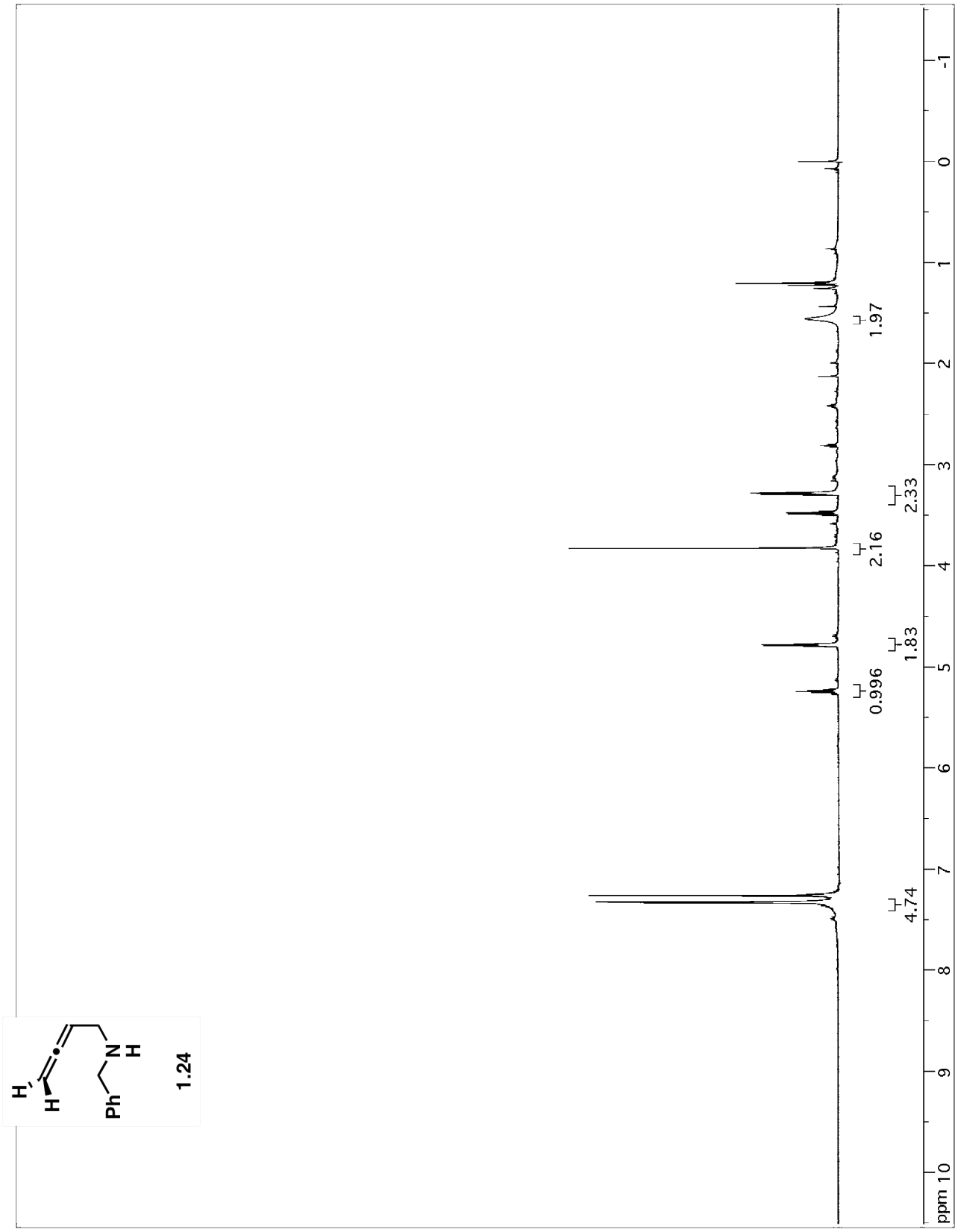
H
H
N
H
Ph
1.24
4.74
0.996
1.83
2.16
2.33
1.97
ppm 10
9
8
7
6
5
4
3
2
1
0
-1

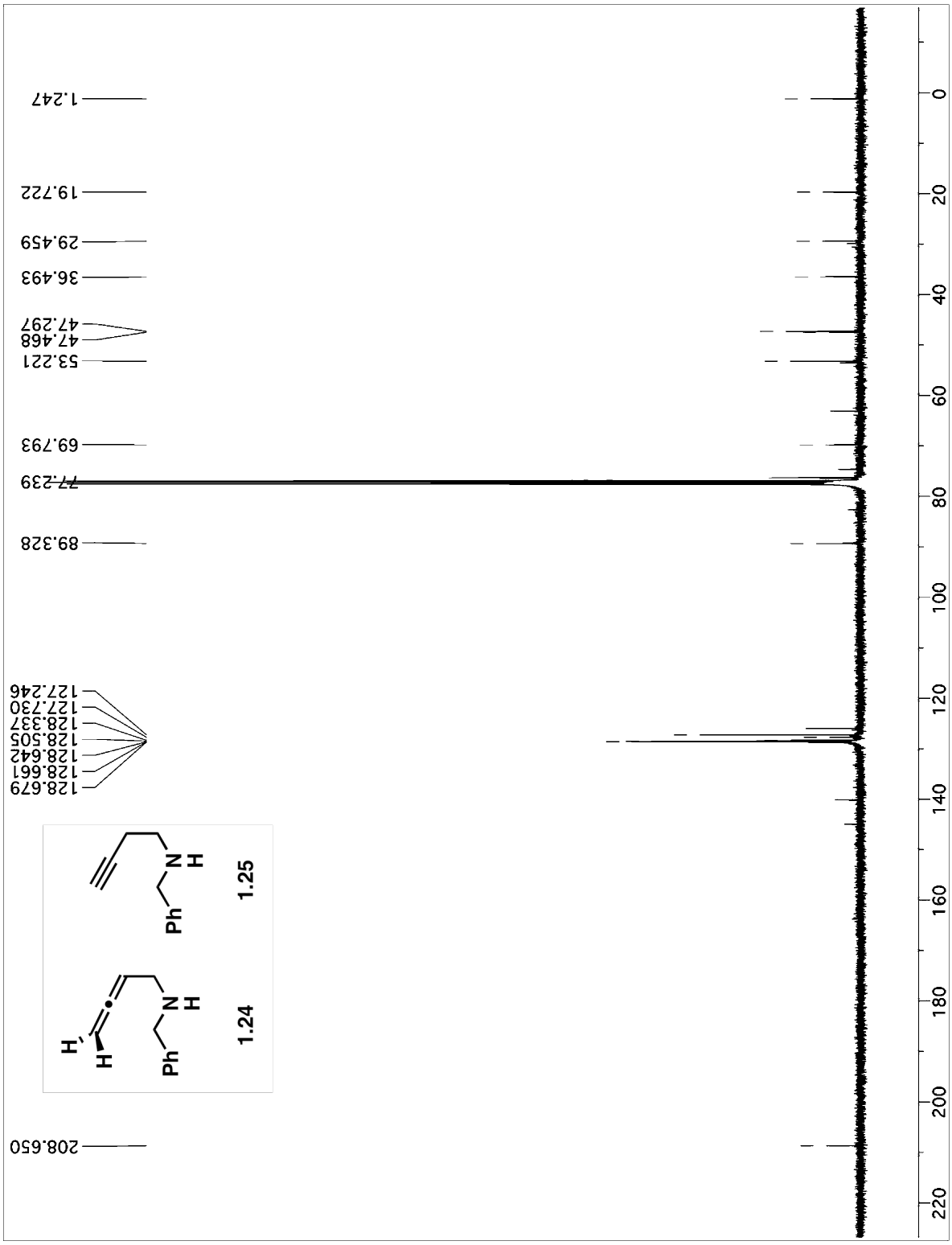
208.650
128.679
128.661
128.642
128.505
128.337
127.730
127.246
89.328
77.239
69.793
53.221
47.468
47.297
36.493
29.459
19.722
1.247
1.25
1.24
Ph
N
H
Ph
N
H
H
H
0
20
40
60
80
100
120
140
160
180
200
220

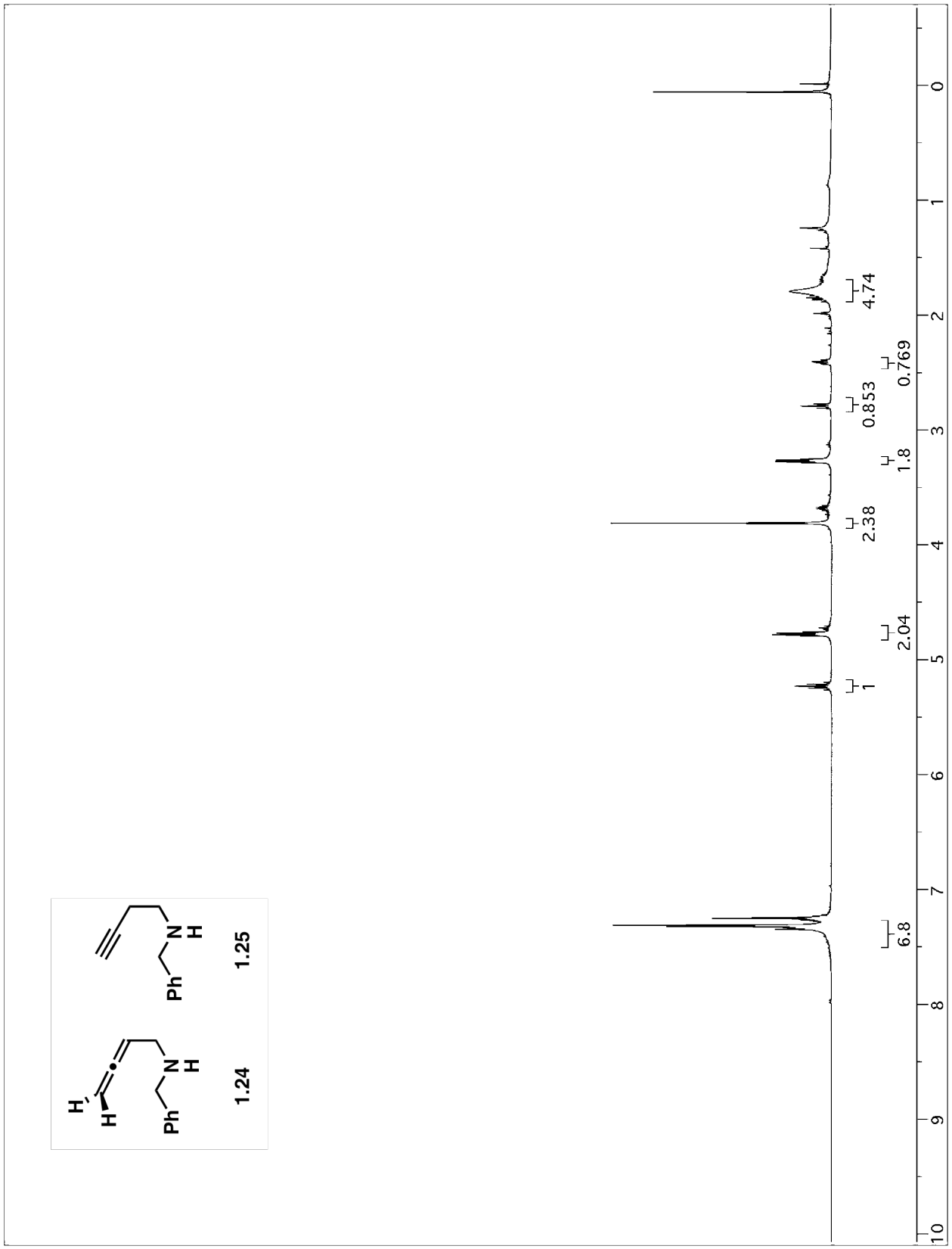
1.24
1.25
6.8
2.04
1
2.38
1.8
0.853
0.769
4.74

Experimental Chapter 2:

For general procedures for producing dithio acids see: D.F. Aycock and G.R. Jurch Jr., *J. Org. Chem.* **44** (1979), pp. 569–572 The dithioacids were prepared according to Aycock et al., and used without further purification. CAUTION: Carbon disulfide vapors are malodorous and cause liver and kidney damage upon inhalation. This reagent is flammable, low boiling, and should be handled in a well-ventilated hood. STENCH: Dithioacids should be handled in a well-ventilated hood.

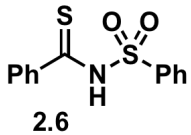

2.6

To a 15 mL round bottom flask charged with 5 mL of MeOH cooled to 0 ^{o}C, was added dithiobenzoic acid **263a** (202 mg, 1.3 mmol) and triethylamine (202 mg, 2.0 mmol). The resultant reddish/dark brown solution was treated with azide **211** (125 mg, 1 mmol) in one portion. Evolution of nitrogen was noted upon addition of azide and precipitation of sulfur was noted during the course of the reaction. The solution was allowed to warm to room temperature, and after 4 h the solution was concentrated in vacuo. Flash column chromatography (3:7 EtOAc/hexanes) provided 187 mg (85%) of thioamide **266** as a viscous yellow oil. IR (neat) mmax 3110, 1717, 1235; ^{1}H NMR (400 MHz, $CDCl_3$) 3.94 (s, 2H), 7.17 (s, 1H), 7.41 (m, 3H), 7.89 (2H),11.2 (br s, 1H); ^{13}C NMR (100 MHz, $CDCl_3$) 37.1, 116.9, 127.1, 129.5, 130.8, 133.4, 149.5, 169.1, 174.8; m/z (ESI-MS), found $[m+Na]^+$ 242.0, calcd. 242.1.

Experimental Chapter 3:

Thio acid/azide Amidation Kinetics Protocol:

Kinetics were conducted utilizing a Shimadzu UV-2401 (PC) spectrophotometer. A Fisher quartz cuvette, 1 cm pathlength, equipped with a micro stir bar and an internal Ωmega thermocouple ± 0.1 ºC was used to react thiobenzoic acid with the corresponding azide. Internal cuvette temperature was regulated using water-jacketed cuvette holder and a Fisher Scientific Isotemp 1006P. Monitored temperature variance over 12 h period was ± 0.1 ºC. Error bars: *x*-axis error bars correspond with the mean variance in temperature and *y*-axis error bars correspond with calculated weighted error in k_{obs}[106] and the error in the measurement of reactants.

UV-Vis kinetics sample preparation, benzene sulfonyl azide and thiobenzoic acid:

MeOH 2.481 g (77.53 mmol), benzenesulfonyl azide 131 mg (0.771 mmol) and 2,6-lutidine 90 mg (0.84 mmol) were weighed into a cuvette via syringe. The clear solution turned yellow upon the injection of 15.0 µl (0.0923 mmol) of thiobenzoic acid via 25 µl Hamilton syringe. The cuvette was then monitored at wavelength 329.0 nm for the disappearance of thiobenzoic acid.

[106] Beving, P. R.; *Data Reduction and Error Analysis for the Physical Sciences*, Mcgraw-Hill, New York, **1969**.

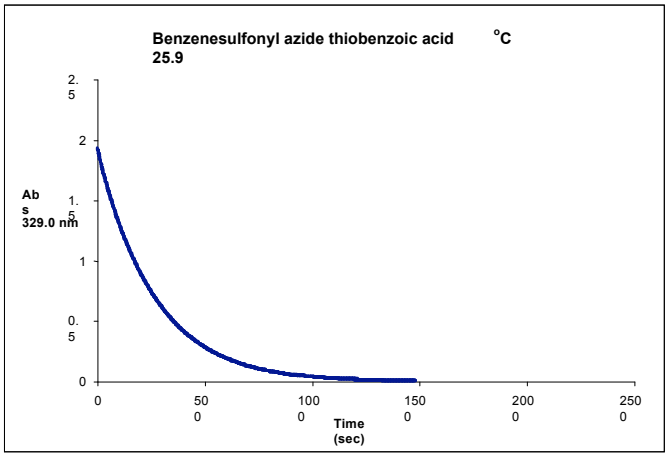

Figure 1. Disappearance of thiobenzoic acid when reacted with benzenesulfonyl azide at 25.9 ºC

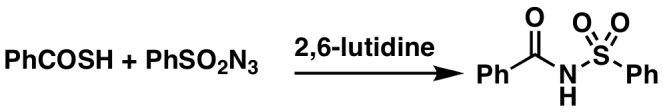

temp in Celsius	ln (k)	1/T
16.3	-5.44525582	0.00345
16.3	-5.47651811	0.00345
21.1	-5.14989339	0.00340
21.1	-5.16365218	0.00340
25.8	-4.85818758	0.00335
25.9	-4.8905719	0.00335
30.5	-4.56304485	0.00329
30.5	-4.52459945	0.00329

39.8	-3.99793119	0.00320
39.7	-4.00979436	0.00320

Table 1. Kinetics plot values for **Table 3.1**

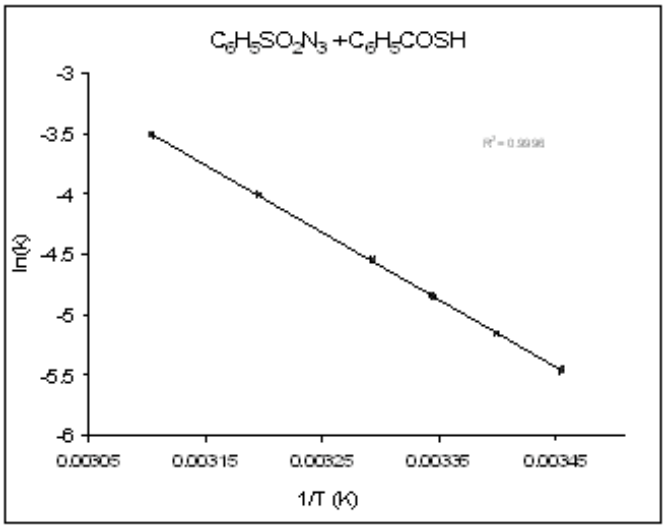

Figure 2. Arrhenius plot used to determine activation para

UV-Vis Kinetics sample preparation, benzyl azide and thiobenzoic acid:

Benzyl azide 3.312 g (24.90 mmol) and 2,6-lutidine 90 mg (0.84 mmol) were weighed (neat) into a cuvette via syringe. The clear solution turned yellow upon the injection of 1.0 µl (0.0061 mmol) of thiobenzoic acid via 5 µl Hamilton syringe. The cuvette monitored at wavelength 400.0 nm for the disappearance of thiobenzoic acid.

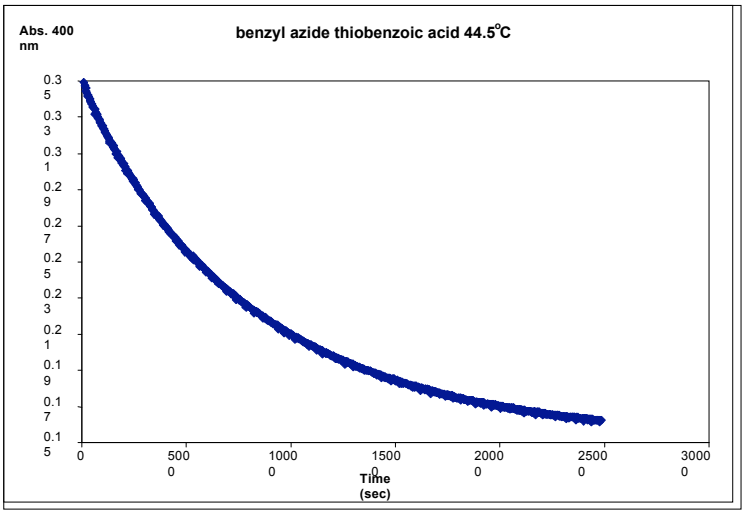

Figure 3. Disappearance of thiobenzoic acid when reacted with benzyl azide at 45 ºC

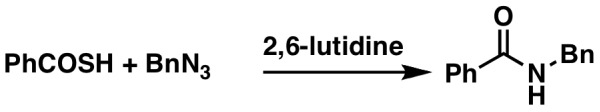

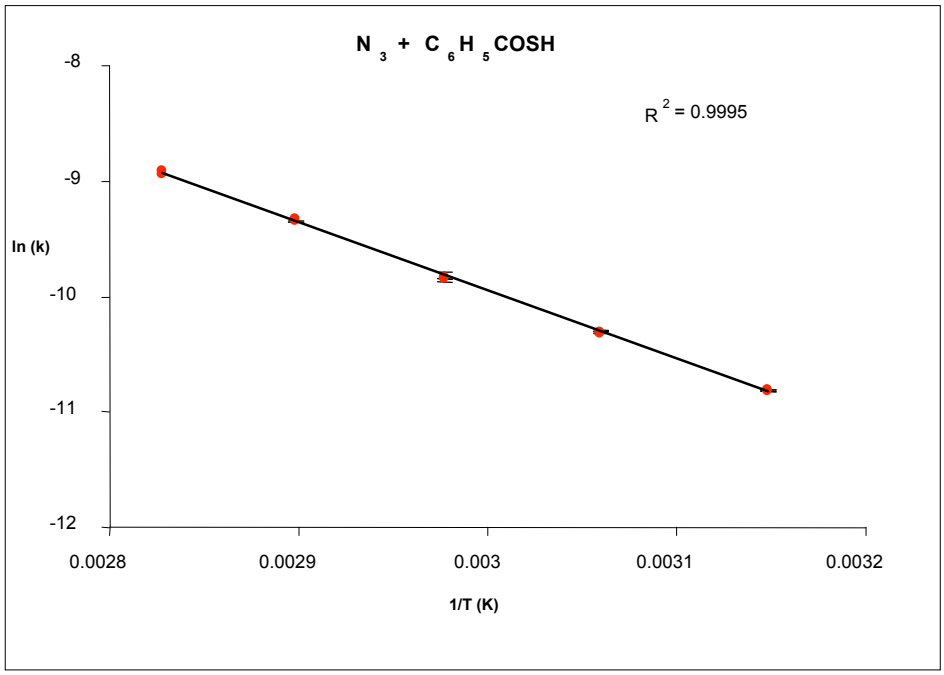

Figure 4. Arrhenius plot used to determine activation parameters. **Table 3.1**

temp in Celsius	ln (k)	1/T
44.5	-10.812925	0.00315
44.5	-10.820376	0.00315
53.7	-10.316158	0.00306
53.7	-10.301947	0.00306
62.7	-9.849537	0.00298
62.7	-9.830337	0.00298
71.9	-9.354435	0.00290
71.9	-9.339287	0.00290
80.4	-8.941085	0.00283
80.4	-8.915901	0.00283

Table 2. Kinetics plot values for **Table 3.1**

Hammett Study

Protocol: Hammett rate constants were conducted utilizing a Shimadzu UV-2401 (PC) spectrophotometer. A Fisher quartz cuvette, 1 cm pathlength, equipped with a micro stir bar and an internal Ωmega thermocouple ± 0.1 ºC was used to react (10.0 µl, 0.0610

mmol) thiobenzoic acid with 1-3 mmol of the corresponding azide, (100 mg, 0.0930 mmol) of 2,6-lutidine and 4.00 g of CH_3Cl_3 as solvent. The reaction was conducted at 30.0 ºC and was monitored a 430.0 nm (except for 3,4-NO_2, 490.0 nm) for the disappearance of thiobenzoic acid. Internal cuvette temperature was regulated using water-jacketed cuvette holder and a Fisher Scientific Isotemp 1006P. Monitored temperature variance over 12 h period was ± 0.1 ºC. Error bars: *y*-axis error bars correspond with calculated weighted error in k_{obs} and the error in the measurement of reactants.

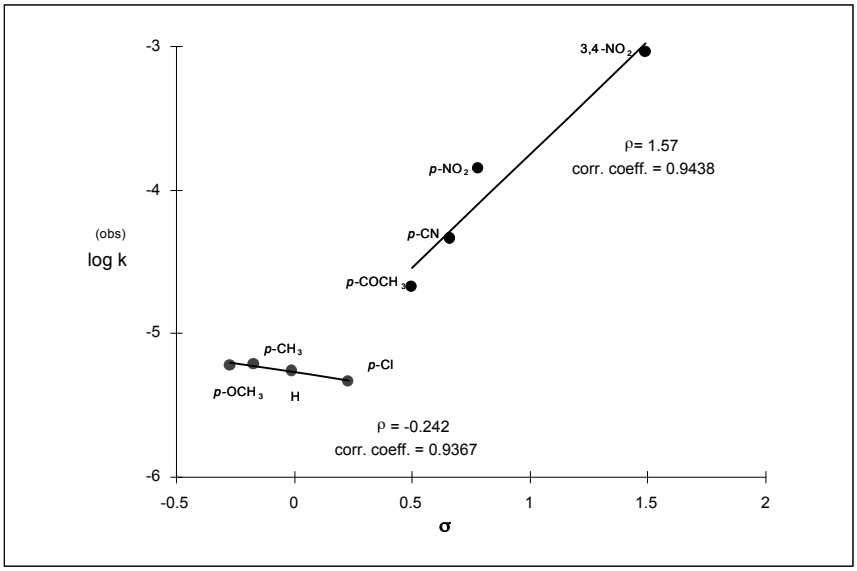

Figure 5. Hammett plot of the pseudo first order rate of thiobenzoic acid and *p*-substituted azides.

Substituent	σ values	log k_{obs}	error ±
CN	0.66	-4.336	0.006
CH_3O	0.50	-4.675	0.006
3,4-NO_2	1.49	-3.042	0.006
Cl	0.23	-5.331	0.005
NO_2	0.78	-3.855	0.005

H	-0.01	-5.259	0.002
CH_3	-0.17	-5.212	0.002
CH_3O	-0.27	-5.219	0.002

Table 3. Hammett plot values for the reaction of thiobenzoic acid and *p*-substituted azides.

III. Intermediate Interception.

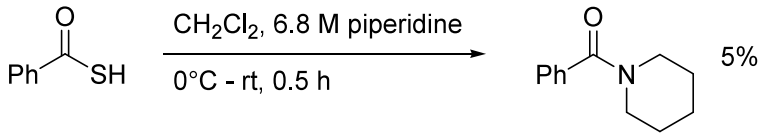

A 10ml round bottom flask, was charged with 500 µl of dichloromethane, 500 µl (6.80 mmol) of piperidine and then submerged into an ice bath, 0 ºC. 138 µl (1.00 mmol) of thiobenzoic acid was then added dropwise to the stirring solution. The yellow solution was stirred for 15 min at 0 ºC and then 15 min at rt. The reaction mixture was concentrated *in vacuo* and subjected to flash column chromatography (FCC), gradient eluent, 1:6 - 1:4 acetone:hexanes. Purification yielded 9 mg of N-benzoylpiperide as a white crystalline solid, 5 % yield. Spectral properties matched those of authentic sample.[108]

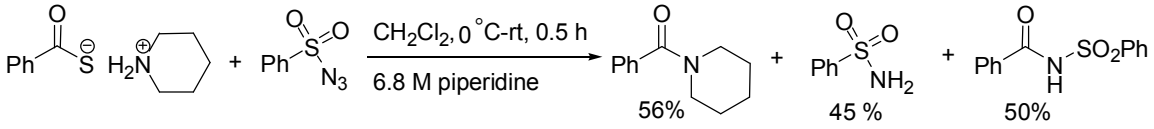

A 10 ml round bottom flask, was charged with 500 µl of dichloromethane, 500 µl (6.80 mmol) of piperidine and then submerged into an ice bath, 0 ºC. 138 µl (1.00 mmol) of thiobenzoic acid was then added dropwise to the stirring solution. The yellow solution was stirred for 10min at 0 ºC upon which time 92 mg (0.50 mmol) of benzene sulfonyl azide was added dropwise to the solution. Bubbling was immediately observed and the reaction was then stirred for an additional 15 min at rt. The reaction mixture was concentrated *in vacuo* and subjected to FCC, gradient eluent, 1:6 – 1:0 acetone:hexanes, 1

% acetic acid. Purification yielded 52 mg of N-benzoylpiperidine as a white crystalline solid, 55 % yield, 37 mg of benzene sulfonamide as a white crystalline solid, 47 % yield and 65 mg of N-phenylsulfonyl benzamide as a white crystalline solid, 50 % yield. Spectral properties were identical with those of authentic sample and reported literature values.[3,109,110]

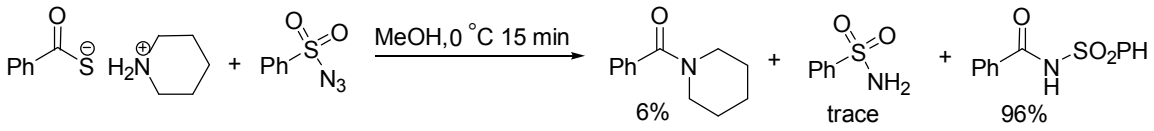

A 10ml round bottom flask, was charged with 2 ml of MeOH, 99 µl (1.00 mmol) of piperidine and then submerged into an ice bath, 0 ºC. 138 µl (1.00 mmol) of thiobenzoic acid was then added dropwise to the stirring solution. 92 mg (0.50 mmol) of benzene sulfonyl azide was then added dropwise (5 min) to the solution. Bubbling was immediately observed upon addition of azide and the reaction was subsequently stirred for an additional 10 min at rt. The reaction mixture was concentrated *in vacuo* and subjected to FCC, gradient eluent, 1:6 – 1:4 acetone:hexanes. Purification yielded 10 mg of N-benzoylpiperidine as a white crystalline solid, 6 % yield, and 125 mg of N-phenylsulfonyl benzamide as a white crystalline solid, 96 % yield. Spectral properties were identical with those of authentic sample and reported literature values.[3,4,5]

III. Thionester Preparation and Spectral Data

Preparation of O-trimethylsilyl benzothioate[111].

To a 50 ml round bottom flask under argon was added 20 ml of dry ether, thiobenzoic acid 1.47 g (10.6 mmol), and chlorotrimethylsilane 1.2 g (11.0 mmol). Triethylamine (1.1 g, 10.9 mmol) was then added and was accompanied by formation of a precipitate. The mixture was stirred for an additional 30 min at rt, followed by filtration and hexanes rinse of residual triethylammonium chloride. The filtrate was dried *in vacuo* to yield a yellow oil. δ_H (400 MHz, $CDCl_3$) 0.53 (s, 9H), 7.38 (t, 2H), 7.54 (m, 1H), 8.24 (d, 2H); δ_c (100 MHz, $CDCl_3$) 0.1, 127.9, 128.8, 132.8, 139.4, 212.4

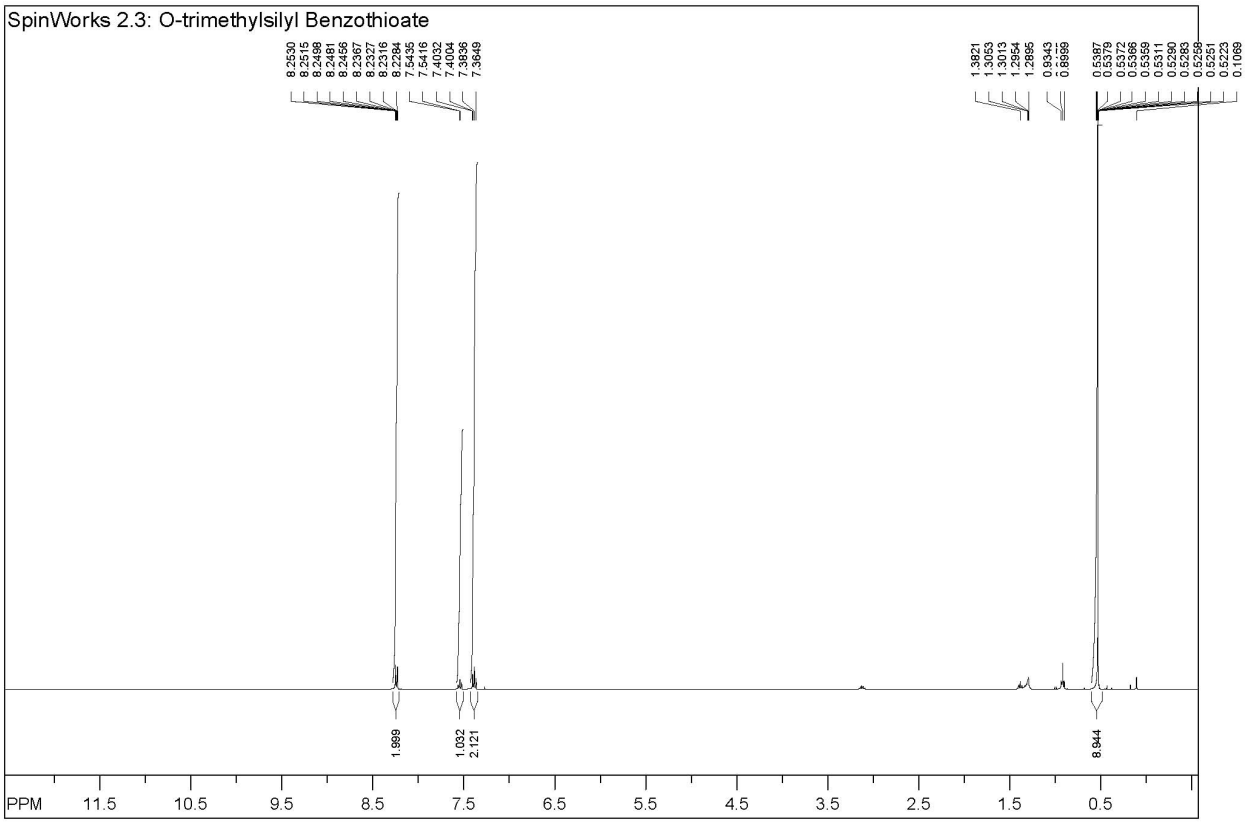

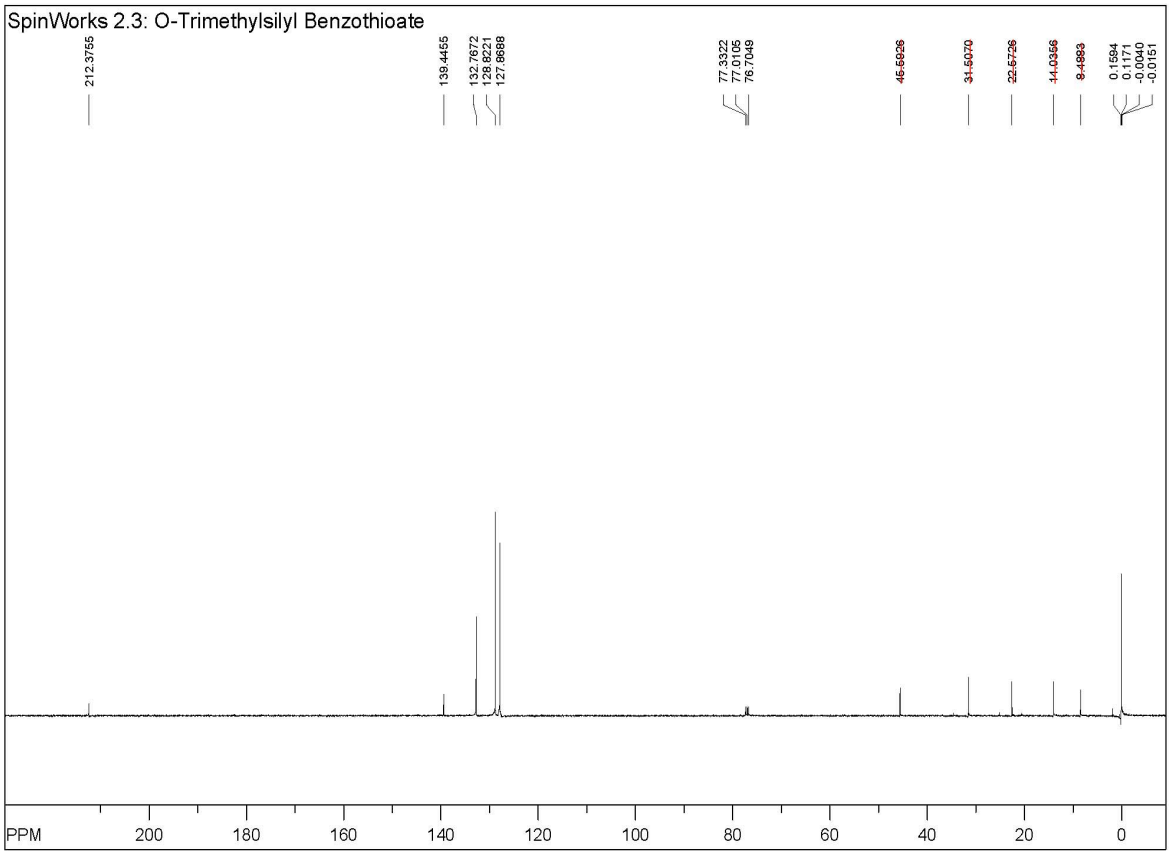
SpinWorks 2.3: O-Trimethylsilyl Benzothioate
212.3755
139.4455
132.7672
128.8221
127.8688
77.3322
77.0105
76.7049
46.6026
31.5070
22.6726
14.0356
9.4883
0.1584
0.1171
-0.0040
-0.0151
PPM
200
180
160
140
120
100
80
60
40
20
0

V. ESI/MS Procedure and Data

Preparation of ESI/MS Sample:

To a 12ml Wheaton sample vial 6 ml MeOH, 20 μmol of azide, 40 μmol of triethylamine and 20 μmol thio acid were added via syringe. The sample vial was then stirrred for 5 minutes, followed by ESI-MS analysis. Sample was collected with the following settings, capillary temperature 180 ºC, spray voltage 4.0 kV, sheath gas flow rate 30 ft/min, and MS/MS+ 20-50% relative collision energy.

ESI/MS **Data:**

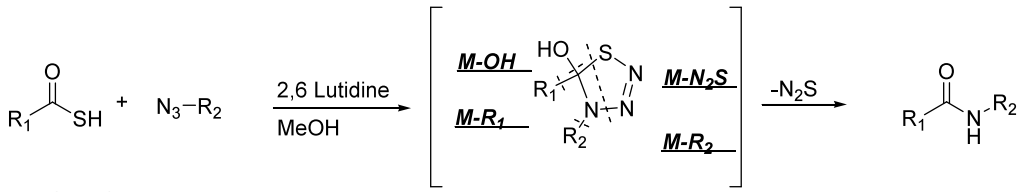

R_1= *CH_3, C_6H_5, Fmoc-Ile,*
R_2= *Benzyl, Dansyl, $SO_2C_6H_4COOH$ Methyl Phenyl Sulphide,*

ESI[MS/MS]+ Ion Trapped Adduct and Corresponding Fragments

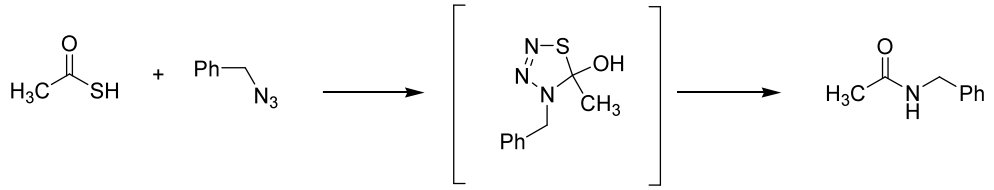

Calc. Mass [$C_9H_{11}N_3OS$]	209.1
Obsv. Mass [$C_9H_{11}N_3OS$] ESI[M+H]	210.1
[**M -N_2S**] Calc: 149.1, Obs: 149.2	
[**M -Bn**] Calc: 194.0, Obs: 194.3	
[**M -CH_3**] Calc: 118.0, Obs: 118.2	
[**M -OH**] Calc: 192.1, Obs: 192.0	

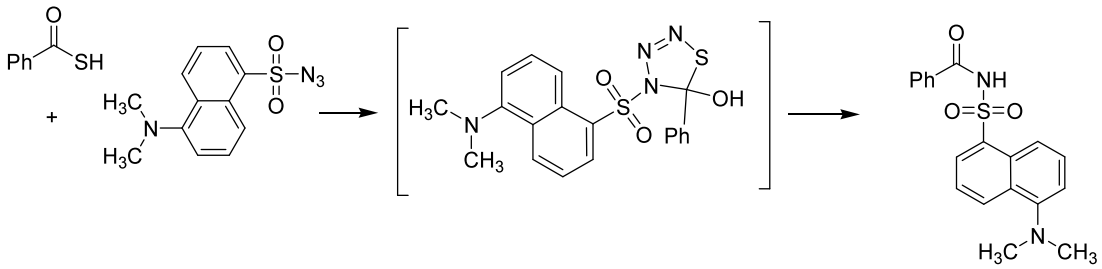

Calc. Mass: [$C_{19}H_{18}N_4O_3S_2$]	414.1
Obsv. Mass: [$C_{19}H_{18}N_4O_3S_2$] ESI[M+H]	415.5
[**M -N_2S**] Calc: 354.1, Obs: 354.2	
[**M -Ph**] Calc: 337.0, Obs: 336.2	
[**M -$C_{12}H_{12}NO_2S$**] Calc: 234.1, Obs: 234.0	
[**M -OH**] Calc: 397.1, Obs: 397.0	

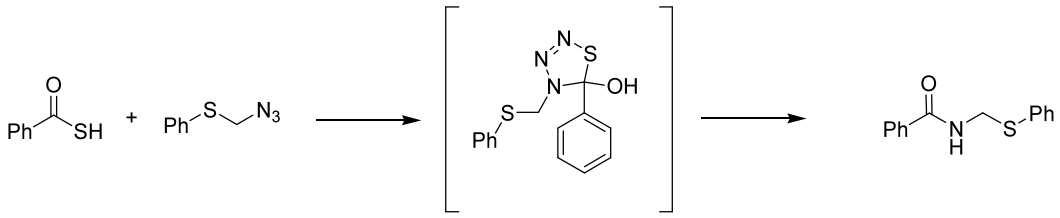

Calc. Mass: $[C_{14}H_{13}N_3OS_2]$ 303.1
Obsv. Mass: $[C_{14}H_{13}N_3OS_2]$ ESI[M+H] 304.3

[**M -N_2S**] Calc: 243.1, Obs: 243.4
[**M -Ph**] Calc: 226.0, Obs: 225.9
[**M -$PhSCH_2$**] Calc:180.0, Obs: 180.1
[**M -OH**] Calc: 286.1, Obs: 286.6

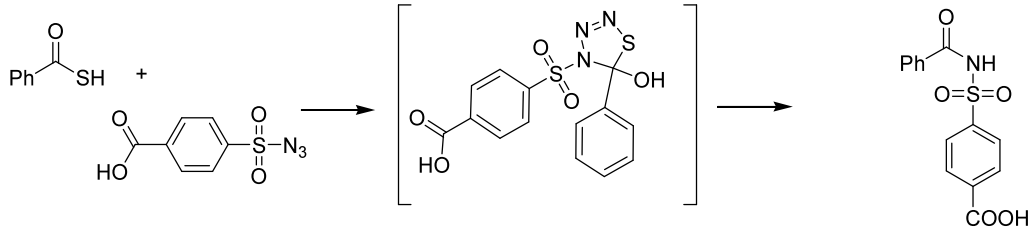

Calc. Mass: $[C_{14}H_{11}N_3O_5S_2]$ 365.0
Obsv. Mass: $[C_{14}H_{11}N_3O_5S_2]$ ESI[M+H] 366.3

[**M -N_2S**] Calc: 305.4, Obs: 305.2
[**M -Ph**] Calc: 288.0, Obs: 287.7
[**M -$C_7H_5O_4S$**] Calc:180.0, Obs: 180.4
[**M -OH**] Calc: 348.0, Obs: 348.2

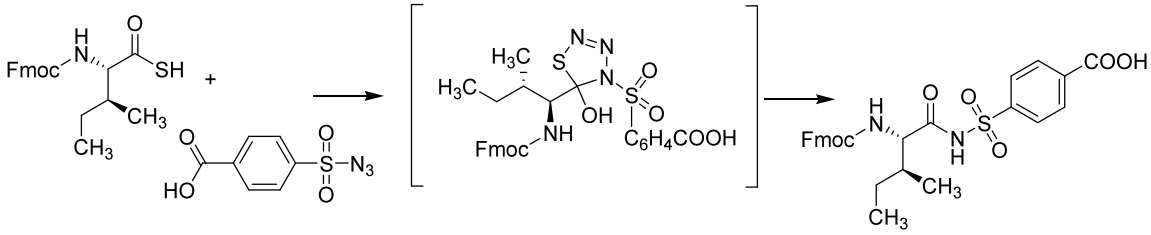

Calc. Mass: $[C_{28}H_{28}N_4O_7S_2]$ 596.1
Obsv. Mass: $[C_{28}H_{28}N_4O_7S_2]$ ESI[M+H] 597.2

[**M -N_2S**] Calc: 536.2, Obs: 536.1
[**M -$C_8H_6N_3O_5S_2$**] Calc: 287.9, Obs: 287.6
[**M -$C_{21}H_{23}N_4O_3S$**] Calc:411.2, Obs: 410.9
[**M -OH**] Calc: 579.2, Obs: 579.3

VI. Computational Data:

Methylazide: **3.21**

7	0.716979	-0.097515	0.000004
7	1.798828	0.272194	-0.000002
7	-0.394748	-0.633787	-0.000002
6	-1.548525	0.285563	0.000000
1	-1.557613	0.920209	0.895348
1	-1.557401	0.920503	-0.895142
1	-2.441246	-0.340330	-0.000207

Low frequencies -11.6080 -4.4042 -0.0011 -0.0007 0.0024 12.8383

Zero-point correction= 0.050446 (Hartree/Particle)
Thermal correction to Energy= 0.054923
Thermal correction to Enthalpy= 0.055867
Thermal correction to Gibbs Free Energy= 0.023852
Sum of electronic and zero-point Energies= -204.051209
Sum of electronic and thermal Energies= -204.046733
Sum of electronic and thermal Enthalpies= -204.045789
Sum of electronic and thermal Free Energies= -204.077804

Methylazide in simulated acetone: SCF Done: E(RB+HF-LYP) = -204.105010

Thioacetic acid: **3.14a**

16	1.338621	-0.073866	0.000000
6	-0.466390	0.229762	0.000000
8	-0.856849	1.372622	0.000000
6	-1.375745	-0.983092	0.000000
1	-1.191274	-1.600344	0.886519
1	-2.414336	-0.643163	-0.000001
1	-1.191273	-1.600345	-0.886518
1	1.286543	-1.435292	0.000002

Low frequencies -0.0010 0.0002 0.0003 8.9624 9.4887 16.9897

Zero-point correction= 0.055977 (Hartree/Particle)
Thermal correction to Energy= 0.061134
Thermal correction to Enthalpy= 0.062079
Thermal correction to Gibbs Free Energy= 0.027708
Sum of electronic and zero-point Energies= -163.913135
Sum of electronic and thermal Energies= -163.907978
Sum of electronic and thermal Enthalpies= -163.907034
Sum of electronic and thermal Free Energies= -163.941404

Thioacetic acid in simulated acetone: -163.973031

Methane sulfonazide: **3.20**

6	-1.794888	1.177777	0.250710
1	-1.852994	1.719264	-0.694394
1	-2.755348	0.728004	0.510819
16	-0.648620	-0.215014	0.014066
1	-1.408098	1.799198	1.058647
7	0.759815	0.780032	-0.551016
7	1.845731	0.301960	-0.173019
7	2.880998	-0.056620	0.130006
8	-1.113422	-1.046304	-1.134272
8	-0.291843	-0.835010	1.328500

Low frequencies -8.2118 -3.7361 -0.0016 0.0011 0.0072 5.0188

Zero-point correction= 0.059342 (Hartree/Particle)
Thermal correction to Energy= 0.067045
Thermal correction to Enthalpy= 0.067989
Thermal correction to Gibbs Free Energy= 0.025990
Sum of electronic and zero-point Energies= -364.519803
Sum of electronic and thermal Energies= -364.512101
Sum of electronic and thermal Enthalpies= -364.511157
Sum of electronic and thermal Free Energies= -364.553155

Methane sulfonazide in siumulated acetone: -364.584701

Thioacetate ion: **3.22**

16	-1.332845	-0.146697	0.236823
6	0.346006	0.220005	-0.100852
8	0.819040	1.325211	-0.412873
6	1.333116	-0.965263	0.003829
1	1.041912	-1.762251	-0.691137
1	2.352413	-0.627409	-0.226132
1	1.304148	-1.393329	1.013229

Low frequencies -10.1498 -0.0014 -0.0011 -0.0005 13.1316 13.7989

Zero-point correction= 0.046351 (Hartree/Particle)
Thermal correction to Energy= 0.051111
Thermal correction to Enthalpy= 0.052055
Thermal correction to Gibbs Free Energy= 0.017130
Sum of electronic and zero-point Energies= -163.383360
Sum of electronic and thermal Energies= -163.378600
Sum of electronic and thermal Enthalpies= -163.377656
Sum of electronic and thermal Free Energies= -163.412581

Thioacetate in simulated acetone: -163.510874

Trimethylsilyl acetate: **3.19b**

16	-1.979874	-1.169117	0.000013
6	-1.514328	0.428947	-0.000062
8	-0.254921	0.857537	0.000009
6	-2.483469	1.583250	0.00001
14	1.245606	0.00433	-0.000001
6	2.461511	1.419496	-0.000029
6	1.399700	-1.016362	1.558599
6	1.399644	-1.016403	-1.558581
1	3.496654	1.053749	0.000037
1	2.335694	2.055376	-0.885150
1	2.335614	2.055465	0.885016
1	0.704056	-1.861122	1.564449
1	2.419951	-1.414267	1.648150
1	1.205468	-0.411288	2.453129
1	0.704295	-1.861408	-1.564200
1	1.204938	-0.411444	-2.453087
1	2.420013	-1.413942	-1.648404
1	-2.305752	2.211501	-0.882391
1	-2.305398	2.211628	0.882265
1	-3.515019	1.231698	0.000241

Low frequencies -11.3996 -0.0021 0.0006 0.0008 7.1020 12.6868

Zero-point correction= 0.161285 (Hartree/Particle)
Thermal correction to Energy= 0.173784
Thermal correction to Enthalpy= 0.174728
Thermal correction to Gibbs Free Energy= 0.122571
Sum of electronic and zero-point Energies= -286.929407
Sum of electronic and thermal Energies= -286.916908
Sum of electronic and thermal Enthalpies= -286.915964
Sum of electronic and thermal Free Energies= -286.968122

Trimethylsilyl acetate in simulated acetone: -287.095057

Linear adduct from methane sulfonazide and thioacetate: **3.23**

S	-1.8495	0.60759	0.02218
C	-3.48172	-0.13789	0.02729
O	-3.74791	-1.32538	-0.02646
C	-4.59561	0.90853	0.10626
N	-0.8672	-1.02947	-0.17582
N	0.36044	-0.85182	-0.18231
N	0.90437	0.34822	-0.04054
S	2.61568	0.2127	-0.10834
H	-4.21608	1.92561	0.24175
H	-5.18103	0.86443	-0.82049
H	-5.26254	0.65044	0.93729
O	3.13911	-0.44064	-1.3705
O	3.14497	1.57953	0.25899
C	3.05988	-0.92885	1.26549
H	2.71011	-0.48331	2.19839
H	2.57459	-1.88683	1.07156
H	4.14812	-1.02212	1.25025

Low frequencies -5.4131 -0.0013 -0.0011 -0.0003 1.1558 5.3065

Zero-point correction= 0.106952 (Hartree/Particle)
Thermal correction to Energy= 0.120233
Thermal correction to Enthalpy= 0.121177
Thermal correction to Gibbs Free Energy= 0.064612
Sum of electronic and zero-point Energies= -527.930725
Sum of electronic and thermal Energies= -527.917444
Sum of electronic and thermal Enthalpies= -527.916500
Sum of electronic and thermal Free Energies= -527.973066

Linear adduct **3.23** in simulated acetone: -528.115065

Transition state from methane sulfonazide and thioacetate: **3.24**

16	2.617961	-0.563849	-0.216803
6	1.209444	0.910727	0.226005
8	1.172999	1.269303	1.400957
6	1.254211	1.924118	-0.919286
7	1.484342	-1.878410	0.146668
7	0.273800	-1.549786	0.123003
7	0.004161	-0.248229	-0.234572
16	-1.673274	0.098851	0.090328
1	2.176886	2.508532	-0.821038
1	1.228036	1.444330	-1.899924
1	0.398444	2.599263	-0.815010
8	-2.149596	-0.230329	1.479595
8	-1.923836	1.480671	-0.461169
6	-2.486833	-1.102321	-1.033544
1	-2.168176	-0.879823	-2.052719
1	-2.183347	-2.102811	-0.724040
1	-3.560433	-0.946833	-0.903479

Low frequencies -160.5580 -8.6870 -5.9905 -2.7563 -0.0004 0.0005

Zero-point correction= 0.107693 (Hartree/Particle)
Thermal correction to Energy= 0.119358
Thermal correction to Enthalpy= 0.120302
Thermal correction to Gibbs Free Energy= 0.069936
Sum of electronic and zero-point Energies= -527.906277
Sum of electronic and thermal Energies= -527.894613
Sum of electronic and thermal Enthalpies= -527.893669
Sum of electronic and thermal Free Energies= -527.944035

Transition state **3.24** in simulated acetone: -528.115065
Intermediate from methane sulfonazide and thioacetate: **3.25**

16	2.657728	-0.392815	-0.118449
6	0.982934	0.875662	0.250440
8	0.770338	1.091589	1.460907

6	1.155471	2.046891	-0.719736
7	1.607683	-1.798761	0.017769
7	0.386585	-1.567093	-0.134550
7	0.057731	-0.240827	-0.440015
16	-1.671229	-0.043425	-0.210752
1	1.996293	2.660009	-0.376604
1	1.336761	1.714103	-1.744558
1	0.244561	2.654784	-0.687478
8	-1.973229	1.406100	-0.481110
8	-2.396444	-1.095108	-1.003999
6	-1.957388	-0.375794	1.564642
1	-1.723623	-1.427548	1.735764
1	-1.280778	0.284094	2.111006
1	-3.012610	-0.160028	1.748206

Low frequencies -3.8628 -0.0007 0.0008 0.0009 9.1974 16.0619

Zero-point correction= 0.108549 (Hartree/Particle)
Thermal correction to Energy= 0.120575
Thermal correction to Enthalpy= 0.121520
Thermal correction to Gibbs Free Energy= 0.070850
Sum of electronic and zero-point Energies= -527.913792
Sum of electronic and thermal Energies= -527.901766
Sum of electronic and thermal Enthalpies= -527.900822
Sum of electronic and thermal Free Energies= -527.951492

Intermediate from **3.25**: -528.094161

Sulfonyl amide: **3.28**

6	-1.667724	0.132478	-0.042468
8	-1.592098	1.325700	0.198031
6	-2.976346	-0.633710	-0.093700
7	-0.536918	-0.634799	-0.307817
16	1.106387	-0.169882	0.114322
1	-3.792244	0.074792	-0.248584
1	-2.988449	-1.389095	-0.886991
1	-3.132038	-1.143156	0.865507
8	1.171308	0.238180	1.547280
8	1.904540	-1.330512	-0.399144
6	1.377240	1.292432	-0.931814
1	1.291200	0.980766	-1.973452
1	0.624786	2.030475	-0.651626
1	2.388258	1.633701	-0.698605
1	-0.604299	-1.639916	-0.442122

Low frequencies -9.1355 -3.3132 -0.0014 -0.0011 0.0002 4.9466

Zero-point correction= 0.110730 (Hartree/Particle)
Thermal correction to Energy= 0.120439
Thermal correction to Enthalpy= 0.121383
Thermal correction to Gibbs Free Energy= 0.075501
Sum of electronic and zero-point Energies= -408.898595
Sum of electronic and thermal Energies= -408.888886
Sum of electronic and thermal Enthalpies= -408.887942

Sum of electronic and thermal Free Energies= -408.933824

Sulfonyl amide **3.28** in simulated acetone: -409.021479

Acetamide: **3.34**

6	0.165899	0.000008	0.481404
8	1.389633	-0.000116	0.366818
6	-0.516357	0.000057	1.840547
1	-1.610352	-0.000116	1.786307
1	-0.188855	-0.882347	2.399668
1	-0.189134	0.882700	2.399460
6	-0.129191	0.000014	-1.964298
1	0.489467	0.886558	-2.139265
1	0.490277	-0.886028	-2.138881
1	-0.966367	-0.000520	-2.666532
7	-0.658010	0.000004	-0.607189
1	-1.658136	0.000171	-0.470897

Low frequencies -12.2715 -11.5560 -0.0007 -0.0005 0.0005 14.2283

Zero-point correction= 0.102127 (Hartree/Particle)
Thermal correction to Energy= 0.108841
Thermal correction to Enthalpy= 0.109786
Thermal correction to Gibbs Free Energy= 0.071150
Sum of electronic and zero-point Energies= -248.435207
Sum of electronic and thermal Energies= -248.428493
Sum of electronic and thermal Enthalpies= -248.427549
Sum of electronic and thermal Free Energies= -248.466184

Acetamide in simulated acetone: -248.548815

Transition state from methane sulfonazide and thioacetic acid: **3.29a**

16	0.303069	-1.422554	-2.350358
6	0.444136	-1.689114	-0.636731
8	1.652273	-1.682224	-0.068096
6	-0.554943	-2.485101	0.156743
7	0.065802	0.770072	-2.308623
7	-0.171279	1.040047	-1.179489
7	-0.349349	0.296695	-0.133851
16	-0.202669	1.158486	1.408745
1	-0.325351	-3.549257	0.015330
1	-0.470455	-2.246800	1.219612
1	-1.568111	-2.292266	-0.194594
8	-0.354065	0.063121	2.416677
8	0.998083	2.051577	1.394445
6	-1.698422	2.208027	1.438304
1	-1.638576	2.910089	0.605257
1	-2.569463	1.555730	1.366592
1	-1.670427	2.732579	2.396148

1	2.304811	-1.295337	-0.682894

Low frequencies -267.3517 -0.0013 -0.0006 -0.0002 1.6783 8.7892

Zero-point correction= 0.119879 (Hartree/Particle)
Thermal correction to Energy= 0.132429
Thermal correction to Enthalpy= 0.133373
Thermal correction to Gibbs Free Energy= 0.080154
Sum of electronic and zero-point Energies= -528.392722
Sum of electronic and thermal Energies= -528.380172
Sum of electronic and thermal Enthalpies= -528.379228
Sum of electronic and thermal Free Energies= -528.432448

Transition state **3.29a** in simulated acetone: -528.533651

Nitrous sulfide:

7	-0.093004	0.000000	-0.008362
7	0.148186	0.000000	1.098804
16	0.492050	0.000000	2.677066

Low frequencies -7.5319 -0.0008 0.0010 0.0013 6.4894 456.4246

Zero-point correction= 0.007708 (Hartree/Particle)
Thermal correction to Energy= 0.010898
Thermal correction to Enthalpy= 0.011842
Thermal correction to Gibbs Free Energy= -0.007276
Sum of electronic and zero-point Energies= -119.584327
Sum of electronic and thermal Energies= -119.581138
Sum of electronic and thermal Enthalpies= -119.580193
Sum of electronic and thermal Free Energies= -119.599311

Nitrogen sulfide in simulated acetone: -119.592632
Thiatriazoline intermediate **3.26**

16	-2.584042	-0.434079	-0.067225
6	-1.100558	0.720630	0.006336
8	-0.911550	1.288355	1.264785
6	-1.204558	1.860794	-0.998543
7	-1.542689	-1.873572	0.039707
7	-0.336765	-1.600996	-0.093494
7	-0.041590	-0.273124	-0.358075
16	1.668609	0.092864	0.099345
1	-2.067629	2.485777	-0.751577
1	-0.300868	2.472702	-0.940223
1	-1.317125	1.467899	-2.010491
8	1.937448	1.462947	-0.431179
8	1.880211	-0.242661	1.541087
6	2.523699	-1.140806	-0.933043
1	2.196491	-2.132311	-0.621495
1	2.282144	-0.931322	-1.975422
1	3.585301	-0.983636	-0.728665
1	-0.844457	0.601320	1.950948

Low frequencies -7.2152 -4.2258 -0.0007 -0.0006 0.0010 7.1340

Zero-point correction=	0.122195 (Hartree/Particle)
Thermal correction to Energy=	0.134204
Thermal correction to Enthalpy=	0.135148
Thermal correction to Gibbs Free Energy=	0.084379
Sum of electronic and zero-point Energies=	-528.420760
Sum of electronic and thermal Energies=	-528.408751
Sum of electronic and thermal Enthalpies=	-528.407807
Sum of electronic and thermal Free Energies=	-528.458576

Thiatriazoline **3.26** in simulated acetone: -528.552348

Transition state for fragmentation of **3.26: 3.27**

16	-2.642793	-0.455157	0.052403
6	-0.867495	0.870997	-0.044639
8	-0.690013	1.355883	1.213253
6	-1.369178	1.960283	-0.977851
7	-1.630160	-1.781128	0.024287
7	-0.469944	-1.831359	-0.168654
7	0.042953	-0.041052	-0.592321
16	1.650328	0.066709	0.060242
1	-2.232222	2.477526	-0.548876
1	-0.555345	2.684906	-1.098172
1	-1.624031	1.544478	-1.953551
8	2.272411	1.336028	-0.440466
8	1.611896	-0.184809	1.557132
6	2.461163	-1.337490	-0.761259
1	2.000885	-2.262707	-0.418174
1	2.353086	-1.196109	-1.837140
1	3.507256	-1.268366	-0.455552
1	-0.071436	0.790675	1.729098

Low frequencies	-384.0524	-0.0002	0.0004	0.0005	5.9229	9.0646

Zero-point correction=	0.120578 (Hartree/Particle)
Thermal correction to Energy=	0.132524
Thermal correction to Enthalpy=	0.133468
Thermal correction to Gibbs Free Energy=	0.082657
Sum of electronic and zero-point Energies=	-528.400650
Sum of electronic and thermal Energies=	-528.388704
Sum of electronic and thermal Enthalpies=	-528.387760
Sum of electronic and thermal Free Energies=	-528.438571

Transition state **3.27** in acetone: -528.528506

Transition state from TMS acetate and methane sulfonazide: **3.29b**

16	-0.958232	2.349869	-0.160550
6	-0.617091	1.062154	0.984622
8	-1.252652	-0.079384	0.949887
6	-0.003291	1.366415	2.328406
7	0.540829	1.967266	-1.660256

7	1.305210	1.170000	-1.214231
7	1.359880	0.635069	-0.031434
16	2.385973	-0.787780	0.071751
8	2.240892	-1.204444	1.503620
8	2.081641	-1.745507	-1.042717
6	4.071967	-0.132638	-0.192137
14	-2.306311	-0.895179	-0.171197
6	-2.460851	-2.561524	0.649253
6	-3.932624	0.022032	-0.195441
6	-1.505276	-1.016171	-1.847285
1	4.117202	0.294691	-1.195077
1	4.268609	0.611012	0.581055
1	4.741408	-0.990815	-0.099957
1	-3.116786	-3.224391	0.069893
1	-1.484126	-3.052626	0.735299
1	-2.882129	-2.476924	1.658391
1	-3.838983	1.005752	-0.667216
1	-4.678468	-0.552268	-0.761786
1	-4.331896	0.165837	0.816387
1	-1.433098	-0.046398	-2.350511
1	-0.500009	-1.450281	-1.789349
1	-2.109756	-1.676285	-2.485087
1	0.690477	2.203876	2.262080
1	0.502929	0.480332	2.719294
1	-0.818374	1.634304	3.014742

Low frequencies -210.3919 -10.6911 -2.2426 -0.0009 -0.0003 0.0006

Zero-point correction= 0.221630 (Hartree/Particle)
Thermal correction to Energy= 0.242011
Thermal correction to Enthalpy= 0.242955
Thermal correction to Gibbs Free Energy= 0.172128
Sum of electronic and zero-point Energies= -651.419439
Sum of electronic and thermal Energies= -651.399058
Sum of electronic and thermal Enthalpies= -651.398114
Sum of electronic and thermal Free Energies= -651.468941

Transition state **3.29b** in simulated acetone: -651.652812

Trimethylsilyl adduct **3.26b**

16	-0.662701	2.445464	-0.041464
6	-0.027623	0.903088	0.849315
8	-0.869351	-0.178296	0.819718
6	0.332815	1.223760	2.299948
7	0.335137	2.107378	-1.479241
7	1.168524	1.207501	-1.275191
7	1.203132	0.696744	0.006391
16	2.052190	-0.887943	0.049713
8	2.197672	-1.217518	1.500439
8	1.421388	-1.854328	-0.900937
6	3.665324	-0.373100	-0.624664
14	-2.137001	-0.811339	-0.126910
6	-2.183500	-2.597379	0.411075

6	-3.712891	0.084265	0.347336
6	-1.803850	-0.665817	-1.960009
1	3.508167	0.001054	-1.636086
1	4.079849	0.386524	0.038549
1	4.270995	-1.282135	-0.621706
1	-1.243162	-3.102259	0.159972
1	-2.331550	-2.686316	1.494319
1	-3.000184	-3.140084	-0.082993
1	-4.580505	-0.372078	-0.148411
1	-3.891568	0.035767	1.429115
1	-3.687395	1.141336	0.057195
1	-0.851318	-1.133404	-2.234083
1	-2.598061	-1.188672	-2.511206
1	-1.790343	0.370631	-2.315110
1	1.063240	2.033909	2.349902
1	0.743723	0.327218	2.770069
1	-0.572574	1.517793	2.839739

Low frequencies -9.3310 -0.0015 -0.0004 0.0004 7.4840 13.2005

Zero-point correction= 0.224323 (Hartree/Particle)
Thermal correction to Energy= 0.243979
Thermal correction to Enthalpy= 0.244923
Thermal correction to Gibbs Free Energy= 0.177075
Sum of electronic and zero-point Energies= -651.444386
Sum of electronic and thermal Energies= -651.424731
Sum of electronic and thermal Enthalpies= -651.423787
Sum of electronic and thermal Free Energies= -651.491634

Trimethylsilyl adduct **3.26b** in simulated acetone: -651.678866 Transition state for methyl azide with thioacetic acid: **3.35**

16	1.557956	.887342	.005641
6	.750254	-.631574	.065055
7	-.517682	2.158203	-.045779
8	.580223	-1.251350	1.268635
6	.838106	-1.641440	-1.055147
7	-1.238073	1.245624	-.155695
7	-1.203328	-.011141	-.346688
6	-2.329830	-.813561	.135082
1	1.815352	-2.135711	-1.000069
1	.067616	-2.412355	-.952453
1	.743069	-1.149278	-2.022864
1	-3.256795	-.527242	-.373361
1	-2.105057	-1.852030	-.114027
1	-2.463443	-.732392	1.220908
1	.792583	-.607018	1.969719

Low frequencies -367.6773 -5.4774 -.0012 -.0011 -.0008 10.9360

Zero-point correction= .111260 (Hartree/Particle)
Thermal correction to Energy= .120478
Thermal correction to Enthalpy= .121422
Thermal correction to Gibbs Free Energy= .076861

Sum of electronic and zero-point Energies= -367.921789
Sum of electronic and thermal Energies= -367.912571
Sum of electronic and thermal Enthalpies= -367.911627
Sum of electronic and thermal Free Energies= -367.956188

Transition state **3.33** in simulated acetone: -368.04669758

Methyl azide-thioacetic acid adduct **3.32**

16	1.617676	-0.455485	-0.115039
6	-0.216226	-0.664784	0.064846
8	-0.598716	-1.062349	1.369859
6	-0.807785	-1.700194	-0.887570
7	1.460487	1.344611	-0.011260
7	0.265079	1.689823	-0.080220
7	-0.655951	0.709090	-0.251301
6	-2.050763	1.102790	-0.062939
1	-0.358232	-2.678606	-0.697901
1	-1.884949	-1.792913	-0.711932
1	-0.628879	-1.412684	-1.925437
1	-2.145076	2.143286	-0.377156
1	-2.691005	0.482150	-0.694936
1	-2.369452	1.002181	0.981019
1	-0.054155	-0.588392	2.021547

Low frequencies -11.4487 -2.3810 -0.0010 0.0004 0.0007 16.9867Zero-point correction= 0.113900 (Hartree/Particle)
Thermal correction to Energy= 0.122527
Thermal correction to Enthalpy= 0.123471
Thermal correction to Gibbs Free Energy= 0.080712
Sum of electronic and zero-point Energies= -367.957587
Sum of electronic and thermal Energies= -367.948960
Sum of electronic and thermal Enthalpies= -367.948016
Sum of electronic and thermal Free Energies= -367.990775

Methyl azide-thioacetic acid adduct **3.32** in simulated acetone: -368.085547

Transition state for fragmentation of **3.32**: **3.33**

16	-1.532251	-0.614086	-0.723716
6	0.779730	-0.527224	0.127573
7	-1.672566	0.715220	0.306026
8	1.643203	-0.824566	-0.884705
6	0.598183	-1.570361	1.203187
7	-0.792936	1.304468	0.898656
7	0.730101	0.765059	0.474343
6	1.273340	1.776049	-0.428427
1	1.681093	-1.785346	-1.015380
1	0.329796	-2.542268	0.778073
1	1.540750	-1.663333	1.762085

1	-0.186587	-1.269829	1.899735
1	1.115818	2.750456	0.039871
1	2.345490	1.607018	-0.562359
1	0.784323	1.761186	-1.412087

Low frequencies -381.1144 -15.3088 -0.0010 -0.0005 0.0010 9.6667

Zero-point correction= 0.111855 (Hartree/Particle)
Thermal correction to Energy= 0.120491
Thermal correction to Enthalpy= 0.121435
Thermal correction to Gibbs Free Energy= 0.078659
Sum of electronic and zero-point Energies= -367.921821
Sum of electronic and thermal Energies= -367.913185
Sum of electronic and thermal Enthalpies= -367.912241
Sum of electronic and thermal Free Energies= -367.955016

Transition state **3.33** in simulated acetone: -368.049788

Experimental Chapter 4:

protocol for thiolate formation:

Method A: Under an argon atmosphere a round bottom flask was charged with 2.50 mL of dry THF and bis(trimethylsilyl)sulfide (1.5 eq in relation to carboxylic acid). 1.2 eq of MeLi was added dropwise at -78 °C and allowed to warm to rt (approx. 30 min).

Method B: Under an argon atmosphere, a round bottom flask was charged with 2.50 mL of dry THF and bis(trimethylsilyl)sulfide (1.5 eq relative to carboxylic acid). 1.2 eq of anhydrous TBAF was added dropwise at -78 °C and the reaction was allowed to warm to rt (approx. 30 min).

General protocol for the conversion of a carboxylic acid to a thio acid: To a round bottom flask charged with dry CH_2Cl_2 under argon, 1 eq of carboxylic acid (azeotroped with toluene) was added, followed by the addition of 2,6-lutidine (3.0 eq) and isobutylchloroformate (1.2 eq) at 0 °C. The reaction mixture was stirred for 30 min then trimethylsilyl thiolate (see **Method A** or **Method B** above) was added via syringe. The reaction mixture was then stirred until TLC analysis indicated complete consumption of the mixed anhydride (30 min to 4 h). The reaction was then quenched with MeOH, dried *in vacuo,* and then azeotroped with MeOH (2 x 10 mL) to remove volatiles. The crude thio acid was taken up in 1.5 ml of MeOH, and to the mixture 2,6-lutidine (1 eq) then sulfonyl azide (0.8 eq) was added. Bubbling was observed after the addition of azide. The reaction was monitored by TLC. Upon completion the reaction was dried *in vacuo* and purified by FCC.

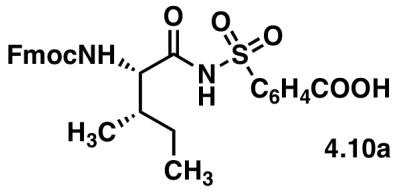

4.10a

10a: 200 mg (0.56 mmol) of Fmoc-Ile-OH, 92 mg (0.68 mmol) of isobutylchloroformate, 350 mg (3.0 mmol) of 2,6-lutidine, 0.152 mg (0.85 mmol) of bis(trimethylsilyl)sulfide , 0.68 mmol of MeLi, and 100 mg (0.44 mmol) of 4-carboxysulfonyl azide were used. FCC, eluted with 2.5:7.5 hexanes:ethyl acetate and 2% acetic acid, furnished 182 mg (86%) of a white solid. IR ν_{max}(KBr)/cm^{-1} 3374, 3068, 1720, δ_H δ_H (400 MHz, $CDCl_3$) 10.22-10.00 (1H, br), 8.17 (2H, d, J=8.0 Hz), 8.08 (2H, d, J=8.0 Hz), 7.76 (2H, d, J=7.2 Hz), 7.56 (2H, d, J=6.8 Hz), 7.40 (2H, t, J=7.2 Hz), 7.29 (2H, td J=7.2, 4.0 Hz), 5.45 (1H, d, J=8.8 Hz), 4.50-4.40 (2H, m), 4.20-4.10 (2H, m), 1.85-1.70 (1H, m), 1.45-1.30 (1H, m), 1.12-1.00 (2H, m), 0.90-0.70 (6H, m); δ_C (100 MHz, $CDCl_3$) 177.0, 169.6, 156.9, 141.3, 134.1, 130.6, 128.5, 127.9, 127.1, 125.0, 120.0, 67.7, 59.6, 46.9, 37.2, 24.6, 15.2, 11.0; *m/z* (ESI/MS) 559 $(M+23)^+$.

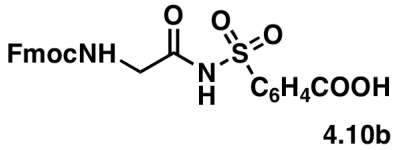

4.10b

10b: 250 mg (0.841 mmol) of Fmoc-Gly-OH, 137 mg (1.01 mmol) of isobutylchloroformate, 350 mg (3.3 mmol) of 2,6-lutidine, 0.265 mg (1.5 mmol) of bis(trimethylsilyl)sulfide , 1.01 mmol of MeLi, and 152 mg (0.80 mmol) of 4-carboxysulfonyl azide were used. FCC, eluted with 1:1 hexanes:ethyl acetate and 2% acetic acid, furnished 268 mg (83%) of a white solid. IR ν_{max}(KBr)/cm^{-1} 3374, 3068, 1715 δ_H (400 MHz, CD_3OD) 8.04 (2H, d, J=8.0 Hz), 7.95 (2H, d, J=8.0 Hz), 7.78 (2H, d, J=7.2

Hz), 7.65 (2H, d, J=7.2 Hz), 7.37 (2H, t, J=7.2 Hz), 7.29 (2H, t J=7.6 Hz), 4.28 (2H, d, J=7.2 Hz), 4.20 (1H, m), 3.73 (2H, s); δ_C (100 MHz, CD_3OD) 176.1, 171.4, 158.4, 144.8, 142.0, 129.8, 128.3, 127.7, 127.5, 125.8, 120.4, 67.5, 47.8, 46.3; *m/z* (ESI/MS) 479 $(M-1)^-$.

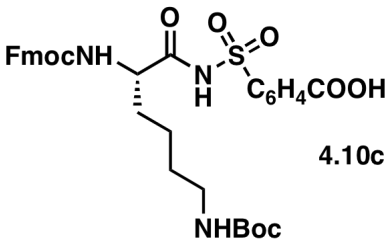

4.10c

10c: 200 mg (0.43 mmol) of Fmoc-Lys-OH, 70 mg (0.52 mmol) of isobutylchloroformate, 200 mg (1.5 mmol) of 2,6-lutidine, 0.114 mg (0.65 mmol) of bis(trimethylsilyl)sulfide , 0.52 mmol of MeLi, and 121 mg (0.34 mmol) of 4-carboxysulfonyl azide were used. FCC, eluted with 5:5 hexanes:ethyl acetate and 2% acetic acid, furnished 217 mg (98%) of a white solid. IR ν_{max}(KBr)/cm^{-1} 3365, 3117, 1719, 1690 δ_H (300 MHz, acetone-d_6) 8.23 (2H, d, J=8.4 Hz), 8.14 (2H, d, J=8.7 Hz), 7.85 (2H, d, J=7.8 Hz), 7.67 (2H, d, J=7.2 Hz), 7.40 (2H, t, J=7.5 Hz), 7.34-7.27 (2H, m), 6.85 (1H, d, J=7.5 Hz), 5.90-6.02 (1H, m), 4.29 (2H, d, J=6.9 Hz), 4.28-4.16 (2H, m), 3.10-2.90 (3H, m), 1.90-1.60 (2H, m), 1.51-1.60 (4H), 1.39 (9H, s); δ_C (100 MHz, CD_3OD) 174.7, 172.9, 167.4, 157.9, 142.1, 136.2, 130.6, 128.8, 128.3, 127.7, 127.6, 125.7, 125.6, 120.4, 79.5, 67.5, 56.1, 47.8, 40.4, 31.5, 29.9, 28.3, 23.5; *m/z* (ESI/MS) 650 $(M-1)^-$.

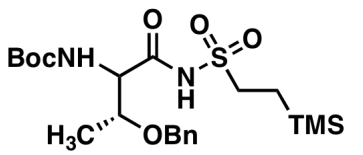

4.10d

10d: 100 mg (0.323 mmol) of Boc-Thr-OH, 53 mg (0.39 mmol) of isobutylchloroformate, 121 mg (1.1 mmol) of 2,6-lutidine, 86 mg (0.49 mmol) of bis(trimethylsilyl)sulfide , 0.38 mmol of MeLi, and 53 mg (0.26 mmol) of SES-azide were used. FCC, eluted with 3:7 hexanes:ethyl acetate and 2% acetic acid, furnished 146 mg (96%) of a white solid. IR ν_{max}(neat)/cm^{-1} 3362, 3244, 1718; δ_H (400 MHz, $CDCl_3$) 9.18-8.82 (1H, br), 7.34-7.27 (5H, m), 5.39 (1H, d, J=6.8 Hz), 4.63 (1H, d, J=11.2 Hz), 4.54 (1H, d, J=11.2 Hz), 4.32 (1H, d, J=4.4 Hz), 4.20-4.12 (1H, m), 3.40-3.28 (2H, m), 1.45 (9H, s), 1.21 (3H, d, J=6.4 Hz), 1.02 (2H, dd, J=10.4, 7.6 Hz), 0.03 (9H, s); δ_C (100 MHz, $CDCl_3$) 170.0, 155.7, 137.1, 128.6, 128.1, 127.8, 81.0, 73.9, 71.7, 58.9, 50.1, 28.2, 15.6, 9.8, -2.1; *m/z* (ESIMS) 471 $(M-1)^-$.

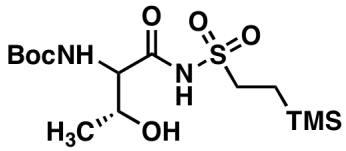

15e: 100 mg (0.46 mmol) of Boc-Thr-OH, 75 mg (0.55 mmol) of isobutylchloroformate, 171mg (1.6 mmol) of 2,6-lutidine, 121 mg (0.69 mmol) of bis(trimethylsilyl)sulfide , 0.55 mmol of MeLi, and 78 mg (0.36 mmol) of SES-azide were used. FCC, eluted with 5:5 hexanes:ethyl acetate and 2% acetic acid, furnished 131 mg (94%) of a white solid. **:** IR ν_{max}(neat)/cm^{-1} 3376, 3253, 1716, 1701 δ_H (400 MHz, $CDCl_3$) 5.64 (1H, d, J=6.8 Hz),

4.34 (1H, m), 4.17 (1H, d, J=6.0 Hz), 3.37-3.23 (2H, m), 1.45 (9H, s), 1.21 (3H, d, J=6.0 Hz), 1.05-1.00 (2H, m), 0.04 (9H, s); δ_C (100 MHz, $CDCl_3$) 170.9, 156.5, 81.2, 66.5, 59.3, 50.0, 28.2, 18.5, 9.8, -2.1; *m/z* (ESI/MS) 381 $(M-1)^-$.

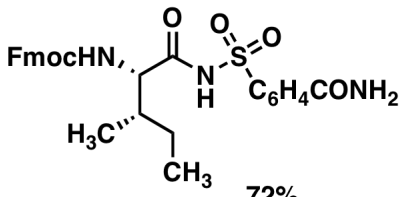

4.13 72%

Wang amide resin (105 mg, 0.11 mmol) was swelled in DMF (4 mL) for 4 h and then treated with 113 mg (0.21 mmol) of **15a**, HOBt 121 mg (4.1 mmol), and DIC 113 mg (4.1 mmol). The mixture was shaken for 8 h, at which time a sample of the derivatized support gave a negative Kaiser test. The solid support was then rinsed with excess CH_2Cl_2, and the sulfonamide was then cleaved from the support using cleavage cocktail K.[1] FCC (1:3 hexanes:ethyl acetate and 2% acetic acid) furnished 52 mg of a white solid [92% yield based on Wang amide resin (0.8 mmol/g); 46% yield based on **15a**].

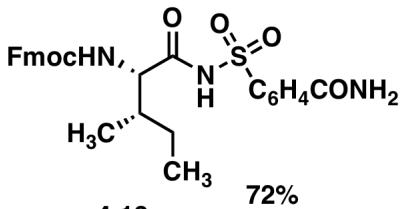

4.13 72%

317 mg (0.9 mmol) of Fmoc-Ile-OH, 184 mg (1.36 mmol) of isobutylchloroformate, 350 mg (3.0 mmol) of 2,6-lutidine, 228 mg (1.35 mmol) of bis(trimethyl)sulfide, and 1.00 mmol of MeLi were used to prepare the thio acid as per Procedure A. Wang amide resin (550 mg, 0.45 mmol) was swelled in DMF (8 mL) for 4 h and then treated with 200 mg (0.9 mmol) of 4-carboxybenzenesulfonazide (**14a**), HOBt 241 mg (1.8 mmol), and DIC 226 mg (1.8 mmol). The mixture was shaken for 8 h, at which time a sample of the derivatized support gave a negative Kaiser test. The solid support was then rinsed with excess CH_2Cl_2. The resin was then treated with 2 mL of 1:1 (v/v) acetic anhydride:pyridine and shaken for one hour. The solid support was then rinsed with excess CH_2Cl_2. The immobilized azide was then treated with the crude Fmoc-Ile-SH (prepared above) and lutidine (0.35 mL) in CH_2Cl_2 (8 mL). Bubbling ensued, and the reaction mixture was shaken for 4h. The sulfonamide was cleaved from solid support using cleavage cocktail K.[112] FCC (1:3 hexanes:ethyl acetate and 2% acetic acid) furnished 169 mg of a white solid, 72%, yield [based on Wang amide resin (0.8 mmol/g)]. δ_H (400 MHz, CD_3CN) 7.98 (2H, d, J=9.5 Hz), 7.87 (2H, d, J=9.5 Hz), 7.83 (2H, d, J=6.1 Hz), 7.64 (2H, d, J=6.0 Hz), 7.40 (2H, t, J=7.3 Hz), 7.31 (2H, td J=7.0, 4.0 Hz), 6.85 (1H, br), 6.14 (1H, br), 5.72 (1H, d, J=7.8Hz), 4.37-4.14 (3H, m), 3.38 (1H, t, J=7.69), 1.75 (1H, m), 1.37-1.29 (1H, m), 1.12-1.00 (2H, m), 0.90-0.78 (6H, m); δ_C (100 MHz, $CDCl_3$) 171.1, 168.5, 156.9, 143.7, 143.2, 141.6, 141.3, 138.0, 128.5, 128.1, 127.8, 127.2, 125.0, 120.0, 67.6, 59.6, 46.9, 37.4, 24.5, 15.3, 11.0; *m/z* (ESI/MS) 558 $(M+23)^+$.

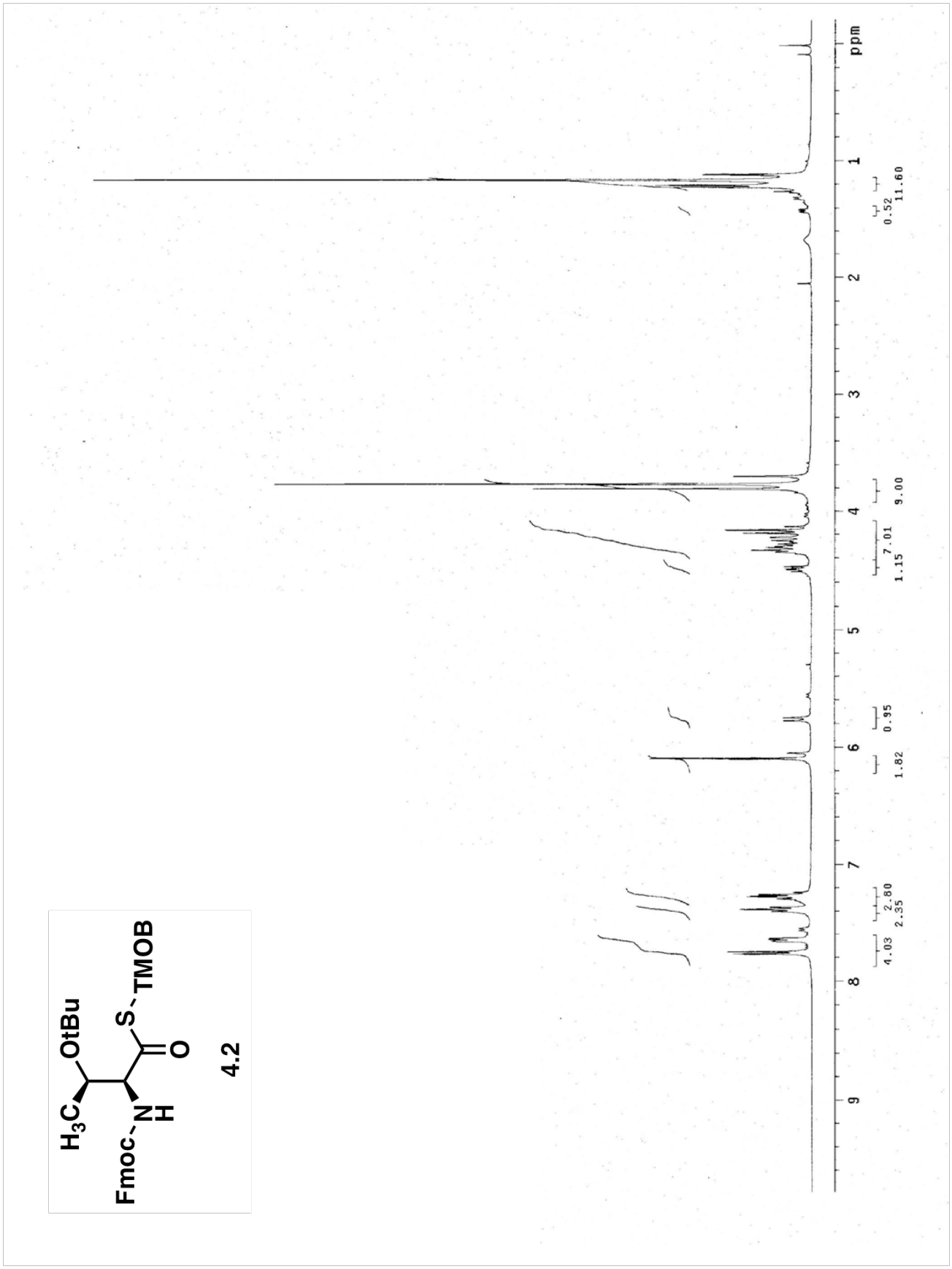
H3C
OtBu
Fmoc
N
H
S
TMOB
O
4.2
ppm
1
2
3
4
5
6
7
8
9
0.52
11.60
7.01
9.00
1.15
0.95
1.82
2.80
2.35
4.03

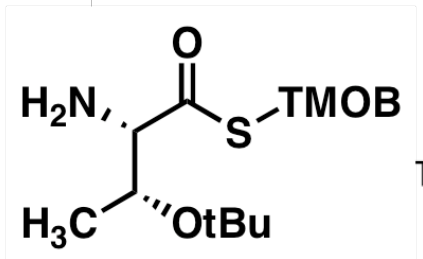

4.3

7

TMOB

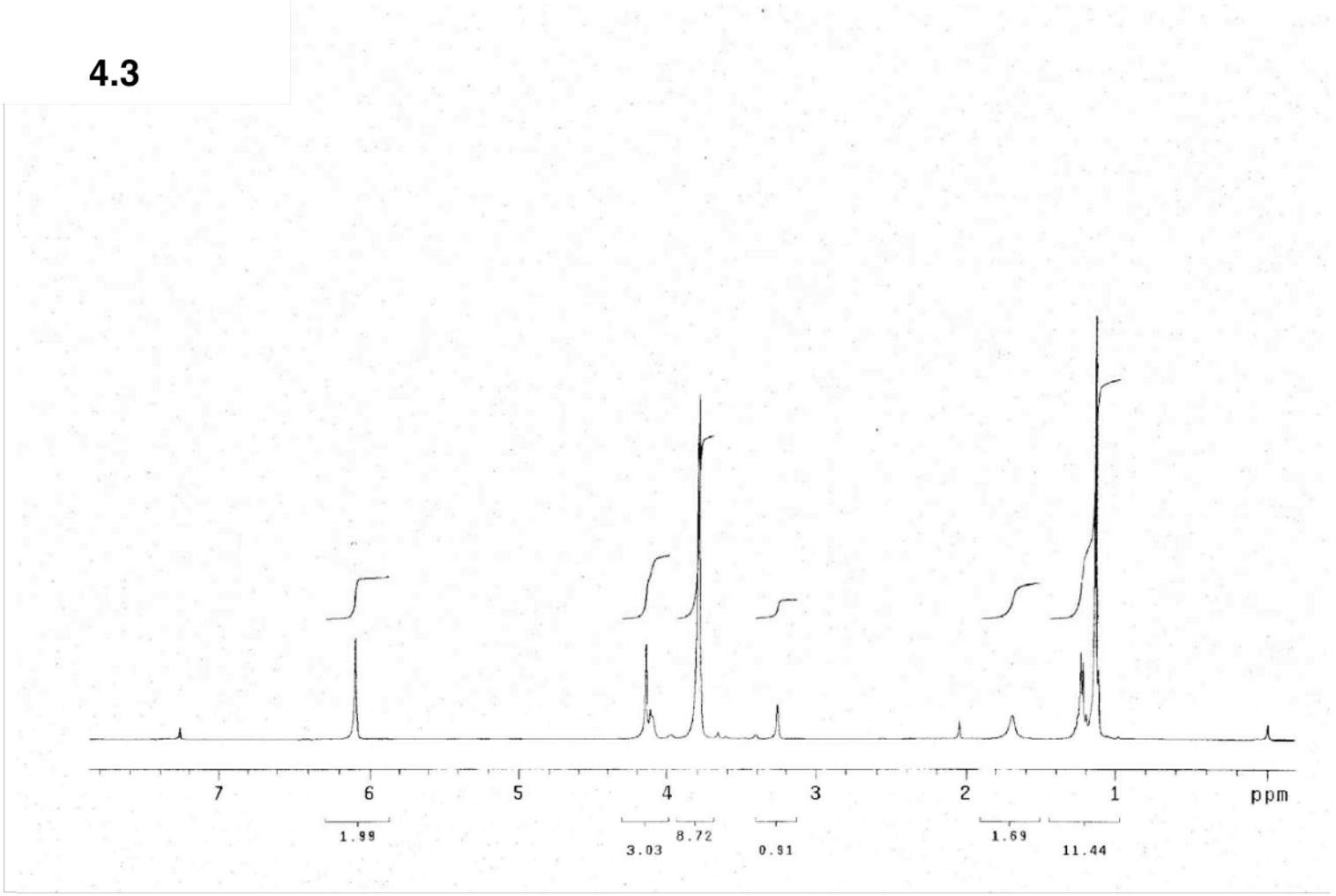

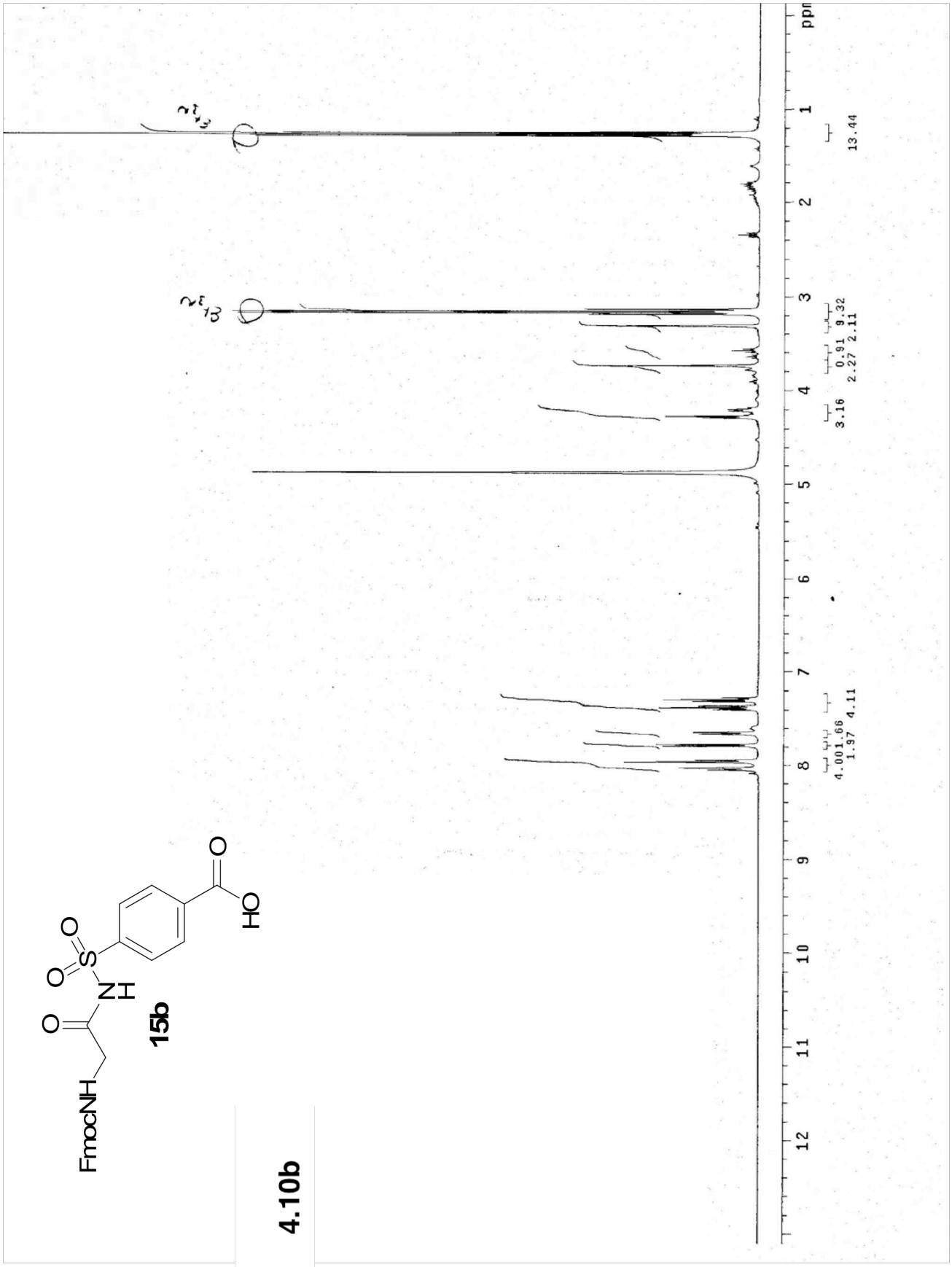
FmocNH
O
O
S
O
NH
O
OH
15b
4.10b
ppm
1
2
3
4
5
6
7
8
9
10
11
12
13.44
3.16
0.91
9.32
2.27
2.11
4.00
1.66
1.97
4.11

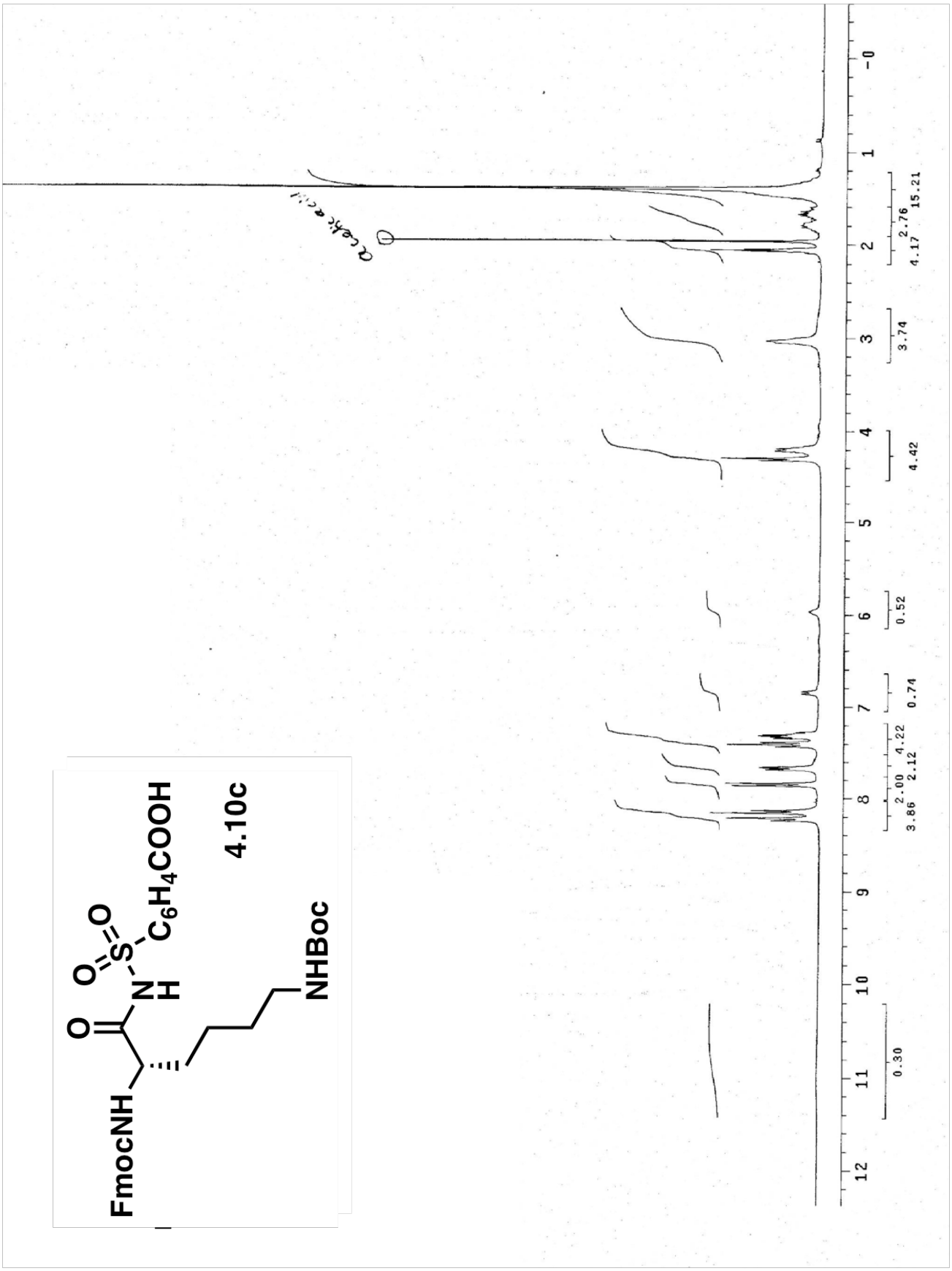
FmocNH
O
O=S=O
N
H
C6H4COOH
NHBoc
4.10c
Oleic acid
12
11
10
9
8
7
6
5
4
3
2
1
-0
0.30
3.86
2.00
2.12
4.22
0.74
0.52
4.42
3.74
4.17
2.76
15.21

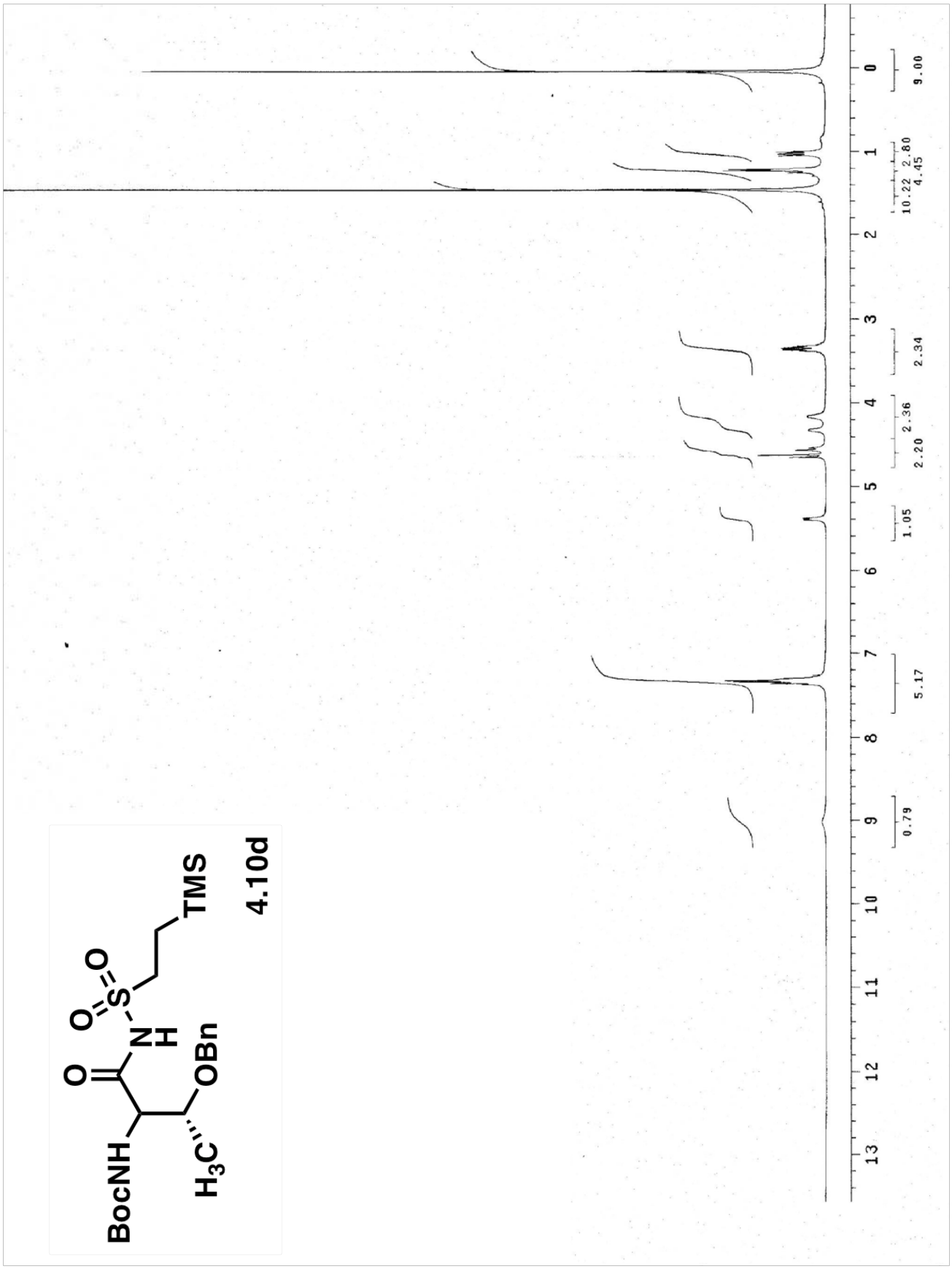
BocNH
O
O
S
O
N
H
OBn
H3C
TMS
4.10d
0.79
5.17
1.05
2.20
2.36
2.34
10.22
2.80
4.45
9.00

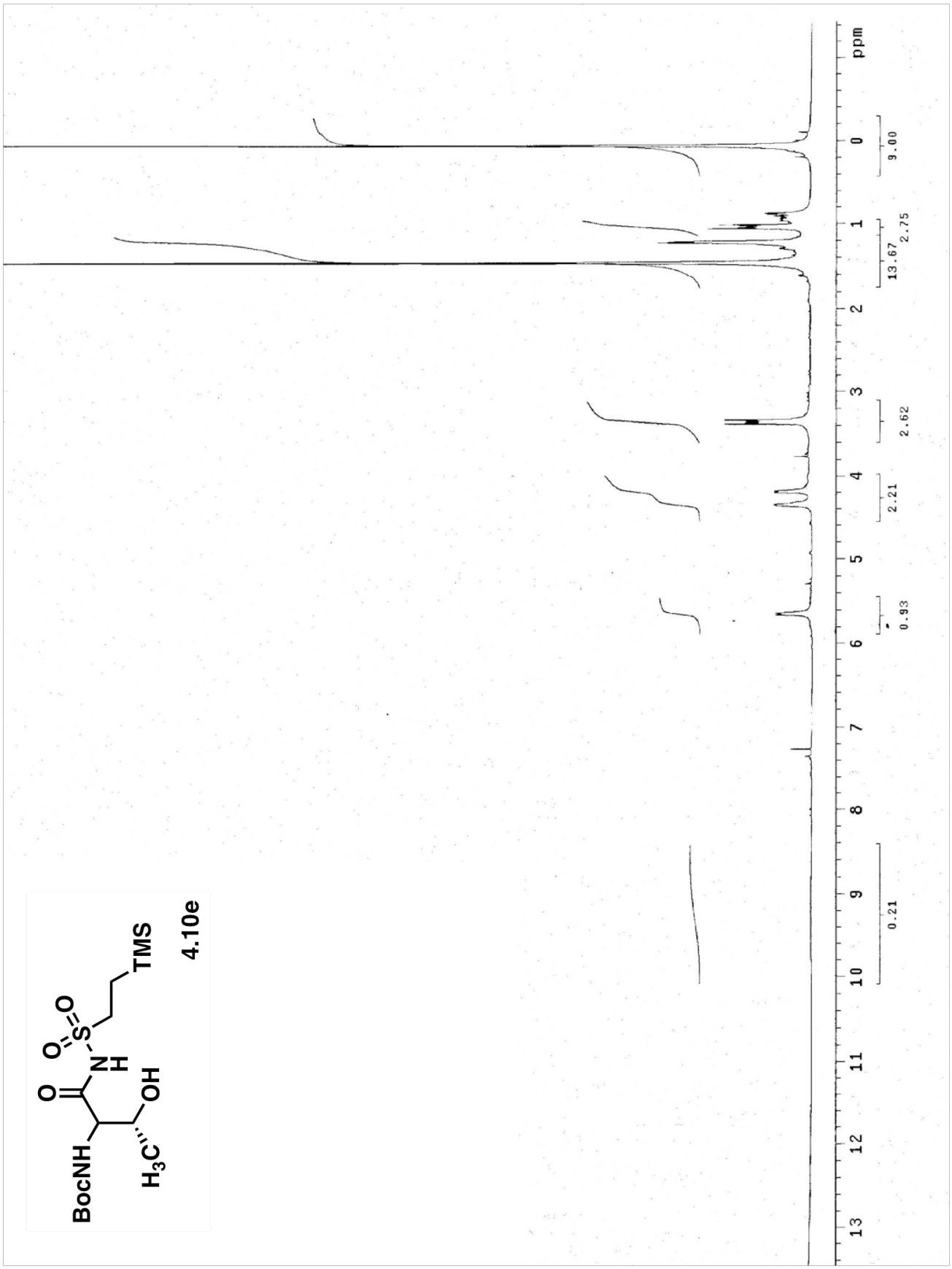
BocNH
O
N
H
O
O
S
TMS
OH
H3C
4.10e
ppm
0.21
0.93
2.21
2.62
13.67
2.75
9.00

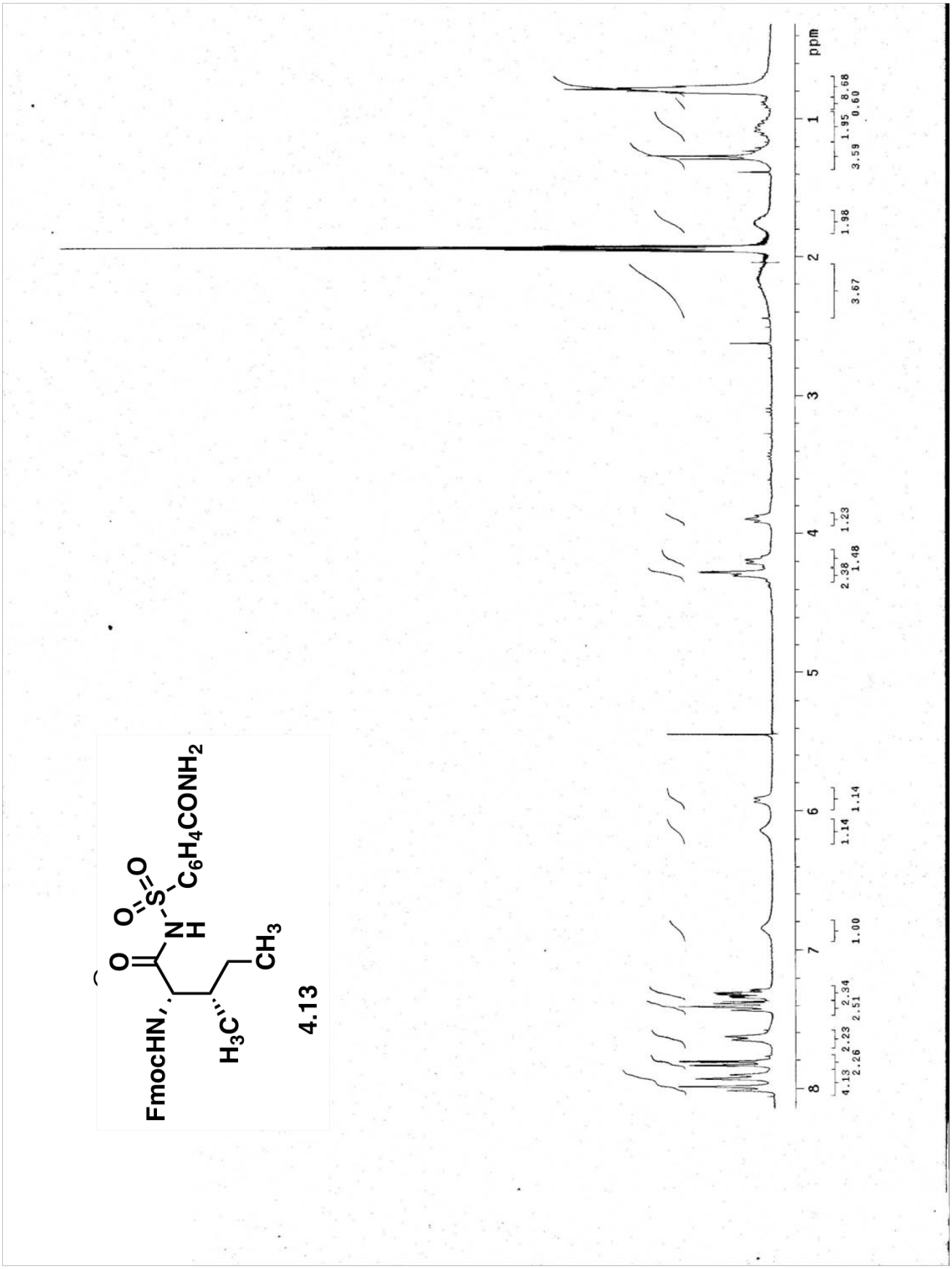
FmocHN
O
O
S
O
N
H
C6H4CONH2
H3C
CH3
4.13
ppm
8
7
6
5
4
3
2
1
4.13
2.23
2.26
2.34
2.51
1.00
1.14
1.14
2.38
1.48
1.23
3.67
1.98
3.59
1.95
8.68
0.60

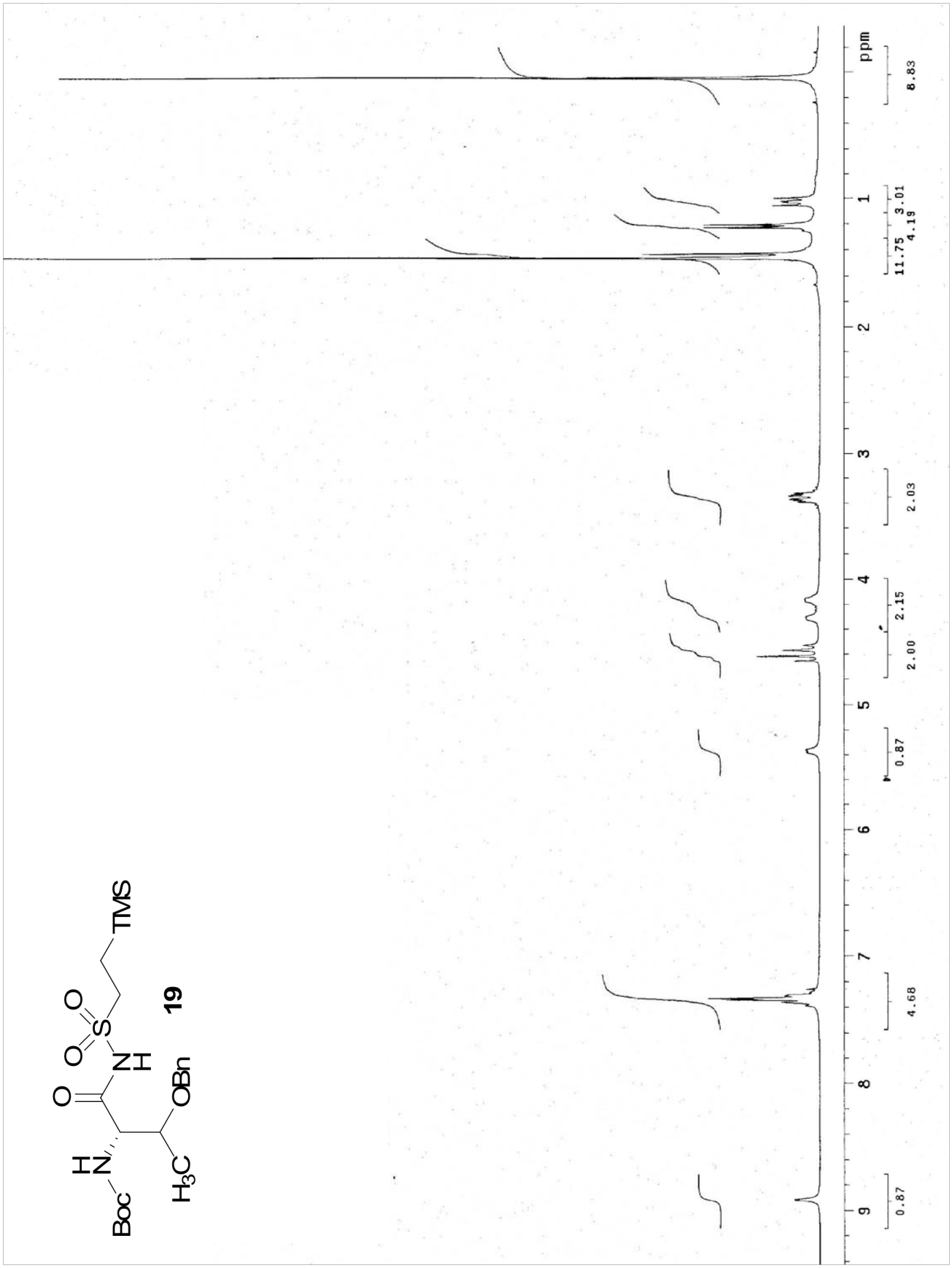
Boc
H
N
O
H
N
O
O
S
O
TMS
H3C
OBn
19
ppm
0.87
4.68
0.87
2.00
2.15
2.03
11.75
3.01
4.19
8.83

Experimental Chapter 5:

I. Distortional Diagrams:

II. Ground State, Transition State and Vibrationally Displaced Bond Lengths:

III. Activation Energies

Cartesian Coordinates:

IV. Transition State Cartesian Coordinates, Energies and Low Frequencies

V. Distortional Cartesian Coordinates, Energies and Olefin Bending Frequencies:

VI: Activation Energy Structure Cartesian Coordinates and Energies:

VII. Product Cartesian Coordinates and Energies:

VIII. Planar Transition State Cartesian Coordinates and Single Point Energies:

I. Distortional Diagrams:

The [2.2.2]-bicyclooctene system was first optimized utilizing B3LYP/6-31g(2d,2p). The anharmonic example was optimized utilizing the B3LYP/6-31+g(d). A frequency calculation was performed with the anharmonic[1] option and harmonic option. The GaussView 4.1.2 package was used to display the anharmonic vibration corresponding with the olefin-bending mode at ~715.00 cm^{-1} and manual displacement of the frequency was used to isolate structures at the appropriate olefin bend. The structures single point energy was then calculated using B3LYP/6-31g(2d,2p) and plotted below.

cyclopropane 1		anharmonic		harmonic
degrees	hartrees	kcal/mol	hartrees	kcal/mol
20	-350.13168054	6.87	-350.13168054	6.87
15	-350.13692422	3.57	-350.13692422	3.57
10	-350.14021415	1.49	-350.14024145	1.49
5	-350.14192145	0.44	-350.14192145	0.44
0	-350.14257669	0.03	-350.14256600	0.03
-1.7	-350.14262106	0.00	-350.14262106	0.00
-5	-350.14236447	0.16	-350.14236447	0.16
-10	-350.14119556	0.89	-350.14119556	0.89
-15	-350.13953462	1.94	-350.13953462	1.94
-20	-350.13527696	4.61	-350.13527696	4.61

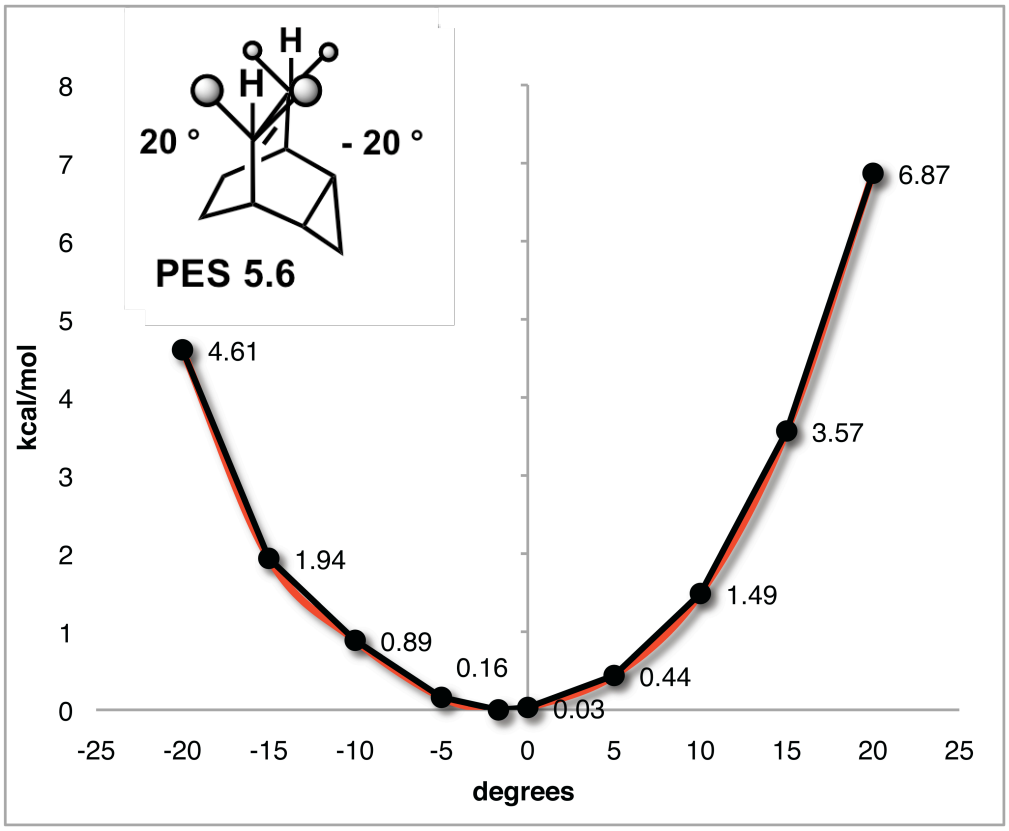

endo nitrile 2		anharmonic		harmonic
degrees	hartrees	kcal/mol	hartrees	kcal/mol
20	-442.37953715	9.90	-442.36312891	9.90
15	-442.37956489	5.19	-442.37063508	5.19
10	-442.38271552	2.38	-442.37511235	2.38
5	-442.38477532	0.85	-442.37774670	0.73
0	-442.38562946	0.07	-442.37880226	0.07
-2.3	-442.38567513	0.00	-442.37891145	0.00
-5	-442.38542850	0.10	-442.37874529	0.10
-10	-442.38432455	0.84	-442.37757365	0.84
-15	-442.38217756	2.36	-442.37515315	2.36
-20	-442.38125950	5.15	-442.37069712	5.15

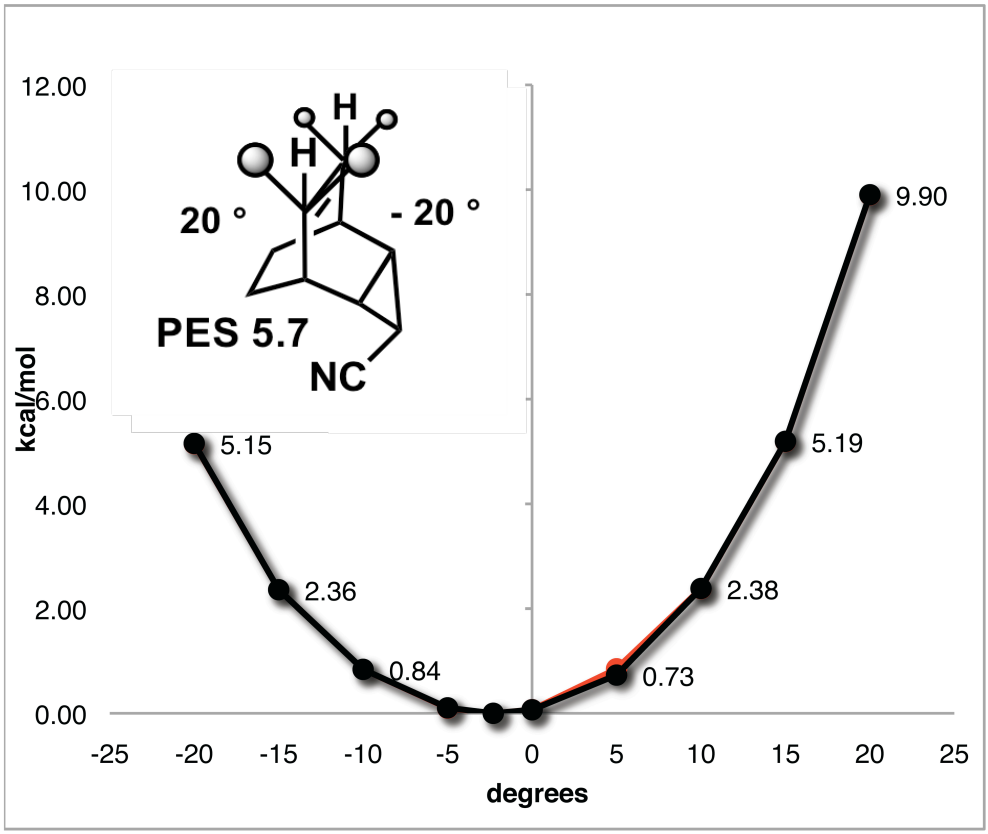

exo nitrile 3		anharmonic		harmonic
degrees	hartrees	kcal/mol	hartrees	kcal/mol
20	-442.37953715	6.78	-442.37488724	6.77
15	-442.37956489	3.83	-442.37956489	3.83
10	-442.38271552	1.86	-442.38298418	1.69
5	-442.38477532	0.56	-442.38491071	0.48
0	-442.38562946	0.03	-442.38562626	0.03
-1.8	-442.38567513	0.00	-442.38567513	0.00
-5	-442.38542850	0.15	-442.38549513	0.11
-10	-442.38432455	0.85	-442.38449530	0.74
-15	-442.38217756	2.19	-442.38218756	2.19
-20	-442.38125950	4.68	-442.37877520	4.33

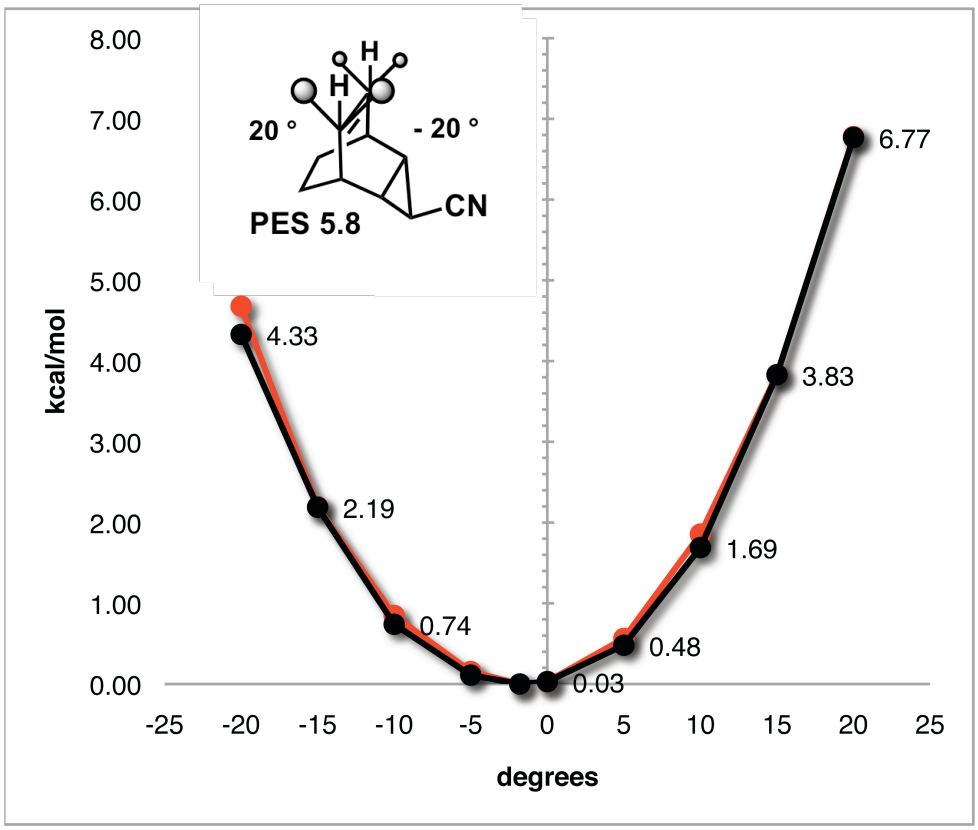

cyclobutane 4		anharmonic		harmonic
degrees	hartrees	kcal/mol	hartrees	kcal/mol
20	-389.45697533	7.19	-389.45634962	7.59
15	-389.46215682	3.94	-389.46257446	3.68
10	-389.46611506	1.46	-389.46586728	1.61
5	-389.46787528	0.35	-389.46787528	0.35
0	-389.46844050	0.00	-389.46844025	0.00
-5	-389.46786844	0.36	-389.46786844	0.36
-10	-389.46608007	1.48	-389.46582763	1.64
-15	-389.46203113	4.02	-389.46245878	3.75
-20	-389.45672269	7.35	-389.45672269	7.35

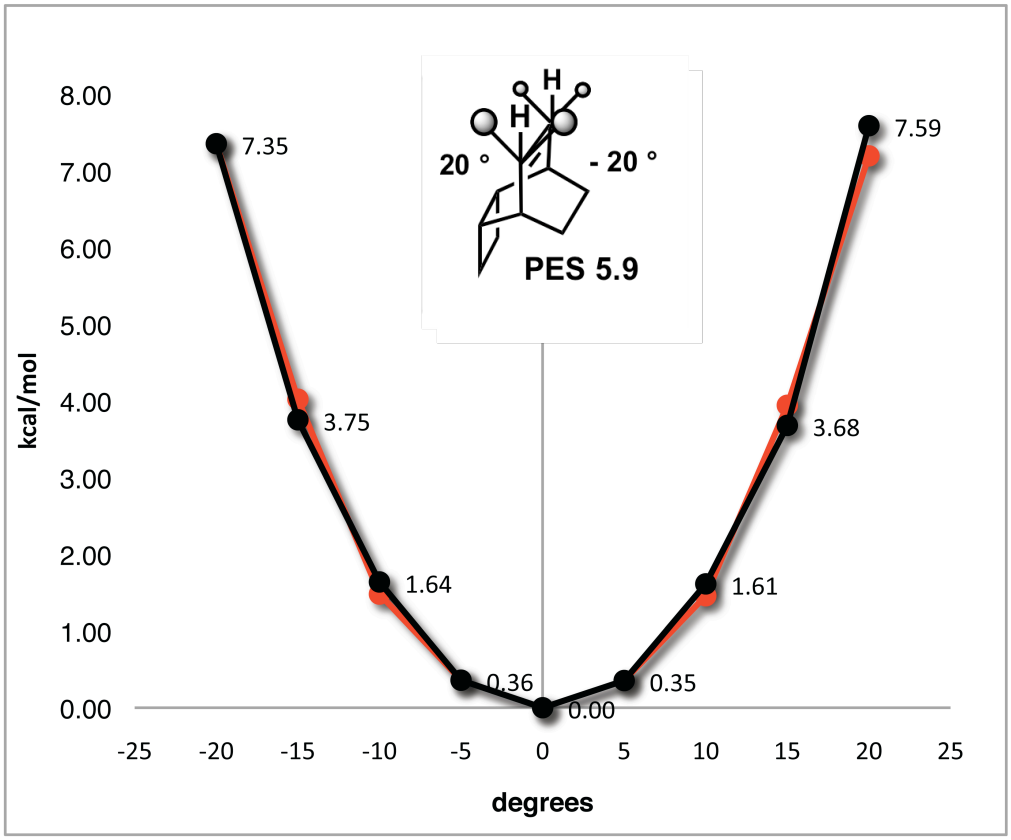

II. Ground State, Transition State and Vibrationally Displaced Bond Lengths:

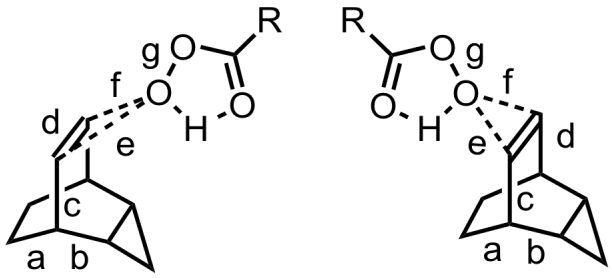

cyclopropane 1[1]	*m*CPBA	PFA	ground state	vibrationally diplaced
syn a	1.563	1.562	1.555	1.565 (10 °)
syn b	1.542	1.542	1.542	1.534 (10 °)
syn c	1.517	1.517	1.521	1.524 (10 °)
syn d	1.373	1.372	1.337	1.337 (10 °)
syn e	2.247	2.252		
syn f	2.252	2.267		
syn d	1.783	1.787		
anti a	1.553	1.553	1.555	1.541 (-10 °)
anti b	1.552	1.551	1.542	1.554 (-10 °)
anti c	1.517	1.518	1.521	1.520 (-10 °)
anti d	1.373	1.372	1.337	1.337 (-10 °)
anti e	2.271	2.267		
anti f	2.261	2.288		
anti g	1.789	1.792		

1. b3lyp/6-31+g(d,p) CPCM=dichloromethane

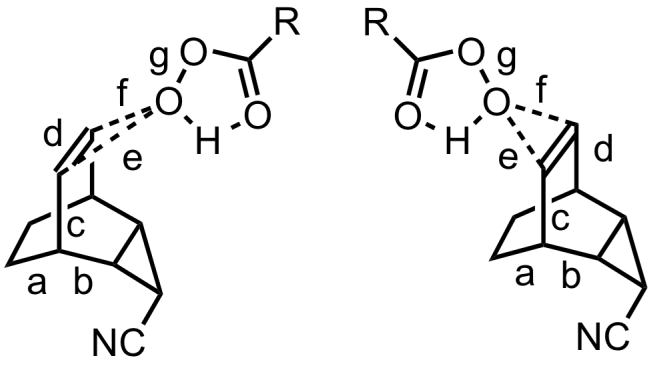

endo nitrile 2[1]	*m*CPBA	ground state	vibrationally diplaced
syn a	1.564	1.555	1.567 (10 °)
syn b	1.540	1.542	1.535 (10 °)
syn c	1.518	1.522	1.524 (10 °)
syn d	1.374	1.336	1.336 (10 °)
syn e	2.215		
syn f	2.221		
syn g	1.803		
anti a	1.553	1.555	1.539 (-10 °)
anti b	1.550	1.542	1.552 (-10 °)
anti c	1.520	1.522	1.520 (-10 °)
anti d	1.375	1.336	1.336 (-10 °)
anti e	2.207		
anti f	2.233		
anti g	1.810		

1. b3lyp/6-31+g(d,p) CPCM=dichloromethane

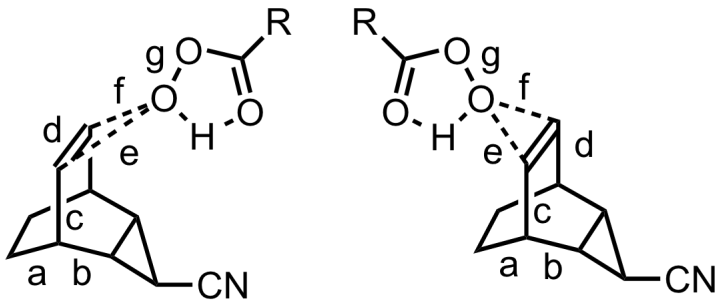

exo nitrile 3[1]	*m*CPBA	ground state	vibrationally diplaced
syn a	1.562	1.554	1.566 (10 °)
syn b	1.539	1.541	1.531 (10 °)
syn c	1.520	1.524	1.525 (10 °)
syn d	1.373	1.336	1.336 (10 °)
syn e	2.222		
syn f	2.223		
syn g	1.797		
anti a	1.552	1.554	1.534 (-10 °)
anti b	1.550	1.541	1.558 (-10 °)
anti c	1.522	1.524	1.523 (-10 °)
anti d	1.375	1.336	1.336 (-10 °)
anti e	2.223		
anti f	2.208		
anti g	1.812		

1. b3lyp/6-31+g(d,p) CPCM=dichloromethane

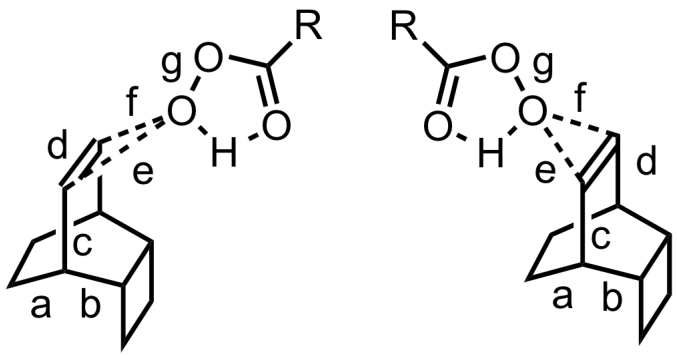

cyclobutane 4[1]	*m*CPBA	ground state	vibrationally diplaced[2]
syn a	1.564	1.553	1.563 (10 °)
syn b	1.551	1.552	1.533 (10 °)
syn c	1.512	1.516	1.518 (10 °)
syn d	1.380	1.338	1.338 (10 °)
syn e	2.126		
syn f	2.127		
syn g	1.852		
anti a	1.552	1.553	1.544 (-10 °)
anti b	1.564	1.552	1.571 (-10 °)
anti c	1.511	1.516	1.514 (-10 °)
anti d	1.375	1.338	1.338 (-10 °)
anti e	2.265		
anti f	2.248		
anti g	1.789		

1. b3lyp/6-31+g(d,p) CPCM=dichloromethane

III. Activation Energies:

TS #	Δ H TS‡ syn a	Δ H products syn b	Δ H TS‡ anti a'	Δ H products anti b'
1	8.1	-53.8	9.6	-53.9
2	9.4	-52.5	12.6	-50.9
3	11.2	-50.7	12.1	-51.4
4	9.6	-52.3	9.8	-53.6
5	8.5	-53.4	10.0	-53.5
6	9.4	-52.5	12.7	-50.8
7	11.5	-50.4	12.3	-51.2
8	9.9	-52.0	10.0	-53.5

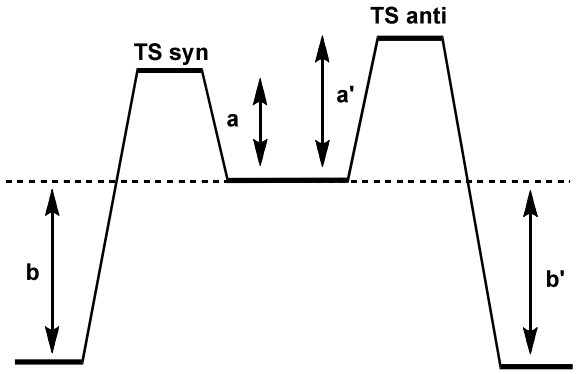

IV. Transition State Cartesian Coordinates, Energy and Low Frequencies

1) B3LYP/6-31+g(d,p) , CPCM , dichloromethane optimized to TS

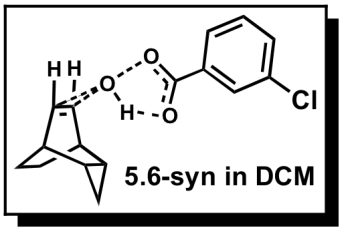

C	-5.23023	0.30848	-0.77962
C	-3.77669	0.06955	-1.30164
C	-2.8277	1.15488	-0.76025
C	-5.22984	0.31294	0.77915
C	-2.82733	1.15884	0.75387
C	-3.77607	0.07633	1.30161
C	-3.37483	-1.25886	-0.68554
C	-3.37485	-1.25537	0.69227
C	-3.32577	2.36686	-0.00629
H	-5.60501	1.2547	-1.18252
H	-5.88514	-0.47857	-1.16667
H	-3.7617	0.03308	-2.3938
H	-1.87806	1.24552	-1.27995
H	-5.88504	-0.47145	1.17107
H	-5.60378	1.26171	1.17679
H	-1.87743	1.25261	1.27254
H	-3.76033	0.04563	2.39392
H	-2.66898	3.23166	-0.00858
H	-4.37868	2.62431	-0.00674
H	-3.30702	-2.16601	-1.2738
H	-3.30714	-2.15956	1.2851
O	-1.38285	-1.51248	0.00267
O	0.43054	-1.84235	0.00067
C	1.00284	-0.67765	0.00201
O	0.37782	0.39906	0.00492
H	-1.13284	-0.54603	0.00592
C	2.50827	-0.70512	0.00027
C	3.1920	0.51772	0.00125
C	3.21991	-1.91184	-0.0021
C	4.58386	0.51401	-0.00018
C	4.61509	-1.89213	-0.00352
H	2.6761	-2.84949	-0.00284
C	5.30893	-0.67909	-0.00255
H	5.17152	-2.82462	-0.00537
H	6.39325	-0.65646	-0.00362
H	2.62868	1.44315	0.00317
Cl	5.45012	2.04756	0.00099

Zero-point correction=	0.294724 (Hartree/Particle)
Thermal correction to Energy=	0.311189
Thermal correction to Enthalpy=	0.312133
Thermal correction to Gibbs Free Energy=	0.248833
Sum of electronic and zero-point Energies =	-1305.424459
Sum of electronic and thermal Energies=	-1305.407995
Sum of electronic and thermal Enthalpies=	-1305.407050
Sum of electronic and thermal Free Energies=	-1305.470350

Low frequencies --- -425.9384 -31.6031 -23.1131 -11.8448 -10.0797 -2.0748

E(RB+HF-LYP) = -1305.7182279

2) B3LYP/6-31+g(d,p) Optimized to TS

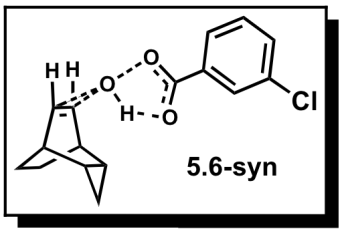

C	5.23571	0.30392	0.77941
C	3.78138	0.07027	1.30197
C	2.83549	1.15701	0.7575
C	5.23562	0.30389	-0.77957
C	2.83541	1.157	-0.75732
C	3.78123	0.07027	-1.30191
C	3.37641	-1.25899	0.68912
C	3.3763	-1.25899	-0.68898
C	3.33588	2.36582	0.00006
H	5.61401	1.25053	1.18066
H	5.88893	-0.48469	1.16887
H	3.76651	0.0369	2.39506
H	1.88584	1.25239	1.27800
H	5.88878	-0.48475	-1.16908
H	5.61388	1.25047	-1.18089
H	1.88568	1.25237	-1.27769
H	3.76616	0.03686	-2.39499
H	2.68005	3.23263	0.00010
H	4.38962	2.62329	0.00001
H	3.30725	-2.16489	1.28042
H	3.30738	-2.16496	-1.28022
O	1.38639	-1.50384	-0.00025
O	-0.42714	-1.82677	-0.00024
C	-1.00445	-0.66388	-0.00004
O	-0.38605	0.41605	0.00010
H	1.14833	-0.53372	-0.00001
C	-2.51006	-0.69993	0.00001
C	-3.2008	0.51914	-0.00005
C	-3.21613	-1.91012	0.00013
C	-4.59273	0.50867	0.00000
C	-4.61164	-1.89767	0.00017
H	-2.66884	-2.84646	0.00019
C	-5.31187	-0.68812	0.00010
H	-5.16342	-2.83392	0.00027
H	-6.39711	-0.67126	0.00013
H	-2.64339	1.44884	-0.00013
Cl	-5.46645	2.03807	-0.00008

Zero-point correction=	0.296629 (Hartree/Particle)
Thermal correction to Energy=	0.313805
Thermal correction to Enthalpy=	0.314749
Thermal correction to Gibbs Free Energy=	0.249106
Sum of electronic and zero-point Energies=	-1305.404548
Sum of electronic and thermal Energies=	-1305.387372
Sum of electronic and thermal Enthalpies=	-1305.386428
Sum of electronic and thermal Free Energies=	-1305.452071

Low frequencies --- -386.9309 -0.0021 -0.0005 0.0005 1.4194 5.5713

E(RB+HF-LYP) = -1305.70117720

3) B3LYP/6-31+g(d,p) CPCM, dichloromethane optimized to TS

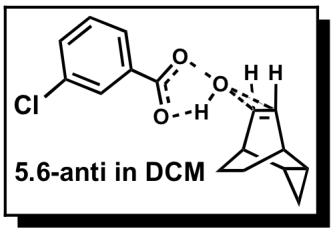

C	-2.93402	1.25256	0.76566
C	-3.81618	0.09242	1.30143
C	-5.26289	0.22411	0.75440
C	-2.93255	1.23299	-0.79208
C	-5.2618	0.20581	-0.75878
C	-3.81437	0.06034	-1.30023
C	-3.32575	-1.21365	0.70353
C	-3.32478	-1.2308	-0.66939
C	-5.73053	1.44115	-0.01735
H	-3.32006	2.20231	1.14968
H	-1.92015	1.14913	1.16367
H	-3.80284	0.07043	2.39568
H	-6.01538	-0.35427	1.28870
H	-1.91799	1.11852	-1.18531
H	-3.31708	2.17312	-1.20049
H	-6.01382	-0.38514	-1.27984
H	-3.79945	0.0112	-2.39358
H	-6.80222	1.62703	-0.0204
H	-5.13225	2.34568	-0.0276
O	0.58801	-1.73927	-0.00578
O	0.5635	0.50226	0.02488
H	-3.15793	-2.12999	-1.25592
H	-3.15493	-2.0971	1.31247
H	-0.99542	-0.47293	0.01706
C	1.18176	-0.57453	0.00848
O	-1.17685	-1.44637	0.00517
C	2.68293	-0.63248	0.00290
C	3.38827	0.57981	0.00305
C	3.37523	-1.85203	-0.00218
C	4.77941	0.54752	-0.00218
C	4.77124	-1.85682	-0.00685
H	2.82551	-2.78908	-0.00212
C	5.48715	-0.65586	-0.00703
H	5.31202	-2.80143	-0.01044
H	6.57507	-0.65535	-0.01085
Cl	5.67126	2.07111	-0.00249
H	2.84935	1.52285	0.00713

Zero-point correction=	0.294057 (Hartree/Particle)
Thermal correction to Energy=	0.310643
Thermal correction to Enthalpy=	0.311588
Thermal correction to Gibbs Free Energy=	0.248217
Sum of electronic and zero-point Energies=	-1305.421947
Sum of electronic and thermal Energies =	-1305.405361
Sum of electronic and thermal Enthalpies=	-1305.404417
Sum of electronic and thermal Free Energies=	-1305.467787

Low frequencies --- -400.6704 -15.5463 -8.2558 -3.3871 -1.5711 2.7842

E(RB+HF-LYP) = -1305.71600421

4) B3LYP/6-31+g(d,p) optimized to TS

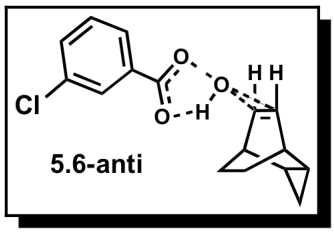

C	-2.80237	1.23136	0.77867
C	-3.71578	0.08986	1.29986
C	-5.15914	0.26896	0.75657
C	-2.80233	1.23102	-0.77907
C	-5.15908	0.26862	-0.75670
C	-3.71568	0.08927	-1.29981
C	-3.27012	-1.22759	0.68911
C	-3.27005	-1.22791	-0.68842
C	-5.59521	1.5057	-0.00035
H	-3.16336	2.18457	1.17687
H	-1.78955	1.09654	1.16659
H	-3.70273	0.05554	2.39202
H	-5.92672	-0.29306	1.28319
H	-1.78948	1.09603	-1.16685
H	-3.16329	2.18404	-1.17770
H	-5.92662	-0.29363	-1.28312
H	-3.70254	0.05445	-2.39194
H	-6.66034	1.72177	-0.00043
H	-4.97387	2.39351	-0.00051
O	0.55464	-1.82309	0.00010
O	0.48135	0.41691	0.00011
H	-3.15772	-2.12664	-1.28204
H	-3.15767	-2.12603	1.28315
H	-0.99216	-0.53041	0.00021
C	1.11801	-0.65443	0.00007
O	-1.26002	-1.49118	0.00016
C	2.62264	-0.66571	-0.00001
C	3.29361	0.56426	0.00004
C	3.34623	-1.86529	-0.00011
C	4.68544	0.57459	-0.00002
C	4.74109	-1.83136	-0.00017
H	2.81195	-2.80842	-0.00014
C	5.42241	-0.61125	-0.00013
H	5.30702	-2.75809	-0.00026
H	6.50644	-0.57760	-0.00017
Cl	5.53610	2.11658	0.00005
H	2.72105	1.48401	0.00012

Zero-point correction=	0.296649 (Hartree/Particle)
Thermal correction to Energy=	0.313818
Thermal correction to Enthalpy=	0.314762
Thermal correction to Gibbs Free Energy=	0.249154
Sum of electronic and zero-point Energies=	-1305.402123
Sum of electronic and thermal Energies=	-1305.384954
Sum of electronic and thermal Enthalpies=	-1305.384010
Sum of electronic and thermal Free Energies=	-1305.449618

Low frequencies --- -381.0152 0.0024 0.0024 0.0029 4.9010 4.9856

E(RB+HF-LYP) = -1305.69877205

5) B3LYP/6-31+g(d,p) CPCM, dichloromethane optimized to TS

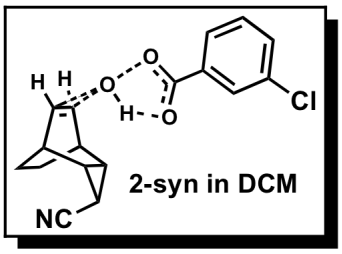

C	-4.93662	-0.49423	-0.77277
C	-3.46543	-0.51516	-1.29774
C	-2.64692	0.67101	-0.75758
C	-4.9347	-0.48433	0.78371
C	-2.64500	0.6804	0.74820
C	-3.46227	-0.49871	1.30537
C	-2.88051	-1.77298	-0.67541
C	-2.87881	-1.76433	0.69771
C	-3.20594	1.88448	-0.01148
H	-5.4596	0.37376	-1.18169
H	-5.45389	-1.37951	-1.15572
H	-3.44201	-0.54535	-2.39088
H	-1.7295	0.88127	-1.30442
H	-5.45111	-1.36463	1.17915
H	-5.45658	0.38884	1.18291
H	-1.72611	0.89742	1.28987
H	-3.43625	-0.51485	2.39877
H	-2.50438	2.72246	-0.01757
H	-2.68835	-2.66364	-1.26758
H	-2.6848	-2.64737	1.30060
O	-0.76566	-1.79345	0.00775
O	1.02555	-1.93172	0.00583
C	1.51536	-0.72073	0.00169
O	0.80472	0.2983	0.00129
H	-0.66628	-0.80628	0.00412
C	3.01603	-0.64846	-0.00257
C	3.61647	0.61913	0.0048
C	3.80877	-1.80534	-0.01378
C	5.00551	0.70401	0.00094
C	5.20008	-1.69259	-0.01793
H	3.33974	-2.78525	-0.01955
C	5.81198	-0.4355	-0.01047
H	5.81860	-2.58819	-0.02702
H	6.89600	-0.34348	-0.01348
H	3.00052	1.51364	0.01342
Cl	5.76649	2.29684	0.01066
C	-4.54793	2.40125	-0.01320
N	-5.58911	2.92320	-0.01542

Zero-point correction=	0.292872 (Hartree/Particle)
Thermal correction to Energy=	0.311187
Thermal correction to Enthalpy=	0.312131
Thermal correction to Gibbs Free Energy=	0.244740
Sum of electronic and zero-point Energies=	-1397.668446
Sum of electronic and thermal Energies=	-1397.650131
Sum of electronic and thermal Enthalpies=	-1397.649187
Sum of electronic and thermal Free Energies=	-1397.716579

Low frequencies --- -410.4031 -13.9083 -8.6110 -3.0241 -1.8403 2.5086

E(RB+HF-LYP) = -1397.96131837

6) B3LYP/6-31+g(d,p) optimized to TS

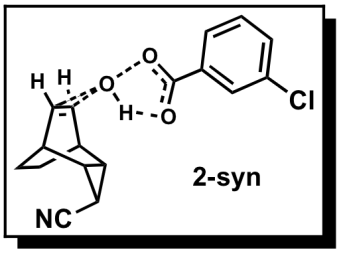

C	4.84869	-0.39652	0.77956
C	3.37925	-0.48486	1.30298
C	2.50395	0.65422	0.75282
C	4.84804	-0.40094	-0.77739
C	2.50341	0.65012	-0.75454
C	3.37819	-0.492	-1.29909
C	2.85736	-1.77794	0.69466
C	2.85657	-1.7817	-0.68319
C	3.00002	1.8856	-0.0044
H	5.32852	0.50159	1.17404
H	5.41006	-1.25048	1.17104
H	3.35689	-0.50656	2.3946
H	1.56385	0.80445	1.2761
H	5.40891	-1.25723	-1.16446
H	5.32778	0.49481	-1.17731
H	1.56292	0.79754	-1.27791
H	3.35493	-0.51976	-2.39055
H	2.25564	2.68001	-0.00626
H	2.72371	-2.67295	1.28977
H	2.7241	-2.68021	-1.27326
O	0.85952	-1.87883	0.00209
O	-0.98215	-2.04171	-0.00155
C	-1.43405	-0.82638	0.00098
O	-0.69581	0.17967	0.00478
H	0.67435	-0.89632	0.00442
C	-2.9319	-0.69511	-0.00093
C	-3.48484	0.59225	0.00202
C	-3.7642	-1.82221	-0.00548
C	-4.86964	0.73302	0.00039
C	-5.14958	-1.65777	-0.00707
H	-3.32093	-2.81138	-0.00771
C	-5.7137	-0.37925	-0.00414
H	-5.79971	-2.52742	-0.0106
H	-6.78991	-0.24481	-0.00533
H	-2.82983	1.4551	0.00556
Cl	-5.57171	2.34705	0.00409
C	4.32052	2.46302	-0.00646
N	5.34669	3.01136	-0.00835

Zero-point correction=	0.295425 (Hartree/Particle)
Thermal correction to Energy=	0.314396
Thermal correction to Enthalpy=	0.315340
Thermal correction to Gibbs Free Energy=	0.245044
Sum of electronic and zero-point Energies=	-1397.641858
Sum of electronic and thermal Energies=	-1397.622887
Sum of electronic and thermal Enthalpies=	-1397.621943
Sum of electronic and thermal Free Energies=	-1397.692239

Low frequencies --- -394.7442 -8.7277 -5.6247 0.0023 0.0031 0.0034

E(RB+HF-LYP) = -1397.93728268

7) B3LYP/6-31+g(d,p) CPCM, dichloromethane optimized to TS

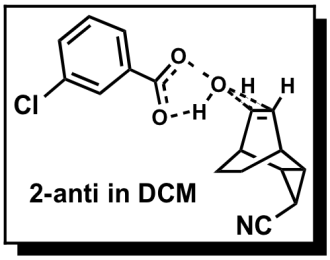

C	-2.59575	0.81318	0.75872
C	-3.38602	-0.40092	1.31547
C	-4.83493	-0.43835	0.76672
C	-2.59455	0.76817	-0.79687
C	-4.83327	-0.48201	-0.73678
C	-3.38293	-0.47641	-1.28332
C	-2.78815	-1.67664	0.74080
C	-2.78589	-1.71666	-0.63348
C	-5.53424	0.67663	-0.01857
H	-3.03961	1.73917	1.13141
H	-1.57744	0.78364	1.15630
H	-3.37993	-0.40209	2.40932
H	-5.51785	-1.08123	1.32062
H	-1.57564	0.71612	-1.19070
H	-3.03885	1.67056	-1.22303
H	-5.51501	-1.15581	-1.25418
H	-3.37455	-0.54185	-2.37520
H	-6.62102	0.55746	-0.01618
O	1.12667	-1.90024	-0.00101
O	0.91413	0.3292	0.05478
H	-2.5574	-2.60957	-1.20822
H	-2.55093	-2.53197	1.36710
H	-0.54537	-0.75351	0.04658
C	1.6214	-0.69287	0.01918
O	-0.67787	-1.73683	0.02324
C	3.12208	-0.62155	-0.00458
C	3.72421	0.64498	0.02185
C	3.91300	-1.77864	-0.05253
C	5.11317	0.72849	-0.00042
C	5.30429	-1.66730	-0.07439
H	3.44227	-2.75755	-0.07305
C	5.91792	-0.41128	-0.04840
H	5.92147	-2.56307	-0.11211
H	7.00189	-0.32024	-0.06517
Cl	5.87640	2.32003	0.032610
H	3.10949	1.53960	0.059200
C	-5.21997	2.07933	-0.0582
N	-5.07799	3.23484	-0.0906

Zero-point correction=	0.292744 (Hartree/Particle)
Thermal correction to Energy=	0.311071
Thermal correction to Enthalpy=	0.312016
Thermal correction to Gibbs Free Energy=	0.244398
Sum of electronic and zero-point Energies=	-1397.665781
Sum of electronic and thermal Energies=	-1397.647454
Sum of electronic and thermal Enthalpies=	-1397.646510
Sum of electronic and thermal Free Energies=	-1397.714128

Low frequencies --- -410.9219 -12.1340 -10.3736 -5.8938 -3.4284 -1.6256

E(RB+HF-LYP) = -1397.95852524

8) B3LYP/6-31+g(d,p) optimized to TS

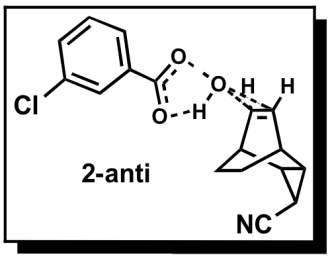

C	-2.48191	0.78681	0.77514
C	-3.29909	-0.42129	1.30340
C	-4.75012	-0.41131	0.75486
C	-2.47887	0.77498	-0.78080
C	-4.74699	-0.42281	-0.75154
C	-3.29367	-0.44112	-1.29378
C	-2.73882	-1.70495	0.70584
C	-2.73542	-1.7155	-0.67413
C	-5.42053	0.73392	-0.00847
H	-2.90877	1.71377	1.1628
H	-1.46317	0.7267	1.16527
H	-3.2944	-0.44495	2.39523
H	-5.44377	-1.05457	1.29097
H	-1.45863	0.70911	-1.16613
H	-2.90442	1.69584	-1.18412
H	-5.43853	-1.07408	-1.28066
H	-3.28446	-0.48168	-2.38508
H	-6.5057	0.63782	-0.00999
O	1.09862	-2.00188	-0.00053
O	0.82164	0.21895	0.01796
H	-2.55906	-2.60674	-1.26296
H	-2.55989	-2.5861	1.30896
H	-0.53406	-0.82393	0.01592
C	1.55666	-0.79005	0.00617
O	-0.75651	-1.80215	0.00835
C	3.05464	-0.66045	-0.00150
C	3.60959	0.62606	0.00688
C	3.88462	-1.78904	-0.01663
C	4.99474	0.76385	-0.00008
C	5.27033	-1.62742	-0.02343
H	3.43886	-2.7771	-0.02294
C	5.83674	-0.34993	-0.01519
H	5.91886	-2.49824	-0.03522
H	6.91318	-0.21733	-0.02037
Cl	5.70072	2.37630	0.01035
H	2.95564	1.48976	0.01859
C	-5.06954	2.13213	-0.01820
N	-4.89257	3.2817	-0.02622

Zero-point correction=	0.295250 (Hartree/Particle)
Thermal correction to Energy=	0.313284
Thermal correction to Enthalpy=	0.314228
Thermal correction to Gibbs Free Energy=	0.247702
Sum of electronic and zero-point Energies=	-1397.636897
Sum of electronic and thermal Energies=	-1397.618863
Sum of electronic and thermal Enthalpies=	-1397.617919
Sum of electronic and thermal Free Energies=	-1397.684445

Low frequencies --- -401.8384 -11.6478 -1.0835 -0.0018 0.0011

E(RB+HF-LYP) = -1397.93214707

9) B3LYP/6-31+g(d,p) CPCM, dichloromethane optimized to TS

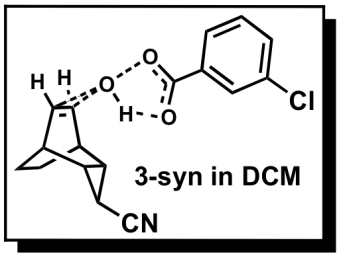

C	5.12931	-0.3873	0.77861
C	3.6589	-0.46559	1.30579
C	2.81863	0.69844	0.74977
C	5.12739	-0.39104	-0.78025
C	2.81688	0.69505	-0.75071
C	3.65567	-0.4717	-1.30339
C	3.12181	-1.74606	0.69184
C	3.12016	-1.74935	-0.68205
C	3.48136	1.85407	-0.00378
H	5.61033	0.51116	1.18027
H	5.68799	-1.24295	1.16985
H	3.63628	-0.48828	2.39911
H	1.90502	0.93598	1.2916
H	5.6851	-1.24855	-1.1688
H	5.60744	0.50554	-1.18728
H	1.90196	0.93014	-1.29142
H	3.63035	-0.49952	-2.39653
H	2.96239	-2.63889	1.2903
H	2.95985	-2.64508	-1.27595
O	1.01882	-1.85449	0.00498
O	-0.77514	-2.03781	0.00332
C	-1.29619	-0.84033	0.00104
O	-0.6138	0.19759	0.00073
H	0.8861	-0.87083	0.00398
C	-2.79902	-0.80978	-0.00122
C	-3.4348	0.44026	0.00286
C	-3.55963	-1.98813	-0.00721
C	-4.8257	0.48668	0.0009
C	-4.95358	-1.91419	-0.0094
H	-3.06361	-2.9546	-0.01037
C	-5.60035	-0.67465	-0.00528
H	-5.5469	-2.82672	-0.01431
H	-6.68649	-0.61263	-0.00681
H	-2.84414	1.35159	0.00761
Cl	-5.63038	2.05796	0.0065
H	4.56267	1.95309	-0.00514
C	2.82055	3.13128	-0.00615
N	2.29925	4.17241	-0.00813

Zero-point correction=	0.292843 (Hartree/Particle)
Thermal correction to Energy=	0.312107
Thermal correction to Enthalpy=	0.313051
Thermal correction to Gibbs Free Energy=	0.241268
Sum of electronic and zero-point Energies=	-1397.675815
Sum of electronic and thermal Energies=	-1397.656552
Sum of electronic and thermal Enthalpies=	-1397.655608
Sum of electronic and thermal Free Energies=	-1397.727390

Low frequencies --- -412.3729 -11.1555 -5.3695 -4.0532 -2.5505 2.4666

E(RB+HF-LYP) = -1397.96865826

10) B3LYP/6-31+g(d,p) optimized to TS

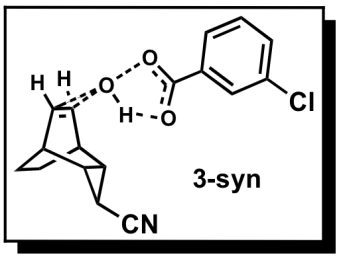

C	-5.03773	-0.27149	-0.77965
C	-3.57212	-0.42216	-1.30337
C	-2.68006	0.70385	-0.75144
C	-5.03747	-0.27083	0.78026
C	-2.67984	0.70427	0.75073
C	-3.57172	-0.42144	1.3036
C	-3.09809	-1.72909	-0.68922
C	-3.09789	-1.72873	0.69003
C	-3.27745	1.89191	-0.0006
H	-5.47511	0.64698	-1.18409
H	-5.64009	-1.09808	-1.1679
H	-3.55114	-0.44985	-2.39487
H	-1.74382	0.88096	-1.27184
H	-5.6401	-1.09676	1.16949
H	-5.47422	0.64823	1.18402
H	-1.7435	0.88183	1.2708
H	-3.55036	-0.44858	2.3951
H	-2.99861	-2.63028	-1.28139
H	-2.99802	-2.62952	1.28272
O	-1.13189	-1.89588	0.00021
O	0.71067	-2.15446	0.0009
C	1.20607	-0.95657	0.00013
O	0.50027	0.0731	-0.00049
H	-0.8846	-0.92166	-0.00008
C	2.70651	-0.87173	-0.00007
C	3.29941	0.39799	0.00032
C	3.50213	-2.02496	-0.00066
C	4.68822	0.49393	0.00013
C	4.89201	-1.9051	-0.0009
H	3.02698	-2.99924	-0.00095
C	5.49613	-0.64502	-0.00049
H	5.51422	-2.79498	-0.0014
H	6.57605	-0.54465	-0.00066
H	2.67207	1.28139	0.00072
Cl	5.44267	2.08363	0.0006
H	-4.35215	2.0305	-0.00047
C	-2.55865	3.1421	-0.00086
N	-1.99602	4.15977	-0.00029

Zero-point correction=	0.295159 (Hartree/Particle)
Thermal correction to Energy=	0.314150
Thermal correction to Enthalpy=	0.315094
Thermal correction to Gibbs Free Energy=	0.244838
Sum of electronic and zero-point Energies=	-1397.646659
Sum of electronic and thermal Energies=	-1397.627667
Sum of electronic and thermal Enthalpies=	-1397.626723
Sum of electronic and thermal Free Energies=	-1397.696979

Low frequencies --- -407.5197 -5.0851 -4.0537 -0.0023 -0.0022 -0.0017

E(RB+HF-LYP) = -1397.94181729

11) B3LYP/6-31+g(d,p) CPCM, dichloromethane optimized to TS

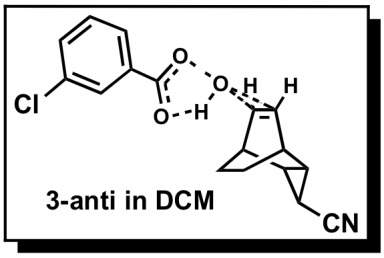

C	2.40715	0.94331	-0.80072
C	3.21635	-0.28953	-1.28775
C	4.66637	-0.23473	-0.74116
C	2.41199	0.99320	0.75658
C	4.67126	-0.18704	0.75698
C	3.22519	-0.20612	1.31627
C	2.65618	-1.54025	-0.62986
C	2.66114	-1.49581	0.74435
C	5.19951	1.01549	-0.03274
H	2.84281	1.85144	-1.23009
H	1.38824	0.87793	-1.19172
H	3.20528	-0.35889	-2.37931
H	5.40051	-0.84965	-1.25930
H	1.39563	0.95337	1.15751
H	2.84988	1.92686	1.12450
H	5.40819	-0.76881	1.30845
H	3.22171	-0.20496	2.41008
O	-1.2480	-1.81713	0.00810
O	-1.08575	0.41671	0.04993
H	2.44915	-2.35623	1.37273
H	2.45363	-2.44237	-1.19982
H	0.39518	-0.63184	0.04685
C	-1.77002	-0.62124	0.01907
O	0.55034	-1.61188	0.02545
C	-3.27177	-0.58331	-0.00037
C	-3.90123	0.67013	0.01075
C	-4.0375	-1.7578	-0.02902
C	-5.29170	0.72323	-0.00747
C	-5.43099	-1.67694	-0.04648
H	-3.54573	-2.72649	-0.03744
C	-6.07169	-0.43427	-0.03596
H	-6.02869	-2.58634	-0.06862
H	-7.15743	-0.36692	-0.04961
Cl	-6.08894	2.2983	0.00599
H	-3.30606	1.57834	0.03331
H	4.63073	1.94094	-0.05987
C	6.62116	1.23557	-0.04451
N	7.77255	1.40964	-0.05382

Zero-point correction=	0.292677 (Hartree/Particle)
Thermal correction to Energy=	0.311050
Thermal correction to Enthalpy=	0.311994
Thermal correction to Gibbs Free Energy=	0.244336
Sum of electronic and zero-point Energies=	-1397.674320
Sum of electronic and thermal Energies=	-1397.655947
Sum of electronic and thermal Enthalpies=	-1397.655003
Sum of electronic and thermal Free Energies=	-1397.722661

Low frequencies --- -410.5603 -13.5367 -6.3562 -3.6356 -1.7145 -1.6225

E(RB+HF-LYP) = -1397.96699687

12) B3LYP/6-31+g(d,p) optimized to TS

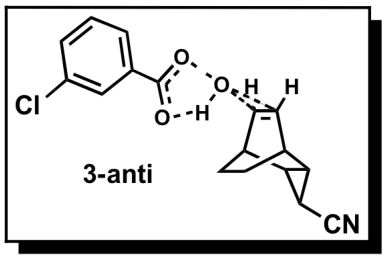

C	-2.27936	0.93414	0.77583
C	-3.12748	-0.25300	1.30658
C	-4.57466	-0.17207	0.75216
C	-2.27557	0.91983	-0.78255
C	-4.57123	-0.18552	-0.74965
C	-3.12153	-0.27639	-1.29571
C	-2.60917	-1.55095	0.70810
C	-2.60555	-1.56348	-0.67141
C	-5.06918	1.05793	-0.01095
H	-2.69027	1.86963	1.16826
H	-1.26187	0.85801	1.16570
H	-3.12174	-0.27600	2.39831
H	-5.32889	-0.74181	1.28735
H	-1.25617	0.83554	-1.16568
H	-2.68346	1.84837	-1.19413
H	-5.32310	-0.76471	-1.27795
H	-3.11072	-0.31918	-2.38680
O	1.22510	-1.92443	0.00016
O	0.98414	0.30077	0.01599
H	-2.45779	-2.46138	-1.25790
H	-2.45783	-2.43703	1.31147
H	-0.38603	-0.72446	0.0159
C	1.70317	-0.7205	0.00583
O	-0.62375	-1.69793	0.00938
C	3.20262	-0.61539	-0.00078
C	3.77850	0.66194	0.00400
C	4.01414	-1.75739	-0.01164
C	5.16563	0.77734	-0.00236
C	5.40227	-1.61820	-0.01758
H	3.55262	-2.73818	-0.01523
C	5.98936	-0.35005	-0.01306
H	6.03657	-2.49942	-0.02594
H	7.06779	-0.23503	-0.01772
Cl	5.89717	2.37831	0.00353
H	3.13906	1.53639	0.01246
H	-4.45999	1.95396	-0.01751
C	-6.48551	1.32847	-0.01653
N	-7.63038	1.53376	-0.02092

Zero-point correction=	0.295237 (Hartree/Particle)
Thermal correction to Energy=	0.314236
Thermal correction to Enthalpy=	0.315180
Thermal correction to Gibbs Free Energy=	0.244759
Sum of electronic and zero-point Energies=	-1397.645356
Sum of electronic and thermal Energies=	-1397.626357
Sum of electronic and thermal Enthalpies=	-1397.625413
Sum of electronic and thermal Free Energies=	-1397.695833

Low frequencies --- -399.1025 -4.4589 -0.0019 -0.0015 -0.0014 1.8062

E(RB+HF-LYP) = -1397.94059272

13) B3LYP/6-31+g(d,p) CPCM, dichloromethane optimized to TS

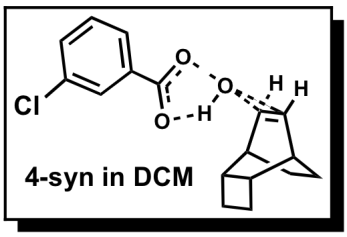

C	5.18326	-0.14299	0.77857
C	3.71649	-0.25446	1.30919
C	2.86175	0.92993	0.78598
C	5.18423	-0.13475	-0.77752
C	2.86169	0.93616	-0.77909
C	3.71833	-0.24283	-1.31140
C	3.18775	-1.51635	-0.69470
C	3.44017	2.37820	0.78857
C	3.43804	2.38516	-0.77034
H	5.76552	-0.98666	1.16377
H	5.64762	0.76322	1.17895
H	3.70594	-0.30379	2.40360
H	1.86752	0.87618	1.24050
H	5.76849	-0.97321	-1.17095
H	5.64733	0.77654	-1.16773
H	1.86771	0.88424	-1.23433
H	3.70951	-0.28237	-2.40622
H	3.00462	-2.41995	1.26559
H	3.00546	-2.40845	-1.28813
H	2.76273	3.10969	1.23941
H	4.42206	2.49984	1.25480
H	2.75775	3.11935	-1.21240
H	4.41818	2.51276	-1.23870
O	1.04616	-1.66023	-0.00473
C	3.18642	-1.52238	0.68034
O	-0.73446	-1.88325	-0.00372
H	0.90467	-0.67999	-0.00738
C	-1.28748	-0.69946	-0.00401
O	-0.63471	0.35642	-0.00684
C	-2.79068	-0.70878	-0.00056
C	-3.52163	-1.90563	0.00576
C	-3.45742	0.52516	-0.00353
C	-4.91708	-1.86634	0.00913
H	-3.00179	-2.85954	0.00811
C	-4.84898	0.53686	0.00002
H	-2.88938	1.45079	-0.00840
C	-5.59460	-0.64334	0.00633
H	-5.48745	-2.79339	0.01412
H	-6.68194	-0.60838	0.00900
Cl	-5.69247	2.08792	-0.00340

Zero-point correction=	0.323219 (Hartree/Particle)
Thermal correction to Energy=	0.340963
Thermal correction to Enthalpy=	0.341907
Thermal correction to Gibbs Free Energy=	0.275643
Sum of electronic and zero-point Energies=	-1344.716916
Sum of electronic and thermal Energies=	-1344.699172
Sum of electronic and thermal Enthalpies=	-1344.698228
Sum of electronic and thermal Free Energies=	-1344.764492

Low frequencies --- - 402.9215 -16.2151 -11.7387 -4.0557 -1.5067 3.0286

E(RB+HF-LYP) = -1345.02349607

14) B3LYP/6-31+g(d,p) optimized to TS

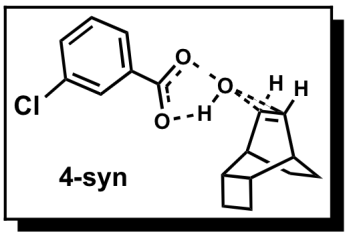

C	-5.09759	-0.08019	-0.77546
C	-3.63501	-0.22821	-1.30841
C	-2.74916	0.93125	-0.78399
C	-5.09570	-0.07814	0.78128
C	-2.74762	0.93383	0.78097
C	-3.63174	-0.22448	1.31103
C	-3.14106	-1.51449	0.69246
C	-3.28734	2.39433	-0.78286
C	-3.28678	2.39662	0.77597
H	-5.70590	-0.90405	-1.16248
H	-5.53846	0.83951	-1.17013
H	-3.62767	-0.27397	-2.40141
H	-1.75428	0.85082	-1.22908
H	-5.70299	-0.9010	1.17203
H	-5.53566	0.84258	1.17454
H	-1.75162	0.85583	1.22398
H	-3.62168	-0.26714	2.40414
H	-3.01191	-2.41889	-1.27222
H	-3.00806	-2.41514	1.27959
H	-2.58879	3.10654	-1.23019
H	-4.26376	2.54943	-1.25035
H	-2.58873	3.11075	1.22101
H	-4.26315	2.55213	1.24341
O	-1.13766	-1.68904	-0.00159
C	-3.14274	-1.51644	-0.68738
O	0.69337	-1.96471	-0.00464
H	-0.90072	-0.7193	0.00072
C	1.21994	-0.77979	-0.00133
O	0.55175	0.27206	0.00153
C	2.72491	-0.74585	-0.00056
C	3.48344	-1.92363	-0.00025
C	3.35975	0.50311	-0.0002
C	4.8767	-1.84913	0.00050
H	2.97672	-2.88182	-0.00062
C	4.75070	0.55402	0.00047
H	2.76057	1.40572	-0.00034
C	5.52214	-0.60965	0.00084
H	5.46942	-2.75898	0.00082
H	6.60472	-0.54436	0.00138
Cl	5.55619	2.12034	0.00084

Zero-point correction=	0.325590 (Hartree/Particle)
Thermal correction to Energy=	0.343956
Thermal correction to Enthalpy=	0.344900
Thermal correction to Gibbs Free Energy=	0.275921
Sum of electronic and zero-point Energies=	-1344.697907
Sum of electronic and thermal Energies=	-1344.679540
Sum of electronic and thermal Enthalpies=	-1344.678596
Sum of electronic and thermal Free Energies=	-1344.747575

Low frequencies --- -384.1483 -7.2821 -3.3728 -0.0018 -0.0014 0.0023

E(RB+HF-LYP) = -1345.02349607

15) B3LYP/6-31+g(d,p) CPCM, dichloromethane optimized to TS

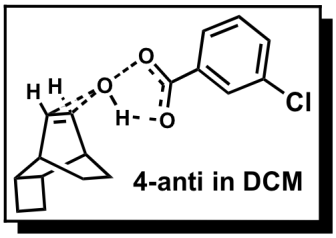

C	2.67012	1.10115	-0.75544
C	3.49128	-0.08961	-1.31669
C	4.96023	-0.03462	-0.7832
C	2.66777	1.06143	0.79979
C	4.95644	-0.07685	0.77984
C	3.48484	-0.15806	1.30203
C	2.96742	-1.37945	-0.72929
C	2.96345	-1.41545	0.64501
H	3.09271	2.04105	-1.12169
H	1.65099	1.0537	-1.15188
H	3.46425	-0.09689	-2.41191
H	1.64729	0.99604	1.19015
H	3.09146	1.98049	1.21449
H	3.45222	-0.2228	2.39522
H	2.78848	-2.3268	1.21074
H	2.78815	-2.25853	-1.34289
H	6.73109	1.25881	-1.18996
C	5.73466	1.32094	-0.74216
H	5.2197	2.17769	-1.1859
C	5.73275	1.2777	0.81559
H	5.2186	2.10939	1.30553
H	6.72822	1.18865	1.26097
H	5.53675	-0.84053	-1.25156
H	5.52943	-0.90776	1.20702
O	0.82137	-1.54601	-0.02443
O	-0.95187	-1.78299	-0.01168
C	-1.51039	-0.60098	-0.01482
O	-0.86043	0.45691	-0.02733
H	0.67215	-0.56685	-0.03133
C	-3.01275	-0.61496	-0.00188
C	-3.73996	-1.81397	0.01622
C	-3.68300	0.61711	-0.00783
C	-5.13546	-1.77857	0.02853
H	-3.21742	-2.76642	0.02093
C	-5.07449	0.62484	0.00462
H	-3.11778	1.54437	-0.02189
C	-5.81651	-0.55753	0.02281
H	-5.70314	-2.70716	0.04288
H	-6.90391	-0.52567	0.03239
Cl	-5.92237	2.17337	-0.00251

Zero-point correction= 0.323113 (Hartree/Particle)
Thermal correction to Energy= 0.340868
Thermal correction to Enthalpy= 0.341812
Thermal correction to Gibbs Free Energy= 0.275318
Sum of electronic and zero-point Energies = -1344.717084
Sum of electronic and thermal Energies= -1344.699329
Sum of electronic and thermal Enthalpies= -1344.698385
Sum of electronic and thermal Free Energies= -1344.764878
Low frequencies --- -401.7843 -18.9873 -10.8981 -3.6895 -1.7202 1.4298

E(RB+HF-LYP) = -1345.04019674

16) B3LYP/6-31+g(d,p) optimized to TS

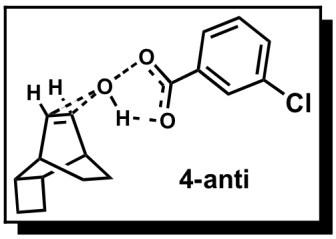

C	-2.54468	1.06163	0.77939
C	-3.39490	-0.12242	1.30846
C	-4.86328	-0.01474	0.78187
C	-2.54418	1.06384	-0.77647
C	-4.86313	-0.01179	-0.78251
C	-3.39472	-0.11825	-1.30938
C	-2.91296	-1.41432	0.68722
C	-2.91305	-1.41217	-0.69221
H	-2.94512	2.00026	1.17195
H	-1.52524	0.98040	1.16605
H	-3.36553	-0.16050	2.40134
H	-1.52450	0.98310	-1.16257
H	-2.94370	2.00388	-1.16657
H	-3.36527	-0.15287	-2.40237
H	-2.78839	-2.31348	-1.28023
H	-2.78871	-2.31753	1.27241
H	-6.60158	1.31041	1.22776
C	-5.60462	1.35951	0.78104
H	-5.06946	2.18884	1.25024
C	-5.60384	1.36279	-0.77664
H	-5.06756	2.19378	-1.2416
H	-6.60031	1.31634	-1.22475
H	-5.46001	-0.81779	1.22655
H	-5.46023	-0.81287	-1.23022
O	-0.90547	-1.60465	-0.00143
O	0.92057	-1.87616	-0.00055
C	1.44375	-0.68916	-0.00094
O	0.77088	0.35985	-0.00179
H	-0.66852	-0.63503	-0.00159
C	2.94797	-0.64916	-0.00013
C	3.71146	-1.82372	0.00097
C	3.57719	0.60271	-0.00048
C	5.10437	-1.74306	0.00172
H	3.20904	-2.78418	0.00122
C	4.9679	0.65969	0.00029
H	2.9741	1.50272	-0.00134
C	5.74429	-0.50072	0.00139
H	5.70112	-2.65025	0.00258
H	6.82658	-0.4307	0.00198
Cl	5.76647	2.22936	-0.00013

Zero-point correction=	0.325617 (Hartree/Particle)
Thermal correction to Energy=	0.343980
Thermal correction to Enthalpy=	0.344924
Thermal correction to Gibbs Free Energy=	0.275707
Sum of electronic and zero-point Energies=	-1344.697823
Sum of electronic and thermal Energies=	-1344.679460
Sum of electronic and thermal Enthalpies=	-1344.678516
Sum of electronic and thermal Free Energies=	-1344.747732

Low frequencies --- -383.2996 -7.7558 -0.0019 -0.0012 0.0013 2.2338

E(RB+HF-LYP) = -1345.02343932

17) B3LYP/6-31+g(d,p) CPCM, dichloromethane optimized to TS

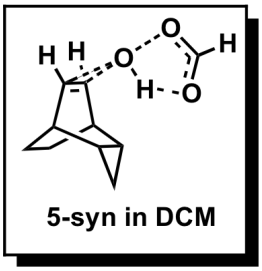

C	-2.74972	-0.40953	-0.77642
C	-1.28560	-0.24541	-1.29820
C	-0.67277	1.06732	-0.76966
C	-2.75321	-0.39011	0.78121
C	-0.67679	1.08699	0.74525
C	-1.29146	-0.21159	1.30505
C	-0.52982	-1.39938	-0.66593
C	-0.53308	-1.38116	0.70625
C	-1.48854	2.10303	-0.02792
H	-3.36964	0.39404	-1.18797
H	-3.15959	-1.35128	-1.15558
H	-1.25889	-0.2886	-2.39162
H	0.20776	1.41751	-1.30641
H	-3.16384	-1.32253	1.18194
H	-3.37538	0.42307	1.16989
H	0.19979	1.45234	1.27835
H	-1.2695	-0.22635	2.39931
H	-1.09642	3.11696	-0.03956
H	-2.57206	2.05717	-0.03021
H	-0.1873	-2.25038	-1.24884
H	-0.18758	-2.21443	1.31270
O	1.59487	-1.05411	-0.00283
O	3.37469	-0.89699	-0.02121
C	3.67913	0.36685	0.00061
H	4.77708	0.52297	-0.00977
O	2.87863	1.30362	0.02692
H	1.48118	-0.0727	0.00331

Zero-point correction=	0.223041 (Hartree/Particle)
Thermal correction to Energy=	0.234814
Thermal correction to Enthalpy=	0.235758
Thermal correction to Gibbs Free Energy=	0.184234
Sum of electronic and zero-point Energies=	-614.822953
Sum of electronic and thermal Energies=	-614.811180
Sum of electronic and thermal Enthalpies=	-614.810236
Sum of electronic and thermal Free Energies=	-614.861760

Low frequencies --- -397.9276 -27.2042 -11.2982 -2.8741 -2.7724 -0.6842

E(RB+HF-LYP) = -615.04599395

18) B3LYP/6-31+g(d,p) optimized to TS

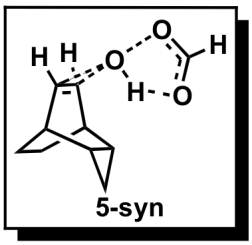

C	-2.69655	-0.40904	-0.77904
C	-1.23432	-0.23152	-1.3008
C	-0.62752	1.07686	-0.76023
C	-2.69769	-0.40466	0.7794
C	-0.62855	1.08163	0.75441
C	-1.2363	-0.22331	1.30231
C	-0.47592	-1.39364	-0.68424

C	-0.4772	-1.38932	0.69428
C	-1.44438	2.1017	-0.00665
H	-3.32073	0.39488	-1.18175
H	-3.10555	-1.34768	-1.16609
H	-1.2094	-0.263	-2.39292
H	0.25874	1.43004	-1.28017
H	-3.10627	-1.3416	1.17099
H	-3.32331	0.4008	1.17681
H	0.25704	1.43776	1.27347
H	-1.21309	-0.24781	2.39465
H	-1.05446	3.11521	-0.00962
H	-2.52744	2.05596	-0.00711
H	-0.15789	-2.24659	-1.27149
H	-0.15848	-2.23791	1.28747
O	1.49985	-1.07223	-0.00021
O	3.35016	-0.87646	-0.00581
C	3.55727	0.39569	0.00012
H	4.63431	0.65028	-0.00148
O	2.69173	1.28012	0.00684
H	1.45955	-0.07818	0.00329

Zero-point correction= 0.224947 (Hartree/Particle)
Thermal correction to Energy= 0.236433
Thermal correction to Enthalpy= 0.237378
Thermal correction to Gibbs Free Energy= 0.186618
Sum of electronic and zero-point Energies= -614.804931
Sum of electronic and thermal Energies= -614.793445
Sum of electronic and thermal Enthalpies= -614.792501
Sum of electronic and thermal Free Energies= -614.843261

Low frequencies --- -378.7117 -22.9152 -11.3519 -0.0010 0.0006 0.0010

E(RB+HF-LYP) = -615.02987878

19) B3LYP/6-31+g(d,p) CPCM, dichloromethane optimized to TS

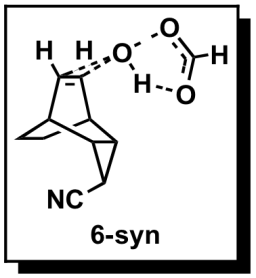

6-syn

Center Number	Atomic Number	Atom Type	Coordinates (Angstroms) X	Y	Z
1	6	0	2.137064	-1.268841	0.776129
2	6	0	0.772030	-0.722550	1.302755
3	6	0	0.468863	0.684218	0.755915
4	6	0	2.133840	-1.267601	-0.780462
5	6	0	0.465678	0.685215	-0.750334
6	6	0	0.766636	-0.720681	-1.300466
7	6	0	-0.253688	-1.661916	0.689101
8	6	0	-0.256740	-1.660878	-0.683798

9	1	0	2.953823	-0.665018	1.179439
10	1	0	2.277347	-2.282683	1.164048
11	1	0	0.742627	-0.735200	2.396108
12	1	0	2.272704	-2.280800	-1.170582
13	1	0	2.948871	-0.663070	-1.186089
14	1	0	0.732533	-0.731780	-2.393701
15	1	0	-0.778034	-2.402203	1.287529
16	1	0	-0.781092	-2.402275	-1.280749
17	8	0	-2.222484	-0.852605	-0.002591
18	8	0	-3.930430	-0.276863	-0.005094
19	6	0	-3.906089	1.020613	0.000484
20	1	0	-4.925127	1.457324	0.002959
21	8	0	-2.889843	1.722073	0.003735
22	1	0	-1.912943	0.086701	-0.000329
23	1	0	1.120148	2.629850	0.002754
24	6	0	1.447361	1.587031	0.001350
25	1	0	-0.294658	1.233798	1.303862
26	1	0	-0.300010	1.235599	-1.294391
27	6	0	2.884943	1.549977	-0.001945
28	7	0	4.046639	1.633058	-0.004518

Zero-point correction=	0.221755 (Hartree/Particle)
Thermal correction to Energy=	0.235277
Thermal correction to Enthalpy=	0.236221
Thermal correction to Gibbs Free Energy=	0.180376
Sum of electronic and zero-point Energies=	-707.067158
Sum of electronic and thermal Energies=	-707.053636
Sum of electronic and thermal Enthalpies=	-707.052692
Sum of electronic and thermal Free Energies=	-707.108537

Low frequencies --- -403.9686 -8.5715 -3.5395 -1.8686 0.8951 7.2576

E(RB+HF-LYP) = -707.288913250

20) B3LYP/6-31++g(d,p) optimized to TS

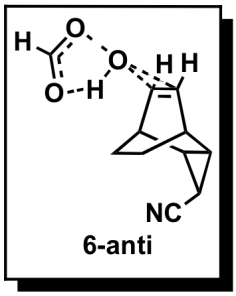

Center Number	Atomic Number	Atomic Type	Coordinates (Angstroms) X	Y	Z
1	6	0	0.000000	0.000000	0.000000
2	6	0	0.000000	0.000000	1.551586
3	6	0	1.442527	0.000000	2.121124
4	6	0	0.794826	1.231543	-0.522443
5	6	0	2.212149	1.192478	1.615231
6	6	0	1.326930	2.056114	0.679381
7	6	0	-0.543128	1.331803	2.052036
8	6	0	0.162131	2.424446	1.588553
9	6	0	2.730667	-0.217871	1.323423
10	1	0	0.433304	-0.933229	-0.364882
11	1	0	-1.032374	0.022804	-0.357356
12	1	0	-0.573485	-0.844523	1.939510
13	1	0	1.517270	-0.275531	3.170336

14	1	0	0.160176	1.870508	-1.141282
15	1	0	1.631443	0.923181	-1.152362
16	1	0	2.830518	1.759312	2.307089
17	1	0	1.868505	2.939431	0.334368
18	1	0	3.566179	-0.482590	1.970440
19	1	0	0.040617	3.424351	1.985598
20	1	0	-1.272992	1.388109	2.849747
21	6	0	2.897100	-0.866873	0.046916
22	7	0	3.124084	-1.433526	-0.943159
23	8	0	-1.796448	2.497147	0.841594
24	8	0	-3.355785	3.147976	0.011648
25	1	0	-4.181806	2.918728	-1.794780
26	6	0	-3.319464	2.629963	-1.165567
27	8	0	-2.434855	1.878797	-1.602880
28	1	0	-1.651296	2.036200	-0.032725

Zero-point correction=	0.223700 (Hartree/Particle)
Thermal correction to Energy=	0.236929
Thermal correction to Enthalpy=	0.237873
Thermal correction to Gibbs Free Energy=	0.182544
Sum of electronic and zero-point Energies=	-707.037646
Sum of electronic and thermal Energies=	-707.024417
Sum of electronic and thermal Enthalpies=	-707.023472
Sum of electronic and thermal Free Energies=	-707.078802

Low frequencies --- -391.7868 -5.6423 0.0003 0.0003 0.0006 1.8909

E(RB+HF-LYP) = -707.2613457

21) B3LYP/6-31+g(d,p) CPCM, dichloromethane optimized to TS

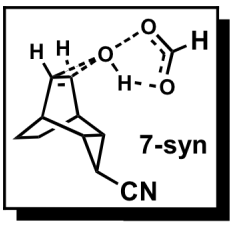

Center Number	Atomic Number	Atomic Type	Coordinates (Angstroms) X	Y	Z
1	6	0	2.371476	-1.449537	0.774321
2	6	0	0.997178	-0.926815	1.305389
3	6	0	0.699422	0.479723	0.752389
4	6	0	2.364571	-1.450250	-0.784096
5	6	0	0.693483	0.478896	-0.748830
6	6	0	0.985619	-0.928222	-1.303065
7	6	0	-0.018125	-1.875294	0.692928
8	6	0	-0.024460	-1.876042	-0.680341
9	1	0	3.176190	-0.823355	1.174637
10	1	0	2.536786	-2.458481	1.164252
11	1	0	0.970179	-0.939448	2.398772
12	1	0	2.526890	-2.459505	-1.174512
13	1	0	3.165511	-0.824079	-1.191924
14	1	0	0.948328	-0.942137	-2.396139
15	1	0	-0.536710	-2.618522	1.292700

16	1	0	-0.545059	-2.622219	-1.274548
17	8	0	-1.984653	-1.077321	-0.001615
18	8	0	-3.699764	-0.513237	-0.010934
19	6	0	-3.682939	0.784457	-0.000196
20	1	0	-4.704550	1.215270	-0.005167
21	8	0	-2.670920	1.491551	0.014370
22	1	0	-1.683765	-0.134534	0.010280
23	6	0	1.770611	1.269815	-0.002861
24	1	0	-0.036944	1.066275	1.298979
25	1	0	-0.046882	1.065702	-1.289624
26	6	0	1.676499	2.704918	-0.003556
27	7	0	1.610322	3.867363	-0.004140
28	1	0	2.800460	0.925649	-0.005789

Zero-point correction=	0.221738 (Hartree/Particle)
Thermal correction to Energy=	0.235260
Thermal correction to Enthalpy=	0.236204
Thermal correction to Gibbs Free Energy=	0.180491
Sum of electronic and zero-point Energies=	-707.074618
Sum of electronic and thermal Energies=	-707.061096
Sum of electronic and thermal Enthalpies=	-707.060152
Sum of electronic and thermal Free Energies=	-707.115865

Low frequencies --- -404.9888 -9.4581 -3.2532 -2.0826 2.0626 8.1594

E(RB+HF-LYP) =-707.2963562

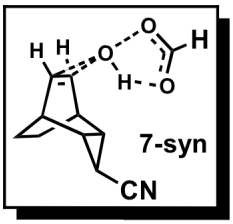

22) B3LYP/6-31++g(d,p) optimized to TS

Center Number	Atomic Number	Atomic Type	Coordinates (Angstroms) X	Y	Z
1	6	0	2.236681	-1.558710	0.779940
2	6	0	0.890849	-0.958998	1.303557
3	6	0	0.678266	0.461710	0.751142
4	6	0	2.236453	-1.558936	-0.779966
5	6	0	0.678035	0.461480	-0.751207
6	6	0	0.890465	-0.959375	-1.303333
7	6	0	-0.169960	-1.857900	0.690267
8	6	0	-0.170173	-1.858079	-0.689490
9	1	0	3.073544	-0.979927	1.183781
10	1	0	2.347837	-2.575218	1.168808
11	1	0	0.859094	-0.972213	2.395054
12	1	0	2.347516	-2.575553	-1.168580
13	1	0	3.073186	-0.980248	-1.184208
14	1	0	0.858351	-0.972885	-2.394816
15	1	0	-0.704068	-2.590124	1.282984
16	1	0	-0.704134	-2.590717	-1.281830

17	8	0	-1.958261	-1.024285	-0.000398
18	8	0	-3.695744	-0.317266	-0.000992
19	6	0	-3.511522	0.956784	0.000179
20	1	0	-4.455143	1.532834	0.000151
21	8	0	-2.412579	1.530984	0.001268
22	1	0	-1.676654	-0.064398	0.000415
23	6	0	1.788840	1.192531	-0.000300
24	1	0	-0.043808	1.083092	1.272117
25	1	0	-0.044224	1.082710	-1.272109
26	6	0	1.793956	2.634744	-0.000476
27	7	0	1.822969	3.797197	-0.000328
28	1	0	2.789052	0.775297	-0.000373

Zero-point correction=	0.223500 (Hartree/Particle)
Thermal correction to Energy=	0.236807
Thermal correction to Enthalpy=	0.237751
Thermal correction to Gibbs Free Energy=	0.182250
Sum of electronic and zero-point Energies=	-707.047361
Sum of electronic and thermal Energies=	-707.034054
Sum of electronic and thermal Enthalpies=	-707.033110
Sum of electronic and thermal Free Energies=	-707.08861

Low frequencies --- -398.1446 -11.3161 -10.6296 -0.0011 -0.0004 0.0006

E(RB+HF-LYP) = -707.270861077

23) B3LYP/6-31+g(d,p) CPCM, dichloromethane optimized to TS

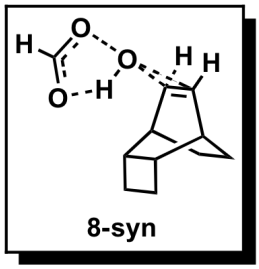

Center Number	Atomic Number	Atomic Type	Coordinates (Angstroms) X	Y	Z
1	6	0	-0.333021	1.141203	0.782659
2	6	0	-0.815622	-0.234523	1.310395
3	6	0	-2.253598	-0.545833	0.779824
4	6	0	-0.330702	1.144140	-0.772856
5	6	0	-2.249909	-0.544618	-0.784494
6	6	0	-0.809908	-0.230171	-1.307338
7	6	0	0.011526	-1.338909	0.691505
8	6	0	0.015005	-1.336411	-0.688531
9	1	0	-0.983124	1.928146	1.174382
10	1	0	0.666894	1.350953	1.172295
11	1	0	-0.779764	-0.262959	2.403348
12	1	0	0.670133	1.356778	-1.158424
13	1	0	-0.980896	1.931600	-1.163423
14	1	0	-0.769122	-0.254830	-2.400212
15	1	0	0.388182	-2.166872	-1.275655
16	1	0	0.383898	-2.170592	1.277430
17	1	0	-4.296210	0.236010	1.221366
18	6	0	-3.353130	0.563198	0.774817

19	1	0	-3.074704	1.511062	1.242147
20	6	0	-3.350899	0.562853	-0.783033
21	1	0	-3.073185	1.510849	-1.250571
22	1	0	-4.292230	0.233353	-1.231571
23	1	0	-2.601111	-1.484229	1.223987
24	1	0	-2.593567	-1.482809	-1.232108
25	8	0	1.988651	-0.950666	0.000692
26	8	0	3.833101	-0.696441	-0.004219
27	6	0	3.987885	0.582742	-0.002638
28	8	0	3.083563	1.428867	0.002933
29	1	0	1.934411	0.042538	0.006670
30	1	0	5.052099	0.884897	-0.006775

Zero-point correction=	0.253883 (Hartree/Particle)
Thermal correction to Energy=	0.266557
Thermal correction to Enthalpy=	0.267501
Thermal correction to Gibbs Free Energy=	0.213476
Sum of electronic and zero-point Energies=	-654.098775
Sum of electronic and thermal Energies=	-654.086101
Sum of electronic and thermal Enthalpies=	-654.085157
Sum of electronic and thermal Free Energies=	-654.139182

Low frequencies --- -373.8829 -10.1377 -9.2594 0.0004 0.0008 0.0010

E(RB+HF-LYP) = -654.3526581

24) B3LYP/6-31+g(d,p) CPCM, dichloromethane optimized to TS

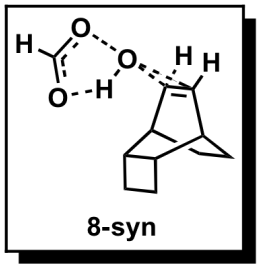

Center Number	Atomic Number	Atomic Type	Coordinates (Angstroms) X	Y	Z
1	6	0	-2.555379	-0.924347	-0.769560
2	6	0	-1.128526	-0.572839	-1.304049
3	6	0	-0.686635	0.822876	-0.790906
4	6	0	-2.557300	-0.905919	0.786331
5	6	0	-0.687491	0.839587	0.774116
6	6	0	-1.130959	-0.545003	1.316150
7	6	0	-0.226952	-1.590475	0.705413
8	6	0	-1.686877	2.019018	-0.801205
9	6	0	-1.688078	2.035527	0.757722
10	1	0	-2.842668	-1.911143	-1.147646
11	1	0	-3.282549	-0.214143	-1.174724
12	1	0	-1.104091	-0.624054	-2.398151
13	1	0	0.273865	1.078637	-1.250288
14	1	0	-2.847966	-1.882703	1.187024
15	1	0	-3.283014	-0.183806	1.172710
16	1	0	0.272403	1.104831	1.229366
17	1	0	-1.108796	-0.572631	2.411139
18	1	0	0.232549	-2.401741	-1.250077
19	1	0	0.235902	-2.370734	1.304097

20	1	0	-1.269864	2.922192	-1.256779
21	1	0	-2.657370	1.826981	-1.267420
22	1	0	-1.272231	2.948297	1.194857
23	1	0	-2.659147	1.852137	1.226220
24	8	0	1.858219	-1.045950	-0.011327
25	6	0	-0.225064	-1.605113	-0.669320
26	8	0	3.630171	-0.737135	-0.032194
27	1	0	1.682082	-0.074467	0.014349
28	6	0	3.812842	0.547683	0.001995
29	8	0	2.924591	1.403513	0.040016
30	1	0	4.889552	0.812950	-0.006766

Zero-point correction=	0.252242 (Hartree/Particle)
Thermal correction to Energy=	0.265132
Thermal correction to Enthalpy=	0.266077
Thermal correction to Gibbs Free Energy=	0.211816
Sum of electronic and zero-point Energies=	-654.115533
Sum of electronic and thermal Energies=	-654.102642
Sum of electronic and thermal Enthalpies=	-654.101698
Sum of electronic and thermal Free Energies=	-654.155959

Low frequencies --- -395.2407 -14.5803 -2.6205 -2.0229 9.8960 9.9322

E(RB+HF-LYP) = -654.3677744

25) B3LYP/6-31+g(d,p) CPCM, dichloromethane optimized to TS

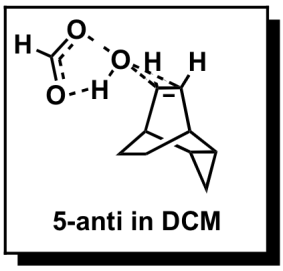

C	-0.61849	1.25398	0.70952
C	-1.1893	-0.06106	1.30611
C	-2.62724	-0.30974	0.77717
C	-0.62018	1.16833	-0.84582
C	-2.62975	-0.3925	-0.7338
C	-1.19412	-0.20416	-1.29184
C	-0.39836	-1.23301	0.75392
C	-0.4001	-1.3083	-0.61687
C	-3.38381	0.72073	-0.03586
H	-1.22093	2.09799	1.06045
H	0.39187	1.41697	1.09757
H	-1.16494	-0.03155	2.39999
H	-3.21194	-1.03142	1.34589
H	0.38979	1.28474	-1.25069
H	-1.2219	1.96983	-1.2862
H	-3.21658	-1.17179	-1.21812
H	-1.17369	-0.29545	-2.38237
H	-4.46825	0.6365	-0.02948
H	-3.0286	1.74371	-0.09265
O	3.53685	-0.83254	-0.0258
O	3.04323	1.36717	0.02158
H	-0.01856	-2.16256	-1.16925
H	-0.00737	-2.01844	1.39500
H	1.67379	0.02052	0.03059
C	3.84447	0.42926	-0.01217

O	1.74955	-0.96314	0.01329
H	4.9416	0.58784	-0.03545

Zero-point correction=	0.222872 (Hartree/Particle)
Thermal correction to Energy=	0.234723
Thermal correction to Enthalpy=	0.235667
Thermal correction to Gibbs Free Energy=	0.183353
Sum of electronic and zero-point Energies=	-614.820667
Sum of electronic and thermal Energies=	-614.808817
Sum of electronic and thermal Enthalpies=	-614.807873
Sum of electronic and thermal Free Energies=	-614.860187

Low frequencies --- -394.0612 -21.8318 -13.3400 -3.8784 -1.8088 1.6118

E(RB+HF-LYP) = -615.04353961

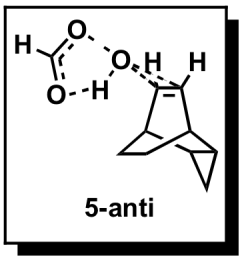

26) B3LYP/6-31+g(d,p) optimized to TS

C	0.57188	1.21416	-0.78276
C	1.13680	-0.13575	-1.29952
C	2.57369	-0.35912	-0.75536
C	0.57179	1.21909	0.77486
C	2.57353	-0.35432	0.75792
C	1.13647	-0.12744	1.30033
C	0.34687	-1.27851	-0.68515
C	0.34680	-1.27412	0.69307
C	3.33397	0.71189	-0.00203
H	1.18029	2.03077	-1.18334
H	-0.43887	1.36183	-1.17177
H	1.11495	-0.16891	-2.39157
H	3.15666	-1.1128	-1.27912
H	-0.43896	1.36944	1.16286
H	1.18033	2.03813	1.17028
H	3.15633	-1.10477	1.28655
H	1.11438	-0.15358	2.39256
H	4.41739	0.62551	-0.00164
H	2.98251	1.73675	-0.00533
O	-3.50729	-0.8132	-0.00162
O	-2.86078	1.34576	0.00112
H	-0.00718	-2.10607	1.28913
H	-0.00637	-2.11447	-1.27598
H	-1.64770	0.01633	0.00125
C	-3.72348	0.45707	-0.00042
O	-1.65353	-0.97802	0.00070
H	-4.80092	0.70778	-0.00108

Zero-point correction=	0.224958 (Hartree/Particle)
Thermal correction to Energy=	0.236452
Thermal correction to Enthalpy=	0.237397
Thermal correction to Gibbs Free Energy=	0.186319
Sum of electronic and zero-point Energies=	-614.802450
Sum of electronic and thermal Energies=	-614.790956

Sum of electronic and thermal Enthalpies= -614.790011
Sum of electronic and thermal Free Energies= -614.841089

Low frequencies --- -371.2204 -14.3565 -8.6457 -0.0006 -0.0005 0.0001

E(RB+HF-LYP) = -615.027407988

27) B3LYP/6-31+g(d,p) CPCM, dichloromethane optimized to TS

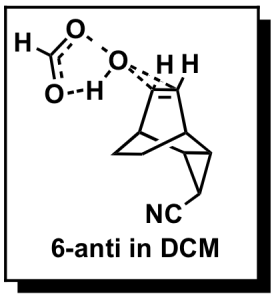

6-anti in DCM

Center Number	Atomic Number	Atomic Type	Coordinates (Angstroms) X	Y	Z
1	6	0	0.386544	0.856209	-0.784693
2	6	0	0.702783	-0.574664	-1.296114
3	6	0	2.055912	-1.090199	-0.744684
4	6	0	0.386745	0.867598	0.771774
5	6	0	2.056366	-1.079157	0.759465
6	6	0	0.703537	-0.555677	1.304161
7	6	0	-0.293748	-1.543407	-0.675696
8	6	0	-0.293025	-1.533443	0.698815
9	6	0	3.105497	-0.258855	0.000993
10	1	0	1.119535	1.558467	-1.188272
11	1	0	-0.582488	1.167849	-1.185249
12	1	0	0.683925	-0.611596	-2.389165
13	1	0	2.468942	-1.947835	-1.274135
14	1	0	-0.582307	1.184838	1.167879
15	1	0	1.119478	1.575751	1.165189
16	1	0	2.469682	-1.928907	1.301259
17	1	0	0.685389	-0.576276	2.397647
18	1	0	4.084116	-0.746190	0.004294
19	1	0	-0.821593	-2.263323	1.305510
20	1	0	-0.819095	-2.284686	-1.271140
21	6	0	3.295188	1.166538	-0.009082
22	7	0	3.559568	2.300740	-0.016725
23	8	0	-2.292469	-0.828205	-0.008762
24	8	0	-4.046086	-0.353541	-0.024704
25	1	0	-5.133142	1.325054	-0.010078
26	6	0	-4.092681	0.941908	-0.001486
27	8	0	-3.115538	1.697883	0.026306
28	1	0	-2.055373	0.131475	0.009916

Zero-point correction= 0.221661 (Hartree/Particle)
Thermal correction to Energy= 0.235169
Thermal correction to Enthalpy= 0.236113
Thermal correction to Gibbs Free Energy= 0.180390
Sum of electronic and zero-point Energies= -707.064394
Sum of electronic and thermal Energies= -707.050886
Sum of electronic and thermal Enthalpies= -707.049942
Sum of electronic and thermal Free Energies= -707.105665

Low frequencies --- -403.8665 -10.6463 -7.6507 -7.2730 -1.6104 5.5189

E(RB+HF-LYP) = -707.2860556

28) B3LYP/6-31++g(d,p) optimized to TS

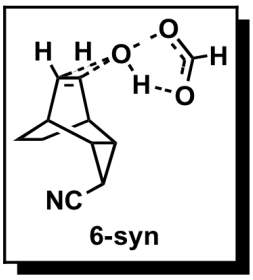

6-syn

Center Number	Atomic Number	Atomic Type	Coordinates (Angstroms) X	Y	Z
1	6	0	0.000000	0.000000	0.000000
2	6	0	0.000000	0.000000	1.561907
3	6	0	1.427452	0.000000	2.136317
4	6	0	0.806417	1.225912	-0.520909
5	6	0	2.208434	1.187078	1.631906
6	6	0	1.347810	2.048654	0.691395
7	6	0	-0.622472	1.340297	1.923085
8	6	0	0.091461	2.425449	1.462034
9	1	0	0.419521	-0.937906	-0.369882
10	1	0	-1.036579	0.039411	-0.348714
11	1	0	-0.580469	-0.839624	1.950074
12	1	0	0.172867	1.878192	-1.129844
13	1	0	1.637453	0.913795	-1.156866
14	1	0	1.898066	2.927673	0.349150
15	1	0	-1.634530	1.413941	2.301795
16	1	0	-0.306520	3.432606	1.443638
17	8	0	0.135344	2.421567	3.575675
18	8	0	0.447962	2.965105	5.330669
19	6	0	1.546180	2.381627	5.664777
20	1	0	1.860262	2.615789	6.698864
21	8	0	2.220422	1.628960	4.946616
22	1	0	0.981078	1.906017	3.677554
23	1	0	3.544087	-0.492606	2.000667
24	6	0	2.716023	-0.225847	1.346214
25	1	0	1.500119	-0.266697	3.187002
26	1	0	2.823616	1.745219	2.332168
27	6	0	2.880265	-0.875990	0.070432
28	7	0	3.090421	-1.437854	-0.926446

Zero-point correction=	0.223816 (Hartree/Particle)
Thermal correction to Energy=	0.237048
Thermal correction to Enthalpy=	0.237992
Thermal correction to Gibbs Free Energy=	0.183138
Sum of electronic and zero-point Energies=	-707.042763
Sum of electronic and thermal Energies=	-707.029531
Sum of electronic and thermal Enthalpies=	-707.028587
Sum of electronic and thermal Free Energies=	-707.083442

Low frequencies --- -384.9375 -6.8924 -4.5993 0.0008 0.0010 0.0011

E(RB+HF-LYP) = -707.266579618

29) B3LYP/6-31+g(d,p) CPCM, dichloromethane optimized to TS

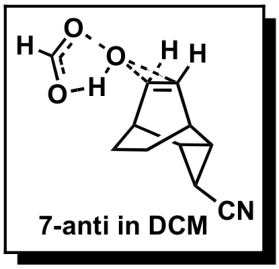

Center Number	Atomic Number	Atomic Type	Coordinates (Angstroms) X	Y	Z
1	6	0	0.067730	1.049641	-0.901173
2	6	0	0.563777	-0.376624	-1.263027
3	6	0	1.979760	-0.622420	-0.682058
4	6	0	0.071740	1.230514	0.646270
5	6	0	1.984193	-0.448135	0.806770
6	6	0	0.571387	-0.075093	1.325185
7	6	0	-0.285927	-1.396481	-0.521723
8	6	0	-0.279353	-1.237762	0.843947
9	1	0	0.709916	1.789599	-1.389752
10	1	0	-0.933991	1.192751	-1.315581
11	1	0	0.545248	-0.534770	-2.345191
12	1	0	-0.927331	1.468076	1.022550
13	1	0	0.716318	2.062134	0.949174
14	1	0	0.559385	0.021133	2.414663
15	1	0	-0.690101	-2.272037	-1.021568
16	1	0	-0.708991	-1.959592	1.533131
17	8	0	-2.359902	-0.910540	0.012634
18	8	0	-4.161012	-0.701522	-0.092395
19	6	0	-4.399957	0.571489	-0.042917
20	1	0	-5.483831	0.798502	-0.097698
21	8	0	-3.547596	1.461465	0.053510
22	1	0	-2.269999	0.072799	0.067986
23	6	0	2.793579	0.519125	-0.063561
24	1	0	2.547425	-1.438494	-1.126404
25	1	0	2.554910	-1.139858	1.424383
26	6	0	4.226444	0.389651	-0.052072
27	7	0	5.385878	0.281737	-0.042265
28	1	0	2.467742	1.548944	-0.183675

Zero-point correction= 0.221521 (Hartree/Particle)
Thermal correction to Energy= 0.235123
Thermal correction to Enthalpy= 0.236067
Thermal correction to Gibbs Free Energy= 0.179688
Sum of electronic and zero-point Energies= -707.073098
Sum of electronic and thermal Energies= -707.059496
Sum of electronic and thermal Enthalpies= -707.058552
Sum of electronic and thermal Free Energies= -707.114930

Low frequencies --- -403.8751 -23.1414 -10.9355 -4.4661 -1.7386 -0.4986

E(RB+HF-LYP) = -707.2946187

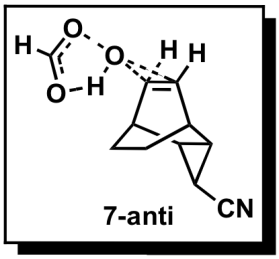

30) B3LYP/6-31++g(d,p) optimized to TS

Center Number	Atomic Number	Atomic Type	Coordinates (Angstroms) X	Y	Z
1	6	0	-0.019355	1.149849	0.772784
2	6	0	-0.516921	-0.221149	1.304620
3	6	0	-1.934620	-0.532649	0.754941
4	6	0	-0.018012	1.138495	-0.785126
5	6	0	-1.932943	-0.543854	-0.747041
6	6	0	-0.514065	-0.240190	-1.297903
7	6	0	0.327365	-1.333028	0.702473
8	6	0	0.329416	-1.343107	-0.677594
9	1	0	-0.662723	1.941921	1.168393
10	1	0	0.982850	1.347837	1.159873
11	1	0	-0.501546	-0.242533	2.396257
12	1	0	0.984790	1.331217	-1.173261
13	1	0	-0.660897	1.924528	-1.193329
14	1	0	-0.496074	-0.277643	-2.389070
15	1	0	0.713022	-2.146548	1.303803
16	1	0	0.711525	-2.167711	-1.265914
17	8	0	2.274422	-0.936629	0.000317
18	8	0	4.131424	-0.662068	-0.009948
19	6	0	4.258560	0.618148	-0.004483
20	1	0	5.313186	0.950120	-0.008953
21	8	0	3.330618	1.441587	0.004889
22	1	0	2.233704	0.060301	0.005305
23	6	0	-2.746917	0.517355	-0.004840
24	1	0	-2.504745	-1.285636	1.291392
25	1	0	-2.501787	-1.304872	-1.273434
26	6	0	-4.183637	0.392615	-0.005512
27	7	0	-5.341377	0.280747	-0.006418
28	1	0	-2.406606	1.545772	-0.012111

Zero-point correction=	0.223672 (Hartree/Particle)
Thermal correction to Energy=	0.236943
Thermal correction to Enthalpy=	0.237888
Thermal correction to Gibbs Free Energy=	0.182579
Sum of electronic and zero-point Energies=	-707.046071
Sum of electronic and thermal Energies=	-707.032800
Sum of electronic and thermal Enthalpies=	-707.031856
Sum of electronic and thermal Free Energies=	-707.087164

Low frequencies --- -389.4204 -0.0009 -0.0004 0.0006 3.5232 9.2956

E(RB+HF-LYP) = -707.2697431

31) B3LYP/6-31+g(d,p) CPCM, dichloromethane optimized to TS

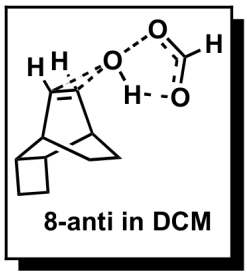

Center Number	Atomic Number	Atomic Type	Coordinates (Angstroms) X	Y	Z
1	6	0	-0.378077	1.157491	0.748762
2	6	0	-0.861687	-0.204415	1.312947
3	6	0	-2.302483	-0.524160	0.795867
4	6	0	-0.381788	1.121704	-0.806403
5	6	0	-2.306639	-0.560018	-0.767245
6	6	0	-0.868640	-0.263824	-1.305797
7	6	0	-0.033812	-1.317250	0.713493
8	6	0	-0.037363	-1.348448	-0.660707
9	1	0	-1.023911	1.956956	1.122960
10	1	0	0.622923	1.371683	1.137288
11	1	0	-0.821032	-0.206621	2.407746
12	1	0	0.617886	1.316577	-1.208326
13	1	0	-1.028073	1.904794	-1.213002
14	1	0	-0.833487	-0.315749	-2.399551
15	1	0	0.364239	-2.180753	-1.232888
16	1	0	0.371535	-2.122568	1.320594
17	1	0	-4.339595	0.274022	1.227892
18	6	0	-3.396911	0.589623	0.770713
19	1	0	-3.112299	1.547753	1.214972
20	6	0	-3.401684	0.553310	-0.787275
21	1	0	-3.121115	1.489971	-1.277199
22	1	0	-4.346793	0.216314	-1.223668
23	1	0	-2.648945	-1.451588	1.265931
24	1	0	-2.655533	-1.508050	-1.192373
25	8	0	2.090071	-0.931440	0.008948
26	8	0	3.870138	-0.723379	-0.002328
27	6	0	4.119100	0.551305	-0.007221
28	8	0	3.273809	1.450412	-0.004012
29	1	0	1.974328	0.049185	0.001985
30	1	0	5.207627	0.761428	-0.016033

Zero-point correction= 0.251838 (Hartree/Particle)
Thermal correction to Energy= 0.264872
Thermal correction to Enthalpy= 0.265816
Thermal correction to Gibbs Free Energy= 0.210553
Sum of electronic and zero-point Energies= -654.115972
Sum of electronic and thermal Energies= -654.102939
Sum of electronic and thermal Enthalpies= -654.101994
Sum of electronic and thermal Free Energies= -654.157257

Low frequencies --- -396.4210 -18.0732 -12.9670 -2.3773 -1.5993 2.5737

E(RB+HF-LYP) = -654.3678103

32) B3LYP/6-31++g(d,p) optimized to TS

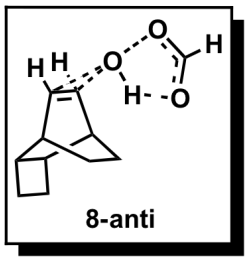

Center Number	Atomic Number	Atomic Type	Coordinates (Angstroms) X	Y	Z
1	6	0	-0.333021	1.141203	0.782659
2	6	0	-0.815622	-0.234523	1.310395
3	6	0	-2.253598	-0.545833	0.779824
4	6	0	-0.330702	1.144140	-0.772856
5	6	0	-2.249909	-0.544618	-0.784494
6	6	0	-0.809908	-0.230171	-1.307338
7	6	0	0.011526	-1.338909	0.691505
8	6	0	0.015005	-1.336411	-0.688531
9	1	0	-0.983124	1.928146	1.174382
10	1	0	0.666894	1.350953	1.172295
11	1	0	-0.779764	-0.262959	2.403348
12	1	0	0.670133	1.356778	-1.158424
13	1	0	-0.980896	1.931600	-1.163423
14	1	0	-0.769122	-0.254830	-2.400212
15	1	0	0.388182	-2.166872	-1.275655
16	1	0	0.383898	-2.170592	1.277430
17	1	0	-4.296210	0.236010	1.221366
18	6	0	-3.353130	0.563198	0.774817
19	1	0	-3.074704	1.511062	1.242147
20	6	0	-3.350899	0.562853	-0.783033
21	1	0	-3.073185	1.510849	-1.250571
22	1	0	-4.292230	0.233353	-1.231571
23	1	0	-2.601111	-1.484229	1.223987
24	1	0	-2.593567	-1.482809	-1.232108
25	8	0	1.988651	-0.950666	0.000692
26	8	0	3.833101	-0.696441	-0.004219
27	6	0	3.987885	0.582742	-0.002638
28	8	0	3.083563	1.428867	0.002933
29	1	0	1.934411	0.042538	0.006670
30	1	0	5.052099	0.884897	-0.006775

Zero-point correction=	0.253883 (Hartree/Particle)
Thermal correction to Energy=	0.266557
Thermal correction to Enthalpy=	0.267501
Thermal correction to Gibbs Free Energy=	0.213476
Sum of electronic and zero-point Energies=	-654.098775
Sum of electronic and thermal Energies=	-654.086101
Sum of electronic and thermal Enthalpies=	-654.085157
Sum of electronic and thermal Free Energies=	-654.139182

Low frequencies --- -373.8829 -10.1377 -9.2594 0.0004 0.0008 0.0010

E(RB+HF-LYP) = -654.3526581

V. Distortional Cartesian Coordinates, Energies and Olefin Bending Frequencies:

The [2.2.2]-bicyclooctene system was first optimized utilizing B3LYP/6-31g(2d,2p). The anharmonic example was optimized utilizing the B3LYP/6-31+g(d). A frequency calculation was performed with the anharmonic[1] option and harmonic option. The GaussView 4.1.2 package was used to display the anharmonic vibration corresponding with the olefin-bending mode at ~715.00 cm^{-1} and manual displacement of the frequency was used to isolate structures at the appropriate olefin bend. The structures' single point energy was then calculated using B3LYP/6-31g(2d,2p) and plotted below.

33) B3LYP/6-31g(2d,2p) optimized, freq=anharmonic B3LYP/6-31g(2d,2p)

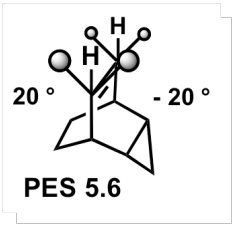

Input orientation:

Center Number	Atomic Number	Atomic Type	Coordinates (Angstroms) X	Y	Z
1	6	0	0.411455	1.391487	0.775187
2	6	0	0.281953	-0.069950	1.289631
3	6	0	-1.016167	-0.708831	0.753678
4	6	0	0.411454	1.389138	-0.779386
5	6	0	-1.016166	-0.711107	-0.751530
6	6	0	0.281952	-0.073848	-1.289414
7	6	0	1.433157	-0.848060	0.669594
8	6	0	1.433157	-0.850080	-0.667031
9	6	0	-2.066060	0.079282	-0.000121
10	1	0	-0.405673	2.000102	1.171856
11	1	0	1.339513	1.818458	1.161933
12	1	0	0.311233	-0.090079	2.380965
13	1	0	-1.343197	-1.600480	1.278269
14	1	0	1.339512	1.814941	-1.167419
15	1	0	-0.405674	1.996553	-1.177891
16	1	0	-1.343194	-1.604340	-1.273422
17	1	0	0.311231	-0.097275	-2.380683
18	1	0	-3.071369	-0.328165	0.000494
19	1	0	-2.041763	1.160725	-0.001758
20	1	0	2.190487	-1.327386	1.279521
21	1	0	2.190487	-1.331248	-1.275506

Zero-point correction= 0.188033 (Hartree/Particle)
Thermal correction to Energy= 0.194485
Thermal correction to Enthalpy= 0.195430
Thermal correction to Gibbs Free Energy= 0.157901
Sum of electronic and zero-point Energies= -349.954673
Sum of electronic and thermal Energies= -349.948220

Sum of electronic and thermal Enthalpies= -349.947276
Sum of electronic and thermal Free Energies= -349.984805

Frequencies -- 712.8523
Red. masses -- 1.6014
Frc consts -- 0.4794
IR Inten -- 24.4017

34) B3LYP/6-31g(2d,2p) optimized, freq=harmonic

Center Number	Atomic Number	Atomic Type	Coordinates (Angstroms) X	Y	Z
1	6	0	0.411455	1.391487	0.775187
2	6	0	0.281953	-0.069950	1.289631
3	6	0	-1.016167	-0.708831	0.753678
4	6	0	0.411454	1.389138	-0.779386
5	6	0	-1.016166	-0.711107	-0.751530
6	6	0	0.281952	-0.073848	-1.289414
7	6	0	1.433157	-0.848060	0.669594
8	6	0	1.433157	-0.850080	-0.667031
9	6	0	-2.066060	0.079282	-0.000121
10	1	0	-0.405673	2.000102	1.171856
11	1	0	1.339513	1.818458	1.161933
12	1	0	0.311233	-0.090079	2.380965
13	1	0	-1.343197	-1.600480	1.278269
14	1	0	1.339512	1.814941	-1.167419
15	1	0	-0.405674	1.996553	-1.177891
16	1	0	-1.343194	-1.604340	-1.273422
17	1	0	0.311231	-0.097275	-2.380683
18	1	0	-3.071369	-0.328165	0.000494
19	1	0	-2.041763	1.160725	-0.001758
20	1	0	2.190487	-1.327386	1.279521
21	1	0	2.190487	-1.331248	-1.275506

Zero-point correction= 0.188033 (Hartree/Particle)
Thermal correction to Energy= 0.194486
Thermal correction to Enthalpy= 0.195430
Thermal correction to Gibbs Free Energy= 0.157901
Sum of electronic and zero-point Energies= -349.954672
Sum of electronic and thermal Energies= -349.948219
Sum of electronic and thermal Enthalpies= -349.947275
Sum of electronic and thermal Free Energies= -349.984804

Frequencies -- 712.8409
Red. masses -- 1.6014
Frc consts -- 0.4795
IR Inten -- 24.4065

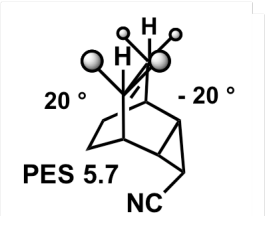

35) B3LYP/6-31g(2d,2p) optimized, freq=anharmonic B3LYP/6-31g(2d,2p)

Center Number	Atomic Number	Atomic Type	Coordinates (Angstroms) X	Y	Z
1	6	0	0.191867	1.373516	0.776808
2	6	0	0.787150	0.032275	1.288893
3	6	0	0.003857	-1.180693	0.749121
4	6	0	0.192566	1.373788	-0.776715
5	6	0	0.003818	-1.180820	-0.748997
6	6	0	0.787067	0.032173	-1.288813
7	6	0	2.174494	-0.080345	0.668206
8	6	0	2.174470	-0.080490	-0.668236
9	1	0	-0.814722	1.520612	1.169598
10	1	0	0.807015	2.188249	1.164552
11	1	0	0.817952	0.019053	2.379321
12	1	0	0.183970	-2.110081	1.278706
13	1	0	0.809300	2.187785	-1.163493
14	1	0	-0.813427	1.522463	-1.170470
15	1	0	0.184187	-2.110171	-1.278563
16	1	0	0.817758	0.018944	-2.379246
17	1	0	3.068458	-0.117621	1.279508
18	1	0	3.068410	-0.117834	-1.279571
19	6	0	-1.331219	-1.138352	0.000024
20	1	0	-1.826809	-2.105699	0.000162
21	6	0	-2.320158	-0.093654	-0.000368
22	7	0	-3.183651	0.679986	-0.000004

Thermal correction to Energy= 0.195112
Thermal correction to Enthalpy= 0.196056
Thermal correction to Gibbs Free Energy= 0.154244
Sum of electronic and zero-point Energies= -442.191975
Sum of electronic and thermal Energies= -442.183791
Sum of electronic and thermal Enthalpies= -442.182846
Sum of electronic and thermal Free Energies= -442.224658

Frequencies -- 714.5649
Red. masses -- 1.9495
Frc consts -- 0.5865
IR Inten -- 19.7740

36) B3LYP/6-31g(2d,2p) optimized, freq=harmonic

Center Number	Atomic Number	Atomic Type	Coordinates (Angstroms) X	Y	Z
1	6	0	0.191867	1.373516	0.776808

2	6	0	0.787150	0.032275	1.288893
3	6	0	0.003857	-1.180693	0.749121
4	6	0	0.192566	1.373788	-0.776715
5	6	0	0.003818	-1.180820	-0.748997
6	6	0	0.787067	0.032173	-1.288813
7	6	0	2.174494	-0.080345	0.668206
8	6	0	2.174470	-0.080490	-0.668236
9	1	0	-0.814722	1.520612	1.169598
10	1	0	0.807015	2.188249	1.164552
11	1	0	0.817952	0.019053	2.379321
12	1	0	0.183970	-2.110081	1.278706
13	1	0	0.809300	2.187785	-1.163493
14	1	0	-0.813427	1.522463	-1.170470
15	1	0	0.184187	-2.110171	-1.278563
16	1	0	0.817758	0.018944	-2.379246
17	1	0	3.068458	-0.117621	1.279508
18	1	0	3.068410	-0.117834	-1.279571
19	6	0	-1.331219	-1.138352	0.000024
20	1	0	-1.826809	-2.105699	0.000162
21	6	0	-2.320158	-0.093654	-0.000368
22	7	0	-3.183651	0.679986	-0.000004

Zero-point correction= 0.186928 (Hartree/Particle)
Thermal correction to Energy= 0.195112
Thermal correction to Enthalpy= 0.196056
Thermal correction to Gibbs Free Energy= 0.154244
Sum of electronic and zero-point Energies= -442.191974
Sum of electronic and thermal Energies= -442.183791
Sum of electronic and thermal Enthalpies= -442.182846
Sum of electronic and thermal Free Energies= -442.224658

Frequencies -- 714.5653
Red. masses -- 1.9493
Frc consts -- 0.5864
IR Inten -- 19.7776

37) B3LYP/6-31g(2d,2p) optimized, freq=anharmonic B3LYP/6-31g(2d,2p)

Center Number	Atomic Number	Atomic Type	Coordinates (Angstroms) X	Y	Z
1	6	0	1.225070	1.339411	0.775039
2	6	0	0.903696	-0.091999	1.291865
3	6	0	-0.458579	-0.566983	0.748119
4	6	0	1.224954	1.336203	-0.780650
5	6	0	-0.458819	-0.570028	-0.745464
6	6	0	0.903322	-0.097272	-1.291537
7	6	0	1.941663	-1.015343	0.670129
8	6	0	1.941421	-1.018135	-0.666353
9	6	0	-1.399907	0.379385	-0.000444
10	1	0	0.499711	2.053946	1.173868
11	1	0	2.201659	1.636860	1.161687
12	1	0	0.922692	-0.117949	2.382188

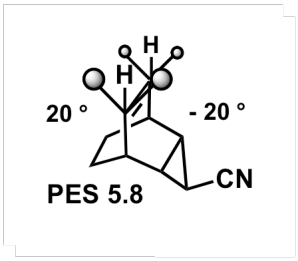

13	1	0	-0.928946	-1.386356	1.278644
14	1	0	2.201505	1.631962	-1.168696
15	1	0	0.499619	2.049158	-1.182328
16	1	0	-0.929359	-1.391554	-1.272493
17	1	0	0.922003	-0.127680	-2.381751
18	1	0	-1.188732	1.439721	-0.002572
19	1	0	2.628631	-1.588363	1.281475
20	1	0	2.628176	-1.593696	-1.275548
21	6	0	-2.805989	0.076487	0.000297
22	7	0	-3.936850	-0.176629	-0.000067

Zero-point correction= 0.186708 (Hartree/Particle)
Thermal correction to Energy= 0.194959
Thermal correction to Enthalpy= 0.195904
Thermal correction to Gibbs Free Energy= 0.153830
Sum of electronic and zero-point Energies= -442.198978
Sum of electronic and thermal Energies= -442.190727
Sum of electronic and thermal Enthalpies= -442.189782
Sum of electronic and thermal Free Energies= -442.231855

Frequencies -- 718.5727
Red. masses -- 1.5002
Frc consts -- 0.4564
IR Inten -- 28.2482

38) B3LYP/6-31g(2d,2p) optimized, freq=harmonic

Center Number	Atomic Number	Atomic Type	Coordinates (Angstroms) X	Y	Z
1	6	0	1.225070	1.339411	0.775039
2	6	0	0.903696	-0.091999	1.291865
3	6	0	-0.458579	-0.566983	0.748119
4	6	0	1.224954	1.336203	-0.780650
5	6	0	-0.458819	-0.570028	-0.745464
6	6	0	0.903322	-0.097272	-1.291537
7	6	0	1.941663	-1.015343	0.670129
8	6	0	1.941421	-1.018135	-0.666353
9	6	0	-1.399907	0.379385	-0.000444
10	1	0	0.499711	2.053946	1.173868
11	1	0	2.201659	1.636860	1.161687
12	1	0	0.922692	-0.117949	2.382188
13	1	0	-0.928946	-1.386356	1.278644
14	1	0	2.201505	1.631962	-1.168696
15	1	0	0.499619	2.049158	-1.182328
16	1	0	-0.929359	-1.391554	-1.272493
17	1	0	0.922003	-0.127680	-2.381751
18	1	0	-1.188732	1.439721	-0.002572
19	1	0	2.628631	-1.588363	1.281475
20	1	0	2.628176	-1.593696	-1.275548

21	6	0	-2.805989	0.076487	0.000297
22	7	0	-3.936850	-0.176629	-0.000067

Zero-point correction= 0.186707 (Hartree/Particle)
Thermal correction to Energy= 0.194958
Thermal correction to Enthalpy= 0.195902
Thermal correction to Gibbs Free Energy= 0.153829
Sum of electronic and zero-point Energies= -442.198979
Sum of electronic and thermal Energies= -442.190728
Sum of electronic and thermal Enthalpies= -442.189783
Sum of electronic and thermal Free Energies= -442.231857

Frequencies -- 718.5685
Red. masses -- 1.5002
Frc consts -- 0.4564
IR Inten -- 28.2485

39) B3LYP/6-31g(2d,2p) optimized, freq=anharmonic B3LYP/6-31g(2d,2p)

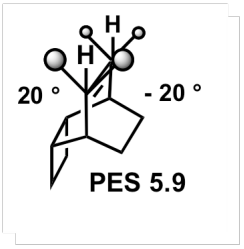

Center Number	Atomic Number	Atomic Type	Coordinates (Angstroms) X	Y	Z
1	6	0	-0.673198	0.776951	1.404060
2	6	0	-0.583038	1.298490	-0.056011
3	6	0	0.709940	0.780532	-0.740692
4	6	0	-0.672657	-0.775921	1.404659
5	6	0	0.710112	-0.780901	-0.740274
6	6	0	-0.582626	-1.298583	-0.055013
7	6	0	-1.727010	-0.669411	-0.824871
8	6	0	2.072529	0.778420	0.020106
9	6	0	2.072749	-0.778109	0.020394
10	1	0	-1.589356	1.162988	1.857533
11	1	0	0.154702	1.169207	1.999750
12	1	0	-0.626368	2.390524	-0.071620
13	1	0	0.779742	1.222679	-1.736879
14	1	0	-1.588324	-1.162281	1.858849
15	1	0	0.155809	-1.167088	2.000280
16	1	0	0.779709	-1.223719	-1.736183
17	1	0	-0.625645	-2.390642	-0.069703
18	1	0	-2.474323	1.271325	-1.329640
19	1	0	-2.473906	-1.272993	-1.328675
20	1	0	2.889311	1.225113	-0.550140
21	1	0	2.065521	1.243887	1.007089
22	1	0	2.889511	-1.224591	-0.550034
23	1	0	2.066202	-1.243445	1.007458
24	6	0	-1.727232	0.668372	-0.825372

Zero-point correction= 0.217018 (Hartree/Particle)
Thermal correction to Energy= 0.224645

Thermal correction to Enthalpy= 0.225589
Thermal correction to Gibbs Free Energy= 0.184761
Sum of electronic and zero-point Energies= -389.251390
Sum of electronic and thermal Energies= -389.243763
Sum of electronic and thermal Enthalpies= -389.242819
Sum of electronic and thermal Free Energies= -389.283647

Frequencies -- 706.9095
Red. masses -- 1.6485
Frc consts -- 0.4854
IR Inten -- 13.8108

40) B3LYP/6-31g(2d,2p) optimized, freq=harmonic

Center Number	Atomic Number	Atomic Type	Coordinates (Angstroms) X	Y	Z
1	6	0	-0.673198	0.776951	1.404060
2	6	0	-0.583038	1.298490	-0.056011
3	6	0	0.709940	0.780532	-0.740692
4	6	0	-0.672657	-0.775921	1.404659
5	6	0	0.710112	-0.780901	-0.740274
6	6	0	-0.582626	-1.298583	-0.055013
7	6	0	-1.727010	-0.669411	-0.824871
8	6	0	2.072529	0.778420	0.020106
9	6	0	2.072749	-0.778109	0.020394
10	1	0	-1.589356	1.162988	1.857533
11	1	0	0.154702	1.169207	1.999750
12	1	0	-0.626368	2.390524	-0.071620
13	1	0	0.779742	1.222679	-1.736879
14	1	0	-1.588324	-1.162281	1.858849
15	1	0	0.155809	-1.167088	2.000280
16	1	0	0.779709	-1.223719	-1.736183
17	1	0	-0.625645	-2.390642	-0.069703
18	1	0	-2.474323	1.271325	-1.329640
19	1	0	-2.473906	-1.272993	-1.328675
20	1	0	2.889311	1.225113	-0.550140
21	1	0	2.065521	1.243887	1.007089
22	1	0	2.889511	-1.224591	-0.550034
23	1	0	2.066202	-1.243445	1.007458
24	6	0	-1.727232	0.668372	-0.825372

Zero-point correction= 0.217019 (Hartree/Particle)
Thermal correction to Energy= 0.224646
Thermal correction to Enthalpy= 0.225590
Thermal correction to Gibbs Free Energy= 0.184763
Sum of electronic and zero-point Energies= -389.251389
Sum of electronic and thermal Energies= -389.243762

Sum of electronic and thermal Enthalpies= -389.242818
Sum of electronic and thermal Free Energies= -389.283645

Frequencies -- 706.9044
Red. masses -- 1.6485
Frc consts -- 0.4854
IR Inten -- 13.8158

VI: Activation Energy Structure Cartesian Coordinates and Energies:

41) B3LYP/6-31+g(d,p) optimized

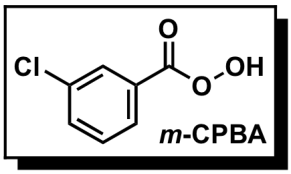

Center Number	Atomic Number	Atomic Type	Coordinates (Angstroms) X	Y	Z
1	6	0	-0.444045	-0.501734	0.000057
2	6	0	-1.793055	-0.155253	0.000004
3	6	0	-2.201545	1.179765	-0.000050
4	6	0	-1.232195	2.185993	-0.000054
5	6	0	0.123747	1.863288	-0.000009
6	6	0	0.518952	0.518622	0.000051
7	1	0	-0.151946	-1.544168	0.000093
8	1	0	-3.258229	1.423660	-0.000089
9	1	0	-1.541863	3.226413	-0.000098
10	1	0	0.886371	2.633883	-0.000020
11	6	0	1.989016	0.243726	0.000095
12	8	0	2.860145	1.076664	0.000062
13	8	0	2.216627	-1.108890	0.000019
14	8	0	3.644769	-1.359532	-0.000164
15	1	0	3.607623	-2.331341	0.000168
16	17	0	-3.004678	-1.428283	0.000003

E(RB+HF-LYP) = -955.56694005

42) B3LYP/6-31+g(d,p) optimized

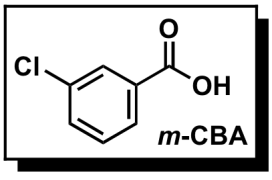

Center Number	Atomic Number	Atomic Type	Coordinates (Angstroms) X	Y	Z
1	6	0	-0.444045	-0.501734	0.000057
2	6	0	-1.793055	-0.155253	0.000004
3	6	0	-2.201545	1.179765	-0.000050

4	6	0	-1.232195	2.185993	-0.000054
5	6	0	0.123747	1.863288	-0.000009
6	6	0	0.518952	0.518622	0.000051
7	1	0	-0.151946	-1.544168	0.000093
8	1	0	-3.258229	1.423660	-0.000089
9	1	0	-1.541863	3.226413	-0.000098
10	1	0	0.886371	2.633883	-0.000020
11	6	0	1.989016	0.243726	0.000095
12	8	0	2.860145	1.076664	0.000062
13	8	0	2.216627	-1.108890	0.000019
14	8	0	3.644769	-1.359532	-0.000164
15	1	0	3.607623	-2.331341	0.000168
16	17	0	-3.004678	-1.428283	0.000003

E(RB+HF-LYP) = -955.566940047

43) B3LYP/6-31+g(d,p) optimized

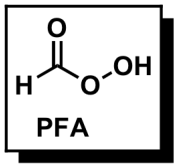

Center Number	Atomic Number	Atomic Type	Coordinates (Angstroms) X	Y	Z
1	6	0	-0.681448	0.354662	0.000006
2	1	0	-0.346446	1.401901	0.000075
3	8	0	-1.811343	-0.048808	0.000073
4	8	0	0.357487	-0.528439	-0.000151
5	8	0	1.600883	0.243937	-0.000210
6	1	0	2.228842	-0.497632	0.000226

E(RB+HF-LYP) = -264.896239174

43) B3LYP/6-31++g(d,p) optimized

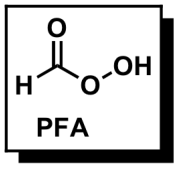

Center Number	Atomic Number	Atomic Type	Coordinates (Angstroms) X	Y	Z
1	6	0	-0.654093	0.333926	0.000067
2	1	0	-0.334079	1.385842	0.000136
3	8	0	-1.778112	-0.085637	0.000135
4	8	0	0.397346	-0.534249	-0.000089
5	8	0	1.629587	0.255802	-0.000149
6	1	0	2.268071	-0.476724	0.000287

E(RB+HF-LYP) = -264.896351795

43) B3LYP/6-31+g(d,p) optimized

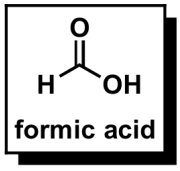

Center Number	Atomic Number	Atomic Type	Coordinates (Angstroms) X	Y	Z
1	8	0	-1.034517	-0.439605	0.000000

2	1	0	-0.669120	-1.342532	0.000000
3	8	0	1.165042	0.107715	0.000000
4	6	0	0.000000	0.423617	0.000000
5	1	0	-0.375077	1.455946	0.000000

E(RB+HF-LYP) = -189.775494996

43) B3LYP/6-31++g(d,p) optimized

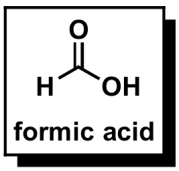

Center Number	Atomic Number	Atomic Type	Coordinates (Angstroms) X	Y	Z
1	8	0	-1.034503	-0.439635	0.000000
2	1	0	-0.669479	-1.342732	0.000000
3	8	0	1.165071	0.107809	0.000000
4	6	0	0.000000	0.423563	0.000000
5	1	0	-0.375065	1.455966	0.000000

E(RB+HF-LYP) = -189.7755956

43) B3LYP/6-31+g(d,p) optimized

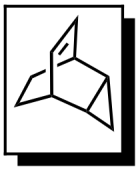

Center Number	Atomic Number	Atomic Type	Coordinates (Angstroms) X	Y	Z
1	6	0	0.415093	1.395126	0.776583
2	6	0	0.282180	-0.068183	1.292532
3	6	0	-1.017796	-0.709777	0.754518
4	6	0	0.415094	1.392779	-0.780759
5	6	0	-1.017781	-0.712086	-0.752338
6	6	0	0.282159	-0.072104	-1.292337
7	6	0	1.433772	-0.849287	0.672463
8	6	0	1.433763	-0.851326	-0.669945
9	6	0	-2.071924	0.075961	-0.000139
10	1	0	-0.402913	2.005819	1.174298
11	1	0	1.345249	1.821865	1.164646
12	1	0	0.309738	-0.088755	2.386304
13	1	0	-1.343827	-1.604222	1.280929
14	1	0	1.345253	1.818372	-1.170075
15	1	0	-0.402909	2.002280	-1.180309
16	1	0	-1.343760	-1.608163	-1.275993
17	1	0	0.309701	-0.095994	-2.386044
18	1	0	-3.078319	-0.335237	0.000479
19	1	0	-2.051934	1.159922	-0.001824
20	1	0	2.192754	-1.331632	1.282751
21	1	0	2.192737	-1.335521	-1.278774

E(RB+HF-LYP) = -350.147120156

43) B3LYP/6-31++g(d,p) optimized

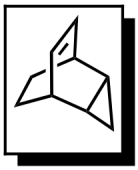

Center Number	Atomic Number	Atomic Type	Coordinates (Angstroms) X	Y	Z
1	6	0	-0.414579	1.588547	-0.148403
2	6	0	-0.282659	0.457974	-1.210503
3	6	0	1.018077	-0.344065	-0.976173
4	6	0	-0.414912	0.958216	1.275480
5	6	0	1.017864	-0.954161	0.401144
6	6	0	-0.282574	-0.588532	1.152807
7	6	0	-1.433132	-0.507632	-0.958495
8	6	0	-1.433054	-1.051177	0.268697
9	6	0	2.069806	0.073518	0.032899
10	1	0	0.404556	2.306615	-0.265564
11	1	0	-1.344202	2.136154	-0.331669
12	1	0	-0.309622	0.880354	-2.219565
13	1	0	1.346198	-0.948865	-1.818734
14	1	0	-1.344830	1.190979	1.803469
15	1	0	0.403890	1.354371	1.886214
16	1	0	1.345403	-1.984727	0.519232
17	1	0	-0.309488	-1.051762	2.143793
18	1	0	3.077583	-0.299227	-0.132013
19	1	0	2.045841	1.064572	0.472156
20	1	0	-2.192227	-0.704217	-1.710807
21	1	0	-2.192119	-1.740373	0.628772

E(RB+HF-LYP) = -350.1473815

44) B3LYP/6-31+g(d,p) optimized

Center Number	Atomic Number	Atomic Type	Coordinates (Angstroms) X	Y	Z
1	6	0	0.199803	1.378610	0.777950
2	6	0	0.789720	0.033142	1.291840
3	6	0	0.002446	-1.179783	0.749532
4	6	0	0.199643	1.378533	-0.777681
5	6	0	0.002663	-1.179854	-0.749400
6	6	0	0.789806	0.033165	-1.291592
7	6	0	2.177913	-0.086917	0.671114
8	6	0	2.177976	-0.086730	-0.670726
9	1	0	-0.807207	1.531160	1.173565
10	1	0	0.819586	2.192392	1.166064
11	1	0	0.818579	0.019241	2.384619

12	1	0	0.182007	-2.111314	1.281397
13	1	0	0.819304	2.192319	-1.165978
14	1	0	-0.807478	1.530957	-1.173108
15	1	0	0.182483	-2.111379	-1.281187
16	1	0	0.818737	0.019312	-2.384372
17	1	0	3.075686	-0.128963	1.281091
18	1	0	3.075811	-0.128666	-1.280620
19	6	0	-1.335127	-1.137088	-0.000178
20	1	0	-1.833536	-2.105583	-0.000244
21	6	0	-2.328622	-0.093612	-0.000544
22	7	0	-3.200186	0.677676	-0.000446

E(RB+HF-LYP) = -442.3849875

44) B3LYP/6-31++g(d,p) optimized

Center Number	Atomic Number	Atomic Type	Coordinates (Angstroms) X	Y	Z
1	6	0	0.199803	1.378610	0.777950
2	6	0	0.789720	0.033142	1.291840
3	6	0	0.002446	-1.179783	0.749532
4	6	0	0.199643	1.378533	-0.777681
5	6	0	0.002663	-1.179854	-0.749400
6	6	0	0.789806	0.033165	-1.291592
7	6	0	2.177913	-0.086917	0.671114
8	6	0	2.177976	-0.086730	-0.670726
9	1	0	-0.807207	1.531160	1.173565
10	1	0	0.819586	2.192392	1.166064
11	1	0	0.818579	0.019241	2.384619
12	1	0	0.182007	-2.111314	1.281397
13	1	0	0.819304	2.192319	-1.165978
14	1	0	-0.807478	1.530957	-1.173108
15	1	0	0.182483	-2.111379	-1.281187
16	1	0	0.818737	0.019312	-2.384372
17	1	0	3.075686	-0.128963	1.281091
18	1	0	3.075811	-0.128666	-1.280620
19	6	0	-1.335127	-1.137088	-0.000178
20	1	0	-1.833536	-2.105583	-0.000244
21	6	0	-2.328622	-0.093612	-0.000544
22	7	0	-3.200186	0.677676	-0.000446

E(RB+HF-LYP) = -442.385270737

45) B3LYP/6-31+g(d,p) optimized

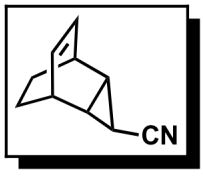

Center Number	Atomic Number	Atomic Type	Coordinates (Angstroms) X	Y	Z
1	6	0	1.230116	1.340453	0.778066
2	6	0	0.905644	-0.093154	1.294430
3	6	0	-0.458338	-0.568971	0.747642
4	6	0	1.229969	1.339550	-0.779708
5	6	0	-0.458456	-0.569863	-0.746773
6	6	0	0.905432	-0.094652	-1.294353
7	6	0	1.942511	-1.018989	0.671404
8	6	0	1.942412	-1.019756	-0.670432
9	6	0	-1.402476	0.378721	-0.000057
10	1	0	0.504188	2.056574	1.178985
11	1	0	2.208606	1.636478	1.166774
12	1	0	0.922692	-0.120188	2.387101
13	1	0	-0.928048	-1.391778	1.279389
14	1	0	2.208371	1.635152	-1.168957
15	1	0	0.503948	2.055180	-1.181330
16	1	0	-0.928247	-1.393305	-1.277465
17	1	0	0.922293	-0.122964	-2.386995
18	1	0	-1.193904	1.442217	-0.000688
19	1	0	2.630497	-1.597899	1.280607
20	1	0	2.630297	-1.599376	-1.279074
21	6	0	-2.811553	0.077737	0.000171
22	7	0	-3.947465	-0.175221	-0.000098

E(RB+HF-LYP) = -442.3926962

46) B3LYP/6-31++g(d,p) optimized

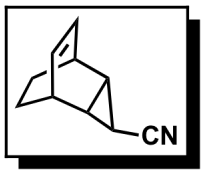

Center Number	Atomic Number	Atomic Type	Coordinates (Angstroms) X	Y	Z
1	6	0	-1.229801	1.340388	-0.778417
2	6	0	-0.905671	-0.093494	-1.294392
3	6	0	0.458207	-0.569526	-0.747547
4	6	0	-1.229606	1.339859	0.779465
5	6	0	0.458349	-0.570033	0.746868
6	6	0	-0.905408	-0.094381	1.294375
7	6	0	-1.942900	-1.018784	-0.671145
8	6	0	-1.942770	-1.019223	0.670711
9	6	0	1.402457	0.378229	-0.000102
10	1	0	-0.503813	2.056273	-1.179557
11	1	0	-2.208305	1.636392	-1.167085
12	1	0	-0.922715	-0.120825	-2.387052
13	1	0	0.927924	-1.392412	-1.279161
14	1	0	-2.208021	1.635617	1.168527
15	1	0	-0.503508	2.055448	1.180951
16	1	0	0.928210	-1.393248	1.277839
17	1	0	-0.922168	-0.122490	2.387021
18	1	0	1.193815	1.441715	0.000263

19	1	0	-2.631160	-1.597460	-1.280261
20	1	0	-2.630906	-1.598302	1.279583
21	6	0	2.811617	0.077473	-0.000202
22	7	0	3.947686	-0.174823	0.000178

E(RB+HF-LYP) = -442.392960816

47) B3LYP/6-31+g(d,p) optimized

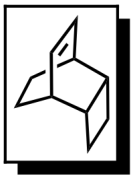

Center Number	Atomic Number	Atomic Type	Coordinates (Angstroms) X	Y	Z
1	6	0	0.674733	-0.777849	1.406213
2	6	0	0.583735	-1.301265	-0.055746
3	6	0	-0.711475	-0.781389	-0.741164
4	6	0	0.674325	0.777409	1.406488
5	6	0	-0.711600	0.781537	-0.740985
6	6	0	0.583469	1.301328	-0.055291
7	6	0	1.729029	0.671876	-0.826435
8	6	0	-2.074959	-0.779087	0.020400
9	6	0	-2.075088	0.778855	0.020537
10	1	0	1.592334	-1.165064	1.860805
11	1	0	-0.155727	-1.170443	2.001985
12	1	0	0.626296	-2.395757	-0.071183
13	1	0	-0.782143	-1.225977	-1.739192
14	1	0	1.591563	1.164959	1.861525
15	1	0	-0.156557	1.169331	2.002124
16	1	0	-0.782172	1.226453	-1.738876
17	1	0	0.625830	2.395833	-0.070304
18	1	0	2.478626	-1.273790	-1.333662
19	1	0	2.478368	1.274648	-1.333220
20	1	0	-2.893325	-1.226397	-0.551839
21	1	0	-2.068636	-1.245357	1.009714
22	1	0	-2.893446	1.226002	-0.551837
23	1	0	-2.069048	1.245102	1.009876
24	6	0	1.729170	-0.671340	-0.826669

E(RB+HF-LYP) = -389.4718863

48) B3LYP/6-31++g(d,p) optimized

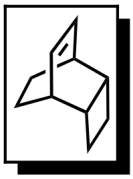

Center Number	Atomic Number	Atom Type	Coordinates (Angstroms) X	Y	Z
1	6	0	-0.675452	0.778643	1.405752
2	6	0	-0.583851	1.301259	-0.056546
3	6	0	0.711760	0.781026	-0.741360
4	6	0	-0.675020	-0.776693	1.406855
5	6	0	0.711872	-0.781743	-0.740552
6	6	0	-0.583416	-1.301393	-0.054700
7	6	0	-1.728588	-0.672481	-0.826344
8	6	0	2.074969	0.779116	0.020727

9	6	0	2.075387	-0.778880	0.020959
10	1	0	-1.593194	1.166177	1.859597
11	1	0	0.154741	1.171581	2.001462
12	1	0	-0.626044	2.395738	-0.072495
13	1	0	0.782535	1.225464	-1.739399
14	1	0	-1.592474	-1.164064	1.861417
15	1	0	0.155489	-1.168334	2.002984
16	1	0	0.782240	-1.227242	-1.738148
17	1	0	-0.625226	-2.395909	-0.069041
18	1	0	-2.478327	1.272433	-1.335137
19	1	0	-2.477972	-1.275045	-1.333224
20	1	0	2.893392	1.226505	-0.551256
21	1	0	2.068248	1.245602	1.009850
22	1	0	2.893763	-1.225918	-0.551363
23	1	0	2.069451	-1.245176	1.010183
24	6	0	-1.728766	0.670844	-0.827362

E(RB+HF-LYP) = -389.472190260

49) B3LYP/6-31+g(d,p) optimized

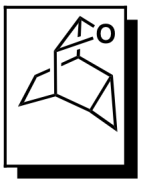

Center Number	Atomic Number	Atomic Type	Coordinates (Angstroms) X	Y	Z
1	6	0	-0.511793	1.529991	0.781834
2	6	0	0.032794	0.174182	1.308641
3	6	0	-0.775283	-1.001263	0.756229
4	6	0	-0.511790	1.529990	-0.781834
5	6	0	-0.775275	-1.001253	-0.756228
6	6	0	0.032799	0.174182	-1.308642
7	6	0	1.460690	0.086615	0.735075
8	6	0	1.460692	0.086617	-0.735074
9	1	0	-1.516284	1.708056	1.178980
10	1	0	0.118746	2.340434	1.165400
11	1	0	0.043013	0.169213	2.403914
12	1	0	0.118756	2.340429	-1.165395
13	1	0	-1.516280	1.708058	-1.178983
14	1	0	0.043018	0.169210	-2.403914
15	1	0	2.270298	0.545398	1.301745
16	1	0	2.270305	0.545397	-1.301738
17	6	0	-2.072296	-0.810049	-0.000003
18	1	0	-0.629230	-1.948732	1.267090
19	1	0	-0.629249	-1.948732	-1.267080
20	1	0	-2.578934	0.149015	0.000000
21	8	0	1.839665	-1.092069	0.000001
22	1	0	-2.754711	-1.655265	-0.000022

E(RB+HF-LYP) = -425.351862450

50) B3LYP/6-31+g(d,p) optimized

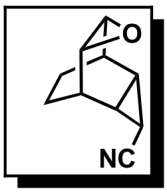

Center Number	Atomic Number	Atomic Type	Coordinates (Angstroms) X	Y	Z
1	6	0	-0.203360	1.458642	0.781188
2	6	0	0.502073	0.179996	1.307875
3	6	0	-0.108094	-1.107582	0.752152
4	6	0	-0.203531	1.458803	-0.780766
5	6	0	-0.108298	-1.107444	-0.752208
6	6	0	0.501721	0.180224	-1.307867
7	6	0	1.932158	0.274714	0.734548
8	6	0	1.931962	0.274837	-0.734902
9	1	0	-1.219121	1.527762	1.176144
10	1	0	0.337004	2.331705	1.164212
11	1	0	0.507645	0.168381	2.402104
12	1	0	0.336831	2.331898	-1.163718
13	1	0	-1.219370	1.528089	-1.175489
14	1	0	0.506998	0.168800	-2.402099
15	1	0	2.673058	0.833712	1.304011
16	1	0	2.672709	0.833931	-1.304468
17	6	0	-1.436231	-1.216559	0.000141
18	1	0	0.186811	-2.015503	1.270261
19	1	0	0.186437	-2.015279	-1.270566
20	8	0	2.458069	-0.846892	-0.000343
21	1	0	-1.818026	-2.235981	0.000120
22	6	0	-2.541106	-0.291335	0.000288
23	7	0	-3.488471	0.384551	-0.000066

E(RB+HF-LYP) = -517.5901788

51) B3LYP/6-31+g(d,p) optimized

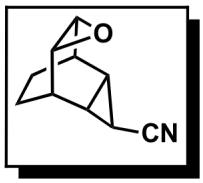

Center Number	Atomic Number	Atomic Type	Coordinates (Angstroms) X	Y	Z
1	6	0	0.904584	1.630373	0.782150
2	6	0	0.704937	0.183424	1.310916
3	6	0	-0.568956	-0.449899	0.749846
4	6	0	0.904623	1.630439	-0.781934
5	6	0	-0.568916	-0.449839	-0.749881
6	6	0	0.705006	0.183534	-1.310831
7	6	0	1.900056	-0.603819	0.735193
8	6	0	1.900094	-0.603756	-0.735111
9	1	0	0.126178	2.288127	1.182527

10	1	0	1.855332	2.016744	1.165249
11	1	0	0.704708	0.171178	2.405105
12	1	0	1.855389	2.016844	-1.164953
13	1	0	0.126236	2.288225	-1.182294
14	1	0	0.704835	0.171378	-2.405021
15	1	0	2.827936	-0.610875	1.305173
16	1	0	2.828003	-0.610766	-1.305043
17	6	0	-1.606246	0.387149	-0.000013
18	1	0	-0.941660	-1.328681	1.266172
19	1	0	-0.941588	-1.328580	-1.266299
20	1	0	-1.521931	1.467855	0.000031
21	8	0	1.636820	-1.811632	-0.000016
22	6	0	-2.972904	-0.069362	-0.000062
23	7	0	-4.075954	-0.439693	-0.000307

E(RB+HF-LYP) = -517.59632304

52) B3LYP/6-31+g(d,p) optimized

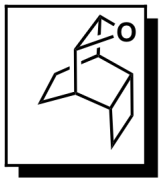

Center Number	Atomic Number	Atomic Type	Coordinates (Angstroms) X	Y	Z
1	6	0	-0.135723	1.655132	-0.779888
2	6	0	-0.356345	0.213203	-1.316147
3	6	0	0.716106	-0.755350	-0.782515
4	6	0	-0.135409	1.654098	0.781891
5	6	0	0.716116	-0.756510	0.781412
6	6	0	-0.356141	0.211519	1.316392
7	6	0	-1.711037	-0.215922	0.735895
8	6	0	2.215602	-0.329196	-0.780682
9	6	0	2.215654	-0.330554	0.780228
10	1	0	-0.933292	2.302805	-1.162731
11	1	0	0.799510	2.066310	-1.171496
12	1	0	-0.375479	0.216159	-2.412610
13	1	0	0.549632	-1.745439	-1.215036
14	1	0	-0.932645	2.301468	1.165927
15	1	0	0.800104	2.064501	1.173662
16	1	0	0.549385	-1.747155	1.212548
17	1	0	-0.375085	0.213119	2.412862
18	1	0	-2.612890	0.023701	-1.299110
19	1	0	-2.612729	0.022086	1.299431
20	1	0	2.881365	-1.072060	-1.230336
21	1	0	2.440417	0.637175	-1.242013
22	1	0	2.881276	-1.074406	1.228453
23	1	0	2.440695	0.634929	1.243304
24	6	0	-1.711132	-0.215030	-0.735978
25	8	0	-1.780802	-1.453941	-0.000813

E(RB+HF-LYP) = -464.675188

53) B3LYP/6-31+g(d,p) optimized

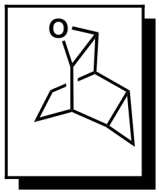

Center Number	Atomic Number	Atomic Type	Coordinates (Angstroms) X	Y	Z
1	6	0	0.085205	1.443876	0.779777
2	6	0	0.018771	-0.005331	1.305336
3	6	0	-1.222970	-0.743080	0.758636
4	6	0	0.085207	1.443876	-0.779778
5	6	0	-1.222968	-0.743081	-0.758640
6	6	0	0.018775	-0.005331	-1.305336
7	6	0	1.213893	-0.791086	0.734035
8	6	0	1.213895	-0.791087	-0.734031
9	1	0	-0.762201	2.009803	1.180200
10	1	0	0.995629	1.916924	1.156068
11	1	0	0.026789	-0.014510	2.400493
12	1	0	0.995631	1.916925	-1.156067
13	1	0	-0.762200	2.009801	-1.180202
14	1	0	0.026797	-0.014511	-2.400493
15	1	0	1.604228	-1.633250	1.303970
16	1	0	1.604232	-1.633251	-1.303963
17	6	0	-2.323528	-0.032923	-0.000004
18	1	0	-1.496476	-1.656291	1.283040
19	1	0	-1.496473	-1.656292	-1.283044
20	1	0	-2.374484	1.050014	-0.000004
21	8	0	2.217586	-0.055010	0.000004
22	1	0	-3.299844	-0.510285	-0.000005

E(RB+HF-LYP) = -425.351827119

54) B3LYP/6-31+g(d,p) optimized

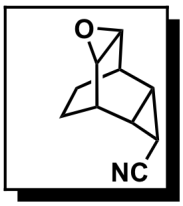

Center Number	Atomic Number	Atomic Type	Coordinates (Angstroms) X	Y	Z
1	6	0	0.068663	-1.314886	-0.779195
2	6	0	0.509471	0.066026	-1.304823
3	6	0	-0.358804	1.217350	-0.754256
4	6	0	0.068529	-1.315060	0.778880
5	6	0	-0.358950	1.217180	0.754411
6	6	0	0.509227	0.065741	1.304890
7	6	0	1.909235	0.382093	-0.734951
8	6	0	1.909097	0.381934	0.735348
9	1	0	-0.917464	-1.563522	-1.177362
10	1	0	0.768173	-2.065484	-1.154590
11	1	0	0.512947	0.078629	-2.399030
12	1	0	0.767991	-2.065729	1.154224

13	1	0	-0.917661	-1.563805	1.176822
14	1	0	0.512499	0.078107	2.399100
15	1	0	2.572144	1.029934	-1.306710
16	1	0	2.571900	1.029649	1.307371
17	6	0	-1.681926	1.069684	-0.000069
18	1	0	-0.260609	2.162119	-1.284685
19	1	0	-0.260871	2.161831	1.285072
20	8	0	2.582441	-0.659320	0.000148
21	1	0	-2.260661	1.992230	-0.000039
22	6	0	-2.581889	-0.056596	-0.000252
23	7	0	-3.386260	-0.897171	-0.000178

E(RB+HF-LYP) = -517.588434040

55) B3LYP/6-31++g(d,p) optimized

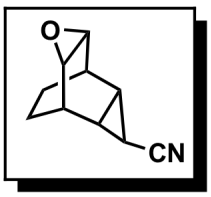

Center Number	Atomic Number	Atomic Type	Coordinates (Angstroms) X	Y	Z
1	6	0	0.068750	-1.314905	-0.779246
2	6	0	0.509538	0.066079	-1.304834
3	6	0	-0.358854	1.217335	-0.754287
4	6	0	0.068616	-1.315080	0.778931
5	6	0	-0.359000	1.217166	0.754442
6	6	0	0.509294	0.065794	1.304901
7	6	0	1.909311	0.382089	-0.734959
8	6	0	1.909173	0.381930	0.735356
9	1	0	-0.917356	-1.563406	-1.177544
10	1	0	0.768235	-2.065459	-1.154705
11	1	0	0.513009	0.078734	-2.399050
12	1	0	0.768053	-2.065703	1.154339
13	1	0	-0.917552	-1.563689	1.177003
14	1	0	0.512560	0.078211	2.399120
15	1	0	2.572153	1.029993	-1.306747
16	1	0	2.571909	1.029708	1.307408
17	6	0	-1.681906	1.069444	-0.000069
18	1	0	-0.260740	2.162107	-1.284723
19	1	0	-0.261001	2.161819	1.285110
20	8	0	2.582706	-0.659288	0.000148
21	1	0	-2.260864	1.991826	-0.000039
22	6	0	-2.581682	-0.057063	-0.000252
23	7	0	-3.387071	-0.896653	-0.000178

E(RB+HF-LYP) = -517.588754736

56) B3LYP/6-31+g(d,p) optimized

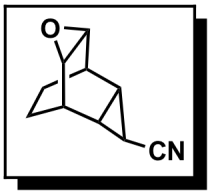

Center Number	Atomic Number	Atomic Type	Coordinates (Angstroms) X	Y	Z
1	6	0	-0.912630	1.442288	-0.781710
2	6	0	-0.626326	0.018969	-1.307557
3	6	0	0.703792	-0.531771	-0.751505
4	6	0	-0.912972	1.443630	0.779154
5	6	0	0.703478	-0.530457	0.753059
6	6	0	-0.626892	0.021228	1.307579
7	6	0	-1.689804	-0.938143	-0.734195
8	6	0	-1.690120	-0.936876	0.735420
9	1	0	-0.166245	2.134275	-1.185722
10	1	0	-1.885281	1.767086	-1.157716
11	1	0	-0.625187	0.005711	-2.401669
12	1	0	-1.885790	1.769079	1.154168
13	1	0	-0.166765	2.136320	1.182294
14	1	0	-0.626230	0.009869	2.401713
15	1	0	-1.952314	-1.827606	-1.304551
16	1	0	-1.952871	-1.825348	1.307209
17	6	0	1.687437	0.365155	0.000196
18	1	0	1.140800	-1.375215	-1.279312
19	1	0	1.140249	-1.372999	1.282501
20	1	0	1.528084	1.437094	-0.000722
21	8	0	-2.785955	-0.355230	-0.000124
22	6	0	3.081592	-0.001406	0.000598
23	7	0	4.204837	-0.304589	-0.000491

E(RB+HF-LYP) = -517.596107249

57) B3LYP/6-31++g(d,p) optimized

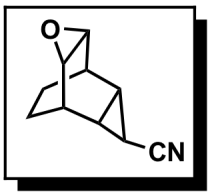

Center Number	Atomic Number	Atomic Type	Coordinates (Angstroms) X	Y	Z
1	6	0	-0.912167	1.442388	-0.781704
2	6	0	-0.626357	0.018918	-1.307562
3	6	0	0.703656	-0.532125	-0.751548
4	6	0	-0.912494	1.443668	0.779266
5	6	0	0.703357	-0.530871	0.753030
6	6	0	-0.626895	0.021072	1.307583
7	6	0	-1.690160	-0.937846	-0.734241
8	6	0	-1.690461	-0.936637	0.735410
9	1	0	-0.165477	2.134016	-1.185734
10	1	0	-1.884685	1.767562	-1.157718
11	1	0	-0.625192	0.005636	-2.401678
12	1	0	-1.885171	1.769462	1.154333

13	1	0	-0.165974	2.135967	1.182465
14	1	0	-0.626185	0.009600	2.401720
15	1	0	-1.952783	-1.827261	-1.304634
16	1	0	-1.953314	-1.825108	1.307168
17	6	0	1.687357	0.364670	0.000186
18	1	0	1.140722	-1.375483	-1.279429
19	1	0	1.140197	-1.373370	1.282470
20	1	0	1.527923	1.436612	-0.000689
21	8	0	-2.786258	-0.354760	-0.000118
22	6	0	3.081634	-0.001562	0.000570
23	7	0	4.205026	-0.304230	-0.000467

E(RB+HF-LYP) = -517.596419435

58) B3LYP/6-31+g(d,p) optimized

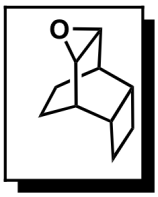

Center Number	Atomic Number	Atomic Type	Coordinates (Angstroms) X	Y	Z
1	6	0	-0.382974	0.779061	1.453994
2	6	0	-0.314145	1.315551	0.009357
3	6	0	0.940385	0.783848	-0.733009
4	6	0	-0.382904	-0.778590	1.454237
5	6	0	0.940390	-0.784027	-0.732816
6	6	0	-0.314092	-1.315536	0.009771
7	6	0	-1.485332	-0.736691	-0.794391
8	6	0	2.334317	0.779824	-0.033633
9	6	0	2.334368	-0.779828	-0.033541
10	1	0	-1.292884	1.155499	1.928737
11	1	0	0.460306	1.173511	2.029363
12	1	0	-0.333887	2.412054	0.009295
13	1	0	0.974537	1.224114	-1.736439
14	1	0	-1.292753	-1.154960	1.929153
15	1	0	0.460445	-1.172781	2.029684
16	1	0	0.974455	-1.224561	-1.736131
17	1	0	-0.333791	-2.412040	0.010063
18	1	0	-1.859682	1.300447	-1.648233
19	1	0	-1.859637	-1.301034	-1.647806
20	1	0	3.129577	1.228458	-0.636327
21	1	0	2.366531	1.242542	0.956782
22	1	0	3.129596	-1.228449	-0.636288
23	1	0	2.366732	-1.242463	0.956908
24	6	0	-1.485355	0.736398	-0.794634
25	8	0	-2.499687	-0.000048	-0.080096

E(RB+HF-LYP) = -464.676012662

59) B3LYP/6-31++g(d,p) optimized

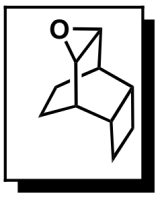

Center Number	Atomic Number	Atomic Type	Coordinates (Angstroms) X	Y	Z
1	6	0	-0.382704	0.779105	1.454038
2	6	0	-0.314152	1.315541	0.009310
3	6	0	0.940327	0.783836	-0.733183
4	6	0	-0.382630	-0.778614	1.454292
5	6	0	0.940333	-0.784024	-0.732982
6	6	0	-0.314095	-1.315526	0.009742
7	6	0	-1.485441	-0.736717	-0.794231
8	6	0	2.334245	0.779847	-0.033699
9	6	0	2.334298	-0.779851	-0.033602
10	1	0	-1.292411	1.155734	1.928958
11	1	0	0.460769	1.173460	2.029156
12	1	0	-0.333755	2.412055	0.009258
13	1	0	0.974343	1.224122	-1.736594
14	1	0	-1.292272	-1.155172	1.929393
15	1	0	0.460916	-1.172696	2.029491
16	1	0	0.974258	-1.224589	-1.736273
17	1	0	-0.333654	-2.412041	0.010061
18	1	0	-1.859640	1.300446	-1.648167
19	1	0	-1.859593	-1.301060	-1.647720
20	1	0	3.129544	1.228530	-0.636259
21	1	0	2.366252	1.242551	0.956692
22	1	0	3.129565	-1.228522	-0.636217
23	1	0	2.366459	-1.242467	0.956825
24	6	0	-1.485465	0.736411	-0.794485
25	8	0	-2.499885	-0.000050	-0.079975

E(RB+HF-LYP) = -464.676353817

VII. Product Cartesian Coordinates and Energies:

60) B3LYP/6-31g(d,p) optimized

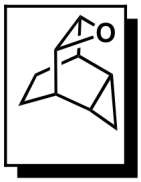

Center Number	Atomic Number	Atom Type	Coordinates (Angstroms) X	Y	Z
1	6	0	-0.516132	1.528126	0.781266
2	6	0	0.032495	0.175428	1.308414
3	6	0	-0.770822	-1.001969	0.755564
4	6	0	-0.516045	1.528209	-0.781188
5	6	0	-0.770802	-1.001884	-0.755672
6	6	0	0.032562	0.175528	-1.308409
7	6	0	1.460060	0.087532	0.734953
8	6	0	1.460100	0.087573	-0.734904
9	1	0	-1.521055	1.703107	1.177469
10	1	0	0.111009	2.340470	1.164949
11	1	0	0.041426	0.172321	2.403552
12	1	0	0.111191	2.340554	-1.164722
13	1	0	-1.520914	1.703298	-1.177475
14	1	0	0.041526	0.172489	-2.403544
15	1	0	2.267627	0.553627	1.299125
16	1	0	2.267705	0.553694	-1.299000
17	6	0	-2.066439	-0.815034	-0.000048
18	1	0	-0.620504	-1.948254	1.266619
19	1	0	-0.620520	-1.948145	-1.266787
20	1	0	-2.576313	0.142125	0.000028
21	8	0	1.836985	-1.088122	0.000002
22	1	0	-2.746923	-1.661371	-0.000092

E(RB+HF-LYP) = -425.3399545

61) B3LYP/6-31g(d,p) optimized

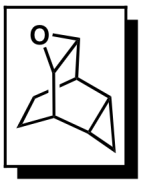

Center Number	Atomic Number	Atomic Type	Coordinates (Angstroms) X	Y	Z
1	6	0	0.089436	1.440898	0.779404
2	6	0	0.017781	-0.007053	1.305342
3	6	0	-1.224697	-0.740981	0.757732
4	6	0	0.089432	1.440875	-0.779444
5	6	0	-1.224697	-0.741006	-0.757708
6	6	0	0.017779	-0.007091	-1.305341
7	6	0	1.213280	-0.791154	0.733750

8	6	0	1.213279	-0.791175	-0.733729
9	1	0	-0.754754	2.010865	1.179611
10	1	0	1.002171	1.908494	1.154954
11	1	0	0.024697	-0.015045	2.400344
12	1	0	1.002163	1.908464	-1.155011
13	1	0	-0.754762	2.010829	-1.179664
14	1	0	0.024694	-0.015113	-2.400343
15	1	0	1.599349	-1.636959	1.301615
16	1	0	1.599346	-1.636997	-1.301571
17	6	0	-2.321323	-0.027671	0.000000
18	1	0	-1.499329	-1.653725	1.281661
19	1	0	-1.499323	-1.653767	-1.281609
20	1	0	-2.368812	1.055195	-0.000018
21	8	0	2.212818	-0.054477	-0.000001
22	1	0	-3.299600	-0.500279	0.000006

E(RB+HF-LYP) = -425.3400369

62) B3LYP/6-31g(d,p) optimized

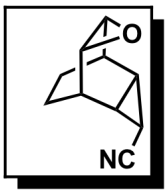

Center Number	Atomic Number	Atomic Type	Coordinates (Angstroms) X	Y	Z
1	6	0	-0.209140	1.456431	0.780666
2	6	0	0.499887	0.181084	1.307737
3	6	0	-0.104310	-1.108288	0.751429
4	6	0	-0.209416	1.456545	-0.780152
5	6	0	-0.104514	-1.108119	-0.751358
6	6	0	0.499484	0.181312	-1.307667
7	6	0	1.929535	0.276493	0.734477
8	6	0	1.929288	0.276649	-0.734803
9	1	0	-1.225612	1.521230	1.173130
10	1	0	0.327886	2.330809	1.163988
11	1	0	0.504023	0.170292	2.401842
12	1	0	0.327581	2.330943	-1.163450
13	1	0	-1.226012	1.521491	-1.172315
14	1	0	0.503244	0.170642	-2.401777
15	1	0	2.667431	0.842550	1.301386
16	1	0	2.667014	0.842805	-1.301831
17	6	0	-1.431617	-1.221746	0.000189
18	1	0	0.195125	-2.014248	1.269524
19	1	0	0.194635	-2.014012	-1.269733
20	8	0	2.454212	-0.842058	-0.000366
21	1	0	-1.809671	-2.242460	0.000025
22	6	0	-2.535668	-0.295939	0.000257
23	7	0	-3.477216	0.387127	-0.000358

E(RB+HF-LYP) = -517.5749176

63) B3LYP/6-31g(d,p) optimized

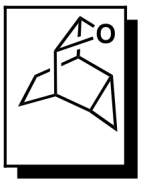

Center Number	Atomic Number	Atomic Type	Coordinates (Angstroms) X	Y	Z
1	6	0	0.066910	-1.311678	-0.778878
2	6	0	0.507129	0.068609	-1.304847
3	6	0	-0.358818	1.220392	-0.753262
4	6	0	0.066899	-1.311871	0.778533
5	6	0	-0.358881	1.220206	0.753462
6	6	0	0.507063	0.068296	1.304848
7	6	0	1.907672	0.378527	-0.734762
8	6	0	1.907628	0.378357	0.734929
9	1	0	-0.919239	-1.561027	-1.175297
10	1	0	0.767864	-2.060226	-1.153918
11	1	0	0.508884	0.081265	-2.398921
12	1	0	0.767834	-2.060526	1.153400
13	1	0	-0.919253	-1.561315	1.174880
14	1	0	0.508752	0.080704	2.398924
15	1	0	2.570009	1.029298	-1.304214
16	1	0	2.569912	1.029009	1.304583
17	6	0	-1.681677	1.072761	0.000047
18	1	0	-0.258168	2.164680	-1.283397
19	1	0	-0.258267	2.164349	1.283863
20	8	0	2.574262	-0.664130	-0.000009
21	1	0	-2.259993	1.995371	0.000153
22	6	0	-2.577069	-0.056804	-0.000179
23	7	0	-3.370509	-0.907044	0.000095

E(RB+HF-LYP) = -517.573357

64) B3LYP/6-31g(d,p) optimized

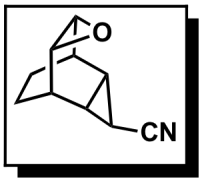

Center Number	Atomic Number	Atomic Type	Coordinates (Angstroms) X	Y	Z
1	6	0	0.906927	1.629491	0.781555
2	6	0	0.705477	0.184022	1.310438
3	6	0	-0.568275	-0.447778	0.749264
4	6	0	0.907013	1.629565	-0.781377
5	6	0	-0.568196	-0.447704	-0.749446
6	6	0	0.705623	0.184146	-1.310418
7	6	0	1.896932	-0.608067	0.735041
8	6	0	1.897013	-0.607996	-0.734964
9	1	0	0.129702	2.288467	1.180988
10	1	0	1.857727	2.014498	1.164513
11	1	0	0.704699	0.173728	2.404479
12	1	0	1.857854	2.014608	-1.164195
13	1	0	0.129831	2.288578	-1.180833
14	1	0	0.704966	0.173955	-2.404460

15	1	0	2.826789	-0.611905	1.302281
16	1	0	2.826932	-0.611782	-1.302102
17	6	0	-1.604835	0.389135	-0.000105
18	1	0	-0.940209	-1.326545	1.265260
19	1	0	-0.940068	-1.326426	-1.265564
20	1	0	-1.517805	1.469628	-0.000061
21	8	0	1.628704	-1.812057	-0.000033
22	6	0	-2.971078	-0.067663	-0.000143
23	7	0	-4.072808	-0.439038	0.000127

E(RB+HF-LYP) = -517.5803694

65) B3LYP/6-31g(d,p) optimized

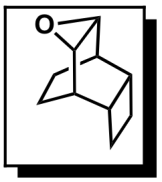

Center Number	Atomic Number	Atomic Type	Coordinates (Angstroms) X	Y	Z
1	6	0	-0.914220	1.438604	-0.782236
2	6	0	-0.624986	0.016556	-1.307543
3	6	0	0.704831	-0.531656	-0.750183
4	6	0	-0.914726	1.440833	0.778013
5	6	0	0.704333	-0.529491	0.752708
6	6	0	-0.625877	0.020298	1.307580
7	6	0	-1.690254	-0.937443	-0.733452
8	6	0	-1.690758	-0.935341	0.735511
9	1	0	-0.170063	2.132439	-1.186044
10	1	0	-1.887706	1.759199	-1.157942
11	1	0	-0.622712	0.003828	-2.401480
12	1	0	-1.888441	1.762551	1.152162
13	1	0	-0.170800	2.135803	1.180300
14	1	0	-0.624355	0.010718	2.401552
15	1	0	-1.948750	-1.829964	-1.301237
16	1	0	-1.949627	-1.826229	1.305686
17	6	0	1.686857	0.367320	0.000297
18	1	0	1.141906	-1.375353	-1.276821
19	1	0	1.141019	-1.371708	1.282034
20	1	0	1.523556	1.438546	-0.001213
21	8	0	-2.782350	-0.352042	-0.000178
22	6	0	3.080797	0.000980	0.000948
23	7	0	4.202683	-0.303923	-0.000776

E(RB+HF-LYP) = -517.5803018

66) B3LYP/6-31g(d,p) optimized

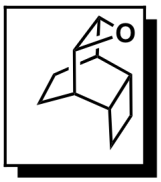

Center Number	Atomic Number	Atom Type	Coordinates (Angstroms) X	Y	Z

1	6	0	-0.135241	1.655538	-0.778444
2	6	0	-0.356691	0.215378	-1.315704
3	6	0	0.713805	-0.754232	-0.782583
4	6	0	-0.134642	1.653644	0.782119
5	6	0	0.713827	-0.756363	0.780557
6	6	0	-0.356299	0.212294	1.316155
7	6	0	-1.709377	-0.218424	0.735557
8	6	0	2.212686	-0.329428	-0.780086
9	6	0	2.212787	-0.331933	0.779241
10	1	0	-0.932003	2.303755	-1.160598
11	1	0	0.799780	2.066866	-1.169458
12	1	0	-0.374692	0.220874	-2.411838
13	1	0	0.544663	-1.743383	-1.214756
14	1	0	-0.930781	2.301308	1.166481
15	1	0	0.800902	2.063549	1.173408
16	1	0	0.544189	-1.746525	1.210195
17	1	0	-0.373951	0.215307	2.412306
18	1	0	-2.612228	0.025754	-1.296128
19	1	0	-2.611929	0.022836	1.296712
20	1	0	2.878152	-1.071016	-1.230912
21	1	0	2.437571	0.636802	-1.240574
22	1	0	2.877998	-1.075350	1.227421
23	1	0	2.438096	0.632655	1.242949
24	6	0	-1.709555	-0.216804	-0.735711
25	8	0	-1.774196	-1.453932	-0.001476

E(RB+HF-LYP) = -464.6636619

67) B3LYP/6-31g(d,p) optimized

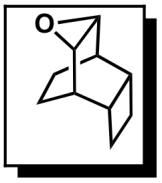

Center Number	Atomic Number	Atom Type	Coordinates (Angstroms) X	Y	Z
1	6	0	0.385407	-0.776081	1.452327
2	6	0	0.312528	-1.315176	0.009959
3	6	0	-0.941663	-0.784330	-0.731802
4	6	0	0.386994	0.780818	1.449863
5	6	0	-0.941438	0.782527	-0.733703
6	6	0	0.313255	1.315300	0.005811
7	6	0	1.485376	0.734606	-0.795035
8	6	0	-2.333381	-0.778872	-0.029963
9	6	0	-2.332771	0.779159	-0.031031
10	1	0	1.296727	-1.151810	1.923604
11	1	0	-0.455533	-1.168521	2.031827
12	1	0	0.330860	-2.411396	0.012882
13	1	0	-0.976380	-1.225738	-1.734210
14	1	0	1.300202	1.155977	1.917867
15	1	0	-0.451816	1.177072	2.029883
16	1	0	-0.976837	1.221176	-1.737286
17	1	0	0.331895	2.411514	0.005138
18	1	0	1.854111	-1.301410	-1.648942

19	1	0	1.854880	1.295245	-1.653271
20	1	0	-3.130000	-1.227391	-0.630032
21	1	0	-2.364158	-1.241329	0.960114
22	1	0	-3.129671	1.227922	-0.630542
23	1	0	-2.361879	1.242484	0.958686
24	6	0	1.484965	-0.737672	-0.792574
25	8	0	2.495247	-0.000685	-0.078603

E(RB+HF-LYP) = -464.6643792

VIII. Planar Transition State Cartesian Coordinates and Single Point Energies:

68) B3LYP/6-31+g(d,p) CPCM, dichloromethane

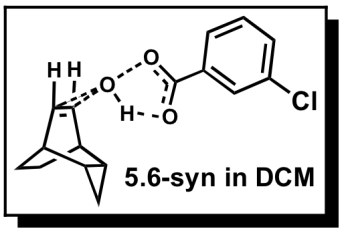

Center Number	Atomic Number	Atomic Type	Coordinates (Angstroms) X	Y	Z
1	6	0	-5.331517	0.241120	-0.778115
2	6	0	-3.871854	0.040639	-1.300746
3	6	0	-2.953389	1.156684	-0.764448
4	6	0	-5.330255	0.252228	0.780013
5	6	0	-2.951942	1.166944	0.749836
6	6	0	-3.869766	0.058632	1.303129
7	6	0	-3.428373	-1.269111	-0.676225
8	6	0	-3.427540	-1.259631	0.696254
9	6	0	-3.487504	2.357377	-0.014890
10	1	0	-5.733108	1.175282	-1.184880
11	1	0	-5.961433	-0.567960	-1.161883
12	1	0	-3.856222	-0.000960	-2.394420
13	1	0	-2.014117	1.281254	-1.299879
14	1	0	-5.960021	-0.550887	1.176367
15	1	0	-5.730511	1.192416	1.174049
16	1	0	-2.011653	1.298575	1.281843
17	1	0	-3.852308	0.032390	2.397255
18	1	0	-2.857098	3.243022	-0.021532
19	1	0	-4.548770	2.579866	-0.015079
20	1	0	-3.137985	-2.135411	-1.264818
21	1	0	-3.136415	-2.117766	1.296423
22	8	0	-1.295674	-1.474122	0.000733
23	8	0	0.465336	-1.756961	-0.006625
24	6	0	1.066783	-0.595401	0.002765
25	8	0	0.459446	0.485812	0.012447
26	1	0	-1.143250	-0.494920	0.005740
27	6	0	2.568367	-0.668343	0.000666

28	6	0	3.285334	0.537077	0.001493
29	6	0	3.249541	-1.894086	-0.001740
30	6	0	4.676147	0.491826	-0.000218
31	6	0	4.645508	-1.912083	-0.003160
32	1	0	2.691211	-2.825980	-0.002222
33	6	0	5.372785	-0.718001	-0.002487
34	1	0	5.177298	-2.861808	-0.004781
35	1	0	6.460672	-0.727717	-0.003649
36	1	0	2.755217	1.485104	0.003449
37	17	0	5.582192	2.007205	0.000709

E(RB+HF-LYP) = -1305.7159197

69) B3LYP/6-31+g(d,p) CPCM, dichloromethane

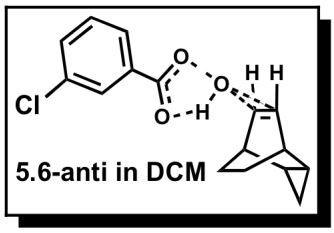

Center Number	Atomic Number	Atomic Type	Coordinates (Angstroms) X	Y	Z
1	6	0	-2.934021	1.252558	0.765663
2	6	0	-3.816181	0.092420	1.301434
3	6	0	-5.262886	0.224114	0.754399
4	6	0	-2.932552	1.232989	-0.792077
5	6	0	-5.261799	0.205805	-0.758778
6	6	0	-3.814367	0.060336	-1.300229
7	6	0	-3.325746	-1.213645	0.703532
8	6	0	-3.324775	-1.230795	-0.669387
9	6	0	-5.730533	1.441145	-0.017346
10	1	0	-3.320056	2.202314	1.149676
11	1	0	-1.920152	1.149128	1.163671
12	1	0	-3.802838	0.070431	2.395683
13	1	0	-6.015379	-0.354271	1.288695
14	1	0	-1.917988	1.118522	-1.185309
15	1	0	-3.317080	2.173120	-1.200487
16	1	0	-6.013817	-0.385137	-1.279843
17	1	0	-3.799448	0.011204	-2.393580
18	1	0	-6.802222	1.627034	-0.020396
19	1	0	-5.132255	2.345682	-0.027602
20	8	0	0.588014	-1.739271	-0.005777
21	8	0	0.563500	0.502256	0.024879
22	1	0	-3.004133	-2.086997	-1.256350
23	1	0	-3.005912	-2.055012	1.312051
24	1	0	-0.995422	-0.472930	0.017062
25	6	0	1.181763	-0.574533	0.008480
26	8	0	-1.176850	-1.446374	0.005173
27	6	0	2.682926	-0.632478	0.002896
28	6	0	3.388268	0.579807	0.003054
29	6	0	3.375232	-1.852028	-0.002182
30	6	0	4.779412	0.547520	-0.002183
31	6	0	4.771244	-1.856815	-0.006850

32	1	0	2.825507	-2.789084	-0.002123
33	6	0	5.487150	-0.655856	-0.007034
34	1	0	5.312021	-2.801429	-0.010435
35	1	0	6.575074	-0.655351	-0.010845
36	17	0	5.671261	2.071110	-0.002494
37	1	0	2.849354	1.522854	0.007131

E(RB+HF-LYP) = -1305.7142023

70) B3LYP/6-31+g(d,p) CPCM, dichloromethane

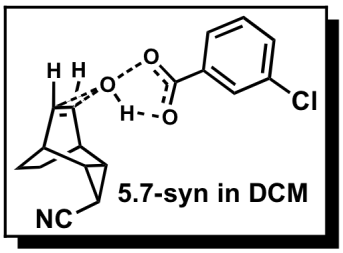

Center Number	Atomic Number	Atomic Type	Coordinates (Angstroms) X	Y	Z
1	6	0	-4.936616	-0.494230	-0.772769
2	6	0	-3.465433	-0.515156	-1.297736
3	6	0	-2.646917	0.671007	-0.757583
4	6	0	-4.934702	-0.484329	0.783712
5	6	0	-2.645000	0.680398	0.748200
6	6	0	-3.462269	-0.498713	1.305370
7	6	0	-2.880506	-1.772982	-0.675411
8	6	0	-2.878807	-1.764330	0.697712
9	6	0	-3.205937	1.884477	-0.011483
10	1	0	-5.459598	0.373758	-1.181691
11	1	0	-5.453894	-1.379514	-1.155724
12	1	0	-3.442007	-0.545351	-2.390883
13	1	0	-1.729503	0.881273	-1.304419
14	1	0	-5.451110	-1.364628	1.179151
15	1	0	-5.456578	0.388840	1.182906
16	1	0	-1.726113	0.897424	1.289867
17	1	0	-3.436253	-0.514845	2.398772
18	1	0	-2.504376	2.722464	-0.017565
19	1	0	-2.499903	-2.600383	-1.268208
20	1	0	-2.496728	-2.584195	1.299968
21	8	0	-0.765657	-1.793447	0.007747
22	8	0	1.025550	-1.931717	0.005830
23	6	0	1.515360	-0.720727	0.001694
24	8	0	0.804722	0.298296	0.001285
25	1	0	-0.666278	-0.806278	0.004122
26	6	0	3.016028	-0.648463	-0.002571
27	6	0	3.616466	0.619127	0.004797
28	6	0	3.808774	-1.805342	-0.013779
29	6	0	5.005514	0.704006	0.000935
30	6	0	5.200076	-1.692593	-0.017930
31	1	0	3.339740	-2.785253	-0.019549
32	6	0	5.811983	-0.435496	-0.010468
33	1	0	5.818604	-2.588192	-0.027020

34	1	0	6.895997	-0.343481	-0.013483
35	1	0	3.000519	1.513636	0.013423
36	17	0	5.766493	2.296841	0.010656
37	6	0	-4.547934	2.401248	-0.013198
38	7	0	-5.589110	2.923200	-0.015419

E(RB+HF-LYP) = -1397.9582974

71) B3LYP/6-31+g(d,p) CPCM, dichloromethane

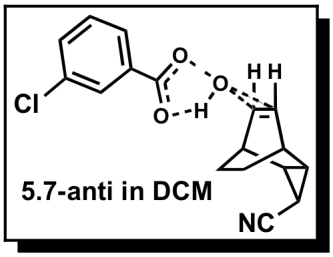

Center Number	Atomic Number	Atomic Type	Coordinates (Angstroms) X	Y	Z
1	6	0	-2.595751	0.813175	0.758717
2	6	0	-3.386022	-0.400916	1.315468
3	6	0	-4.834926	-0.438352	0.766724
4	6	0	-2.594548	0.768170	-0.796874
5	6	0	-4.833272	-0.482014	-0.736777
6	6	0	-3.382932	-0.476406	-1.283324
7	6	0	-2.788146	-1.676644	0.740795
8	6	0	-2.785891	-1.716660	-0.633483
9	6	0	-5.534239	0.676631	-0.018570
10	1	0	-3.039610	1.739167	1.131406
11	1	0	-1.577444	0.783639	1.156299
12	1	0	-3.379931	-0.402090	2.409324
13	1	0	-5.517850	-1.081231	1.320623
14	1	0	-1.575635	0.716120	-1.190704
15	1	0	-3.038845	1.670558	-1.223031
16	1	0	-5.515008	-1.155810	-1.254183
17	1	0	-3.374546	-0.541846	-2.375200
18	1	0	-6.621021	0.557456	-0.016184
19	8	0	1.126672	-1.900243	-0.001008
20	8	0	0.914131	0.329196	0.054778
21	1	0	-2.396565	-2.551082	-1.209658
22	1	0	-2.400691	-2.476304	1.365722
23	1	0	-0.545365	-0.753506	0.046576
24	6	0	1.621398	-0.692869	0.019178
25	8	0	-0.677867	-1.736826	0.023235
26	6	0	3.122080	-0.621553	-0.004578
27	6	0	3.724211	0.644979	0.021850
28	6	0	3.912996	-1.778637	-0.052533
29	6	0	5.113169	0.728490	-0.000421
30	6	0	5.304288	-1.667297	-0.074389
31	1	0	3.442269	-2.757554	-0.073047
32	6	0	5.917921	-0.411275	-0.048403
33	1	0	5.921471	-2.563073	-0.112105
34	1	0	7.001886	-0.320239	-0.065167

35	17	0	5.876397	2.320031	0.032612
36	1	0	3.109490	1.539601	0.059200
37	6	0	-5.219974	2.079332	-0.058199
38	7	0	-5.077990	3.234841	-0.090602

E(RB+HF-LYP) = -1397.9564188

72) B3LYP/6-31+g(d,p) CPCM, dichloromethane

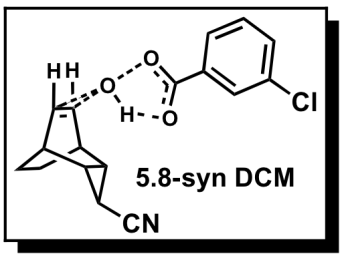

Center Number	Atomic Number	Atomic Type	Coordinates (Angstroms) X	Y	Z
1	6	0	5.129313	-0.387301	0.778613
2	6	0	3.658898	-0.465585	1.305791
3	6	0	2.818633	0.698435	0.749769
4	6	0	5.127395	-0.391035	-0.780247
5	6	0	2.816879	0.695045	-0.750711
6	6	0	3.655668	-0.471704	-1.303393
7	6	0	3.121814	-1.746063	0.691836
8	6	0	3.120155	-1.749352	-0.682047
9	6	0	3.481357	1.854074	-0.003777
10	1	0	5.610331	0.511164	1.180272
11	1	0	5.687990	-1.242951	1.169854
12	1	0	3.636283	-0.488283	2.399108
13	1	0	1.905021	0.935975	1.291597
14	1	0	5.685095	-1.248546	-1.168797
15	1	0	5.607444	0.505535	-1.187277
16	1	0	1.901960	0.930136	-1.291416
17	1	0	3.630351	-0.499522	-2.396533
18	1	0	2.771208	-2.582438	1.290391
19	1	0	2.768132	-2.588529	-1.275857
20	8	0	1.018820	-1.854487	0.004975
21	8	0	-0.775141	-2.037812	0.003316
22	6	0	-1.296187	-0.840326	0.001043
23	8	0	-0.613804	0.197590	0.000732
24	1	0	0.886095	-0.870827	0.003983
25	6	0	-2.799023	-0.809778	-0.001216
26	6	0	-3.434795	0.440261	0.002855
27	6	0	-3.559626	-1.988125	-0.007213
28	6	0	-4.825701	0.486680	0.000901
29	6	0	-4.953581	-1.914187	-0.009398
30	1	0	-3.063614	-2.954602	-0.010373
31	6	0	-5.600354	-0.674645	-0.005283
32	1	0	-5.546896	-2.826716	-0.014312
33	1	0	-6.686489	-0.612626	-0.006806
34	1	0	-2.844142	1.351594	0.007609

35	17	0	-5.630382	2.057959	0.006495
36	1	0	4.562669	1.953089	-0.005143
37	6	0	2.820553	3.131280	-0.006152
38	7	0	2.299252	4.172409	-0.008134

E(RB+HF-LYP) = -1397.9656272

73) B3LYP/6-31+g(d,p) CPCM, dichloromethane

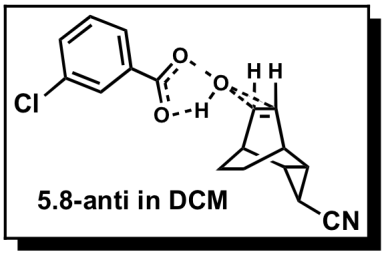

Center Number	Atomic Number	Atomic Type	Coordinates (Angstroms) X	Y	Z
1	6	0	2.407150	0.943314	-0.800716
2	6	0	3.216352	-0.289528	-1.287746
3	6	0	4.666367	-0.234726	-0.741156
4	6	0	2.411990	0.993202	0.756577
5	6	0	4.671264	-0.187039	0.756981
6	6	0	3.225185	-0.206119	1.316269
7	6	0	2.656180	-1.540248	-0.629859
8	6	0	2.661135	-1.495809	0.744346
9	6	0	5.199514	1.015488	-0.032743
10	1	0	2.842812	1.851443	-1.230087
11	1	0	1.388242	0.877930	-1.191717
12	1	0	3.205276	-0.358893	-2.379312
13	1	0	5.400510	-0.849650	-1.259303
14	1	0	1.395629	0.953366	1.157506
15	1	0	2.849883	1.926859	1.124500
16	1	0	5.408191	-0.768809	1.308449
17	1	0	3.221707	-0.204958	2.410081
18	8	0	-1.248003	-1.817131	0.000807
19	8	0	-1.085750	0.416713	0.049927
20	1	0	2.296905	-2.304515	1.371605
21	1	0	2.287742	-2.387453	-1.200994
22	1	0	0.395183	-0.631839	0.046847
23	6	0	-1.770021	-0.621238	0.019069
24	8	0	0.550341	-1.611881	0.025446
25	6	0	-3.271767	-0.583308	-0.000367
26	6	0	-3.901230	0.670126	0.010753
27	6	0	-4.037504	-1.757799	-0.029016
28	6	0	-5.291701	0.723230	-0.007469
29	6	0	-5.430991	-1.676937	-0.046477
30	1	0	-3.545727	-2.726492	-0.037444

31	6	0	-6.071688	-0.434272	-0.035959
32	1	0	-6.028687	-2.586335	-0.068620
33	1	0	-7.157427	-0.366917	-0.049605
34	17	0	-6.088941	2.298299	0.005988
35	1	0	-3.306061	1.578339	0.033305
36	1	0	4.630729	1.940940	-0.059866
37	6	0	6.621164	1.235569	-0.044508
38	7	0	7.772551	1.409641	-0.053822

E(RB+HF-LYP) = -1397.9648385

78) B3LYP/6-31+g(d,p) CPCM, dichloromethane

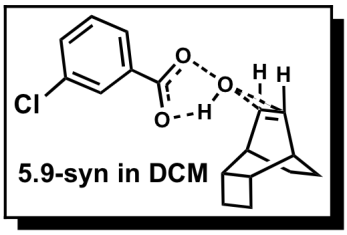

Center Number	Atomic Number	Atomic Type	Coordinates (Angstroms) X	Y	Z
1	6	0	5.183259	-0.142993	0.778568
2	6	0	3.716492	-0.254461	1.309192
3	6	0	2.861748	0.929927	0.785976
4	6	0	5.184227	-0.134749	-0.777519
5	6	0	2.861694	0.936161	-0.779090
6	6	0	3.718326	-0.242826	-1.311398
7	6	0	3.187750	-1.516347	-0.694695
8	6	0	3.440172	2.378203	0.788568
9	6	0	3.438040	2.385161	-0.770338
10	1	0	5.765521	-0.986664	1.163769
11	1	0	5.647615	0.763222	1.178945
12	1	0	3.705941	-0.303790	2.403598
13	1	0	1.867519	0.876178	1.240499
14	1	0	5.768486	-0.973212	-1.170952
15	1	0	5.647328	0.776543	-1.167734
16	1	0	1.867709	0.884243	-1.234333
17	1	0	3.709513	-0.282365	-2.406219
18	1	0	2.833944	-2.367587	1.265659
19	1	0	2.836397	-2.356412	-1.288062
20	1	0	2.762733	3.109694	1.239408
21	1	0	4.422056	2.499836	1.254801
22	1	0	2.757746	3.119354	-1.212395
23	1	0	4.418175	2.512755	-1.238700
24	8	0	1.046162	-1.660232	-0.004725
25	6	0	3.186421	-1.522383	0.680341
26	8	0	-0.734463	-1.883253	-0.003718
27	1	0	0.904666	-0.679989	-0.007376
28	6	0	-1.287475	-0.699459	-0.004008
29	8	0	-0.634712	0.356421	-0.006838

30	6	0	-2.790684	-0.708783	-0.000563
31	6	0	-3.521628	-1.905628	0.005756
32	6	0	-3.457418	0.525158	-0.003527
33	6	0	-4.917077	-1.866339	0.009125
34	1	0	-3.001791	-2.859542	0.008112
35	6	0	-4.848977	0.536858	0.000020
36	1	0	-2.889384	1.450789	-0.008397
37	6	0	-5.594597	-0.643339	0.006328
38	1	0	-5.487446	-2.793390	0.014124
39	1	0	-6.681936	-0.608377	0.009000
40	17	0	-5.692475	2.087922	-0.003399

E(RB+HF-LYP) = -1345.0377928

79) B3LYP/6-31+g(d,p) CPCM, dichloromethane

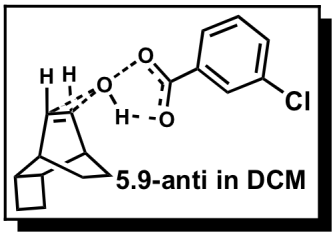

Center Number	Atomic Number	Atomic Type	Coordinates (Angstroms) X	Y	Z
1	6	0	2.670120	1.101147	-0.755435
2	6	0	3.491279	-0.089611	-1.316688
3	6	0	4.960233	-0.034619	-0.783195
4	6	0	2.667772	1.061428	0.799791
5	6	0	4.956438	-0.076846	0.779843
6	6	0	3.484841	-0.158062	1.302029
7	6	0	2.967420	-1.379448	-0.729294
8	6	0	2.963453	-1.415447	0.645010
9	1	0	3.092706	2.041048	-1.121691
10	1	0	1.650994	1.053698	-1.151884
11	1	0	3.464254	-0.096888	-2.411910
12	1	0	1.647292	0.996043	1.190152
13	1	0	3.091457	1.980491	1.214492
14	1	0	3.452224	-0.222795	2.395215
15	1	0	2.615028	-2.274984	1.211601
16	1	0	2.622346	-2.208224	-1.342049
17	1	0	6.731086	1.258808	-1.189956
18	6	0	5.734661	1.320941	-0.742155
19	1	0	5.219701	2.177688	-1.185897
20	6	0	5.732752	1.277700	0.815594
21	1	0	5.218598	2.109391	1.305527
22	1	0	6.728223	1.188647	1.260973
23	1	0	5.536750	-0.840530	-1.251556
24	1	0	5.529426	-0.907762	1.207023
25	8	0	0.821370	-1.546014	-0.024431
26	8	0	-0.951866	-1.782989	-0.011682
27	6	0	-1.510386	-0.600981	-0.014821
28	8	0	-0.860427	0.456909	-0.027332
29	1	0	0.672150	-0.566852	-0.031329
30	6	0	-3.012750	-0.614962	-0.001879
31	6	0	-3.739964	-1.813968	0.016220

32	6	0	-3.683001	0.617107	-0.007833
33	6	0	-5.135462	-1.778569	0.028527
34	1	0	-3.217421	-2.766419	0.020933
35	6	0	-5.074493	0.624841	0.004622
36	1	0	-3.117776	1.544374	-0.021894
37	6	0	-5.816508	-0.557533	0.022810
38	1	0	-5.703136	-2.707160	0.042881
39	1	0	-6.903909	-0.525671	0.032385
40	17	0	-5.922370	2.173368	-0.002508

E(RB+HF-LYP) = -1345.0378663

80) B3LYP/6-31+g(d) CPCM, dichloromethane

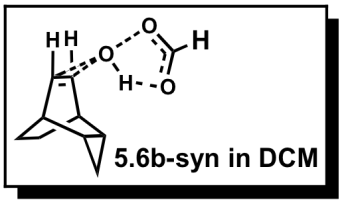

Center Number	Atomic Number	Atomic Type	Coordinates (Angstroms) X	Y	Z
1	6	0	2.684657	-0.388970	0.779451
2	6	0	1.221606	-0.230855	1.301395
3	6	0	0.596303	1.065938	0.757258
4	6	0	2.684996	-0.389807	-0.778446
5	6	0	0.596668	1.065640	-0.757952
6	6	0	1.222280	-0.231313	-1.301279
7	6	0	0.477386	-1.405050	0.689288
8	6	0	0.477653	-1.405282	-0.689210
9	6	0	1.394670	2.099756	-0.000374
10	1	0	3.298773	0.424775	1.178835
11	1	0	3.107229	-1.321038	1.169001
12	1	0	1.199295	-0.260168	2.394251
13	1	0	-0.300369	1.402406	1.270437
14	1	0	3.106758	-1.322800	-1.166679
15	1	0	3.300194	0.422796	-1.178504
16	1	0	-0.299810	1.401824	-1.271663
17	1	0	1.200612	-0.260908	-2.394138
18	1	0	0.989412	3.107818	-0.000645
19	1	0	2.479036	2.072998	-0.000113
20	1	0	-0.009021	-2.172011	1.280008
21	1	0	-0.008493	-2.172391	-1.279955
22	8	0	-1.463071	-1.087821	-0.000485
23	8	0	-3.312339	-0.869510	0.000197
24	6	0	-3.497738	0.403461	0.000254
25	1	0	-4.572802	0.672965	0.000670
26	8	0	-2.627522	1.281639	-0.000152
27	1	0	-1.418244	-0.091841	-0.000301

E(RB+HF-LYP) = -615.0025199

81) B3LYP/6-31+g(d) CPCM, dichloromethane

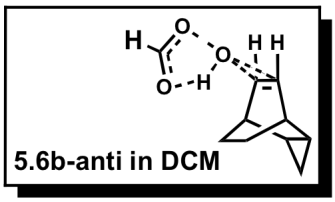

Center Number	Atomic Number	Atomic Type	Coordinates (Angstroms) X	Y	Z
1	6	0	-0.537881	1.206216	0.776804
2	6	0	-1.118057	-0.133629	1.299897
3	6	0	-2.556586	-0.341680	0.756347
4	6	0	-0.537282	1.203297	-0.780710
5	6	0	-2.556097	-0.344484	-0.755792
6	6	0	-1.117252	-0.138435	-1.299219
7	6	0	-0.340441	-1.288653	0.691706
8	6	0	-0.339959	-1.291230	-0.686275
9	6	0	-3.303478	0.733194	-0.001977
10	1	0	-1.136042	2.032775	1.173377
11	1	0	0.476161	1.342905	1.161648
12	1	0	-1.096701	-0.161159	2.392672
13	1	0	-3.147710	-1.087636	1.282950
14	1	0	0.477097	1.338323	-1.165236
15	1	0	-1.134934	2.028496	-1.180863
16	1	0	-3.146898	-1.092326	-1.280086
17	1	0	-1.095212	-0.169931	-2.391875
18	1	0	-4.388420	0.659876	-0.002209
19	1	0	-2.941969	1.755083	-0.003782
20	8	0	3.477211	-0.802684	-0.001608
21	8	0	2.799917	1.349529	0.001110
22	1	0	0.166216	-2.043338	-1.278766
23	1	0	0.165326	-2.038549	1.287349
24	1	0	1.614365	0.003611	0.001385
25	6	0	3.669388	0.468961	-0.000582
26	8	0	1.625010	-0.992341	0.000916
27	1	0	4.744174	0.736965	-0.001318

E(RB+HF-LYP) = -615.000239

82) B3LYP/6-31+g(d,p) CPCM, dichloromethane

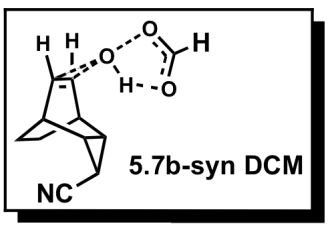

Input orientation:

Center Number	Atomic Number	Atomic Type	Coordinates (Angstroms) X	Y	Z
1	6	0	2.137064	-1.268841	0.776129
2	6	0	0.772030	-0.722550	1.302755
3	6	0	0.468863	0.684218	0.755915
4	6	0	2.133840	-1.267601	-0.780462
5	6	0	0.465678	0.685215	-0.750334
6	6	0	0.766636	-0.720681	-1.300466
7	6	0	-0.253688	-1.661916	0.689101

8	6	0	-0.256740	-1.660878	-0.683798
9	1	0	2.953823	-0.665018	1.179439
10	1	0	2.277347	-2.282683	1.164048
11	1	0	0.742627	-0.735200	2.396108
12	1	0	2.272704	-2.280800	-1.170582
13	1	0	2.948871	-0.663070	-1.186089
14	1	0	0.732533	-0.731780	-2.393701
15	1	0	-0.921106	-2.275937	1.287943
16	1	0	-0.926898	-2.274071	-1.280328
17	8	0	-2.222484	-0.852605	-0.002591
18	8	0	-3.930430	-0.276863	-0.005094
19	6	0	-3.906089	1.020613	0.000484
20	1	0	-4.925127	1.457324	0.002959
21	8	0	-2.889843	1.722073	0.003735
22	1	0	-1.912943	0.086701	-0.000329
23	1	0	1.120148	2.629850	0.002754
24	6	0	1.447361	1.587031	0.001350
25	1	0	-0.294658	1.233798	1.303862
26	1	0	-0.300010	1.235599	-1.294391
27	6	0	2.884943	1.549977	-0.001945
28	7	0	4.046639	1.633058	-0.004518

E(RB+HF-LYP) = -707.2861095

83) B3LYP/6-31+g(d,p) CPCM, dichloromethane

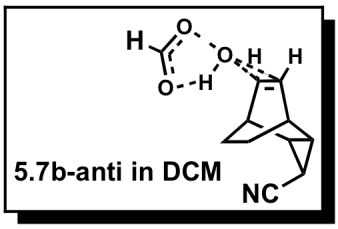

Center Number	Atomic Number	Atomic Type	Coordinates (Angstroms) X	Y	Z
1	6	0	0.386544	0.856209	-0.784693
2	6	0	0.702783	-0.574664	-1.296114
3	6	0	2.055912	-1.090199	-0.744684
4	6	0	0.386745	0.867598	0.771774
5	6	0	2.056366	-1.079157	0.759465
6	6	0	0.703537	-0.555677	1.304161
7	6	0	-0.293748	-1.543407	-0.675696
8	6	0	-0.293025	-1.533443	0.698815
9	6	0	3.105497	-0.258855	0.000993
10	1	0	1.119535	1.558467	-1.188272
11	1	0	-0.582488	1.167849	-1.185249
12	1	0	0.683925	-0.611596	-2.389165
13	1	0	2.468942	-1.947835	-1.274135
14	1	0	-0.582307	1.184838	1.167879
15	1	0	1.119478	1.575751	1.165189
16	1	0	2.469682	-1.928907	1.301259
17	1	0	0.685389	-0.576276	2.397647
18	1	0	4.084116	-0.746190	0.004294
19	1	0	-0.939966	-2.161453	1.304834
20	1	0	-0.941277	-2.180089	-1.271834
21	6	0	3.295188	1.166538	-0.009082
22	7	0	3.559568	2.300740	-0.016725
23	8	0	-2.292469	-0.828205	-0.008762

24	8	0	-4.046086	-0.353541	-0.024704
25	1	0	-5.133142	1.325054	-0.010078
26	6	0	-4.092681	0.941908	-0.001486
27	8	0	-3.115538	1.697883	0.026306
28	1	0	-2.055373	0.131475	0.009916

E(RB+HF-LYP) = -707.2841401

84) B3LYP/6-31+g(d,p) CPCM, dichloromethane

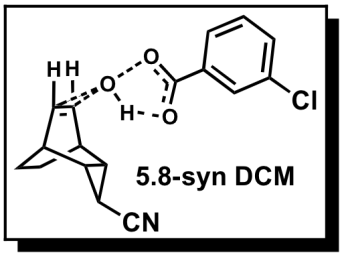

Center Number	Atomic Number	Atomic Type	Coordinates (Angstroms) X	Y	Z
1	6	0	2.371476	-1.449537	0.774321
2	6	0	0.997178	-0.926815	1.305389
3	6	0	0.699422	0.479723	0.752389
4	6	0	2.364571	-1.450250	-0.784096
5	6	0	0.693483	0.478896	-0.748830
6	6	0	0.985619	-0.928222	-1.303065
7	6	0	-0.018125	-1.875294	0.692928
8	6	0	-0.024460	-1.876042	-0.680341
9	1	0	3.176190	-0.823355	1.174637
10	1	0	2.536786	-2.458481	1.164252
11	1	0	0.970179	-0.939448	2.398772
12	1	0	2.526890	-2.459505	-1.174512
13	1	0	3.165511	-0.824079	-1.191924
14	1	0	0.948328	-0.942137	-2.396139
15	1	0	-0.678208	-2.495702	1.293286
16	1	0	-0.689967	-2.497022	-1.273948
17	8	0	-1.984653	-1.077321	-0.001615
18	8	0	-3.699764	-0.513237	-0.010934
19	6	0	-3.682939	0.784457	-0.000196
20	1	0	-4.704550	1.215270	-0.005167
21	8	0	-2.670920	1.491551	0.014370
22	1	0	-1.683765	-0.134534	0.010280
23	6	0	1.770611	1.269815	-0.002861
24	1	0	-0.036944	1.066275	1.298979
25	1	0	-0.046882	1.065702	-1.289624
26	6	0	1.676499	2.704918	-0.003556
27	7	0	1.610322	3.867363	-0.004140
28	1	0	2.800460	0.925649	-0.005789

E(RB+HF-LYP) = -707.2937155

85) B3LYP/6-31+g(d,p) CPCM, dichloromethane

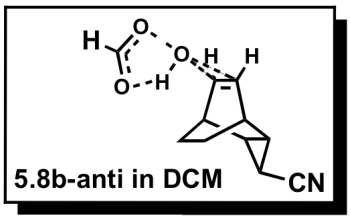

Center Number	Atomic Number	Atomic Type	Coordinates (Angstroms) X	Y	Z
1	6	0	0.067730	1.049641	-0.901173
2	6	0	0.563777	-0.376624	-1.263027
3	6	0	1.979760	-0.622420	-0.682058
4	6	0	0.071740	1.230514	0.646270
5	6	0	1.984193	-0.448135	0.806770
6	6	0	0.571387	-0.075093	1.325185
7	6	0	-0.285927	-1.396481	-0.521723
8	6	0	-0.279353	-1.237762	0.843947
9	1	0	0.709916	1.789599	-1.389752
10	1	0	-0.933991	1.192751	-1.315581
11	1	0	0.545248	-0.534770	-2.345191
12	1	0	-0.927331	1.468076	1.022550
13	1	0	0.716318	2.062134	0.949174
14	1	0	0.559385	0.021133	2.414663
15	1	0	-0.841920	-2.177831	-1.031786
16	1	0	-0.830014	-1.881248	1.524608
17	8	0	-2.359902	-0.910540	0.012634
18	8	0	-4.161012	-0.701522	-0.092395
19	6	0	-4.399957	0.571489	-0.042917
20	1	0	-5.483831	0.798502	-0.097698
21	8	0	-3.547596	1.461465	0.053510
22	1	0	-2.269999	0.072799	0.067986
23	6	0	2.793579	0.519125	-0.063561
24	1	0	2.547425	-1.438494	-1.126404
25	1	0	2.554910	-1.139858	1.424383
26	6	0	4.226444	0.389651	-0.052072
27	7	0	5.385878	0.281737	-0.042265
28	1	0	2.467742	1.548944	-0.183675

E(RB+HF-LYP) = -707.2925467

86) B3LYP/6-31+g(d,p) CPCM, dichloromethane

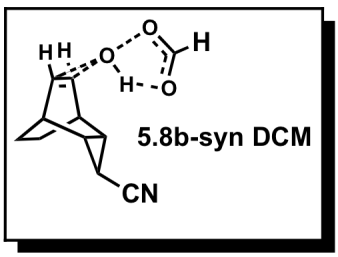

Center Number	Atomic Number	Atomic Type	Coordinates (Angstroms) X	Y	Z
1	6	0	-2.555379	-0.924347	-0.769560
2	6	0	-1.128526	-0.572839	-1.304049
3	6	0	-0.686635	0.822876	-0.790906
4	6	0	-2.557300	-0.905919	0.786331

5	6	0	-0.687491	0.839587	0.774116
6	6	0	-1.130959	-0.545003	1.316150
7	6	0	-0.226952	-1.590475	0.705413
8	6	0	-1.686877	2.019018	-0.801205
9	6	0	-1.688078	2.035527	0.757722
10	1	0	-2.842668	-1.911143	-1.147646
11	1	0	-3.282549	-0.214143	-1.174724
12	1	0	-1.104091	-0.624054	-2.398151
13	1	0	0.273865	1.078637	-1.250288
14	1	0	-2.847966	-1.882703	1.187024
15	1	0	-3.283014	-0.183806	1.172710
16	1	0	0.272403	1.104831	1.229366
17	1	0	-1.108796	-0.572631	2.411139
18	1	0	0.375101	-2.299947	-1.250965
19	1	0	0.371704	-2.272877	1.303242
20	1	0	-1.269864	2.922192	-1.256779
21	1	0	-2.657370	1.826981	-1.267420
22	1	0	-1.272231	2.948297	1.194857
23	1	0	-2.659147	1.852137	1.226220
24	8	0	1.858219	-1.045950	-0.011327
25	6	0	-0.225064	-1.605113	-0.669320
26	8	0	3.630171	-0.737135	-0.032194
27	1	0	1.682082	-0.074467	0.014349
28	6	0	3.812842	0.547683	0.001995
29	8	0	2.924591	1.403513	0.040016
30	1	0	4.889552	0.812950	-0.006766

E(RB+HF-LYP) =- 654.3656012

87) B3LYP/6-31+g(d,p) CPCM, dichloromethane

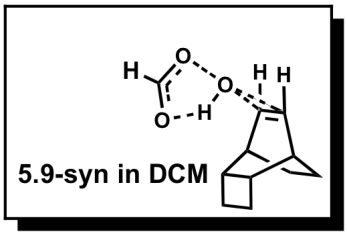

Center Number	Atomic Number	Atomic Type	Coordinates (Angstroms) X	Y	Z
1	6	0	-0.378077	1.157491	0.748762
2	6	0	-0.861687	-0.204415	1.312947
3	6	0	-2.302483	-0.524160	0.795867
4	6	0	-0.381788	1.121704	-0.806403
5	6	0	-2.306639	-0.560018	-0.767245
6	6	0	-0.868640	-0.263824	-1.305797
7	6	0	-0.033812	-1.317250	0.713493
8	6	0	-0.037363	-1.348448	-0.660707
9	1	0	-1.023911	1.956956	1.122960
10	1	0	0.622923	1.371683	1.137288
11	1	0	-0.821032	-0.206621	2.407746
12	1	0	0.617886	1.316577	-1.208326
13	1	0	-1.028073	1.904794	-1.213002
14	1	0	-0.833487	-0.315749	-2.399551
15	1	0	0.511172	-2.090293	-1.235321
16	1	0	0.517840	-2.032415	1.318169
17	1	0	-4.339595	0.274022	1.227892
18	6	0	-3.396911	0.589623	0.770713

19	1	0	-3.112299	1.547753	1.214972
20	6	0	-3.401684	0.553310	-0.787275
21	1	0	-3.121115	1.489971	-1.277199
22	1	0	-4.346793	0.216314	-1.223668
23	1	0	-2.648945	-1.451588	1.265931
24	1	0	-2.655533	-1.508050	-1.192373
25	8	0	2.090071	-0.931440	0.008948
26	8	0	3.870138	-0.723379	-0.002328
27	6	0	4.119100	0.551305	-0.007221
28	8	0	3.273809	1.450412	-0.004012
29	1	0	1.974328	0.049185	0.001985
30	1	0	5.207627	0.761428	-0.016033

E(RB+HF-LYP) = -654.3656004

Robert V. Kolakowski

Education and Research Experience

Rutgers, The State University of New Jersey	Ph.D. Organic Chemistry, 2010, Prof. L. J. Williams
Rutgers, The State University of New Jersey	B.S. Chemistry, 2004

Publications and Presentations

(1) Kolakowski, Robert V.; Williams, Lawrence J. *Nature Chemistry* **2010**, *2*, 303-307. "Strereoinduction by Distortional Asymmetry."

(2) Kolakowski, Robert V.; Williams, Lawrence J. *J. Am. Chem. Soc.* **2009**, *49*, 12910-12911. "Allene Synthesis via C−C Fragmentation: Method and Mechanistic Insight."

(3) Kolakowski, Robert V.; Williams, Lawrence J. *Tetrahedron Lett.* **2007**, *48*, 4761-4764. "Synthesis of the C21-C28 segment of pectenotoxin-4."

(4) Barlett, Kristin N.; Kolakowski, Robert V.; Katukojvala, Sreenivas; Williams, Lawrence J. *Org. Lett.* **2006**, *8*, 823-826. "Thio Acid/Azide Amidation: An Improved Route to N-Acyl Sulfonamides."

(5) Kolakowski Robert V; Shangguan Ning; Sauers Ronald R; Williams Lawrence J. *J. Am. Chem. Soc.* **2006**, *128*, 5695-702. "Mechanism of thio acid/azide amidation."

(6) Kolakowski, Robert V.; Shangguan, Ning; Williams, Lawrence J. *Tetrahedron Lett*. **2006**, 47, 1163-1166. "Thioamides via thiatriazolines."